RESEARCH REPORT

[redacted]

GPO PRICE $ _____

CFSTI PRICE(S) $ _____

Hard copy (HC) $ 6.00

Microfiche (MF) $ 1.25

ff 653 July 65

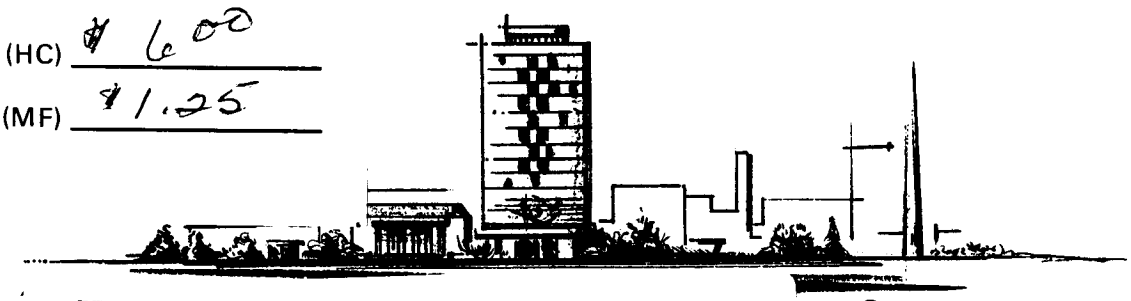

BATTELLE MEMORIAL INSTITUTE

COLUMBUS LABORATORIES

BATTELLE MEMORIAL INSTITUTE

COLUMBUS LABORATORIES • 505 KING AVENUE • COLUMBUS, OHIO 43201

DEDICATED TO THE ADVANCEMENT OF SCIENCE

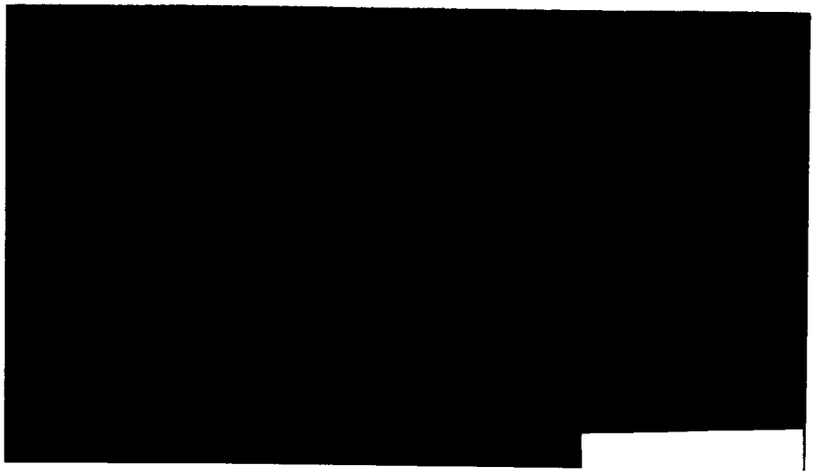

FIELDS OF RESEARCH

Aeronautics — Astronautics
Agricultural Chemistry
Agricultural Economics
Alloy Development
Applied Mathematics
Area Economics
Biochemistry
Biophysics — Bionics
Catalysis — Surface Chemistry
Ceramics
Chemical Engineering
Chemical Processes
Communications Science
Computer Technology
Corrosion Technology
Earth — Atmospheric Sciences
Electrochemistry
Electronics
Energy Conversion
Engineering — Structural Materials
Environmental Systems
Extractive Metallurgy
Extreme-Temperature Technology
Ferrous Metallurgy
Food Technology
Foundry Practice
Fuels — Combustion
Glass Technology
Graphic Arts Technology
Immunology — Cancer Studies
Industrial Economics
Industrial Physics
Information Research
Inorganic Chemistry
Instrumentation
Light Alloys — Rare Metals
Lubricant Technology
Materials Separation — Concentration
Mechanical Engineering
Metal Fabrication Engineering
Metal Finishing
Metallurgical Processes
Microbiology
Microscopy — Mineralogy
Nondestructive Evaluation Technology
Nonferrous Metallurgy
Nucleonics
Ocean Engineering
Organic Chemistry
Organic Coatings
Packaging Research
Particle Dynamics
Petrochemicals
Petroleum Engineering
Pharmaceutical Chemistry
Physical Chemistry
Production Engineering
Psychological Sciences
Pulp — Paper Technology
Radioisotopes — Radiation
Reactor Technology
Refractories
Reliability Engineering
Rubber — Plastics
Semiconductors — Solid-State Devices
Sound — Vibration
Systems Engineering
Textiles — Fibers
Theoretical — Applied Mechanics
Thermodynamics
Transportation
Welding — Metals-Joining Technology
Wood — Forest Products

FINAL REPORT

(June 27, 1964 - July 28, 1965)

on

WELDING-BASE METAL INVESTIGATION

to

GEORGE C. MARSHALL SPACE FLIGHT CENTER
NATIONAL AERONAUTICS AND SPACE ADMINISTRATION

Contract NAS8-11445

July 28, 1965

by

D. L. Cheever, P. A. Kammer, R. E. Monroe, and D. C. Martin

BATTELLE MEMORIAL INSTITUTE
505 King Avenue
Columbus, Ohio 43201

ABSTRACT

13076

A program was conducted to investigate the effects of factors associated with aluminum-base plate and filler wire on the occurrence of weld defects. The materials studied were experimental alloys of 2219-T87 and 2014-T6 base plate and 2319 and 4043 filler wire. In the program, four factors that determine the weld defect potential of a material were considered:

1. Chemical content.
2. Internal impurities.
3. Hydrogen content.
4. External impurities.

Chemical content is used to describe all the intentional alloy additions specified as ranges. Internal impurities were those elements limited by specifications to a maximum level. The hydrogen content was determined by vacuum fusion analysis. External impurities is used to describe the variation in hydrated surface oxide layers possible with aluminum. Actual control of external impurities was achieved by moisture additions to the weld shielding gas.

Welds were made with the experimental plate and wire using precisely regulated welding equipment and accurate instrumentation. The welds were then examined by radiographic and sectioning techniques. The occurrence of pores, which were the only weld defects observed, was related to variations of each of the four factors between a high and a low level. Statistical methods were used in this analysis.

The conclusions reached and recommendations to insure that materials with a low weld defect potential are available are presented. In addition, a potential method of monitoring weld shielding gas purity is described.

FOREWORD

The "Welding-Base Metal Investigation", Contract NAS8-11445, was performed by the Columbus Laboratories of Battelle Memorial Institute from June 27, 1964, to July 28, 1965. The program was under the sponsorship of the Welding Development Branch, Manufacturing Engineering Laboratories of the George C. Marshall Space Flight Center, National Aeronautics and Space Administration. Primary responsibility for conduct of the program was held by the Columbus Laboratories Materials Joining Division--D. L. Cheever, Project Engineer; P. A. Kammer, Project Leader; R. E. Monroe, Associate Division Chief; and D. C. Martin, Division Chief. S. J. Dearring was responsible for the performance of the investigations conducted in the Welding Laboratory. The preparation of the experimental materials was performed by the Nonferrous Metallurgy Division--Dr. D. N. Williams, Associate Chief and K. R. Grube, Metallurgist. C. R. Thompson of the Metallographic Laboratory prepared and photographed the microsections of the welds. The vacuum-fusion analyses were performed by M. A. VanCamp of the Analytical Chemistry Division with M. W. Mallett of the Physical Chemistry Divison consulting. G. R. Beatty of the Applied Statistics Division was responsible for the initial statistical planning and analyses.

Many helpful comments and suggestions were received during the program from the NASA personnel who monitored and co-ordinated the results of this investigation with the other NASA-sponsored research. The help of R. Poorman, R. Hoppes, and H. Brennecke was of paricular importance. The results of this program were co-ordinated by NASA-MSFC with four other programs related to the improvement of the performance of welded aluminum alloy. These programs were:

1. Contract NAS8-1135: Effects of Porosity Level; Martin - Denver.
2. Contract NAS8-11332: Mechanisms of Porosity Formation; Douglas.
3. Contract NAS8-11435: Transferability of Set-Up Perameters; Lockheed-Georgia.
4. Contract NAS8-11723: Design, Development, and Fabrication of a Portable Spectrometer Monitor - IIT Research Institute.

TABLE OF CONTENTS

LIST OF TABLES

LIST OF FIGURES

WELDING-BASE METAL INVESTIGATIONS

D. L. Cheever, P. A. Kammer, R. E. Monroe, and D. C. Martin

INTRODUCTION

In critical applications of welded aluminum alloy structures, such as those of the Saturn program, weld quality must be consistently maintained at a high level. The problem of insuring weld quality can be approached by considering two areas: (1) the welding materials, base plate and filler metal, and (2) the welding process, including the arc shielding gas. This research program studied the materials area.

The objective of this program was to determine the contribution of several specially-defined factors--chemical content, hydrogen content, internal impurities, and external impurities--to the weld defect potential of two base plate alloys, 2219 and 2014, and two filler metal alloys, 2319 and 4043. A base plate or filler metal of given surface quality (external impurities) and chemical composition (alloying elements, metallic impurities, and hydrogen content) can be considered to possess a specific weld defect potential. During welding, this defect potential is released. Part may result in defects and part may be dissipated by the welding process. With the results of this program, revised specifications can be suggested so that the contribution of the welding materials to the occurrence of weld defects can be minimized.

SUMMARY

The work performed during this program determined the relationship of four factors related to base and filler metal composition to the occurrence of weld defects. In additon, other important observations were made which were not included in the original program plan. The four factors that are involved in base metal composition as defined for this program were:

1. Chemical content. The metallic alloying elements for which the materials specifications used by NASA-MSFC allowed the compositions to range between high and low weight percentages. (Cu, Mn, Ti, V, Zr for 2219 and 2319 alloys; Cu, Mn, Si, Mg for 2014 alloy, Si for 4043 alloy).
2. Internal impurity content. The metallic* impurity elements for which the materials specifications used by NASA-MSFC specified only the allowable maximum weight percentages.
3. Gas content. The hydrogen content of the experimental welding materials before welding as measured by the Battelle vacuum-fusion analysis method.
4. External impurities. The amount of moisture present in the welding arc shielding gas (to simulate variations in the hydrated surface oxide layer.)

*Non-metallic internal impurities such as dross were not studied during the program and are not referred to as internal impurities.

Experimental base plates 1/4- and 3/4-inch thick by 36 inches long of X2219-T87* and X2014-T6 were fabricated and welded during the studies. The filler wires studied were 1/16-inch diameter experimental X2319 and X4043 alloys. All experimental materials were analyzed to determine chemical, internal impurity, and hydrogen content.

The program was conducted in two phases. In Phase I, plate material was welded without the addition of filler metal. The four factors were varied between high and low levels. Experiments were planned and analyzed statistically to determine the significance of each factor in promoting weld defects. The completed welds were studied by radiography and by microscopic inspection of transverse weld sections. The significance of the base material composition upon the size, location, frequency, and type of weld defect was shown. Pores were the only weld defects formed during the program.

In Phase II weld beads were deposited on commercial 2219 plate with experimental X2319 filler wire and on commercial 2014 plate with experimental X4043 filler wire. The same variable factors and methods of analyses used during Phase I were used during Phase II.

The welding process was gas-tungsten-arc (GTA) using straight polarity d-c current. The automatic welding head, power supply, and travel movement were carefully regulated. Recorders with an accuracy of 0.25% were used during the program. Radiography, ultrasonic inspection, and photomicrography conformed to widely used industrial and government standards.

---

*The prefix "X" denotes experimentally prepared alloys to distinguish them from commercial alloys.

The four variable factors were ranked in order of the strength of the relationship between the factor level and the weld porosity level. The external impurities factor was the strongest factor and was trailed in strength by the chemical content, internal impurities, and hydrogen content. The hydrogen content of the experimental base plate was significant only at a level above the hydrogen content of the commercial base plate available and above the majority of the experimental base plate hydrogen contents. The hydrogen content of the filler wire was not significant in the majority of the statistical comparisons studied. An interaction existed between chemical content and internal impurities which apparently affected the significance of the relationship of each factor to the porosity level. Minimum weld defect potential exists when all four factors are at a low level.

The size and distribution of pores within the welds were related to the composition of the weld metal. Segregation layers were observed in the welds in which pores formed preferentially. The segregation layer's appearance changed for different combinations of the variable factors.

The hydrogen content of the experimental base plate was low for low chemical content and low internal impurities and was high for high chemical content and high internal impurities. The hydrogen content was independent of the control methods used during casting except for one severe treatment.

The porosity level of the welds increased with increasing hydrogen content of the experimental base plate.

The arc voltage and arc current waveform changed form and developed inflection points when moisture was present in the helium shielding gas.

The following recommendations were made for full utilization of the program results.

All possible sources of moisture contamination of the helium shielding gas should be minimized when critical aluminum alloy assemblies are welded. A means should be provided to determine the actual quality of the shielding gas at the welding arc.

One or more of three basic approaches should be taken to determine and to decrease the weld defect potential of the commercial aluminum alloy studied. The approach(es) used would be dependent upon applicable time and priority factors.

1. The present specifications for chemical content should be lowered for the materials studied. The ranges of the hydrogen content in the commercial material should be determined.
2. An extensive program should determine the size of variations in hydrogen content, chemical content, and internal impurities in commercial base plate and filler wire materials.
3. A determination should be made of the contribution of each metallic element to the total weld defect potential or of intermediate levels of chemical content and internal impurities. The determination could take the form of an extensive casting, fabrication, welding, and defect analyses program in which a large number of variations of composition were made. A simpler determination should be considered which would study existing welds in existing variations

of weld composition. Studies should be made in this latter investigation to determine the relation of the pore occurrence to specific elements or intermetallics. In addition, the relation between hydrogen content and the level of specific elements should be determined.

The hydrogen content of the base plate should remain below 1.0 ppm, by weight.

The possibility of controlling the weld porosity size and grouping by controlling the weld metal composition should be studied.

The feasibility of developing an arc shield contamination monitor should be investigated.

PROGRAM STATISTICAL PLAN

The program plan was prepared to make maximum utilization of the experimental work and results. The initial plan allowed the program to yield the expected results, and additional meaningful observations were obtained which contributed to the Saturn V welding program and to the welding of aluminum in general practice.

Initial Plan

The initial plan divided the study into two phases. During Phase I, the effect of the experimental base plate composition upon the occurrence of weld defects was studied. Each of the four factors of weld metal composition (chemical content, internal impurity content, gas content, and external impurities) were studied at high and low levels. Of the possible 16 (2^4) combinations of two levels of the 4 factors, 8 were selected for study. The combinations selected are specified as types in Table 1. The selection of the 8 combinations was made so that the analysis of results was suitable for a one-half fractional factorial analysis, a method of statistical analysis which allows strong conclusions to be made from a study of a fraction of the possible combinations of factors. Appendix F discusses fractional factorial analysis more completely. Figure 1 illustrates the symmetrical selection of combinations of the composition factors studied. For Phase I, four separate welds (specimens) were made on each base plate thickness with each alloy. For Phase II, the number of replications was changed to two.

TABLE 1. LEVELS OF FOUR FACTORS OF COMPOSITION SELECTED FOR STUDY

Type Number	Phase I and II			Phase I	Phase II
	Chemical Content	Gas Content	Internal Impurities	External Impurities	External Impurities
1	L[a]	L	L	L	H
2	L	H[b]	H	L	H
3	L	L	H	H	H
4	L	H	L	H	H
5	H	H	L	L	H
6	H	L	H	L	H
7	H	L	L	H	H
8	H	H	H	H	H

(a) L - Low level.

(b) H - High level.

		Low Chemical Content		High Chemical Content	
		Low Gas Content	High Gas Content	Low Gas Content	High Gas Content
Low External Impurities	Low Internal Impurities	Type 1	-	-	Type 5
	High Internal Impurities	-	Type 2	Type 6	-
High External Impurities	Low Internal Impurities	-	Type 4	Type 7	-
	High Internal Impurities	Type 3	-	-	Type 8

FIGURE 1. COMBINATIONS OF FACTORS OF COMPOSITION INITIALLY PLANNED FOR THE INVESTIGATION

Phase I

Eight types (combinations of compositional factors) of experimental X2219 and X2014 base plate were prepared and welded in conformance with the initial plan. The analysis of the results from Phase I was limited by the relatively strong effect of the external impurity level upon weld defect occurrence. The strength of this one factor did not allow strong conclusions to be drawn about the effect of the three weaker composition factors upon weld defects.

Phase II

The plan was slightly modified for Phase II so that the stronger factor of external impurities was fixed at one level to allow a determination of the effect of the levels of chemical content, internal impurity content, and gas content upon the weld defect level. In addition, the results from Phase I indicated that the commercial 2219-T87 and 2014-T6 obtained from NASA-MSFC had a sufficiently low weld defect potential for use in Phase II. The analysis of Phase I results also indicated that the four weld replications (specimens) made for each thickness of each alloy could be reduced to two during Phase II without an appreciable decrease in the significance of the results obtained.

MATERIALS FABRICATION

All of the combinations of base plate and filler wire composition were cast, fabricated, and heat-treated at Battelle. For this reason, the

program results were based solely upon study of variations of composition levels of experimental materials. Although the materials could not possibly be cast in massive ingots and fabricated to plate with large reductions of thickness as in commercial practice, the results have good validity for predicting the effect of the composition of commercial materials upon weld defect occurrence.

Base Plate Casting

Materials with low metallic impurities were prepared using high purity master alloys and 99.99% super-purity aluminum ingots. High purity Al-Cu, Al-Si, Al-Fe, and Al-Cu-Zr master alloys were prepared because commercial alloys were not readily available or were not of sufficient purity (see Appendix A for the composition of the commercial and Battelle master alloys).

All material compositions were melted in clean silicon-carbide crucibles placed in a gas-fired furnace. As soon as the aluminum charge was molten, master alloys were added in order of the melting point of each addition. The highest melting point addition was made last. After treating the melt to achieve the desired level of hydrogen content, the ingots were cast at temperatures ranging from 1275 to 1350 F. Appendix A contains details of the melting process. Each material composition of X2014 and X2219 was cast in a steel book mold coated with a zirconite wash. The mold was rotated through a 75-degree arc as shown in Figures 2A and B to provide minimum turbulence during pouring. After casting, each ingot was radiographed to determine if any defects were present. The ingots

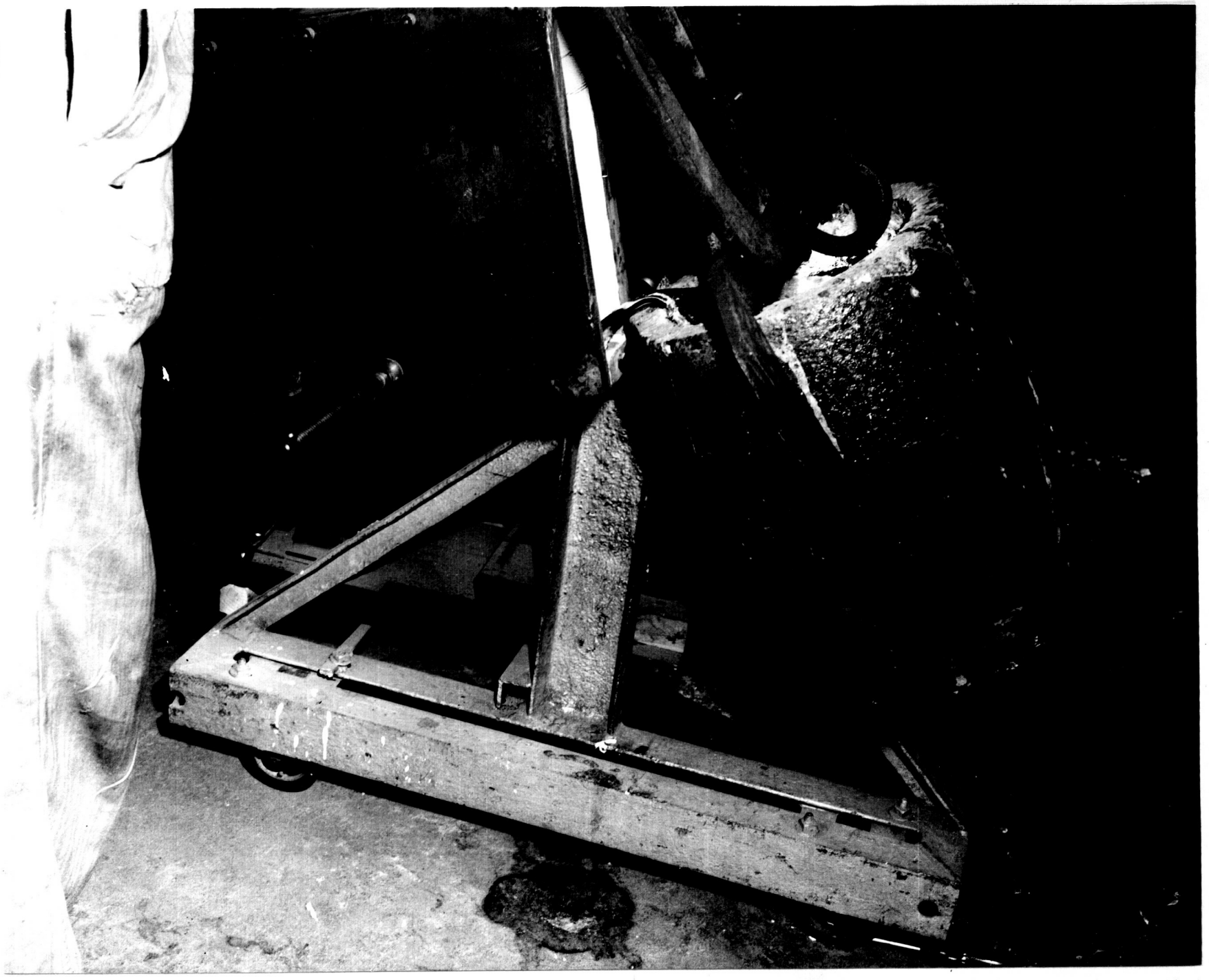

16454

FIGURE 2A. START OF POURING OF INGOT FOR 3/4-INCH-THICK PLATES

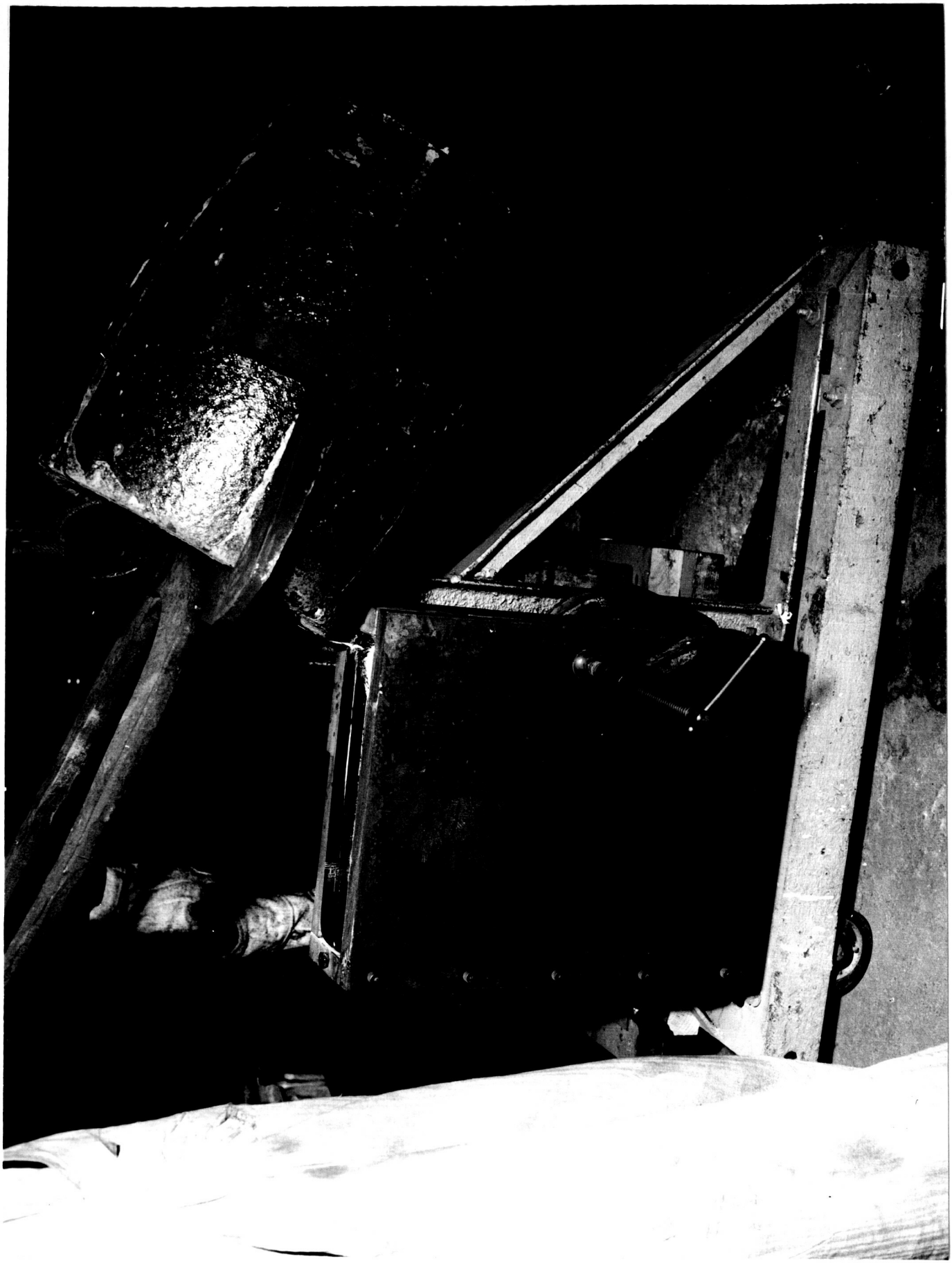

FIGURE 2B. FINISH OF POURING OF INGOT FOR 3/4-INCH-THICK PLATES

16452

used for plate fabrication were all free of radiographically detectable defects.

Hydrogen Content Control

One well-known method for bringing the hydrogen content to a low level in aluminum alloys is to bubble a gas with limited solubility in molten aluminum, generally chlorine, through the molten metal prior to casting. The general explanation for the success of this method is that the gas bubbles form interfaces within the aluminum solution that provide favorable sites for the nucleation and growth of bubbles of hydrogen. The bubbles of hydrogen eventually escape to the atmosphere. Without the introduction of the bubble interfaces, the hydrogen might remain in the molten aluminum alloy.

Control of hydrogen content during this program initially was attempted by means of two procedures:

Low Gas Content: Chlorinate 15 to 20 minutes with a decreasing melt temperature, and cast at a low temperature after a minimum holding time.

High Gas Content: Chlorinate for 5 to 10 minutes at a high temperature, hold a long period at high temperature to promote hydrogen absorption, and cast at a high temperature.

After these procedures were used on half of the X2219 alloys and one-fourth of the X2014 alloys, several modifications were made to control the hydrogen content more directly. These changes were made when vacuum-fusion analyses of samples from the previously cast ingots showed the same average hydrogen

content for alloys cast using the low hydrogen content procedures as for the high hydrogen content procedures. Despite the use of methods of introducing hydrogen to the melt such as playing a fuel gas flame over the surface of the melt or inserting a water-covered rod into the melt (X2014 Type 4 only), the hydrogen analyses of the ingots continued to show that the resulting hydrogen content was not completely controlled by the procedure used. The data contained in Appendix A details the chlorination times, temperatures, and any other treatment of the alloys during melting. The results of the hydrogen content analyses are tabulated in the section on materials analyses.

Base Plate Fabrication

The ingots were prepared for hot rolling by first removing 1 to 2 inches from the ingot top and at least 0.050 inch from the bottom and sides. Samples for the preliminary analyses of hydrogen content were also cut at this time. Figure 3 shows the uniform grain structure of the X2014 ingot tops. After cutting the ingot for the 3/4-inch-thick base plate in half along the length, the ingots were rolled to plate. Figure 4 shows typical ingots prior to rolling. Rolling temperatures were maintained at 850 to 900 F; two to three passes per reheat were made in the rolling mill shown in Figure 5. Surface cracking, particularly in the 3/4-inch-thick plate, necessitated machining of 0.050-inch from the surface of the plates at intermediate stages of fabrication. Figure 6 shows the plates after

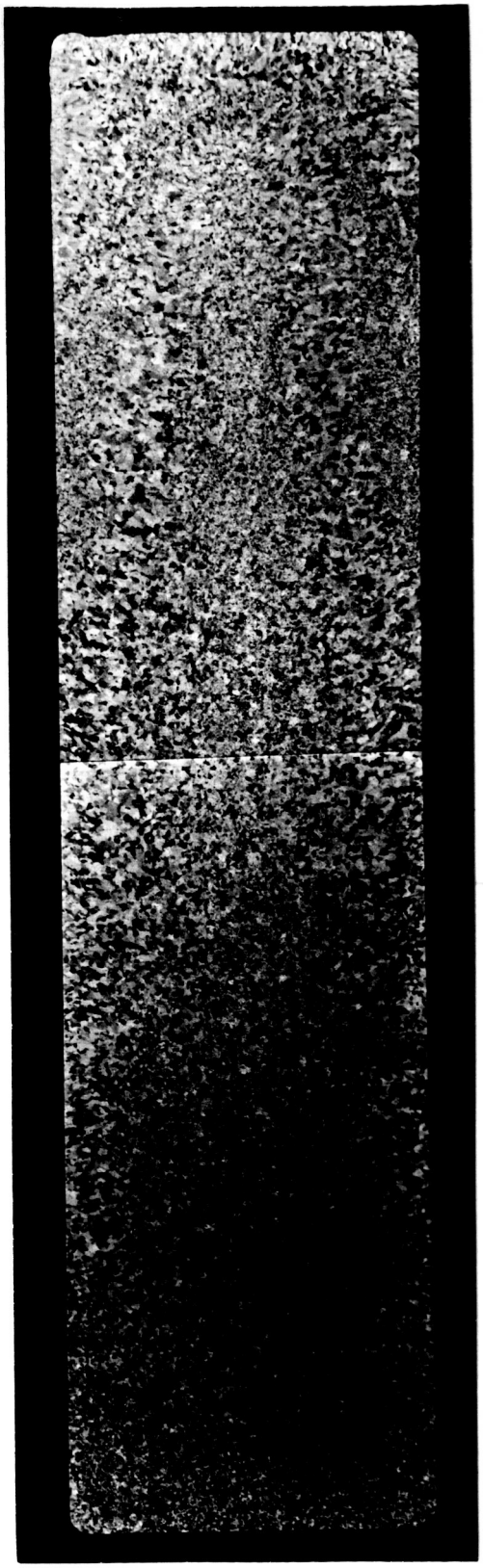

1X Flick's Etch 18128

A. Ingot for 1/4-Inch-Thick Plates

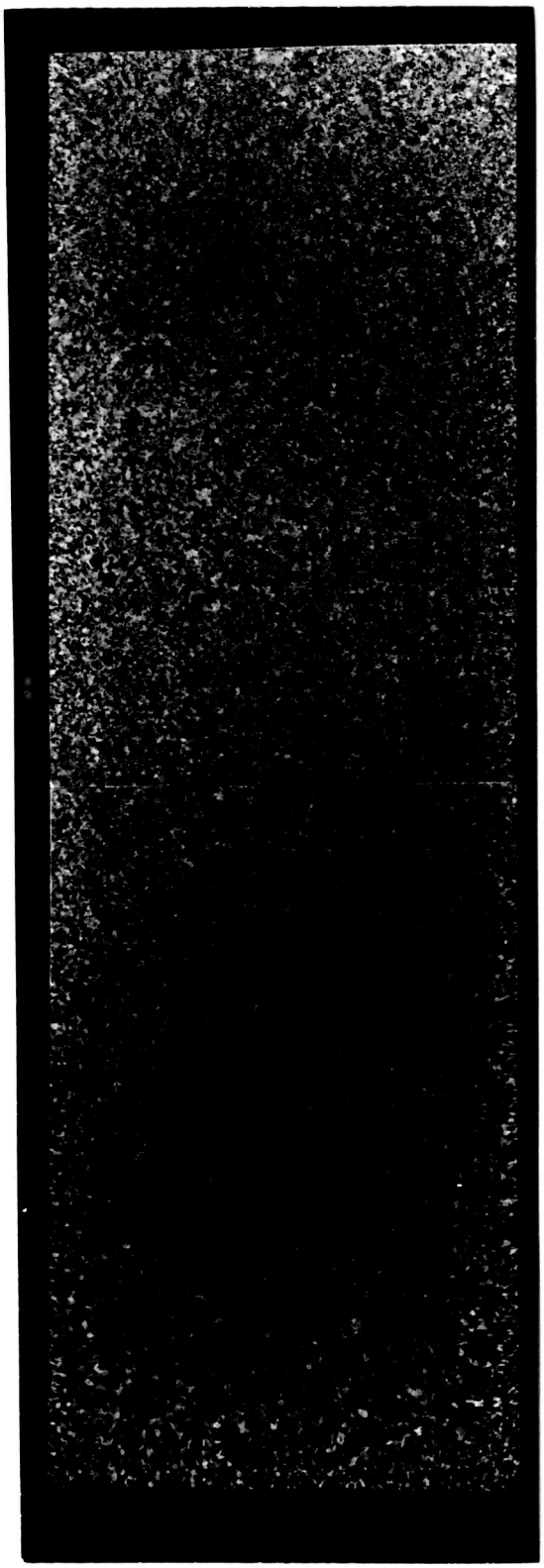

1X Flick's Etch 18130

B. Two-Thirds of Ingot for 3/4-Inch-Thick Plates

FIGURE 3. ETCHED CROSS SECTIONS OF X2014 INGOT TOPS

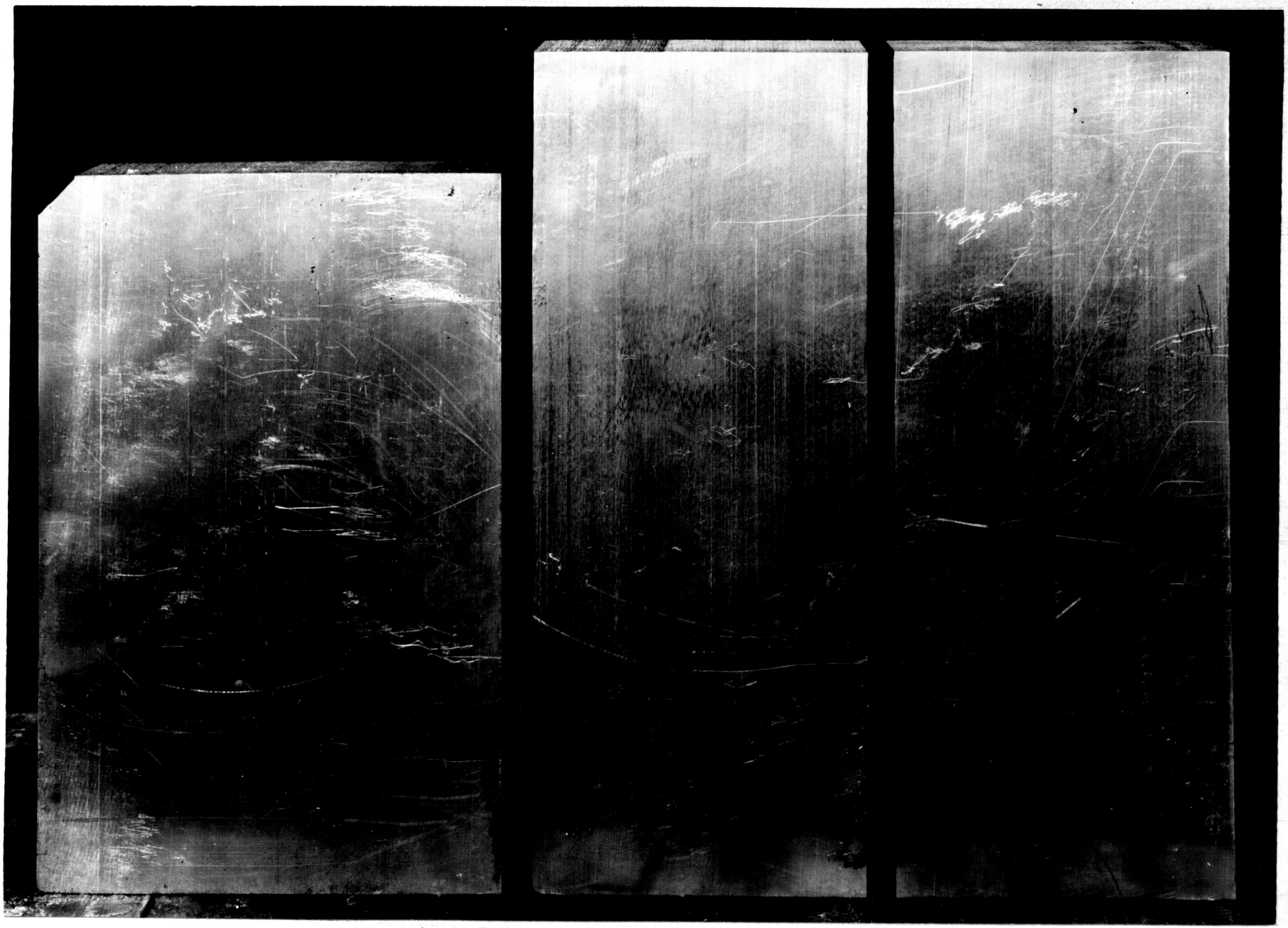

~1/3X

16518

a. Ingot for 1/4-Inch-Thick Plates

b. Ingots for 3/4-Inch-Thick Plates

FIGURE 4. INGOTS AFTER TOPPING, MILLING, AND SECTIONING

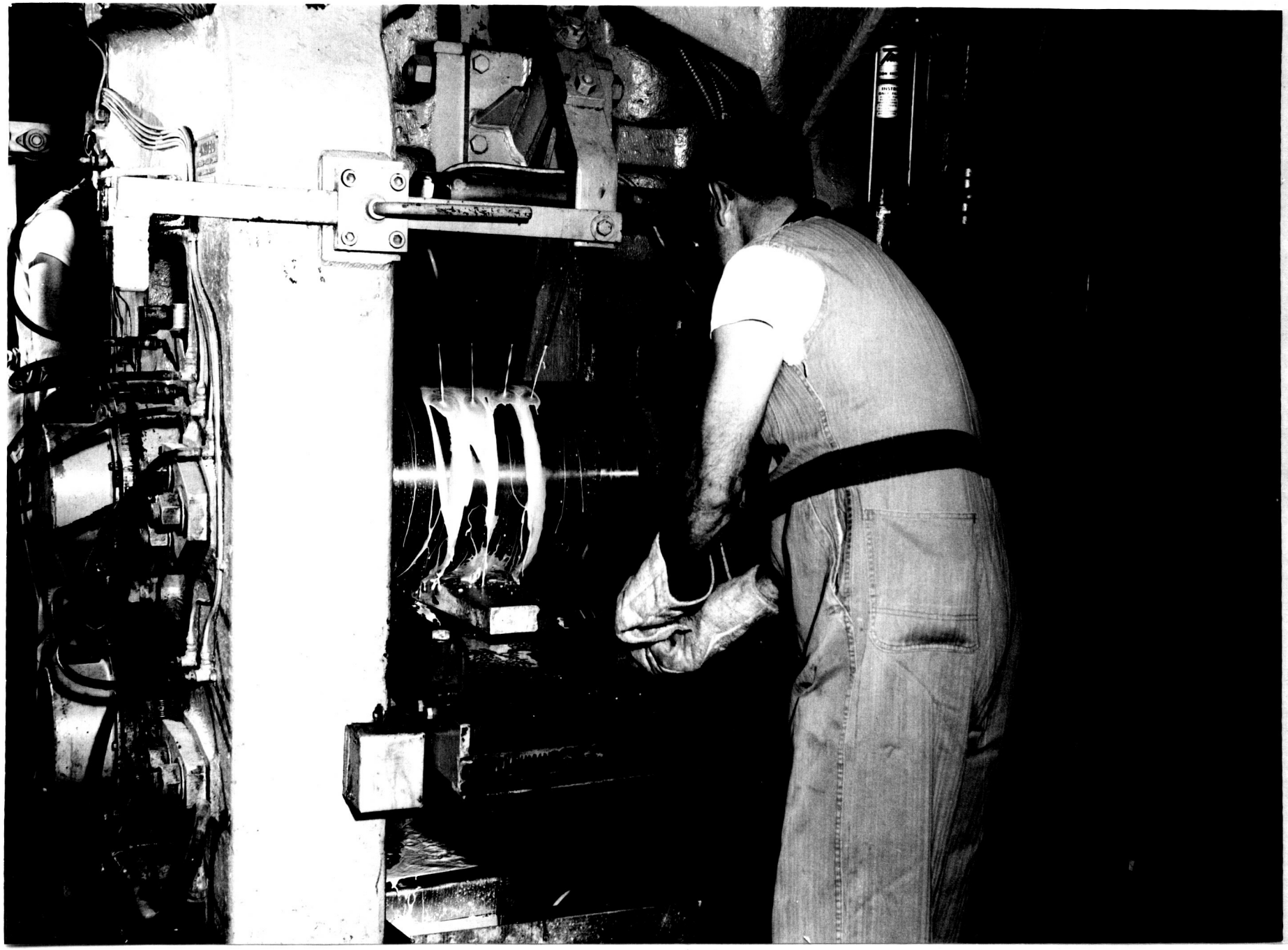

16484

FIGURE 5. SECOND ROLLING PASS ON INGOT FOR 3/4-INCH-THICK PLATE

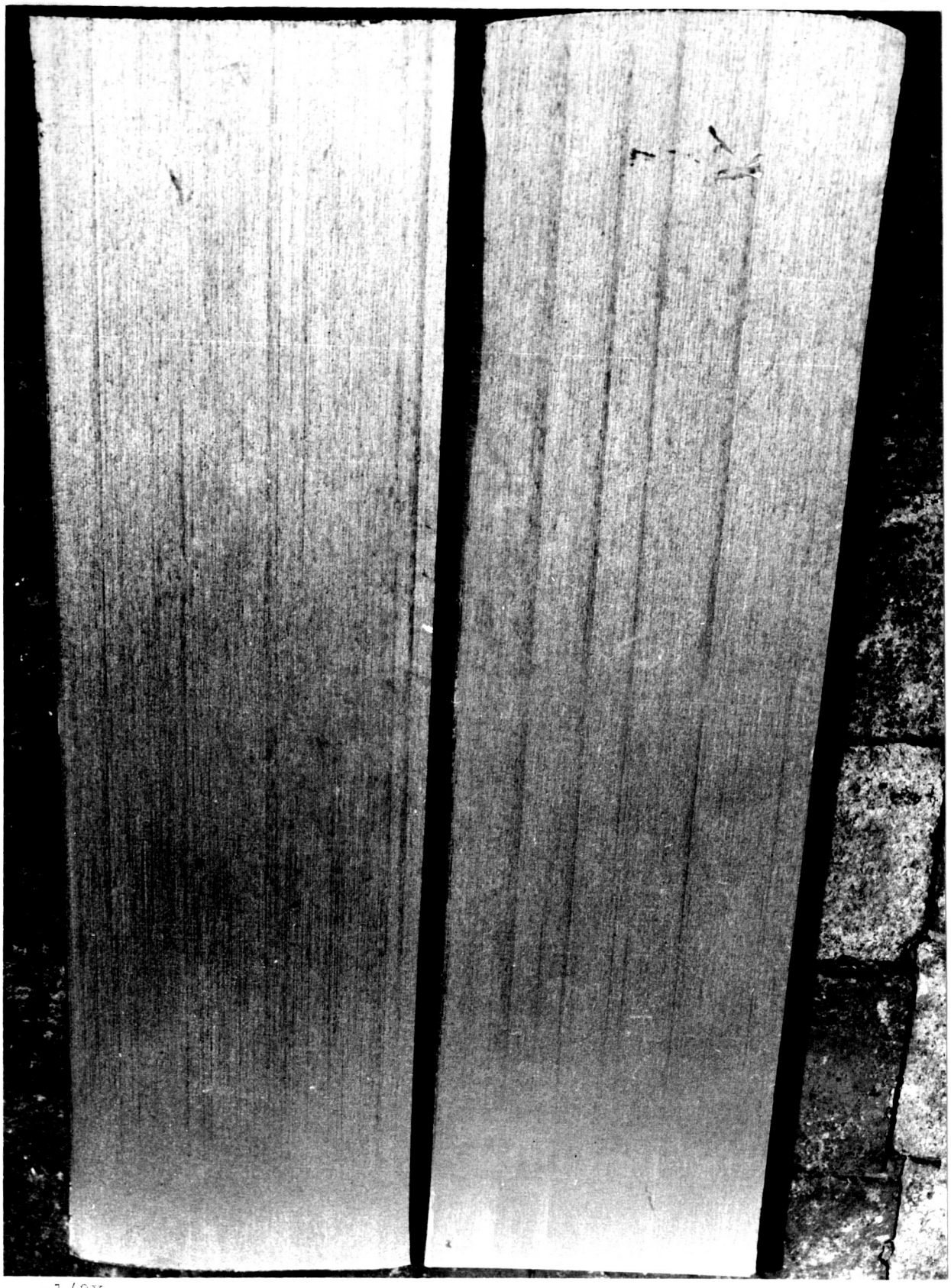

~1/2X

17052

FIGURE 6. PLATE AT INTERMEDIATE STAGE OF FABRICATION AFTER SURFACE MILLING

surface milling. The fabrication of X2014 plate was more difficult than the X2219 plate fabrication because the X2014 plates were more susceptible to surface cracking. Type 4 and Type 7 of X2014 plate cracked so severely during initial fabrication that the plates were remelted and recast. These replacement ingots were successfully fabricated to plate. Appendix A summarizes all of the plate fabrication data.

Heat Treatment

The X2219 plate was heat treated to approximate the T87 temper. The plates were solution annealed for one hour between 980 and 1014 F and then water quenched. The plate was then cold rolled immediately to final size (about an 8% reduction). Finally, the plate was aged 10 hours at 340 F. The X2014 plate was heat treated to approximate the T6 temper. The plates were solution annealed for one hour at 925 to 945 F, water quenched and aged for 10 hours at 340 F. Both the X2219 and X2014 plates were straightened as required by three point bending prior to aging.

Experimental Filler Wire Fabrication

Eight compositions of X2319 and of X4043 filler wire were cast and fabricated to rod at Battelle. The rod was drawn to 1/16-inch-diameter wire by a commercial drawer for use in Phase II.

X2319 Filler Wire

The X2319 ingots were cast as 2 by 8-1/4 by 14-inch ingots. Two compositions were cast from each melt. For example, Types 1 and 4 had the

same chemical content and internal impurity content, but were to have different levels of hydrogen content. The ingot of Type 1 composition was cast after the melt was thoroughly degassed. The remainder of the melt was reheated after the first pouring, treated for high hydrogen content and cast as Type 4. (See Appendix A for the details of the melt preparation.) After machining 0.050 inch from each side and sectioning the ingot into two pieces 2 by 4 by 12 inches, the pieces were preheated for 16 hours at 950 F and upset-forged to form a 12-inch long octagon. The billets were heated to 930 F, then hammer forged to 2-inch-diameter billets. The hammer-forged billets were then reheated to 925 F and rod-rolled to 1.0 inch-diameter round bars with one intermediate reheat. The bars were reheated to 900 F and rod-rolled to 0.625-inch-diameter round bar. Any fins formed during rod rolling were removed by filing and grinding. The bars were reduced to 0.375-inch-diameter rod by cold swaging. After swaging, a commercial firm removed 30 mils from the diameter by a rotating tool-bit process. The removal of the outside surface completely prevented the possibility of fins being present during the wire drawing process, thus preventing surface inclusions in the filler wire.

X4043 Filler Wire

The X4043 was cast in a tapered circular mold which was water cooled. Two compositions were cast from one melt just as the X2319 compositions were (see Appendix A). The round, tapered ingots were about

3-7/8-inch diameter and 12 inches long. The ingot top was removed and the billets were machined to 3.25-inch diameters. The billets were extruded to 0.343-inch-diameter rod at 650 F for low internal impurity compositions and at 750 F for high external impurity compositions. Table 2 illustrates the considerable difference between the extrusion force required for the eight types. The 50-foot lengths of extruded rod were of high-quality surface finish with some extrusion marks along the rod axis.

Wire Drawing

The X2319 and X4043 rod fabricated at Battelle was sent to a commercial drawer of welding wire for the final fabrication to super-clean finished 1/16-inch-diameter wire. The rod was drawn in several passes with up to a total of 3 annealing periods, depending upon the composition type (See Appendix A). The wire with low internal impurities was drawn with fewer anneals. The resulting wire was of good surface finish quality. All wire was inspected by eddy-current techniques. The individual reels were received in sealed, evacuated wrappings and were stored in a controlled low-humidity area until the time of use. The wrapping was first opened no longer than 2 hours before the wire reel was placed in the welding chamber and the chamber was evacuated. The surface quality of the wire as shown in Figure 7 was good with no excessive surface scoring. The wire was consistent in visual appearance from point to point and from reel to reel.

TABLE 2. EXTRUSION CONDITIONS FOR X4043 ROD

Alloy	Billet[a] Temperature, F	Container Temperature, F	Starting Pressure, tons	Comments
1	650	670	400	
4	650	700	375	
7	650	600	500	
5	650	600	450	
3	750	700	520	
2	750	700	525	
6	750	700	475	First attempt to extrude at 650 F failed
8	650	680	650	

(a) Original billet 10 inches long by 3.25-inch diameter extruded to 0.343-inch-diameter rod.

FIGURE 7. COMPARISON OF SURFACE FINISH OF EXPERIMENTAL X2319 FILLER WIRE WITH COMMERCIAL 2319 FILLER WIRE

MATERIAL ANALYSES

All of the materials for the program were analyzed for chemical content, internal impurity content, gas (hydrogen) content, and the presence of any structural defects.

Analysis of Chemical and Internal Impurity Content

The weight percentages of the elements present in all the materials used during the program were determined by a commercial testing laboratory (Laboratory 1). This laboratory melted sections of the samples supplied in an inert gas furnace and chill cast "buttons". Laboratory 1 analyzed all of the samples supplied by spectrochemical analysis except for the copper in X2219, which was determined by wet chemistry methods. Discrepancies were noted between the known amount of copper added during material fabrication and the amount of copper that was reported by Laboratory 1. As a check upon Laboratory 1, samples of X2219 plate and X2319 ingots for Phase II were analyzed by Laboratory 2. Laboratory 2 machined the samples before analysis. Spectrochemical analysis was used for all of the elements except copper and vanadium, which were determined by wet chemical analysis. Because the analyses of the laboratories were quite different for two adjacent X2319 sections having 2-inch diameters and of less than 1/2-inch thickness, the degree of certainty of the chemical analyses was questioned. Subsequent checking showed no definite cause of the differences other than a possible volatilization of magnesium and zinc

by Laboratory 1 during their remelting despite their specific efforts to avoid this occurrence. Thus, the exact composition of the materials used during the program was not determined to a high degree of certainty. Nevertheless, the analyses did definitely determine whether the levels of the chemical content were high or low. For the statistical plan used, the results of the chemical analyses were more than sufficient.

Comparison of the specified alloy compositions in Table 3 to the chemical analyses in Tables 4 through 6 shows that distinct and definite high and low levels corresponding to the statistical plan were achieved for chemical content and internal impurities. In the few cases where one laboratory reported an analysis outside the specified range (those numbers which are underlined in the tables), the second laboratory rarely agreed. The high magnesium content in four of the eight X2319 alloys was as much as 5 times higher than the specifications and resulted from incorrect placement of a decimal point in the melt calculations. The reported analyses that did exceed the specified range were too few, uncertain, and insignificant to justify making new compositions which completely conformed to the material specifications. In addition, it was unlikely that any of the variations from the composition specifications that were encountered during the program could significantly affect the major conclusions drawn. Had the program studied effects of several levels of a few elements upon weld defects instead of two levels of all principal elements, these variations might have detracted from the results.

TABLE 3. SPECIFIED COMPOSITIONS OF THE ALUMINUM ALLOYS STUDIED

Composition, percent by weight											
Military Specification MIL-A-8920A (ASG) for 2219 Aluminum Alloy[b]											
Cu	Mn	Ti	V	Zr	Si	Fe	Mg	Zn	Others, each	Others, total	
5.8-6.8	0.20-0.40	0.02-0.10	0.05-0.15	0.10-0.25	0.20[a]	0.30[a]	0.02[a]	0.10[a]	0.05[a]	0.15[a]	
Aerospace Material Specification AMS 4014 for 2014 Aluminum Alloy[c]											
Cu	Mn	Si	Mg	Fe	Zn	Ti	Cr		Others, each	Others, total	
3.9-5.0	0.4-1.2	0.5-1.2	0.2-0.8	1.0[a]	0.25[a]	0.15[a]	0.10[a]		0.05[a]	0.15[a]	
National Aeronautics and Space Administration, George C. Marshall Space Flight Center Specification M-ME-MPROC-700.1 for 2319 Aluminum-Alloy Wire[d]											
Cu	Mn	Ti	V	Zr	Si	Fe	Zn	Mg	Be	Others, each	Others, total
5.8-6.8	0.20-0.40	0.10-0.20	0.05-0.15	0.10-0.25	0.20[a]	0.30[a]	0.10[a]	0.02[a]	0.0008[a]	0.05[a]	0.15[a]
Aerospace Material Specification AMS 4190A for 4043 Aluminum-Alloy Wire[e]											
Si	Mn	Cu	Fe	Zn	Mg	Ti			Others, each	Others, total	
4.5-6.0	0.05[a]	0.30[a]	0.8[a]	0.10[a]	0.05[a]	0.20[a]			0.05[a]	0.15[a]	

(a) Maximum permissible.
(b) 5-20-63
(c) 6-30-64
(d) 12-4-62
(e) 6-15-52

TABLE 4. CHEMICAL ANALYSES OF X2219 BASE PLATE

Type	Thickness, inch	Laboratory[a]	Analysis[b], percent by weight: Chemical Content Cu	Mn	Ti	V	Zr	Internal Impurities Si	Fe	Mg	Zn
1	1/4	1	6.06	0.20	0.02	0.065	0.13	0.009	0.007	<0.001	0.01
1	3/4	1	5.75	0.20	0.03	0.065	0.12	0.008	0.007	<0.001	0.01
1	3/4	2	5.92	0.27	0.023	0.092	0.093	<0.01	0.013	0.002	0.035
2	1/4	1	5.76	0.25	0.04	0.07	0.13	0.19	0.31	0.007	0.10
2	3/4	1	5.95	0.26	0.04	0.07	0.13	0.20	0.30	0.015	0.10
3	1/4	1	5.76	0.25	0.04	0.07	0.13	0.19	0.32	0.002	0.09
3	3/4	1	5.95	0.26	0.04	0.07	0.13	0.20	0.30	0.004	0.08
3	3/4	2	5.74	0.29	0.023	0.089	0.083	0.18	0.25	0.008	0.085
4	1/4	1	5.81	0.21	0.07	0.13	0.16	0.010	0.007	<0.001	<0.01
4	3/4	1	6.07	0.21	0.08	0.14	0.16	0.009	0.009	0.002	<0.01
4	3/4	2	5.89	0.28	0.023	0.096	0.079	<0.01	0.014	<0.002	0.030
5	1/4	1	5.63	0.37	0.07	0.14	0.23	0.010	0.008	0.001	<0.01
5	3/4	1	6.10	0.37	0.07	0.14	0.21	0.008	0.007	<0.001	<0.01
5	3/4	2	6.57	0.55	0.063	0.19	0.19	0.01	0.026	<0.002	0.056
6	1/4	1	6.72	0.46	0.08	0.13	0.18	0.23	0.37	0.004	0.10
6	3/4	1	6.98	0.43	0.08	0.13	0.19	0.26	0.37	0.008	0.10
6	3/4	2	6.34	0.57	0.071	0.19	0.205	0.25	0.28	0.015	0.115
7	1/4	1	6.21	0.38	0.07	0.13	0.23	0.010	0.007	0.001	<0.01
7	3/4	1	6.05	0.38	0.08	0.14	0.22	0.009	0.007	0.001	<0.01
7	3/4	2	6.51	0.47	0.066	0.19	0.18	<0.01	0.023	<0.002	0.051
8	1/4	1	6.78	0.47	0.08	0.12	0.18	0.23	0.37	0.004	0.10
8	3/4	1	7.08	0.46	0.08	0.13	0.18	0.23	0.37	0.010	0.10
8	3/4	2	6.30	0.46	0.063	0.19	0.17	0.20	0.26	0.017	0.115

(a) Laboratory 1 analyzed samples from the plate at an intermediate stage of fabrication; Laboratory 2 analyzed samples from the fabricated plate.

(b) Underlined numbers are those reported compositions which were not the specified compositions in Table 3.

TABLE 5. CHEMICAL ANALYSES OF X2014 BASE PLATE[a]

Type	Thickness, inch	Analysis[b], percent by weight							
		Chemical Content				Internal Impurities			
		Cu	Mn	Si	Mg	Fe	Zn	Ti	Cr
1	1/4	3.82	0.32	0.46	0.22	<0.01	<0.01	<0.01	<0.006
1	3/4	3.85	0.39	0.45	0.23	<0.01	<0.01	<0.01	<0.006
2	1/4	4.31	0.50	0.62	0.33	0.72	0.34	0.12	0.09
2	3/4	3.82	0.39	0.45	0.23	0.82	0.24	0.14	0.09
3	1/4	4.45	0.50	0.62	0.24	0.73	0.37	0.11	0.09
3	3/4	4.53	0.49	0.58	0.35	0.75	0.20	0.13	0.08
4	1/4	4.31	0.39	0.55	0.26	0.02	<0.01	<0.01	<0.005
4	3/4	4.11	0.48	0.68	0.35	0.03	0.02	0.01	0.003
5	1/4	4.78	0.83	0.99	0.63	0.01	<0.01	<0.01	<0.006
5	3/4	4.90	0.87	1.01	0.72	0.01	<0.01	<0.01	<0.005
6	1/4	4.53	0.80	0.99	0.76	0.82	0.24	0.14	0.09
6	3/4	4.36	0.84	0.94	0.77	0.81	0.24	0.14	0.09
7	1/4	5.00	0.88	1.08	0.73	0.02	<0.01	<0.01	<0.005
7	3/4	4.50	0.83	1.02	0.68	0.04	0.02	0.01	0.003
8	1/4	4.53	0.87	0.87	0.72	0.86	0.22	0.13	0.08
8	3/4	4.53	0.88	0.88	0.76	0.91	0.24	0.13	0.08

(a) Sample taken from plate at intermediate stage of fabrication.

(b) Underlined numbers are those reported compositions which were not the specified compositions in Table 3.

TABLE 6. CHEMICAL ANALYSES OF EXPERIMENTAL FILLER WIRE INGOT[a]

Type	Laboratory	Reported Analysis of X2319[b], percent by weight								
		Chemical Content					Internal Impurities			
		Cu	Mn	Ti	V	Zr	Si	Fe	Zn	Mg
1	1	6.23	0.20	0.09	0.075	0.13	0.06	0.007	<0.01	<0.001
1	2	5.96	0.28	0.088	0.095	0.092	0.032	0.015	0.038	<0.002
2	1	6.48	0.21	0.10	0.08	0.14	0.17	0.26	0.10	0.10
2	2	5.45	0.31	0.10	0.10	0.088	0.18	0.25	0.105	0.105
3	1	5.82	0.20	0.09	0.075	0.14	0.19	0.26	0.13	0.05
3	2	5.93	0.35	0.11	0.099	0.069	0.24	0.31	0.115	0.076
4	1	5.32	0.20	0.13	0.085	0.14	0.02	0.007	<0.01	<0.001
4	2	5.52	0.27	0.12	0.10	0.08	0.026	0.018	0.03	<0.002
5	1	6.05	0.36	0.19	0.15	0.23	0.01	0.007	<0.01	<0.001
5	2	6.27	0.53	0.14	0.17	0.165	0.012	0.02	0.044	<0.002
6	1	5.82	0.20	0.09	0.075	0.14	0.19	0.26	0.13	0.05
6	2	6.32	0.55	0.18	0.19	0.15	0.18	0.25	0.13	0.05
7	1	6.01	0.39	0.19	0.16	0.24	0.01	0.008	<0.01	<0.001
7	2	6.54	0.56	0.17	0.18	0.125	0.014	0.026	0.049	<0.002
8	1	6.05	0.39	0.15	0.15	0.23	0.20	0.35	0.14	0.04
8	2	6.30	0.60	0.17	0.19	0.12	0.19	0.29	0.125	0.115

		Reported Analysis of X4043, percent by weight						
		Chemical Content	Internal Impurities					
		Si	Mn	Cu	Fe	Zn	Mg	Ti
1	1	4.89	<0.005	<0.001	<0.002	<0.01	<0.002	<0.005
2	1	5.08	0.039	0.20	0.70	0.10	0.036	0.17
3	1	4.99	0.039	0.20	0.69	0.10	0.050	0.17
4	1	4.89	<0.005	<0.001	<0.002	<0.01	<0.002	<0.005
5	1	5.68	<0.005	<0.001	<0.002	<0.01	<0.002	<0.005
6	1	5.80	0.037	0.19	0.69	0.10	0.053	0.15
7	1	5.73	<0.005	<0.001	<0.002	<0.01	<0.002	<0.005
8	1	5.74	0.038	0.19	0.70	0.10	0.047	0.15

(a) Underlined numbers are those reported compositions which were not the specified compositions in Table 3.

(b) Samples of X2319 sent to the two laboratories were adjacent cross-sections from ingots.

Commercial Base Plate

Specimens chosen at random from the commercial base plate used during Phase II were chemically analyzed. The results are shown in Table 7.

Gas Content Analysis

The hydrogen content of the material compositions studied was measured by the Battelle vacuum-fusion methods discussed in Appendix B. A 5 to 15-gram sample of the material to be analyzed was abraded to remove the sample surface layer and cleaned. After exposure to ambient conditions for 25 minutes, the abraded sample was placed in the vacuum-fusion apparatus. A molten tin bath in the apparatus was held at 1200 F while the apparatus was vacuum-purged. The sample was then dropped into the tin bath and the released gases were collected and measured. The collected gas was circulated through hot copper oxide, which oxidized any hydrogen present to water vapor. The hydrogen in the form of water vapor was frozen in a cooling section and the resulting drop in pressure of the collected gas sample indicated the amount of hydrogen present. After correction for the moisture on the surface of the abraded specimen and the blank rate of the measurement apparatus, the internal hydrogen content was calculated. The total hydrogen content (corrected for blank rate) only was determined for the filler wire. The total hydrogen contents are suitable for statistical analysis because the surface correction factor is

TABLE 7. CHEMICAL ANALYSES OF COMMERCIAL BASE PLATE USED FOR PHASE II

Lot	Plate Thickness, inch	Analysis of 2219 Base Plate, percent by weight								
		Chemical Content					Internal Impurities			
		Cu	Mn	Ti	V	Zr	Si	Fe	Zn	Mg
9535-9653-738	1/4	6.29	0.32	0.08	0.09	0.13	0.14	0.26	0.02	0.01
9535-9653-738	1/4	6.34	0.31	0.08	0.09	0.13	0.14	0.26	0.02	0.01
9535-9653-738	1/4	6.25	0.31	0.08	0.09	0.13	0.14	0.27	0.02	0.01
9535-781-6410	3/4	6.07	0.30	0.09	0.09	0.13	0.13	0.24	0.01	0.007
9535-781-6410	3/4	6.20	0.31	0.08	0.10	0.14	0.12	0.24	0.01	0.007
9535-781-6410	3/4	6.14	0.30	0.08	0.10	0.14	0.13	0.27	0.01	0.007

		Analysis of 2014 Base Plate, percent by weight							
		Chemical Content				Internal Impurities			
		Cu	Mn	Si	Mg	Fe	Zn	Ti	Cr
9535-766085	1/4	4.51	0.88	1.12	0.53	0.37	0.02	0.025	0.01
9535-766085	1/4	4.61	0.88	1.18	0.55	0.39	0.02	0.025	0.01
9535-9752719	3/4	4.69	0.75	0.99	0.52	0.38	0.02	0.040	0.01
9535-9752719	3/4	4.63	0.75	0.96	0.53	0.36	0.02	0.040	0.01

essentially constant for each alloy. Tables 8 through 10 record the reported hydrogen content for the materials used during the program.

Ultrasonic Inspection

All of the experimental base plates for Phase I were inspected for structural defects under Class A of MSFC-SPEC-283 (12-10-63). Class A is the more rigorous of the two classes in the specification. Each plate was inspected for structural defects to within at least an inch of the plate edges. Inspection of the edges was difficult (because of ultrasonic edge effects) and unnecessary because the welds were not located at the edge of the plates. The results of the ultrasonic inspection are listed in Table 11. All X2219 plate was accepted under Class A. Some small indications were detected, but they were not of significant size. The inspection of the X2014 plate reflected the surface-cracking difficulties encountered during fabrication. Several plates were unacceptable under the Class A standard. The location of all defects of significant size was clearly marked on the plate surfaces to prevent any study or analysis of weld defects which did not consider the presence of the ultrasonically located plate defect. None of the weld sections studied for the statistical analysis were taken at the location of defects found during the ultrasonic inspection.

TABLE 8. VACUUM-FUSION ANALYSES OF X2219 AND X2014 BASE PLATE

Type	Thickness, inch	Internal H_2 Content, ppm by weight	
		Ingot	Fabricated Plate[a]
		X2219 Base Plate	
1	1/4	0.2	0.1
1	3/4	0.2	0.3
2	1/4	0.7	0.8
2	3/4	--	0.5
3	1/4	0.6	0.6
3	3/4	--	0.5
4	1/4	0.5	0.3
4	3/4	0.2	0.1
5	1/4	0.4	1.1
5	3/4	0.4	0.7
6	1/4	1.1	0.5
6	3/4	--	0.4
7	1/4	0.2	0.1
7	3/4	0.2	0.1
8	1/4	0.6	0.7
8	3/4	--	0.5
		X2014 Base Plate	
1	1/4	0.8	0.3
1	3/4	--	0.3
2	1/4	0.6	0.7
2	3/4	--	1.9
3	1/4	3.1	0.4
3	3/4	--	0.7
4	1/4	0.2	0.4
4	3/4	0.2	1.8
5	1/4	0.5	0.6
5	3/4	0.5	0.5
6	1/4	0.9	0.8
6	3/4	--	0.7
7	1/4	1.0	0.5
7	3/4	0.7	0.3
8	1/4	0.6	0.9
8	3/4	--	0.8

(a) Samples taken from plate edge midway between the ends.

TABLE 9. VACUUM-FUSION ANALYSES OF EXPERIMENTAL FILLER WIRE[a]

Type	H_2 Analysis, ppm by weight	
	Ingot[b]	Wire[c]
	X2319 Filler Wire	
1	0.3	1.4
2	0.4	1.7
3	1.2	2.5
4	0.3	3.1
5	0.9	3.4
6	0.7	2.5
7	0.3	1.5
8	0.2	2.0
	X4043 Filler Wire	
1	0.2	1.5
2	0.3	1.8
3	0.3	2.5
4	0.4	4.0
5	0.4	2.4
6	0.1	1.8
7	0.6	2.2
8	0.4	2.9

(a) Wire sample was adjacent to last weld made using the wire.

(b) Internal hydrogen content.

(c) Total hydrogen content (internal plus surface correction factor).

TABLE 10. VACUUM-FUSION ANALYSES OF COMMERCIAL BASE PLATE USED FOR PHASE II

Specimen	Thickness, inch	Internal Hydrogen Content, ppm by weight
	2219-T87 Base Plate	
1	1/4	0.1
2	1/4	0.2
3	1/4	0.4
4	3/4	0.1
5	3/4	0.1
6	3/4	0.1
	2014-T6 Base Plate	
1	1/4	0.6
2	1/4	0.4
3	3/4	0.9
4	3/4	0.5

TABLE 11. RESULTS OF ULTRASONIC INSPECTION OF EXPERIMENTAL BASE PLATE[a]

Alloy	Type	Sample Number 1	2	3	4	6	7	8	9
X2219	1	A	A	A	A	A	A	A	A
X2219	2	A	A	A	A	A	A	A	A
X2219	3	A	A	A	A	A	A	A	A
X2219	4	A	A	A	A	A	A	A	A
X2219	5	A	A	A	A	A	A	A	A
X2219	6	A	A	A	A	A	A	A	A
X2219	7	A	A	A	A	A	A	A	A
X2219	8	A	A	A	A	A	A	A	A
X2014	1	A	R	A	A	R	R	R	R
X2014	2	A	A	A	-	R	R	R	R
X2014	3	A	A	A	-	A	A	A	A
X2014	4	A	A	A	R	R	R	A	A
X2014	5	A	A	A	A	A	A	A	A
X2014	6	R	A	A	R	A	A	A	A
X2014	7	R	A	A	A	R	R	A	A
X2014	8	A	A	A	A	R(b)	R(b)	R(b)	R(b)

(a) All plate accepted (A) or rejected (R) under requirements for Class A of MSFC-SPEC-283 (12-10-63).

(b) Rejected because of lamination.

WELDING

A total of 192 three-foot long bead-on-plate welds were welded using experimental materials. In addition, another 400 welds, which were not part of the statistical plan, were made to establish welding conditions and to evaluate the effects of the shielding gas dewpoint, tungsten electrode shape, and other factors.

Equipment

All welding was performed in an 8-foot long, 30-inch-diameter vacuum-purged chamber. The use of the chamber prevented variables such as drafts, ambient humidity, and the relative position of the shield to the electrode tip from influencing the test results. In all cases, the chamber was evacuated to a pressure of 10 microns of mercury or lower before back filling. The chamber was pumped a minimum of 12 hours at 10 microns or less before each series of test welds.

Figure 8 shows the welding chamber and a portion of the equipment used during the program. Appendix C lists the specific equipment used. At the far left in the photograph is one of the two precision (±0.25% accuracy) recording electronic millivolt potentiometers used to record arc voltage, arc current, travel speed, and filler wire speed. The recorder is mounted above the equipment cabinet for the automatic voltage-regulating welding head.

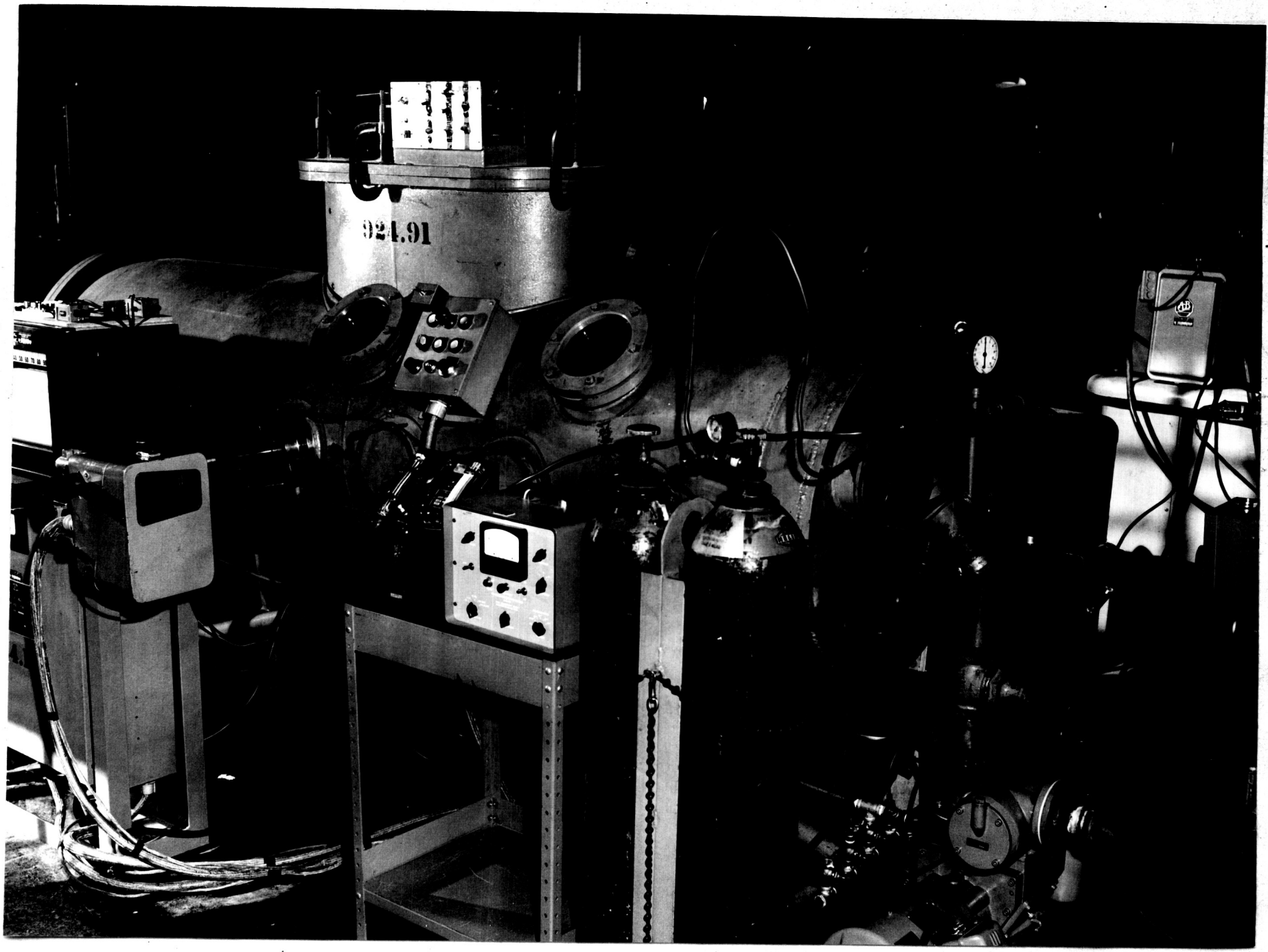

14723

FIGURE 8. WELDING CHAMBER AND A PORTION OF THE WELDING EQUIPMENT AND INSTRUMENTATION

The automatic voltage-regulating head was used during gas-tungsten-arc welding with d-c straight polarity. The head was located in the horizontal position outside the chamber. The torch inside the chamber was connected to a shaft which passed through a vacuum seal to the voltage-regulating head.

The plates were clamped horizontally in a work holder with provision for minimum heat sink during the bead-on-plate welding. The work holder was driven by a machine-screw connected to a variable speed motor.

During Phase II a pull-type wire feeder fed 1/16-inch-diameter filler wire in the forehand position at 3 to 4o'clock in the weld pool.

Additional comments on the equipment are given in Appendix C.

Instrumentation

Accurate instrumentation of the experimental setup for the welding program was initially felt to be essential to minimize experimental error. All recorders used during the welding of experimental materials had ±0.25% accuracy. The actual recorder accuracy was thus well under the maximum limits of accuracy imposed upon the program. Table 12 compares the specified and actual instrumentation accuracy. All shunts, voltage dividers, and recorders were calibrated periodically against at least secondary standards of the U. S. Bureau of Standards.

TABLE 12. COMPARISON OF SPECIFIED[(a)] AND ACTUAL INSTRUMENTATION ACCURACY

Accuracy	Arc Voltage, volts	Arc Amperage, percent	Arc Travel, inch/minute	Wire Feed, percent
Specified	±0.1	±1.0	±0.1	±3.0
Maximum Actual	±0.03	±0.6	±0.03	±0.03

(a) Specified by the Sponsor, NASA, George C. Marshall Space Flight Center.

Appendix D details the descriptions of the recording electronic millivolt potentiometers and the tachometer generators used during the program. In addition, Appendix D contains a discussion of the characteristics necessary to fully describe a recording system.

Arc Current

The arc current was measured during Phase I across a precision 200 ampere - 50 millivolt shunt that was located along one power lead. During Phase II, a precision 300 ampere-50 millivolt shunt was used. The shunts were calibrated prior to use. These shunt values were selected so that the recordings were made close to full scale on the recorder. Small variations within the current were more easily detected by placing the recording level close to the full scale level.

Arc Voltage

The arc voltage leads were connected directly to the work and to the tungsten electrode. The arc voltage leads passed through a precision calibrated 1500 to 1 voltage divider. The lower ratio voltage was supplied directly to the input of a recorder.

Travel Speed

The travel speed of the work was measured by a generator-tachometer mounted directly on the drive shaft of the drive motor. The

tachometer was located before the 10 to 1 worm gear speed reducer which was mounted in the motor housing and before the 5 to 1 worm gear speed reducer mounted beyond the output shaft of the drive motor. The speed limitations of the tachometers available and the chamber configuration made measurement of the travel speed more directly than this setup quite difficult. The speed of the motor drive closely reflected that of the travel speed since worm gear speed reducers and metallic couplings were used. The output voltage of the generator tachometer passed through a precision 2000 to 1 voltage divider. The lower ratio voltage was supplied directly to a recorder input.

Filler Wire Speed

During Phase II, the addition of filler wire required measurement of the filler wire speed. Because the travel speed recordings showed no extreme variations during Phase I, a timer-relay was installed to alternate signals from the travel speed and the wire speed tachometers. The wire speed was recorded 50 seconds of every minute while travel speed was recorded the remaining 10 seconds.

The filler wire speed was recorded at a point between the wire feeder and the reel. The wire was used to drive a pressure roll to which a precision (0.0002-inch tooth-to-tooth composite error) 48 pitch gear was mounted. The gear on the pressure roll drove a second gear on a generator-tachometer shaft at five times the rotational speed of the pressure

roll. The output of the generator-tachometer passed through a 2000 to 1 voltage divider. The lower ratio voltage was supplied directly to the recorder input.

Trial Welds

Welds other than those used in the statistical plan were made to establish welding conditions, to evaluate the effects of surface contaminants, to evaluate the effects of electrode shapes, and to determine the effect of moisture-contaminated helium upon arc voltage and arc amperage.

Establishment of Welding Conditions

The values of arc voltage, arc current, travel speed, and filler wire speed were established at levels approximating those used at NASA-MSFC for the same materials. The final conditions were determined by the amount of undercut (first priority), the amount of penetration (second priority), and the weld contour. During Phase I full penetration was not achieved on either thickness of the two experimental alloys. During Phase II, full penetration was achieved with 1/4-inch thick 2219 and 2014 base plates. Undercut was generally negligible and never was above 4% of the plate thickness when it occurred. The welding conditions established for the program are summarized in Table 13.

Effect of Surface Contaminants

The method of controlling the factor of external impurities for the statistical plan was established after the evaluation of welds made on

TABLE 13. WELDING CONDITIONS[a] ESTABLISHED FOR PROGRAM

Base Plate	Arc Voltage, volts	Arc Amperage, amperes	Work Travel, inches/minute	Wire Speed, inches/minute
		Phase I		
1/4-Inch-Thick X2219-T87	13.5	140	11.2	--
1/4-Inch-Thick X2014-T6	13.5	145	11.2	--
3/4-Inch-Thick X2219-T87	13.5	170	11.2	--
3/4-Inch-Thick X2014-T6	14.1	220	11.2	--
		Phase II		
1/4-Inch-Thick 2219-T87	13.5	180	11.2	64
1/4-Inch-Thick 2014-T6	13.5	180	11.2	64
3/4-Inch-Thick 2219-T87	13.5	280	11.2	64
3/4-Inch-Thick 2014-T6	13.5	280	11.2	64

(a) DC straight polarity gas tungsten-arc welding.

plates with different surface treatments. The intent of the search for a method of controlling external impurities was to select a controllable (and measurable) process for reproducing external impurities such as surface oxides which are encountered during production welding. The objective was also to find a method which would consistently produce fine, evenly spaced pores which would increase either in frequency or size, or both, for high weld defect potential weld materials and decrease for low weld defect potential materials.

The first methods studied boiled plates in water for up to 30 minutes. This treatment was then followed up by exposure to air for as long as 48 hours. The radiographs of the welds made on this plate after surface preparation showed two small widely-separated pores. The excessive oxide layer formed during boiling made welding difficult.

The next method studied thick coats of vacuum pump and diffusion pump oils which were applied over two clean plates. These low-vapor pressure oils yielded irregular amounts of large pores visible in radiographs. Thin coatings of oil-acetone mixtures of up to 75% oil on clean plates also yielded no radiographically visible porosity.

The third method studied was to machine grooves, holes, or notches in plate surfaces in such a way that the water vapor driven off by the heat of welding would be trapped in the groove, hole, or notch until it was brought into the molten weld pool. In addition, this method increased the plate surface area to volume ratio. The plates were boiled

as long as 3 minutes after exposure to air at 75 F in 100 percent humidity for 1 hour. After boiling, the plates were exposed to ambient air for 20 hours before being welded. No radiographically visible pores occurred.

A material (ball clay) with a high temperature for the release of water of hydration was dusted over the surfaces of several plates. No porosity was observed in radiographs of the welds.

Water Addition to Shielding Gas

Because none of the previous techniques studied had yielded controllable porosity, the effects of moisture added to the helium shielding gas were studied. Moisture was added to the helium as the controlled-atmosphere chamber was backfilled. The helium passed through a heated aspirator bottle into which a measured volume of distilled water had been placed. The water evaporated in the helium flow long before the chamber backfilling was complete. The dewpoint of the chamber atmosphere was measured by a standard dewpointer after the lines and instrument had been well purged with the moisture-containing helium atmosphere. Dewpoints determined before and after the first and succeeding welds showed a substantial dewpoint increase after the first weld and constant dewpoint readings during the succeeding welds. Accordingly, a weld was made on scrap plate prior to beginning welding tests so that the atmosphere was thoroughly mixed.

Dewpoint Evaluation. The dewpoints initially investigated ranged from -60 F (no moisture addition) to +40 F*. Pores were not visible

*A dewpoint of -60 F results from a moisture content of about 0.0055 percent by volume; 0 F from 0.150 percent.

in radiographs or microscopic sections of the welds until the dewpoint was about -10 F. As the dewpoint increased above -10 F, the number and size of pores increased. Replications of welds made at the same dewpoint in different atmospheres showed that this method of porosity control was reasonably reproducible. However, the distribution of pores throughout the bead-on-plate welds was uneven despite the precise regulation of the welding variables and the use of commercial base plate.

The use of moisture additions to the shielding gas was selected as the best method studied for achieving controllable and consistent pore formation. The external impurity of moisture addition was also felt to be the most realistic method studied since porosity caused by insufficient shielding gas protection, leaks in the water-cooling system of the welding torch, aspiration of humid air in shielding gas line leaks, or moisture contamination of the shielding gas cylinder can be encountered in welding practice.

Selection of Phase I Dewpoint Level. The dewpoint level for welding during Phase I was selected on the criterion that the high dewpoint level was to produce fine scattered porosity in radiographs of bead-on-plate welds with no filler wire addition. The final high dewpoint levels selected were +10 F for the X2219 base plate and +6 F for the X2014 base plate for high external impurities and -60 F (no moisture addition) for low external impurities with both alloys.

Selection of Phase II Dewpoint Level. The dewpoint level for welding during Phase II was selected on the criterion that the dewpoint was to be just above the porosity threshold so that fine pores were microscopically visible in a weld section. The sections of the bead-on-plate welds with filler wire addition showed that the threshold for microscopically visible pores ranged from -20 to -10 F for welds made on both thicknesses of 2014 plate with X4043 filler wire and of 2219 plate with 2319 filler wire. The dewpoint level selected for Phase II was fixed at the single level of -3 F in accordance with the revised statistical plan.

In practice, the dewpoints measured during the experimental welding generally ranged ±5 F from the selected level despite the use of a standard volume of water addition. The variations from weld to weld were quite small except during Phase II where the dewpoint consistently dropped 1 to 2 F between each weld. The drop during Phase II welds was ascribed to the "gettering" of moisture by the large amount of finely divided metallic vapor released when both filler and base metal were melted. Some of the variation between the values measured was, no doubt, due to the error of the dewpointer whose accuracy was approximately ±2 F.

Effect of Electrode Shape. The most difficult problem during the establishment of welding conditions for both phases was the stabilizing of the arc voltage and arc current to variations within the values specified in Table 14. The equipment used throughout the program was capable of operating well within these specified variations. However, the arc

TABLE 14. SPECIFIED[(a)] MAXIMUM ARC VARIATIONS

Welding Variable	Maximum Variations
Arc Voltage	±0.3 volts
Arc Current	±1.0%
Travel Speed	±0.1 inches/minute
Filler Wire Speed	No specification

(a) Specified by Sponsor, NASA, George C. Marshall Space Flight Center.

instability in the moisture-contaminated shielding gas was observed to increase with increasing dewpoint.

During the evaluation of surface contaminants, welds were made on thickly oiled plates. On one plate, the voltage recording showed the initial variation of ±0.25 volts abruptly dropped to ±0.03 volts in the middle of the weld and continued to be low until the end of the weld. Inspection of the electrode showed that the tip, which had been ground to a 30° included angle, had melted off and the electrode after welding had a hemispherical tip. A radiograph of the weld located a large tungsten inclusion at the point where the voltage variations abruptly dropped. In addition, the visual appearance of the weld length before the tungsten tip melted was rougher than the last portion of the weld.

A series of tests then were run in shielding gas with no moisture additions to determine if the electrode shape had any relation to the arc stability. The electrode shapes studied ranged from a square blunt end to hemispherical ends to 45° included angles. Arcs were generally more stable with blunt electrode tips. The results of the tests indicated that 3/32-inch-diameter 1 percent thoriated tungsten electrode gave the most stable arc when a 15° taper was used to bring the electrode diameter to 1/16 inch and the point was then formed at a 45° included angle. This shape was used throughout the program.

Effect of Moisture on Arc Waveforms. During all welds made in moisture-contaminated shielding gas, the recordings of the arc voltage and amperage were observed to change from the start of the weld. The

arc voltage and arc amperage recordings remained stable at first and then gradually grew more unstable. This same behavior has been observed on recordings from Martin-Denver which were made during the addition of hydrogen to the arc under Contract NAS8-11335.

An oscilloscope was used to monitor the arc voltage and amperage waveform during welding with dry helium (-60 F) and moisture-contaminated helium (+10 F). The waveforms during welding in dry helium did not change but remained regular and periodic during 5 minutes of continuous welding. With moisture in the shielding gas, significant changes occurred in the waveform. Initially, the voltage and amperage waveforms were similar to those previously observed. Within 45 seconds after the start, a small amplitude peak became superimposed on the voltage waveform at the same frequency as the voltage waveform. The voltage waveform continued to grow more distorted and subject to sharp spikes or inflection points until the weld ended (as shown in Figure 9). The current waveform never changed shape, but spikes began occurring within 165 seconds after the weld started and continued to become more severe. It was also noted that after the spikes had been observed in a waveform that the spikes would appear without a time lapse after the arc had been shut off for a period of time and then restarted. Replacing the old tungsten electrode with a freshly ground electrode caused the spikes to occur only after a time delay as originally observed. Apparently, the tungsten electrodes were "contaminated" in such a manner that regrinding was necessary to remove the "contamination".

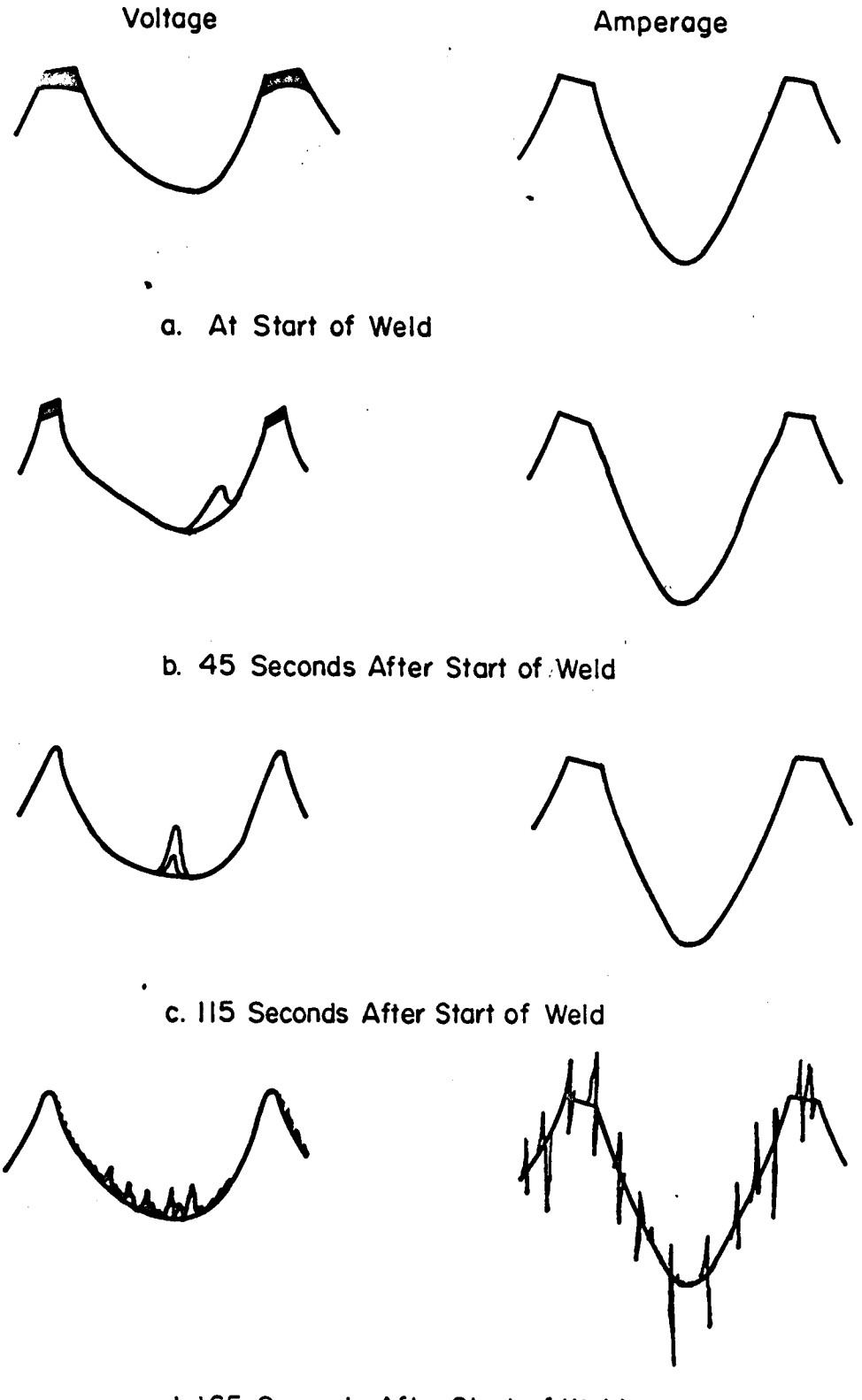

FIGURE 9. VARIATION OF ARC WAVEFORMS FOR CONTAMINATED HELIUM

Program Welding

Prior to welding, all of the base plate used in the statistically planned program was vapor-degreased and then alkaline- and acid-etched until all visible surface dirt and inhomogeneous surfaces were removed. The resulting plates were bright and showed no water marks. Table 15 contains the plate cleaning specification prepared for the program. After cleaning and during loading into the chamber, the plates were handled with white gloves and at the edges only. The cleaned plates were never allowed to be exposed to the atmosphere more than 1-1/2 hours before they were placed inside the welding chamber and the chamber was evacuated. Inside the chamber, the plates were handled by their edges only prior to welding to avoid surface contamination by the rubber gloves. Welding was performed only after the chamber had been evacuated to 10 microns or less for a minimum of 12 hours.

Welding During Phase I

The 126 three-feet long experimental welds for Phase I were made over a 6-week period. Welds were deposited in the middle of the 4 by 36 by 1/4-inch-thick experimental base plate on one side only along the rolling direction. Two welds were deposited on opposite sides at the one-third and two-third points of the 6 by 36 by 3/4-inch-thick experimental base plate. Generally, 8 separate welds were made for each backfilling. The low dewpoint atmospheres for Phase II were obtained by

TABLE 15. SPECIFICATION FOR BASE PLATE CLEANING

1. Vapor-degrease all samples.
2. Remove remaining grease or dirt marks with acetone.
3. Cleaning bath procedure:

   Alkaline Etch - 40 grams sodium hydroxide + 1-liter water

   Temperature: room; immersion time: 1 to 2 minutes after uniform gassing on surface; rinse: hot, running tap water for 2 minutes.

   Acid Etch - 1-liter nitric acid ($42^{o}Be'$) + 1-liter water

   Temperature: room; immersion time: 15 to 30 seconds; rinse: hot, running tap water for 2 minutes; dry in air, avoid water spots.

4. Standard practices:

   a. Mix new alkaline solution for each six plates cleaned.

   b. Place plates in chamber for vacuum purging as soon as possible. Allow no more than 1-1/2 hours between cleaning and vacuum purging.

   c. Repeat cleaning procedure if plate surface is not uniformly bright.

backfilling the chamber directly from a helium cylinder through a vacuum-purged line. High dewpoint atmospheres were obtained by backfilling the chamber with helium which passed through a heated aspirator bottle containing a fixed amount of distilled water that evaporated completely during backfilling. All of the plates of the same composition type were welded in the same atmosphere in a random order. A freshly ground tungsten electrode was used for each weld. Dewpoint determinations were taken before and after each weld.

The work travel speed varied less than ±0.05 inch per minute throughout most of the welds. The arc voltage was ±0.2 voltfor most of the welds made at low dewpoint and ±0.45 volt for most of the welds made at a high dewpoint. Arc current similarly ranged up to ±0.5% to ±1.5% for most of the welds made at high dewpoint. These variations reflected the more severe arc fluctuations which occur when moisture is present within the arc shielding gas even when accurate and precision welding equipment is used. Figure 10 compares typical recordings for welds made at high and low dewpoints.

Weld Appearance. Figure 11 shows the overall appearance of welds made during Phase I on X2219 base plate at low dewpoints. Figure 12, a photograph of one of the welds in Figure 11, shows the smooth weld surface (the dark spots along the edge of the weld are a surface residue).

The rough herringbone appearance of welds made at high dewpoints is shown in Figure 13. The rough appearance is probably caused by oxygen

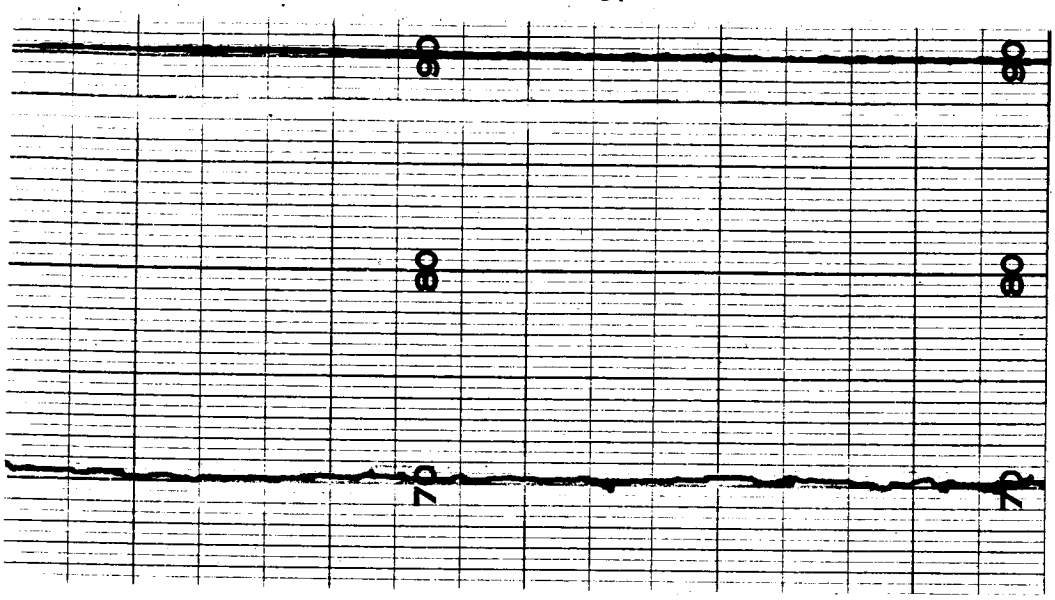

Voltage: 13.5 volts
(100 = 15 volts)

Current 140 amp
(100 = 200 amp)

a. Low Dewpoint

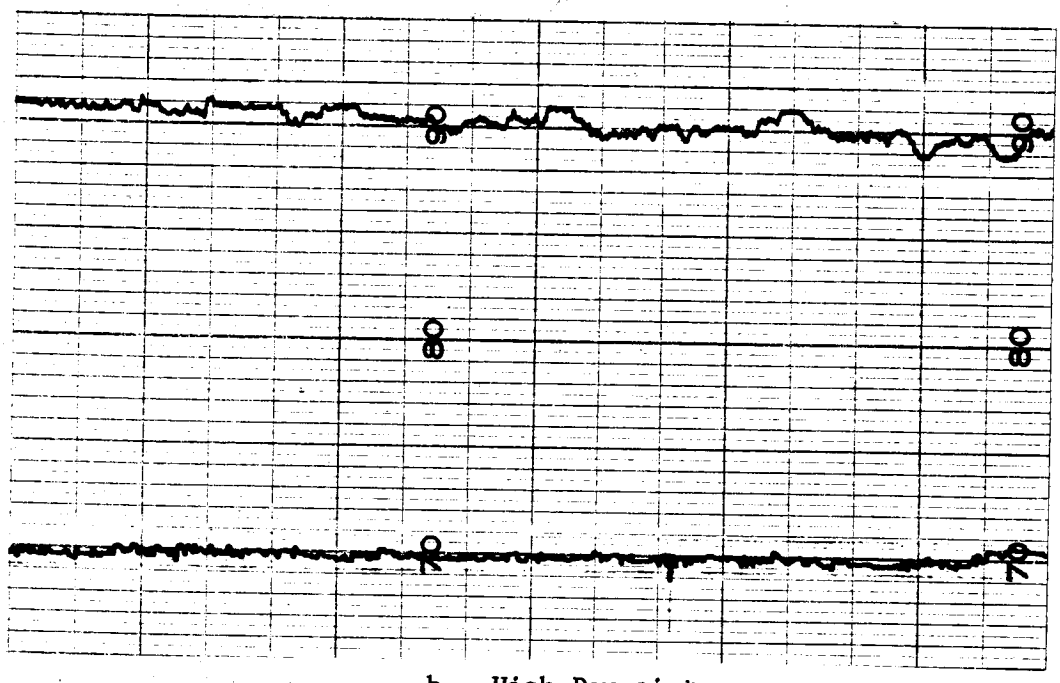

Voltage: 13.5 volts
(100 = 15 volts)

Current: 140 amp
(100 = 200 amp)

b. High Dewpoint

FIGURE 10. ARC-VOLTAGE AND ARC-CURRENT VARIATIONS FOR PHASE I

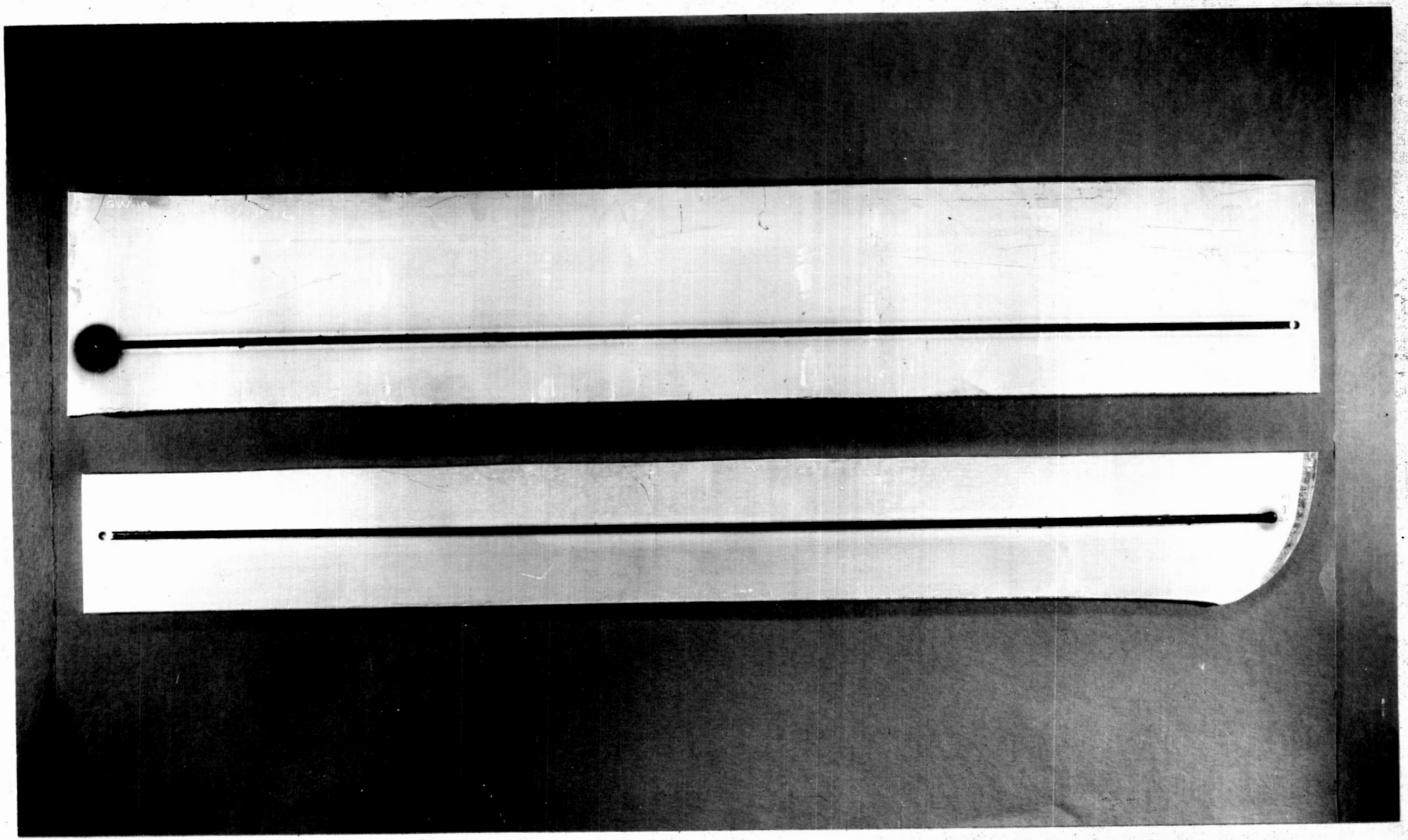

~1/4X

17754

FIGURE 11. TYPICAL WELDS ON X2219 BASE PLATE MADE AT LOW DEWPOINT

Top: 3/4-inch-thick plate; bottom: 1/4-inch-thick plate.

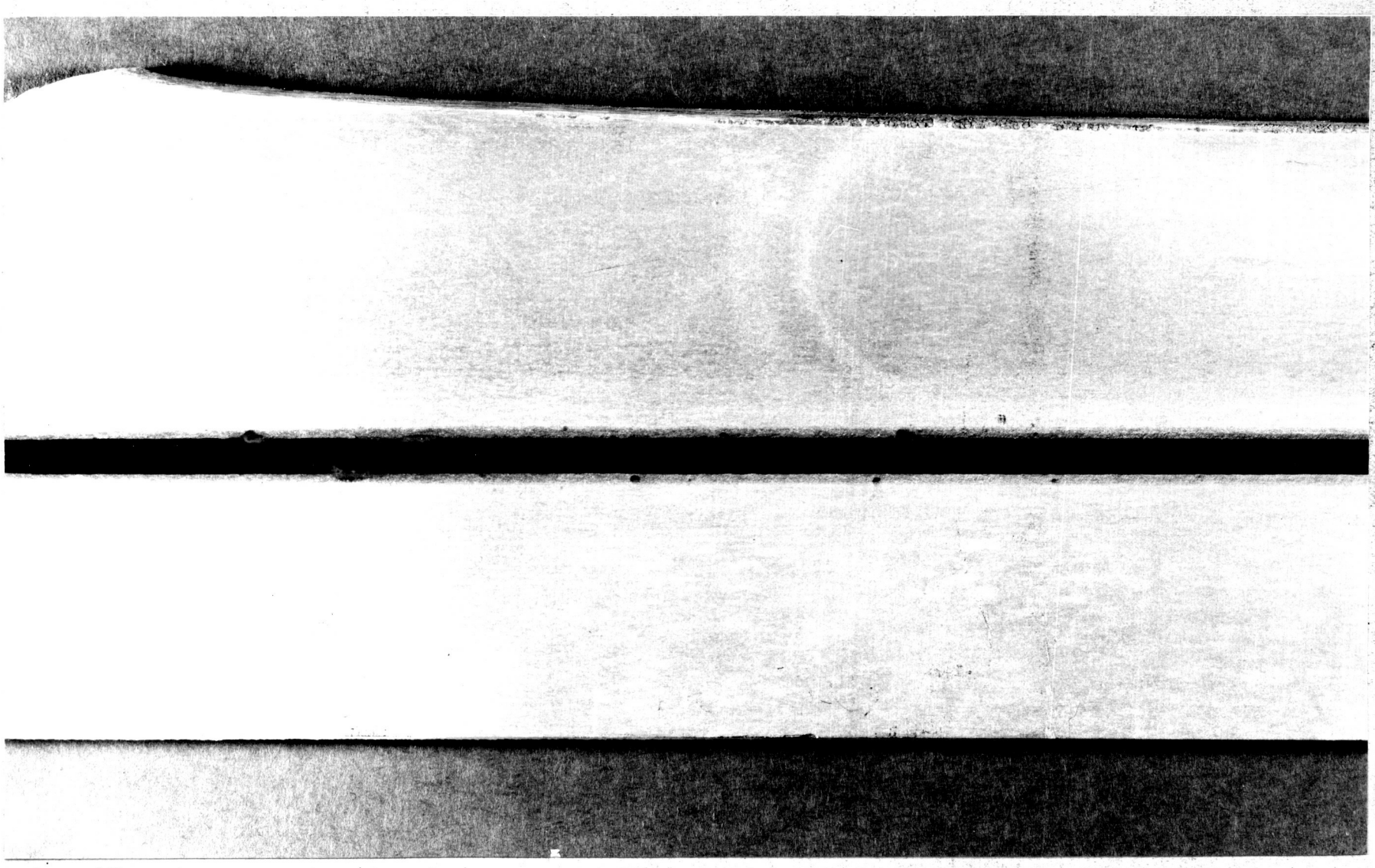

1X

17755

FIGURE 12. SURFACE OF WELD MADE AT LOW DEWPOINT

One quarter -inch-thick X2219 base plate; discontinuities are in thin residue covering the weld.

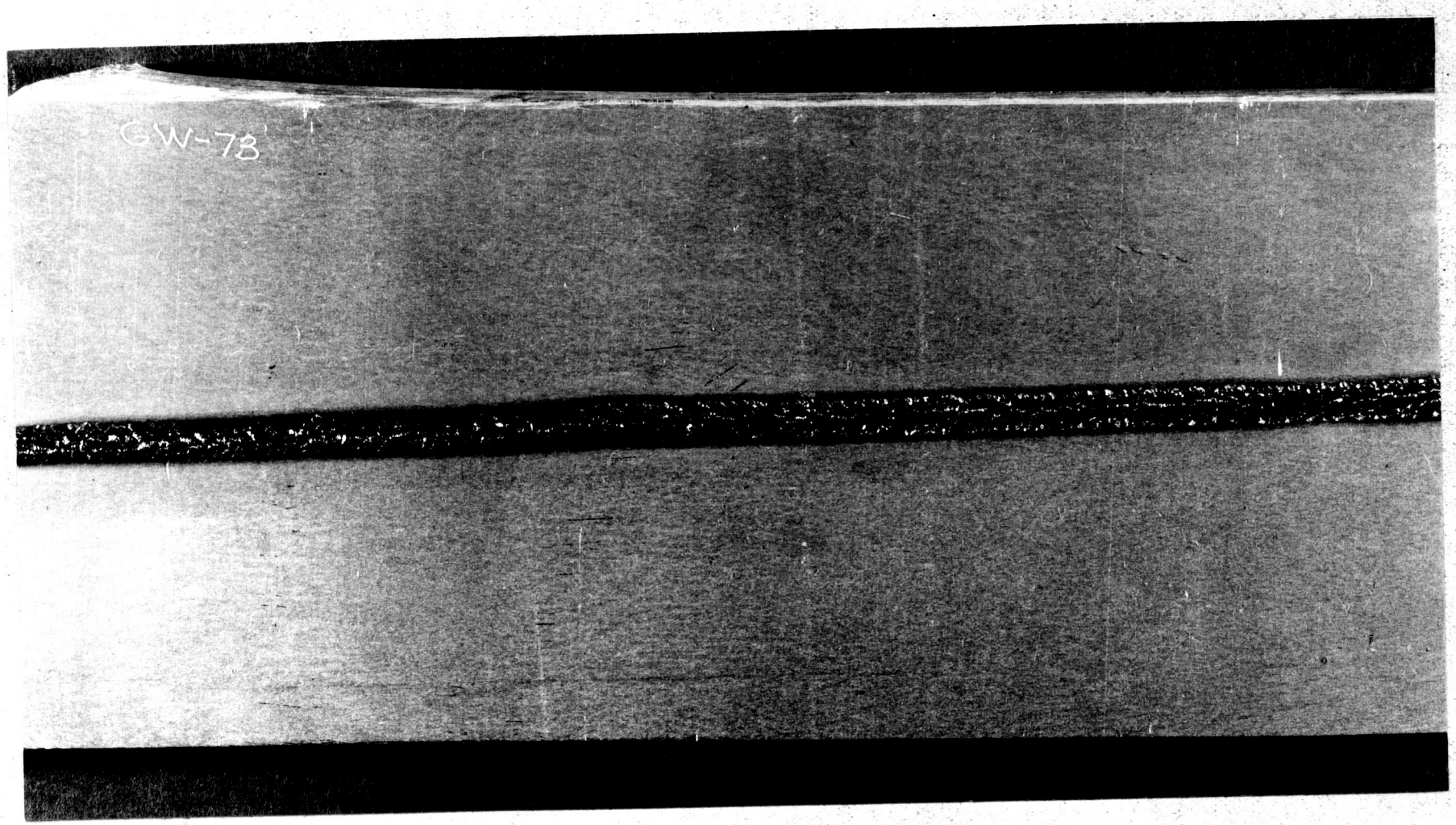

1X

17681

FIGURE 13. SURFACE OF WELD MADE AT HIGH DEWPOINT

One quarter-inch-thick X2219 plate.

which formed when water vapor dissociated in the welding arc and reacted with the molten aluminum to form a thick oxide skin. The observation was made that, at high dewpoints, the crater of molten metal surrounding the arc had steeper sides than when no moisture was in the shielding gas. This was probably due to the oxide "skin" increasing the surface tension of the molten weld pool.

Welding Residue. During the welding of each different composition type, a residue of finely divided particles formed on the plate at both high and low dewpoints. The residue was the same color and was present in the same amount for welds of the same composition. The color of the residue ranged from a light grey trace, to golden brown with black, to a dark smudged grey. The brown color darkened with prolonged exposure to air. Figure 14 shows the difference in the residue appearance for two compositions of X2014 base plate. The residue from one of the plates shown in Figure 13 was qualitatively analyzed by spectroscopy and found to contain an aluminum major with smaller amounts of copper, magnesium, zinc, silicon, manganese, iron, titanium, tungsten, nickel, and zirconium. The latter three elements were not present in the base plate in amounts over 0.05 percent by weight. The tungsten doubtless came from the welding electrode.

Welding During Phase II

The 66 three-feet-long experimental welds for Phase II were made over a 4-week period. The welds were positioned in the middle of 4 by 36-inch wide commercial base plate on one side only. Four separate welds were made for each chamber backfilling. All of the plates of the same

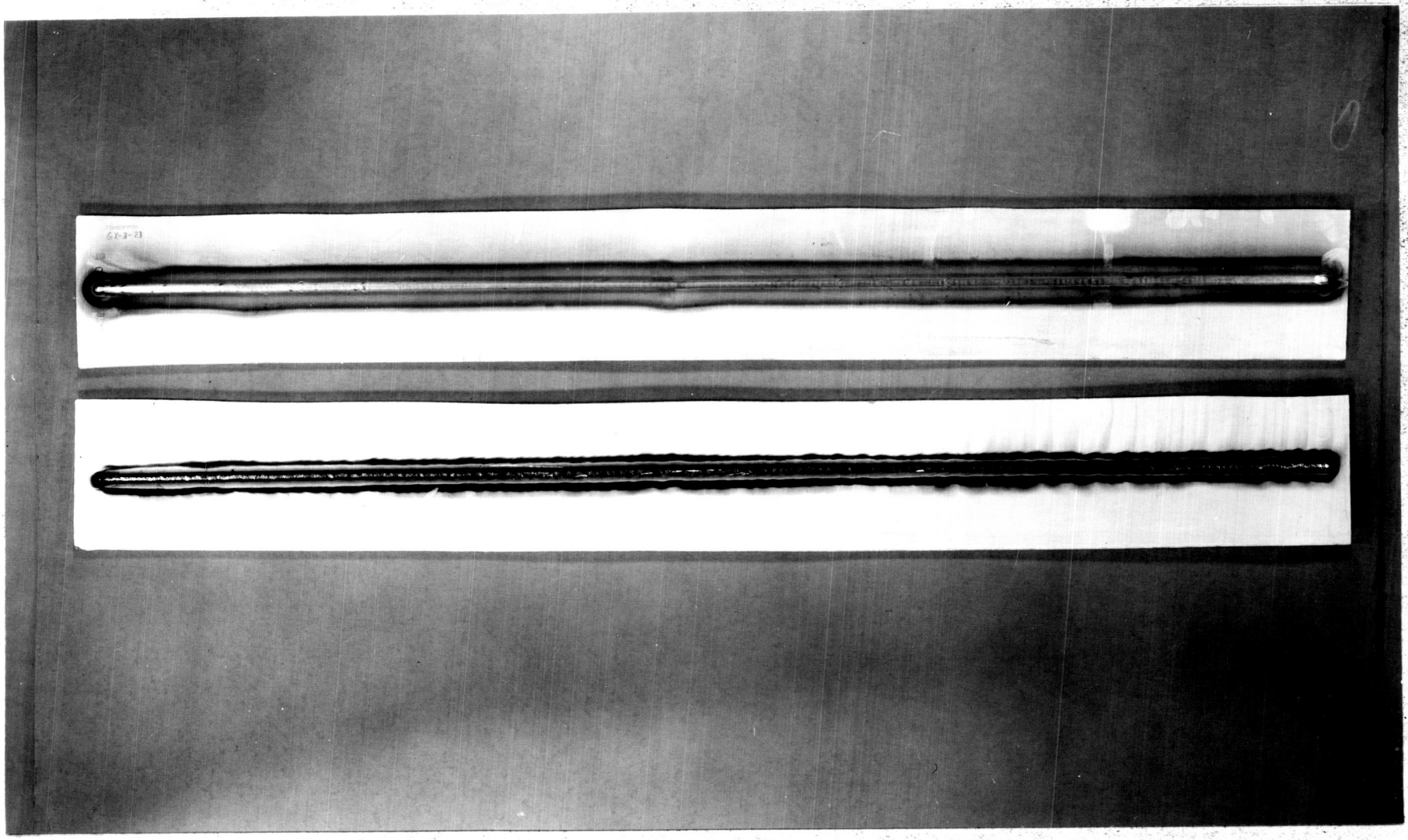

~1/4X

18151

FIGURE 14. RESIDUE FORMED ON PLATE DURING WELDING

Top: Type 2, X2014 1/4-inch-thick plate;
Bottom: Type 7, X2014 1/4-inch-thick plate.

composition type were welded in the same atmosphere in a random order. A new tungsten electrode was used for each weld. Dewpoint determinations were taken before and after each weld.

The work travel speed varied less than ±0.05 inch per minute throughout most of the welds. The arc voltage and arc amperage were more difficult to control when filler wire was added. The arc voltage generally varied up to ±0.50 volt for most of the welds. The arc amperage varied up to ±2.0% for most of the welds. The filler wire speed varied as much as ±10 percent for some welds. Figure 15 is a typical recording made during Phase II. These arc variations again reflected the difficulty of precisely controlling the arc variations in high dewpoint shielding gas even when precision welding equipment was used.

The surface of the welds was not as rough as those made during Phase I at high dewpoints. The weld appearance was uniform. Residue formed along the welds as in Phase I.

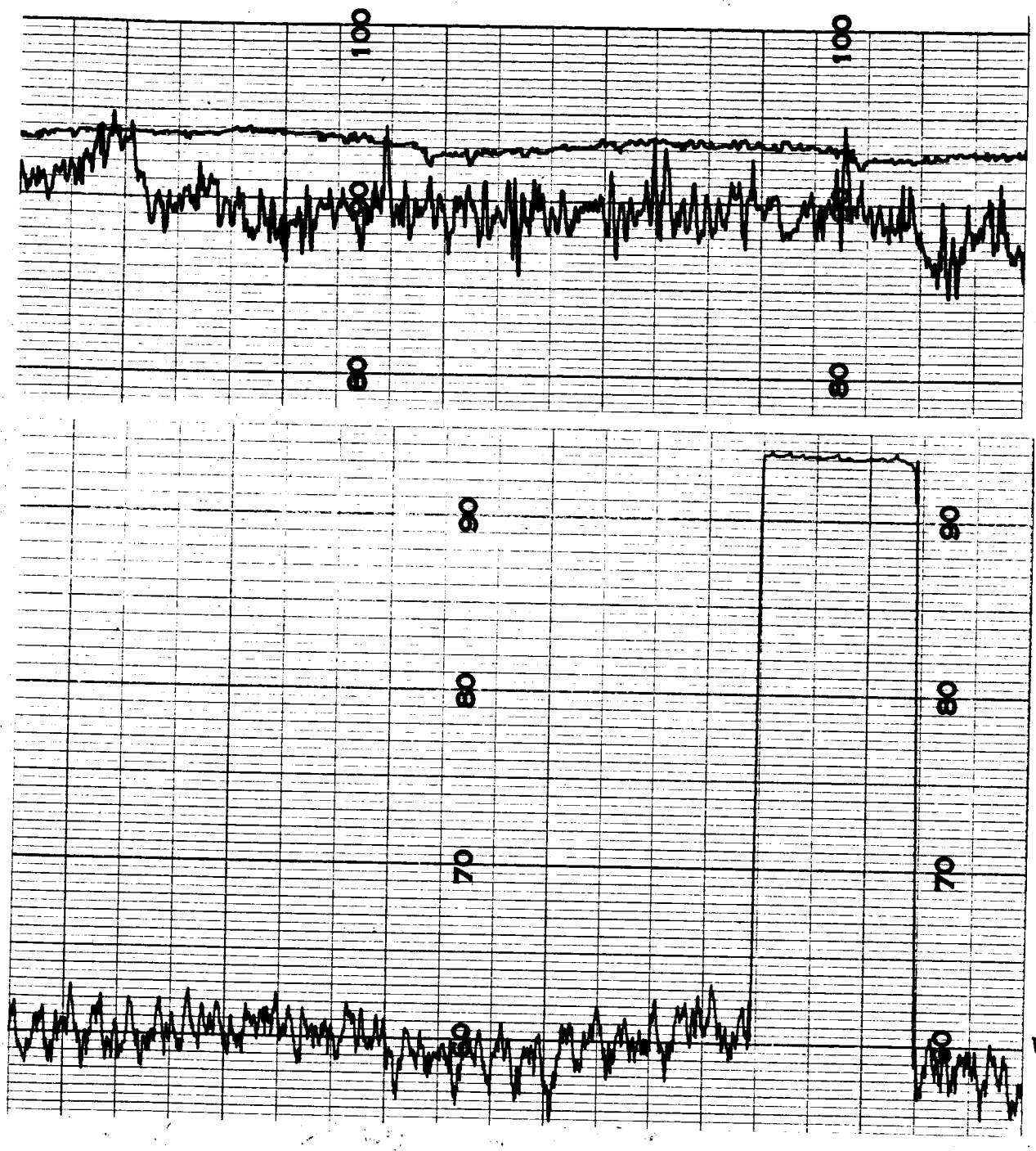

Current:
280 amp
(100=300 amp)

Voltage:
135 volts
(100=15 volts)

Travel Speed:
11.2 ipm
(100=11.9 ipm)

Wire Speed:
64 ipm
(100=106 ipm)

FIGURE 15. TYPICAL RECORDING MADE DURING PHASE II

WELD DEFECT ANALYSES

Weld defects were detected by two inspection methods. The welds were first X-rayed along their complete length. The radiographs were then inspected and graded. After radiography, random transverse weld sections were cut, mounted, polished, photographed, and studied. Defects within the first and last four inches of the weld length were not studied for statistical analysis. The only defects found in the welds were pores and crater cracks at the ends of the welds. The crater cracks were of the same general size throughout the program and were not considered significant.

After welding the experimental plates for Phase I, the welds were taken to a commercial radiographer. The resulting radiographs conformed to the minimum standards of MIL-STD-453 (October 29, 1962*). The welds from Phase II were cut from the base plate in 1-1/2-inch-wide strips and radiographed at Battelle with methods and radiographic sensitivity well within the most stringent standards of MIL-STD-453 (October 29, 1962). The radiographs were individually classified using the method of ABMA-PD-R-27A (August 14, 1959). All but two of the welds were graded under the scattered porosity classifications of this specification. The two exceptions were graded to the linear porosity classifications. Tables 16 and 17 tabulate the radiographic classifications. The weld porosity shown in the radiographs was not statistically analyzed because most of the pores were not of sufficient size to be visible in the radiographs. In some cases, welds were classified to be Class I (defect free) when the pore volume was 10% of the weld volume (as determined by microscopic examination) because the pores were all very fine.

---

* MIL-STD-453 superseded MIL-I-6865 which was referenced in the contract.

TABLE 16. RADIOGRAPHIC CLASSIFICATION OF PHASE I WELDS[a]

Alloy	Type[b]	Sample Number[b] 1/4-Inch-Thick Material 1	2	3	4	3/4-Inch-Thick Material 6	7	8	9
X2219	1	I	I	I	I	I	I	I	I
X2219	2	I	I	I	I	I	I	I	I
X2219	3	I	I	I	I	I	I	I	I
X2219	4	I	I	II	I	I	I	I	I
X2219	5	I	V[c]	I	II[c]	I	I	I	I
X2219	6	I	I	I	I	I	I	I	I
X2219	7	I	I	I	I	I	I	I	I
X2219	8	I	I	I	I	II	II	II	II
X2014	1	I	I	I	I	I	I	I	I
X2014	2	I	I	I	-[d]	I	I	I	I
X2014	3	II	II	I	-[d]	II	II	II	II
X2014	4	II	I	I	II	II	II	II	II
X2014	5	I	II	I	III	I	-[d]	I	-[d]
X2014	6	II	II	I	I	I	I	I	I
X2014	7	III	II	II	III	II	-[d]	I	-[d]
X2014	8	III	III	III	IV	IV	IV	III	III

(a) The scattered porosity classification of ABMA-PD-R-27A was used unless otherwise noted.

(b) See Appendix A for a definition of type and sample numbers.

(c) The linear porosity classification of ABMA-PD-R-27A was used.

(d) No material was available for these replications.

TABLE 17. RADIOGRAPHIC CLASSIFICATIONS OF PHASE II WELDS[a]

Alloy[c]	Type[b]	Sample Number[b] 1/4-Inch-Thick Base Plate 1	1/4-Inch-Thick Base Plate 2	3/4-Inch-Thick Base Plate 6	3/4-Inch-Thick Base Plate 7
X2319	1	II	II	I	I
X2319	2	II	I	I	I
X2319	3	II	II	I	I
X2319	4	I	II	I	I
X2319	5	I	II	I	I
X2319	6	III	II	I	I
X2319	7	II	II	I	I
X2319	8	II	II	I	I
X4043	1	I	I	I	I
X4043	2	III	I	I	I
X4043	3	II	II	I	I
X4043	4	II	II	I	I
X4043	5	II	III	I	I
X4043	6	II	I	I	I
X4043	7	III	II	I	I
X4043	8	II	II	I	I

(a) The scattered porosity classification of ABMA-PD-R-27A was used exclusively; porosity at start and end of weld was ignored.

(b) See Appendix A for a definition of type and sample numbers.

(c) Filler wire which was used for welds on base plate.

All radiographs of the experimental welds made during the program were sent to NASA-MSFC at the close of the contract.

Microscopic Studies

The most valuable data and observations during the program came from the transverse weld sections that were polished and photographed at 20 times enlargement according to ASTM-E-2-49T. Over 600 separate cross-sections were cut and photographed during the program. Because weld defects were of prime interest, the samples were photographed either in as-polished condition or with a light etch-polish. The light etching prevented confusion of small intermetallics with fine pores.

Point Counting Technique

The most useful method describing the occurrence of porosity was to determine the volume percentage of pores volume within the weld metal. A well-developed and widely-used technique was used for determination of the pore volume. (References 8,9, and 10 in Appendix G) During the printing of the 5-inch by 7-inch negative taken of each transverse weld section, a ruled grid of lines was placed between the negative and the photographic paper. The resulting print had a finely-lined grid over the entire surface. The pore volume was determined by counting the number of grid intersections which coincided with the pores within the weld section. The total number of grid intersections within the weld was then determined. The porosity level of the cross-section was defined as the ratio of grid intersections coinciding with pores in the weld to the total number of grid intersections

within the weld as determined by the use of a polar planimeter and a grid of known spacing. The area of the 20X photograph was measured by the polar planimeter. The measured area, when multiplied by the number of grid intersections per square inch, yielded the total number of grid intersections within the weld. Figure 16 contains a typical print with a grid and details the necessary calculations. Originally, a grid with 400 intersections per square inch was used, but a 100 grid per square inch grid was used for most of the program when studies showed that the accuracy of the porosity level determination was not appreciably changed by the decrease in grid density.

The results of the porosity level determinations are tabulated in Tables 18 through 21. The location of the cross-section from the end of each weld is also specified in these tables.

Typical cross-sections for each weld made with each composition of experimental material on each base plate thickness are included in Appendix E.

Pore Size and Distribution

Methods of determining pore size and distribution within welds were studied for use in a statistical analysis of the program results. The most promising method is illustrated in Figure 17. All of the 20X weld section micrographs were studied for X4043, Types 2, 3, 4, 5, and 8 filler wire on 1/4-inch-thick 2014 base plate. Five random, two-inch-long lines were drawn across each micrograph. The diameter of all pores intersecting the lines was determined for nine different pore diameter intervals. The

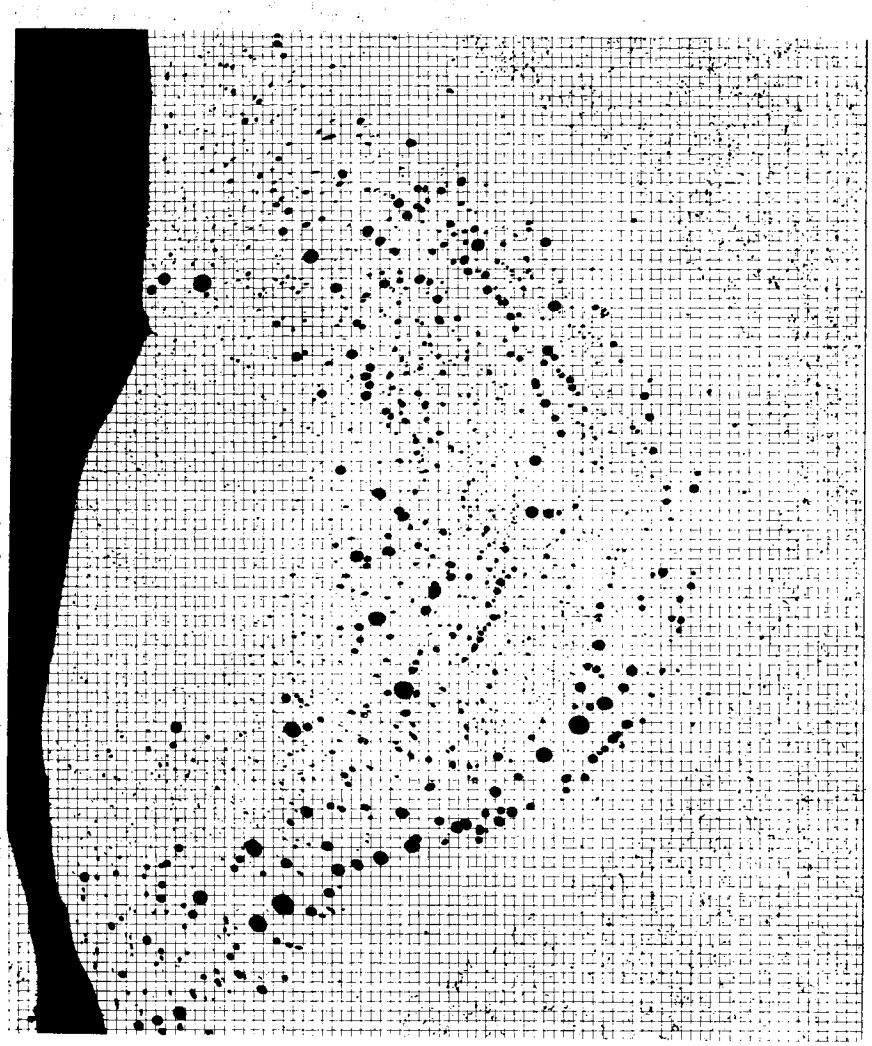

20X RM40104

Area of a fusion zone (measured by polar planimeter) = 11.69 square inches.

Total number of grid intersections in fusion zone = $\frac{400 \text{ grid intersections}}{\text{square inch}}$ X 11.69 square inches = 4676.

Number of grid intersections coincident with pores in fusion zone (determined by counting) = 454.

Porosity level = $\frac{\text{coincident intersections}}{\text{total intersections}}$ X 100% = $\frac{454}{4676}$ X 100% = 4.71%.

FIGURE 16. SAMPLE DETERMINATION OF POROSITY LEVEL

TABLE 18. POROSITY LEVEL AND LOCATION OF WELD SECTIONS ON X2219 BASE PLATE

Type[b]	Porosity Level, percent and Location, inch[a] Sample Number							
	1	2	3	4	6	7	8	9
3	1.1(4)	6.3(18)	4.9(12)	5.5(7)	4.7(11)	4.6(4)	11.8(4)	7.2(11)
3	2.2(10)	5.1(27)	6.7(19)	7.1(16)	3.7(18)	4.6(6)	8.9(10)	11.7(20)
3	--	--	--	--	8.8(21)	8.4(22)	4.2(14)	2.6(22)
3	--	--	--	--	6.0(27)	3.4(31)	1.1(25)	3.8(24)
4	4.4(14)	4.2(15)	2.4(16)	0.9(9)	1.6(10)	8.4(13)	7.1(7)	2.5(7)
4	3.6(15)	7.4(20)	2.5(27)	1.0(13)	0.7(19)	1.3(26)	8.6(10)	1.1(12)
4	5.3(17)	8.7(26)	--	0.7(16)	--	--	--	4.0(16)
4	4.8(21)	8.6(29)	--	0.5(26)	--	--	--	--
7	3.5(11)	2.0(7)	3.5(10)	5.4(19)	6.4(12)	5.3(26)	5.6(6)	1.5(11)
7	4.4(12)	1.0(22)	3.8(19)	4.7(20)	5.9(32)	4.3(29)	5.7(12)	0.8(20)
7	4.1(20)	--	--	--	--	--	1.9(15)	6.1(21)
7	4.6(31)	--	--	--	--	--	2.3(18)	5.9(27)
8	6.0(4)	9.1(3)	3.5(6)	6.1(8)	9.5(5)	7.7(6)	11.5(4)	9.5(7)
8	4.5(5)	10.4(6)	4.3(8)	5.8(11)	7.3(7)	11.2(9)	11.7(8)	12.2(12)
8	3.6(11)	7.8(10)	2.9(9)	4.8(13)	9.1(10)	11.0(10)	8.0(14)	14.3(13)
8	3.2(12)	10.9(11)	3.6(12)	6.4(15)	8.9(12)	7.5(12)	10.6(16)	10.3(14)
8	5.1(15)	7.6(12)	6.8(14)	6.7(17)	8.8(16)	8.0(14)	13.0(18)	11.5(16)
8	6.7(20)	6.6(13)	8.7(18)	7.6(20)	11.2(21)	10.4(16)	11.2(19)	11.8(20)
8	5.8(22)	5.0(14)	7.8(21)	6.4(26)	9.2(23)	10.2(17)	11.8(20)	11.9(23)
8	4.4(28)	5.3(17)	12.8(24)	8.0(29)	7.9(26)	9.8(18)	10.0(25)	9.1(24)
8	--	5.9(20)	7.0(27)	--	--	9.8(19)	--	9.9(26)
8	--	5.5(22)	--	--	--	10.0(21)	--	--
8	--	6.3(28)	--	--	--	5.9(26)	--	--
8	--	--	--	--	--	9.4(27)	--	--
8	--	--	--	--	--	12.7(29)	--	--
8	--	--	--	--	--	11.3(31)	--	--

(a) The location of each section from the end of the weld is at the right of the porosity level in parentheses.

(b) Types 1 and 6: No Porosity.

Types 2 and 5: Slight Porosity (<0.2%).

(See Appendix A for a definition of type and sample numbers)

TABLE 19. POROSITY LEVEL AND LOCATION OF WELD SECTIONS ON X2014 BASE PLATE

Type[b]	Porosity Level, percent and Location, inch[a] Sample Number 1	2	3	4	6	7	8	9
3	8.8(9)	10.3(20)	11.5(8)	--	7.2(18)	12.0(9)	13.3(15)	22.1(12)
3	8.8(29)	10.0(29)	8.3(22)	--	11.1(24)	11.6(11)	11.6(21)	24.6(15)
4	5.4(3)	9.8(15)	1.8(5)	3.4(6)	21.6(9)	22.0(10)	18.7(18)	24.1(14)
4	8.7(8)	5.9(31)	1.4(18)	2.7(16)	14.5(11)	22.6(23)	15.2(31)	21.1(28)
5	7.9(18)	6.4(16)	0.9(17)	1.5(10)	--	--	--	--
5	1.2(25)	5.3(21)	2.1(30)	2.1(19)	--	--	--	--
5	--	--	--	1.3(21)	--	--	--	--
5	--	--	--	3.1(27)	--	--	--	--
6	4.3(9)	3.7(5)	1.4(13)	2.1(24)	--	--	--	--
6	3.9(20)	5.1(24)	1.0(22)	2.7(29)	--	--	--	--
7	8.6(16)	6.6(8)	3.8(6)	7.8(20)	13.1(5)	--	9.8(10)	--
7	8.8(24)	6.1(14)	2.6(17)	7.2(22)	20.2(14)	--	11.1(13)	--
8	14.0(13)	11.5(16)	8.0(7)	9.6(7)	17.0(7)	14.7(16)	12.6(24)	19.9(9)
8	11.6(20)	13.2(23)	8.5(17)	12.8(16)	12.3(24)	14.4(23)	7.5(28)	17.4(29)

(a) The location of each section from the end of the weld is at the right of the porosity level in parentheses.

(b) Types 1 and 2 and Samples 6, 7, 8, and 9 of Types 5 and 6: Slight Porosity (<0.2%). (See Appendix A for a definition of type and sample numbers)

TABLE 20. POROSITY LEVEL AND LOCATION OF WELD SECTIONS IN WELDS USING X2319 FILLER WIRE

Type[b]	Porosity Level, percent and Location, inch[a] Sample Number 1	2	6	7
1	2.5(11)	1.1(11)	2.5(21)	2.4(12)
1	4.4(13)	1.3(21)	5.0(23)	2.1(21)
2	0.3(16)	0.5(7)	0.8(9)	1.6(7)
2	0.4(17)	0.4(11)	0.2(23)	1.3(21)
3	0.7(16)	0.8(11)	2.3(7)	2.4(4)
3	0.6(23)	2.0(24)	1.4(18)	2.6(13)
4	0.6(21)	1.9(7)	5.0(6)	8.2(23)
4	1.3(30)	0.8(14)	6.0(12)	4.1(28)
5	2.7(6)	2.0(6)	3.3(9)	3.0(11)
5	2.4(24)	2.9(25)	2.3(15)	2.7(23)
6	1.0(21)	0.5(10)	3.8(11)	1.6(10)
6	1.6(22)	3.4(19)	4.2(13)	1.3(25)
7	1.6(6)	1.9(12)	4.2(9)	2.9(10)
7	1.1(9)	2.2(26)	3.0(26)	2.6(17)
8	1.8(5)	1.8(7)	1.0(5)	2.1(8)
8	2.8(10)	1.2(8)	1.5(14)	5.5(16)

(a) The location of each section from the end of the weld is at the right of the porosity level in parentheses.

(b) See Appendix A for a definition of type and sample numbers.

TABLE 21. POROSITY LEVEL AND LOCATION OF WELD SECTIONS IN WELDS USING X4043 FILLER WIRE

Type[b]	Porosity Level, percent and Location, inch[a] Sample Number 1	2	6	7
1	3.5(11)	0.6(14)	0.7(24)	0.8(14)
1	2.3(20)	1.0(23)	0.8(26)	1.4(24)
2	4.8(24)	5.5(12)	0.7(14)	1.3(18)
2	4.3(26)	7.7(20)	0.9(24)	1.3(24)
3	1.9(23)	2.7(14)	1.4(17)	3.7(4)
3	1.9(27)	3.2(20)	0.7(18)	3.2(21)
4	2.3(19)	2.8(16)	1.1(6)	4.5(20)
4	2.6(23)	6.6(23)	0.7(20)	6.2(26)
5	1.3(5)	2.7(28)	1.4(7)	3.0(7)
5	1.6(26)	3.1(29)	3.3(13)	4.0(15)
6	4.4(13)	6.5(19)	1.8(4)	1.6(8)
6	6.7(14)	6.5(24)	2.4(17)	4.2(24)
7	3.0(13)	0.6(16)	3.1(4)	2.8(9)
7	3.9(23)	2.0(23)	2.0(5)	1.8(17)
8	2.0(20)	1.3(8)	2.0(19)	2.0(10)
8	0.6(21)	3.5(19)	2.8(22)	1.4(26)

(a) The location of each section from the end of the weld is at the right of the porosity level in parentheses.

(b) See Appendix A for a definition of type and sample numbers.

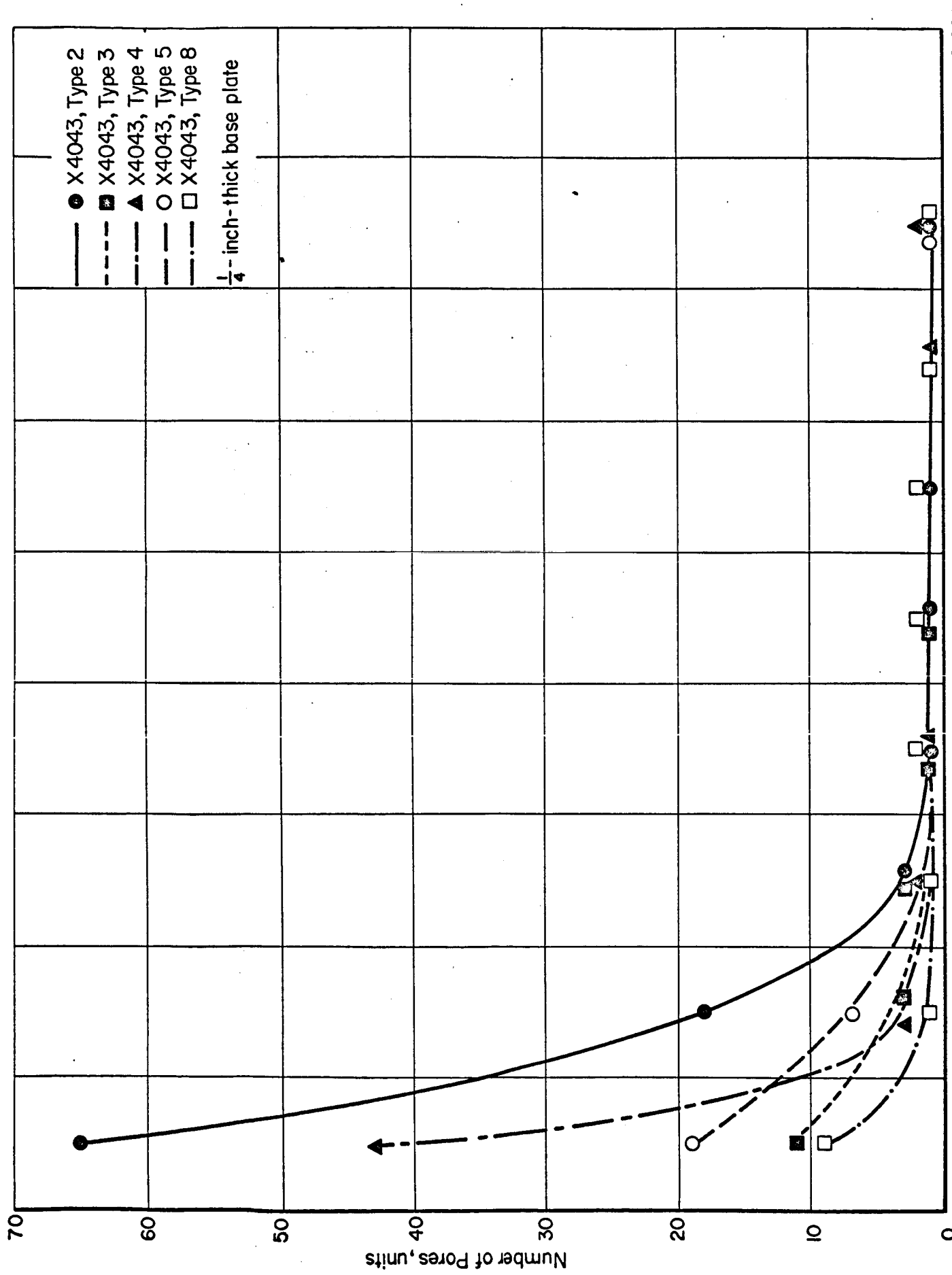

FIGURE 17. DISTRIBUTION OF PORE DIAMETERS IN WELDS ON 2014 BASE PLATE

total of the diameters of all the pores intersected by each line for all micrographs of all welds using the same wire type is plotted in Figure 17. As shown in the figure, the majority of the pores were 0 to 0.001-inch diameter. This diameter range is about 1/12 of the minimum pore diameter that would be visible in a radiograph having 2 per cent sensitivity of a 1/4-inch-thick plate. Radiographically visible pores composed a small percentage of the total number of pores in the weld sections.

Pores were not analyzed statistically for frequency and distribution within this program because the results would have limited significance at this time. All weld micrographs made during the project are available for meaningful statistical analysis when the NASA-sponsored program on effects of porosity level determines the significance of the pore size and distribution upon weld strength.

Weld at Low Dewpoint. As a check upon the quality of the experimental welding wire surfaces, two welds were made on 1/4- and 3/4-inch-thick 2219 base plate using X2319 Type 8 filler wire. Figure 18 shows the micrograph of the weld section containing the most pores. The porosity in the other three sections ranged from 0 to the 15 to 20 small pores shown in the figure. The surface of the experimental filler wire was judged to be more than adequately clean for use in Phase II of the program without any cleaning of the wire surface.

Pores Due to Surface Cracks in Base Plate

After welding 1/4-inch-thick X2219 Type 5 base plates, two of the four plates were found to have a blistered appearance near the weld. Examination of the weld radiographs showed that several extremely large

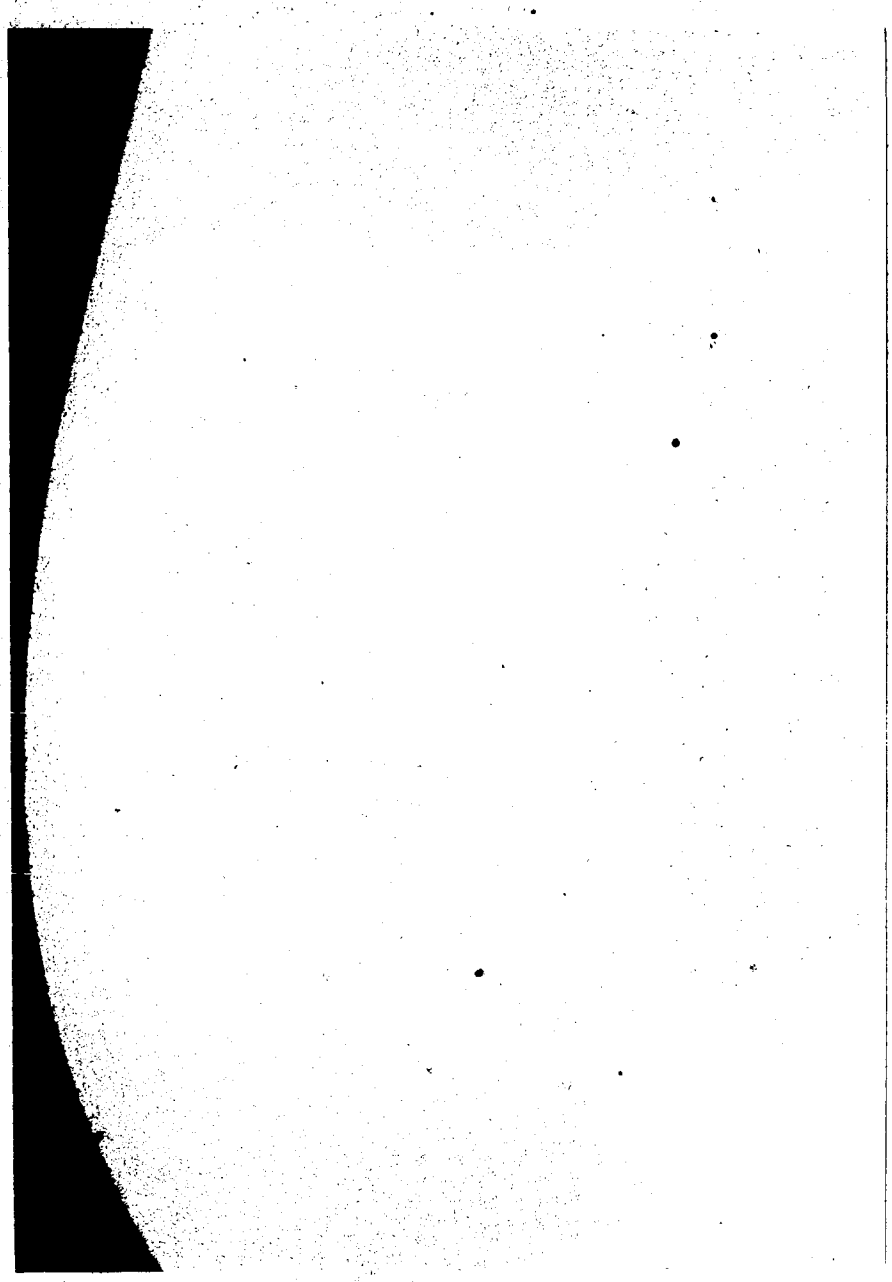

20X RM43740

FIGURE 18. SECTION OF WELD MADE AT LOW DEWPOINT WITH EXPERIMENTAL X2319, TYPE 8 FILLER WIRE

pores had formed along the welds in the two plates. Micrographs of the weld sections containing the blisters also contained a series of enlarged cracks within the weld as shown in Figure 19. Figure 20 shows one of the large pores formed within the weld even though the dewpoint of the shielding gas was low (-60 F). Examination of base plate sections showed that long, fine cracks ran parallel and just below the outside surface except at one end of the crack which was joined to the outer surface. An internal hydrogen content analysis of samples with the outer surface lightly draw-filed (removal of less than 0.001 inch) and heavily draw-filed (removal of 0.02 inch) yielded the following:

	Hydrogen Content, ppm, by weight
Lightly filed surface	2.3
Heavily filed surface	1.1

The difference between the two analyses were attributed to the removal of the cracks which probably contained hydrated aluminum oxide or rolling lubricants.

These studies showed the extreme sensitivity of the base plate appearance after welding and of the radiographic appearance of the weld to the presence of fine surface cracks. The blisters and large pores were never observed in any other than the two X2219 Type 5 1/4-inch-thick plates. Thus, the surface quality of all but two of the 96 plates fabricated for the program was demonstrated to be high.

20X RM40400

FIGURE 19. ,MICROSCOPIC APPEARANCE OF A SECTION THROUGH A WELD BLISTER

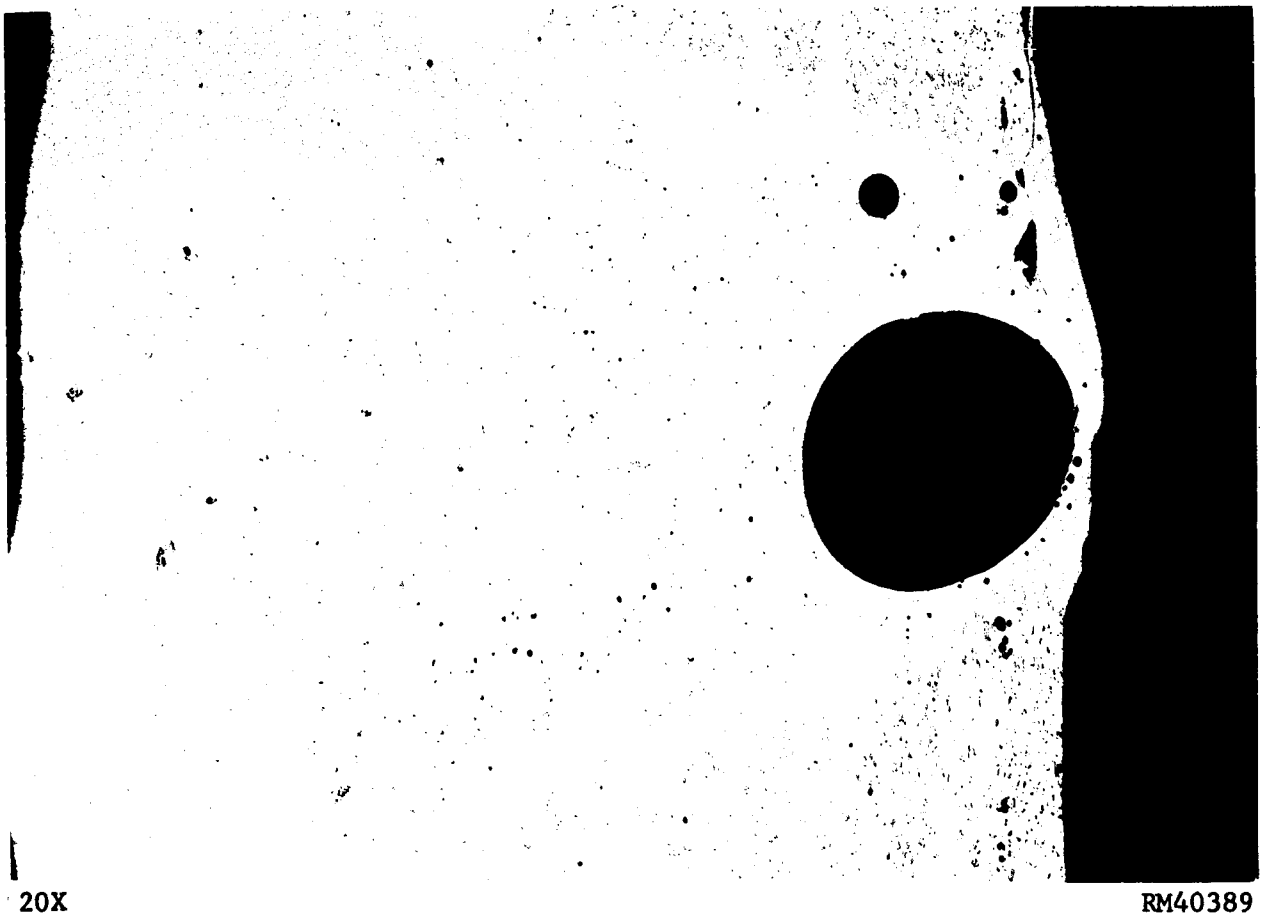

20X RM40389

FIGURE 20. MICROSCOPIC APPEARANCE OF A SECTION THROUGH A LARGE PORE IN A BLISTERED WELD

Pores Outside Fusion Zone

In several sections of welds made on experimental and commercial base plate, pores were observed grouped outside the fusion zone. Figure 21 shows a typical occurrence of this phenomenon. No specific reason or explanation for this pore formation was found. The composition types of X2219 and X2014 base plate in which the pores most frequently appeared outside the fusion zone were Types 7 and 8 (welded at high dewpoint).

Effect of Arc Variations Upon Porosity Level

Over seventy weld sections were cut from welds on X2219 Type 8 plate to determine the effect of arc variations that were beyond the limits specified for the program in Table 14. Sections were taken where arc variations were as much as three times or as little as 1/10 of the specified maximum variations. The results of the tests of statistical significance that were made for these weld sections is included in the section on statistical analyses.

Effect of Base Plate Defects

Welds were deliberately made over defects detected by ultrasonic inspection in X2014 Type 1, 4, and 6 base plate. These defects were not visible in radiographs which had better radiographic sensitivity than is required by MIL-STD-453. A longitudinal cross-section was cut along the weld axis near the center of the weld extending one inch beyond either side of the reported defect location. No defects or significant weld heterogeneity were observed in the cross-sections. Because the defects indicated by ultrasonic inspection were not located or identified, this study was terminated with no conclusive results.

FIGURE 21. PORES FORMED OUTSIDE FUSION ZONE IN X2219, TYPE 7 BASE PLATE

Hardness Variations Within Weld Sections

An apparent relation between porosity and segregation in the weld metal was observed in metallographic cross-sections. Weld cross-sections of all materials usually contained ordered groupings of pores as shown in Appendix E. Pores in the lower half of the weld were gathered in bands parallel to the boundary between the fusion and the heat-affected zone. Often, a band composed of the largest pores in the weld cross-section extended completely across the width of the weld at the midplane. The upper part of the weld cross-section contained a large number of fine pores (usually less than 0.0025-inch diameter) and some larger pores. The distribution of fine pores was observed to vary widely both in the number present and the degree and form of ordering for the different weld compositions.

Light and dark bands parallel to the boundary between the fusion and the heat-affected zones were observed in many etch-polished weld cross-sections. The microstructures of the light and dark bands were noticeably different. A microhardness traverse along the line indicated in Figure 22 was made on a cross-section containing these light and dark bands. Hardness variations above Point 6 were observed, but resolution of the bands in this area was difficult. Therefore, the results for these points were inconclusive. A definite hardness difference between points located in the light and in the dark bands was clearly established for Points 1 through 6 (See Figure 22). Additional tests beside these points verified the differences observed. Similar microhardness variations in steel welds have been reported by Gurev and Stout (Reference 2 in Appendix G).

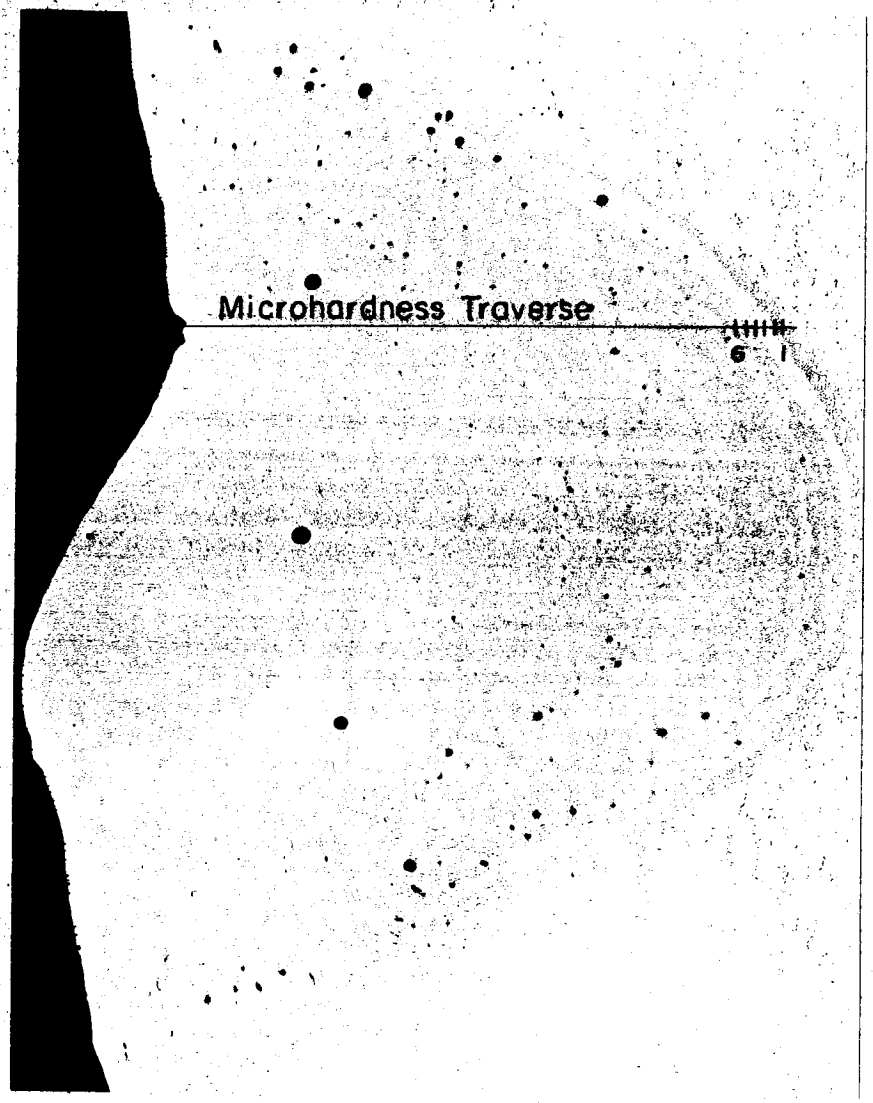

20X Etch-polish RM40635

Point[a]	Knoop Hardness Number (50 gram load)	Band
1	83.0	Dark
2	83.0	Dark
3	73.5	Light
4	71.5	Light
5	80.5	Dark
6	77.0	Dark

(a) Results above Point 6 not reported due to interpretation difficulties.

FIGURE 22. LOCATION OF MICROHARDNESS VARIATIONS IN X2219 WELD

Preferential Pore Occurrence

The apparent preferential occurrence of pores in the light bands of weld sections was of particular interest. The observations of preferential pore grouping in light or dark bands would probably have been more numerous if the metallographic procedure had been different. Etch-polishing, which was not used on X2014 cross-sections, and special oblique lighting were found to develop the contrast between the light and dark bands.

Examination of longitudinal cross-sections taken along the centerline of 8 different X2014 welds disclosed an ordered occurrence of pores, as shown in Figure 23. Pores in the lower half of the X2014 Type 4 weld were grouped in families of curves spaced about 0.03-inch apart. Halfway from the top of the weld a band of larger pores in no ordered grouping extended along the length of the weld. The upper half of the X2014 Type 4 weld contained fine pores arranged in families of curves.

Examination of longitudinal cross-sections of nonporous X2014 Type 6 welds showed some light and dark bands grouped in curves similar to the curves of pores shown in Figure 23. The appearance of the upper half of welds of each of the three types of X2014 examined was markedly different in both thickness and appearance. In the upper part of the X2014 Type 6 weld, distinct light and dark bands were grouped in straight lines which intersected the top surface at an included angle of less than 5 degrees as shown in Figure 24. The X2014 Type 1 weld section in Figure 25

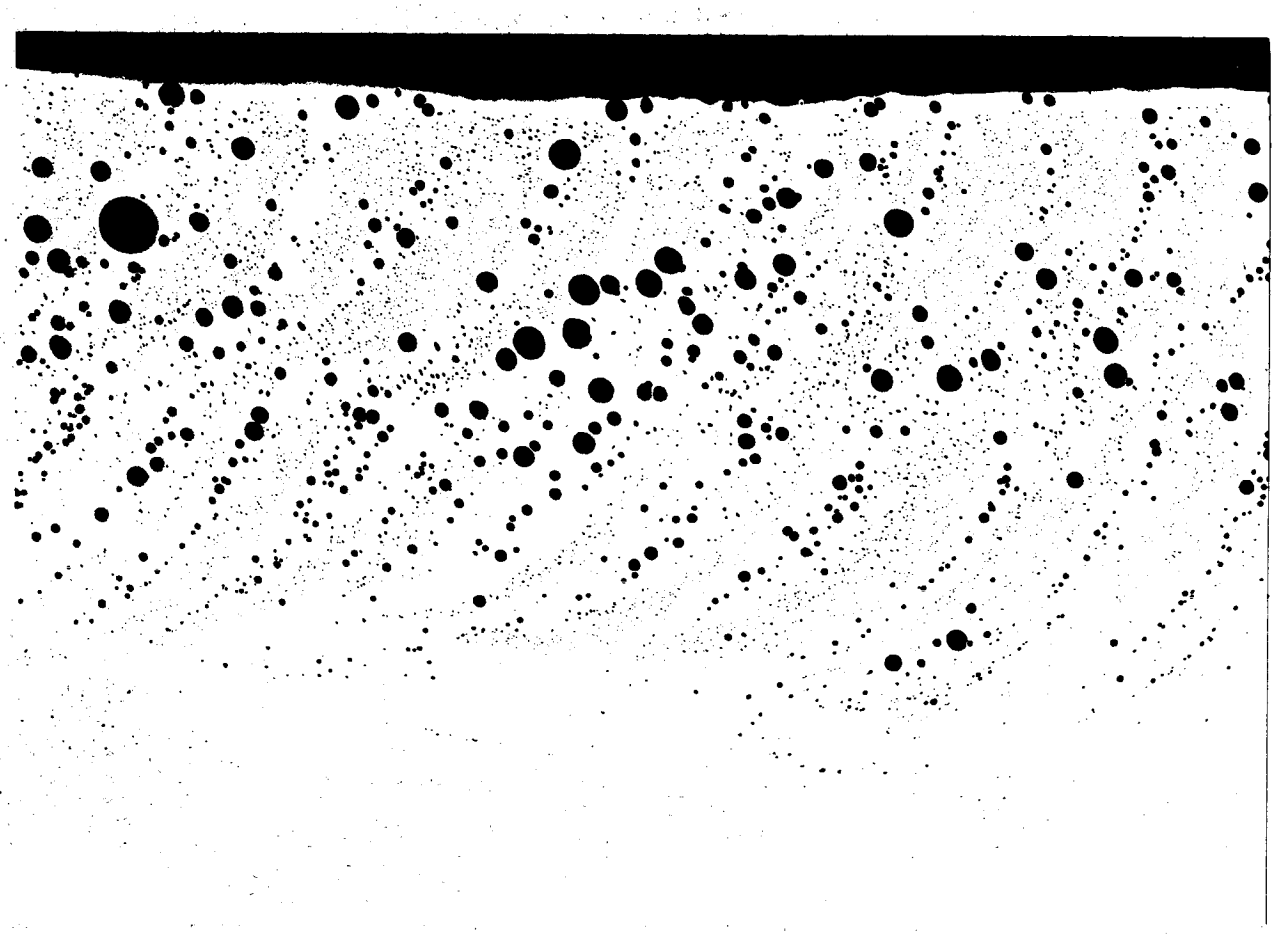

20X 5% HF Etch RM41860

FIGURE 23. ORDERING OF PORES ALONG TRANSVERSE SECTION OF WELD IN X2014, TYPE 4 BASE PLATE

20X 5% HF Etch RM41864

FIGURE 24. SEGREGATION ALONG TRANSVERSE SECTION OF WELD IN X2014, TYPE 6 BASE PLATE

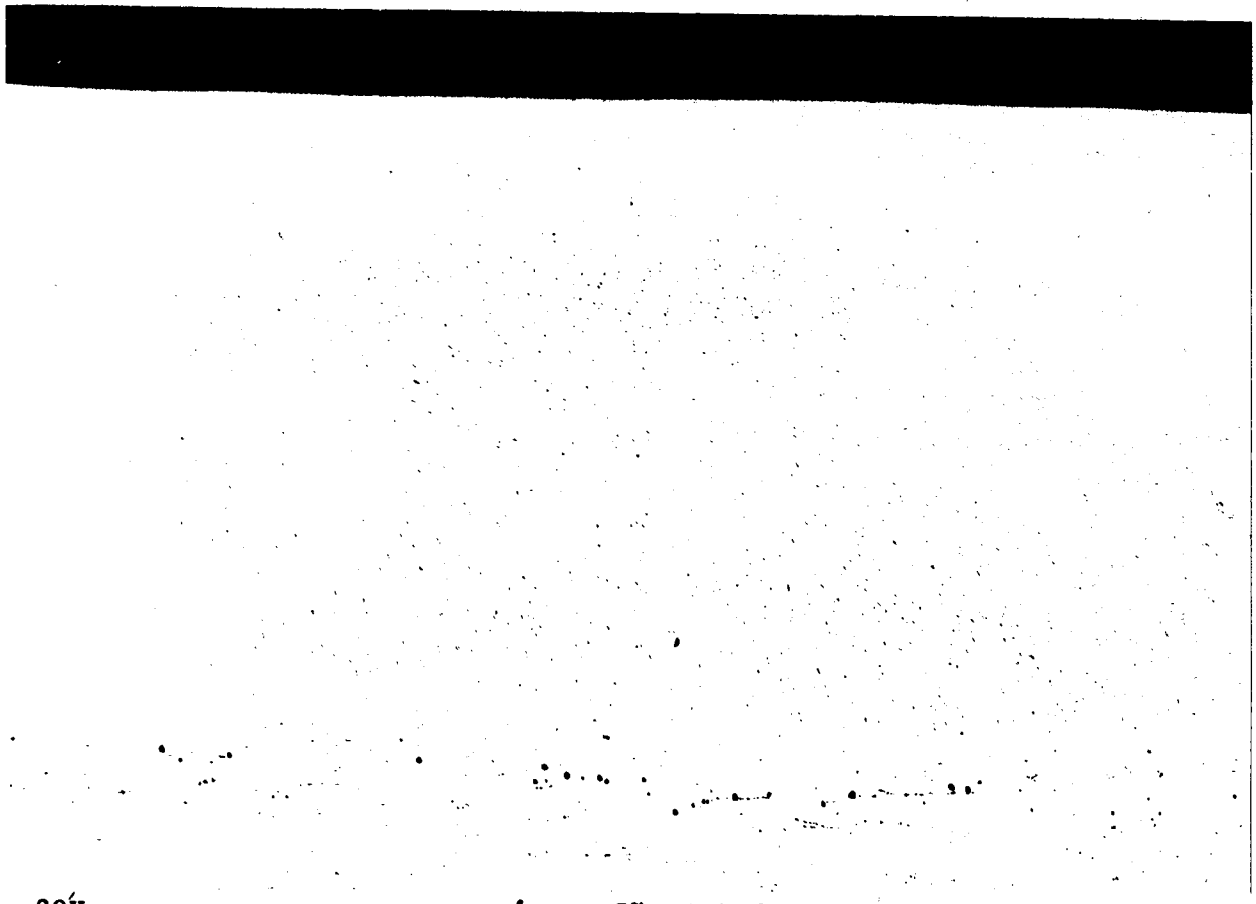

20X 5% HF Etch RM41845

FIGURE 25. SEGREGATION ALONG TRANSVERSE SECTION OF WELD IN X2014, TYPE 1 BASE PLATE

contained visible light and dark bands. A boundary between the upper and lower part of the weld cross-section was visible near the top.

Analysis of Experimental Base Plate Intermetallics

The intermetallics (metallic inclusions) in X2219 base plate were primarily $CuAl_2$ and AlCuFeMn. Non-metallic inclusions were not observed at any time during the program studies. The intermetallics in X2014 base plate were $CuAl_2$ and alpha AlFeSi. A minor phase associated with the $CuAl_2$ was identified as AlCuMn. Phase identifications were made by following the etching procedures described by F. Keller and G. W. Wilcox in "Identification of Constituents of Aluminum Alloys".

STATISTICAL ANALYSIS

The significance of the relationships between the four factors of weld composition and the occurrence of weld defects was determined by statistical analysis. The difficulty of controlling the hydrogen content of the experimental materials to exact and distinct high and low levels caused the statistical analysis to be modified. The fractional factorial method of analysis was discarded in both phases. A limited, but valuable, number of observations were made during Phase I by paired comparisons. For Phase II, the level of external impurities was set at a fixed value to allow study of the three weaker factors of composition. A large number of paired comparisons were analyzed for Phase II.

Phase I Analyses

The fractional factorial design for the program is presented in the previous discussion and in Appendix E. Instead of studying all 16 (2^4) combinations of two levels of the four factors, eight combinations were planned for study. Except for gas content, the desired combinations of the four factors were obtained in all of the plate fabricated for use in the program. The actual level of each of the four factors is shown in Table A-11 of Appendix A. The one-half factorial design was planned to supply the following information on weld defects for each of the four materials:

1. Effect of high versus low chemical content
2. Effect of high versus low gas content
3. Effect of high versus low internal impurities
4. Effect of high versus low external impurities

5. The significance of each of the four factors.

This statistical design does not allow for analysis of specific interactions between the four factors.

Two events caused the method of analysis to be changed in the program. First, as previously reported, the actual hydrogen content varied from the target content. Second, the welds made at low dewpoints contained no porosity except for two compositions of 1/4-inch-thick X2014. All welds which contained no porosity were assigned the same defect rating--zero. Thus, all of the comparisons contained in the original statistical plan could not be made between welds which were not porous. The problem was simply that at low dewpoints, only high quality welds could be made. Consequently, half of the planned comparisons were not suitable for statistical analysis. Specific, but incomplete statistical results, also were obtained for each material studied. The variation of the gas content from the target content was much more beneficial than harmful to the program. The variations in gas content allowed significant interactions among the four factors to be definitely established. These interactions could not have been discovered by the original statistical program.

Comparisons of Materials

A separate analysis was made between composition types of the experimental materials which were the same alloy, the same base plate thickness, and the same hydrogen content. This procedure isolated the effects of the variables so that they could be measured. Careful examination

of the results of the microscopic examinations led to the results listed in Table 22. Columns 1 and 2 show that at least one comparison was made for each thickness of each material. Column 3 of the table shows which material types were compared. Column 4 shows which variables were constant and at what level. Column 5 shows the variable whose effect was being tested. The last column shows the degree of certainty associated with the conclusion that the variable being tested was a real cause of porosity. The conclusions based on relationships which have a degree of certainty of 95% or more are generally thought of as being soundly based upon the data considered. For lower degrees of certainty, the conclusiveness of the results diminishes greatly with each percentage point (an exponential sort of relationship). Thus, results with a degree of certainty from 90 to 95 percent one of interest, but should not be used completely to establish conclusions. A degree of certainty from 80 to 90 is low, but could be considered. Below 80% degree of certainty, the relationships observed are considered to have very little significance.

Effect of Arc Variables

An analysis of variance was made to determine the effects of arc variations upon the porosity level of welds. The porosity levels of the sections of Type 8 X2219 were arranged in two groups for each base plate thickness. One group contained sections where the arc variables had exceeded the maximum variations specified for the program. The second group contained sections that were taken at points along the welds where the arc variations were well within the maximum specified variations. The

TABLE 22. RESULTS OF SIGNIFICANCE TESTS ON PAIRED COMPARISONS FOR PHASE I.

Material	Thickness, inch	Types Compared	Fixed Variables: Chemical Content	Fixed Variables: Internal Impurities	Fixed Variables: External Impurities	Respective Hydrogen Content, ppm by weight	Effect Tested[a]	Degree of Certainty, percent
X2219	1/4	7 with 8	High	---	High	0.1,0.7	I and G	98.2
X2219	3/4	3 with 8	----	High	High	0.5,0.5	C	99.8
X2219	3/4	4 with 7	----	Low	High	0.1,0.1	C	81
X2014	1/4	3 with 4	Low	----	High	0.4,0.4	I	95
X2014	1/4	5 with 7	High	Low	----	0.6,0.5	E	93
X2014	1/4	6 with 8	High	High	----	0.8,0.9	E	99.9
X2014	3/4	6 with 8	High	High	----	0.7,0.8	E	>99.9

[a] C - Chemical content.
I - Internal impurities.
G - Hydrogen content.

analysis of variance showed that the difference in porosity levels for the two groups was insignificant.

Phase II Analyses

Phase II was planned so that the effect of external impurities, the factor most significantly related to weld porosity, was limited and the effects of the less significant factors could be studied. Accordingly, the level of the external impurities was fixed throughout Phase II. As in Phase I, only paired comparisons were made in the analysis. Table 23 tabulates the results for each variable studied.

Examination of Table 23 shows that the results of changes in hydrogen content generally had a low degree of certainty or no significance at all. Accordingly, twelve more paired comparisons were made between compositions which had hydrogen content values within 0.4 ppm of each other. The statistical comparisons are listed in Table 24 and should be used with full knowledge that 0.4 ppm difference in hydrogen content was considered negligible for the purposes of the statistical analyses. The analysis of X4043 Type 5 with Type 7 in Table 23 is of interest because the chemical contents, internal impurity contents, and hydrogen contents for each type were reported to be the same. The statistical comparison shows that there is no significant difference in the porosity levels of the two types. This comparison shows that the experimental error involved was quite small, in this case.

TABLE 23. RESULTS OF SIGNIFICANCE TESTS ON PAIRED COMPARISONS FOR PHASE II.

Material	Base Plate Thickness, inch	Types Compared	Fixed Variables[a]			Effect Tested[b]	Degree of Certainty, percent
			Chemical Content	Internal Impurities	Respective Hydrogen Content, ppm by weight		
X2319	1/4	1 with 7	---	Low	1.4,1.5	C	Not significant
X2319	3/4	1 with 7	---	Low	1.4,1.5	C	Not significant
X2319	1/4	3 with 6	---	High	2.5,2.5	C	83
X2319	3/4	3 with 6	---	High	2.5,2.5	C	Not significant
X2319	1/4	2 with 7	---	----	1.5,1.7	C+I	93.5
X2319	3/4	2 with 7	---	----	1.5,1.7	C+I	90.5
X2319	1/4	1 with 4	Low	Low	1.4,3.1	G	Not significant
X2319	3/4	1 with 4	Low	Low	1.4,3.1	G	Not significant
X2319	1/4	2 with 3	Low	High	1.7,2.5	G	84
X2319	3/4	2 with 3	Low	High	1.7,2.5	G	81
X2319	1/4	5 with 7	High	Low	3.4,1.5	G	85
X2319	3/4	5 with 7	High	Low	3.4,1.5	G	Not significant
X2319	1/4	6 with 8	High	High	2.5,2.0	G	Not significant
X2319	3/4	6 with 8	High	High	2.5,2.0	G	Not significant
X4043	1/4	2 with 6	----	High	1.8,1.8	C	Not significant
X4043	3/4	2 with 6	----	High	1.8,1.8	C	91
X4043	1/4	3 with 5	----	----	2.5,2.4	C+I	Not significant
X4043	3/4	3 with 5	----	----	2.5,2.4	C+I	Not significant
X4043	1/4	1 with 4	Low	Low	1.5,4.0	G	Not significant
X4043	3/4	1 with 4	Low	Low	1.5,4.0	G	Not significant
X4043	1/4	2 with 3	Low	High	1.8,2.5	G	89
X4043	3/4	2 with 3	Low	High	1.8,2.5	G	Not significant
X4043	1/4	5 with 7	High	Low	2.4,2.2	Error	Not significant
X4043	3/4	5 with 7	High	Low	2.4,2.2	Error	Not significant
X4043	1/4	6 with 8	High	High	1.8,2.9	G	97.1
X4043	3/4	6 with 8	High	High	1.8,2.9	G	Not significant

(a) External impurities fixed at uniform, high level.
(b) C - Chemical content. I - Internal impurities. G - Hydrogen content.

TABLE 24. RESULTS OF SUPPLEMENTARY SIGNIFICANCE TESTS ON PAIRED COMPARISONS FOR PHASE II.[a]

Material	Base Plate Thickness, inch	Types Compared	Fixed Variables[b]			Effect Tested[c]	Degree of Certainty, percent
			Chemical Content	Internal Impurities	Respective Hydrogen Content, ppm by weight		
X2319	1/4	1 with 2	Low	----	1.4,1.7	I	77
X2319	3/4	1 with 2	Low	----	1.4,1.7	I	85
X2319	1/4	4 with 5	----	High	3.1,3.4	C	97.8
X2319	3/4	4 with 5	----	High	3.1,3.4	C	98.7
X2319	1/4	2 with 8	----	High	1.7,2.0	C	93.5
X2319	3/4	2 with 8	----	High	1.7,2.0	C	Not significant
X4043	1/4	1 with 2	Low	----	1.5,1.8	I	87.5
X4043	3/4	1 with 2	Low	----	1.5,1.8	I	Not significant
X4043	1/4	1 with 6	----	----	1.5,1.8	I+C	91
X4043	3/4	1 with 6	----	----	1.5,1.8	I+C	93
X4043	1/4	6 with 7	High	----	1.8,2.2	I	91
X4043	3/8	6 with 7	High	----	1.8,2.2	I	Not significant

(a) Analyses based on results in Table 23 which showed differences in hydrogen content alone were not significant. The results here assume that a difference of hydrogen content up to 0.4 ppm is negligible.

(b) External impurities fixed at uniform, high level.

(c) C - Chemical content. I - Internal impurities. G - Hydrogen content.

PROGRAM RESULTS

The large amount of data and tests resulting from the investigation allowed studies to be made that were not originally planned in the proposal. The most interesting studies were of the relation of hydrogen content of the experimental materials to material composition or to the porosity level of a weld using the experimental materials.

Statistical Plan

The planned levels for chemical content, internal impurities, and external impurities as specified in Table 1 were satisfactorily met during all work in Phase I and Phase II. The control of the hydrogen content of the experimental base plate hydrogen content did not allow the separation of values of hydrogen content into two separate and distinct levels. Figure 26 shows the reported hydrogen content for the base plate ingots prior to fabrication for each composition. Because not all of the ingots were analyzed, the figure does not include all the possible points. In most cases, the level of hydrogen as determined by the analysis was completely opposite to that which was expected. After fabrication, the hydrogen content values were at the levels shown in Figure 27. Figure 27 shows a definite increase in the internal hydrogen content accompanying a change from the low chemical content, low internal impurities compositions to the high chemical content, high internal impurities compositions. The single anomalous result at the low chemical content, low internal impurities composition was the material which was treated for high hydrogen content by stirring of the melt with a frequently-moistened graphite rod. This

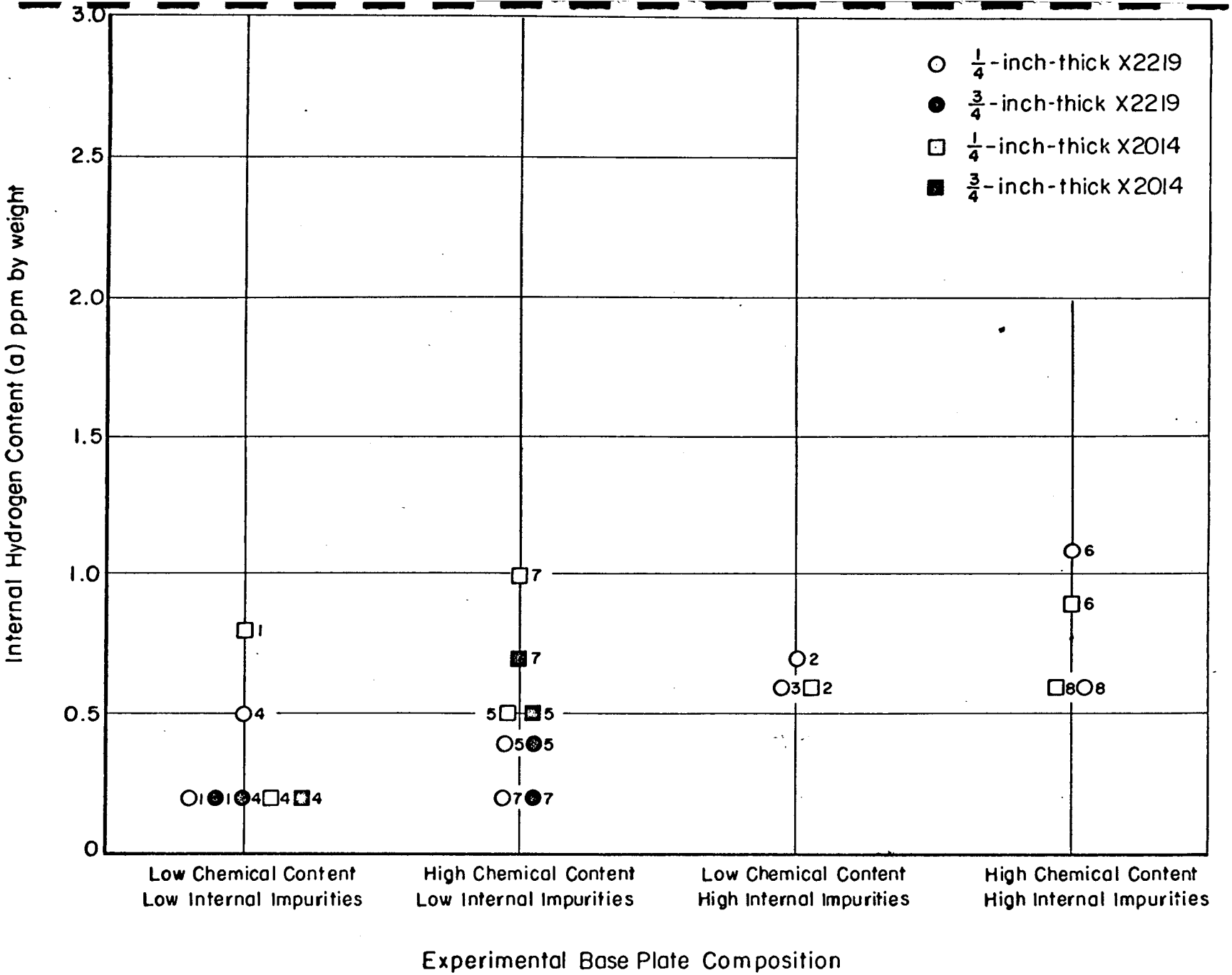

FIGURE 26. RELATIONSHIP BETWEEN EXPERIMENTAL BASE-PLATE COMPOSITION AND INTERNAL HYDROGEN CONTENT

(a) Hydrogen content of ingots prior to fabrication.
Type number is indicated beside each point.

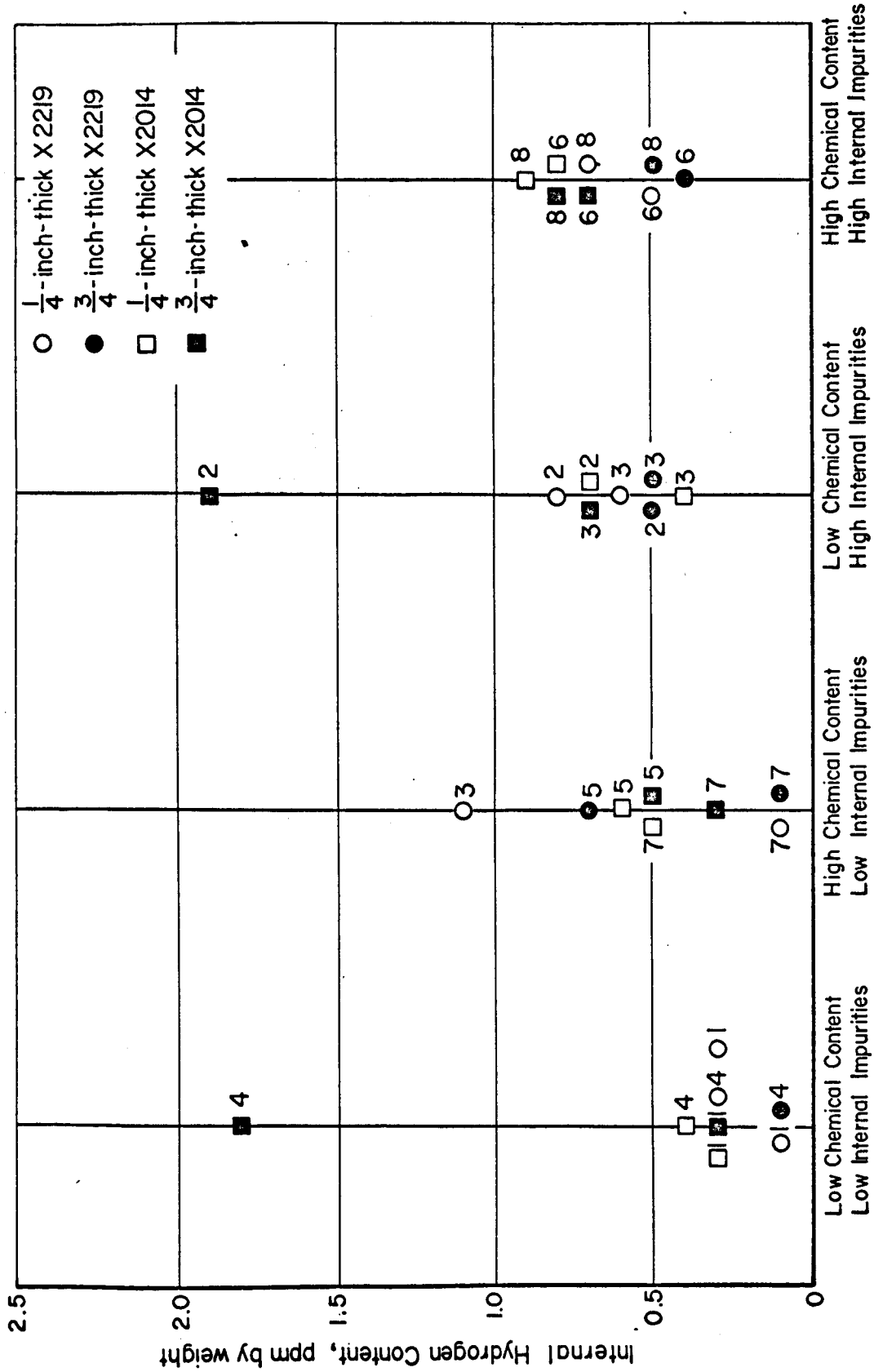

FIGURE 27. RELATIONSHIP BETWEEN EXPERIMENTAL BASE-PLATE COMPOSITION AND INTERNAL HYDROGEN CONTENT

(a) Hydrogen content of base plate after fabrication.
Type number is indicated beside each point.

rather severe preparation method explains the large difference between this single high hydrogen content value and the group of the remaining hydrogen content values. Thus, this single deviation does not seriously detract from the observed relationship of base plate composition and hydrogen content. If this point is ignored, the degree of certainty for the relationship between increasing hydrogen content and the composition level is greater than 99.9 per cent. The two intermediate compositions in Figure 27 have hydrogen contents scattered about levels intermediate to the hydrogen content levels of the two endpoint compositions.

Filler Wire Hydrogen Content

The filler wire hydrogen content was successfully controlled by the casting methods used (See Appendix A). Figure 28 shows the total internal hydrogen content of the X4043 and X2319 ingots. The difference between the analyses of the ingot in Figure 28 and the drawn wire in Figure 29 was caused by two factors. The hydrogen content in Figure 29 is the internal hydrogen content plus a surface hydrogen correction factor of about 0.3 ppm. (A definite surface hydrogen correction factor was never determined for the filler wire, but the indications were that it was about 0.5 ppm). In addition, the surface area to volume ratio of the wire sample was much greater than the ingot sample so that the analyses were more sensitive to the surface condition of the wire.

Figure 29 shows that both of the filler wire alloys, despite differences in their alloying elements, shared the same median. In addition, the median for all of the analyses was the median for each combination of the material composition factors. Twelve of the sixteen

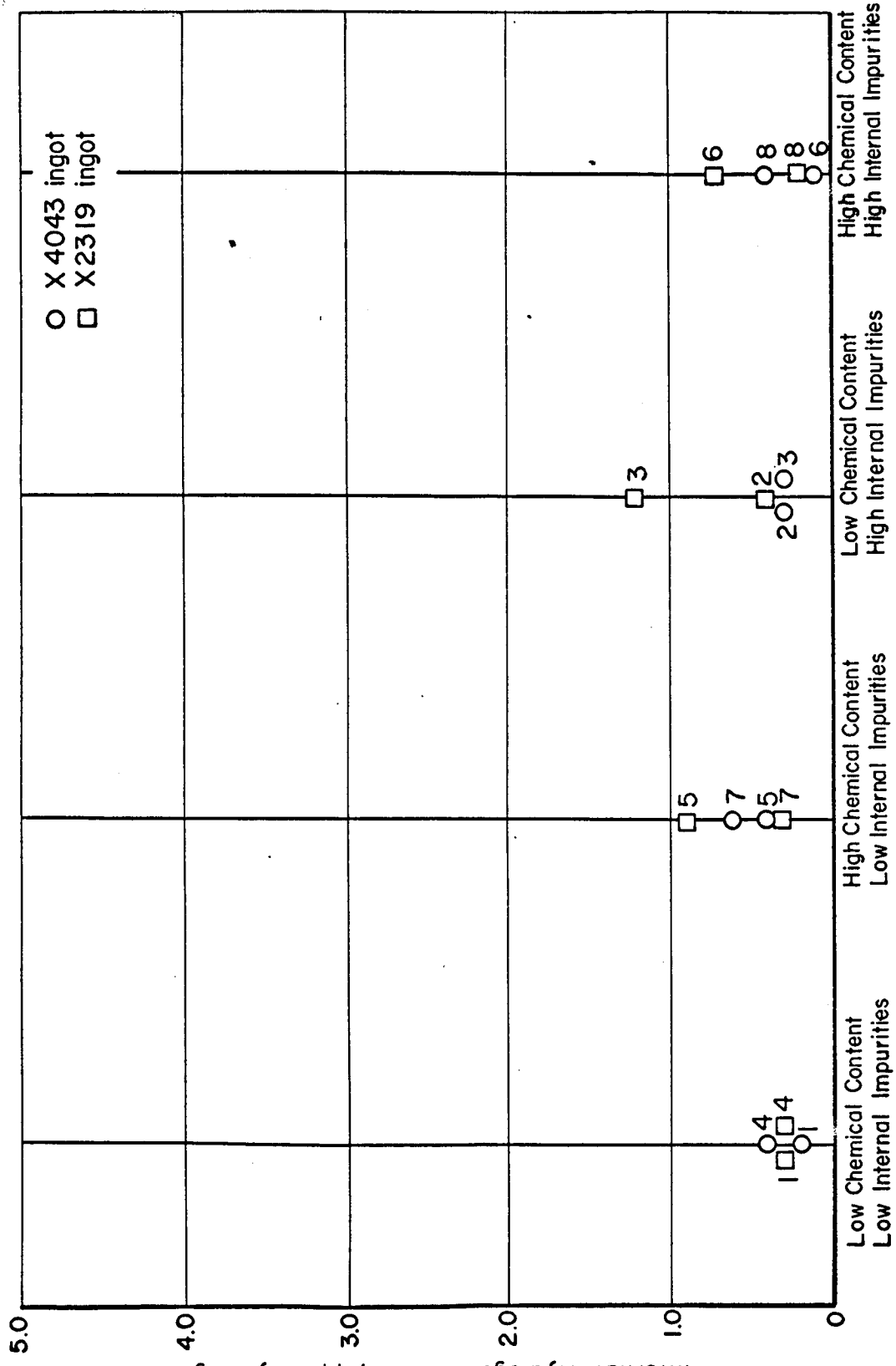

FIGURE 28. RELATIONSHIP BETWEEN EXPERIMENTAL FILLER-WIRE COMPOSITION AND INTERNAL HYDROGEN CONTENT

(a) Hydrogen content of ingot prior to fabrication. Type number is indicated beside each point.

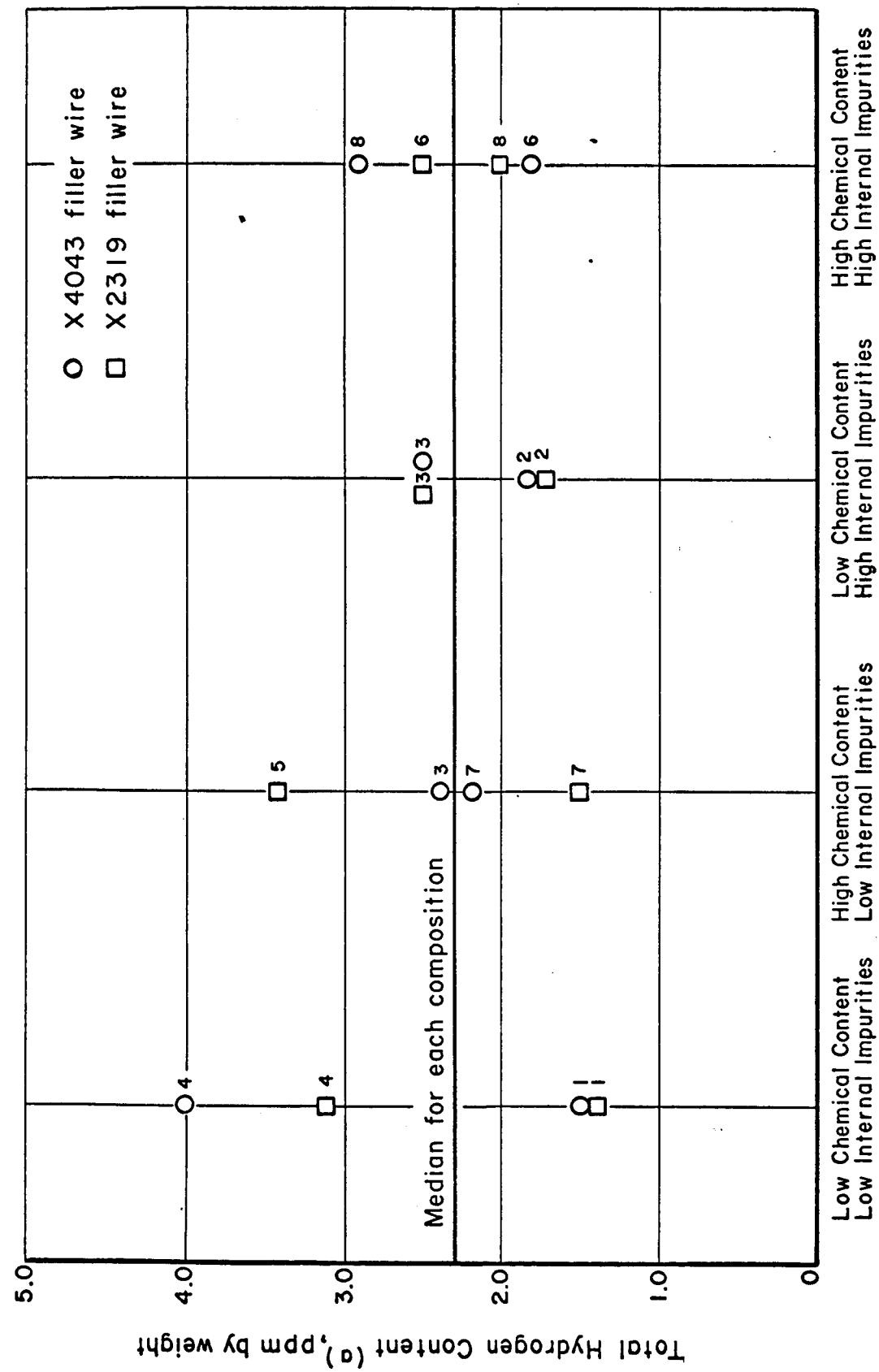

FIGURE 29. RELATIONSHIP BETWEEN EXPERIMENTAL FILLER-WIRE COMPOSITION AND TOTAL HYDROGEN CONTENT

(a) Hydrogen content of filler wire after fabrication. Type number is indicated beside each point.

types cast had the intended high or low level of hydrogen content (relative to the median) that was desired.

Hydrogen Content and Porosity Level

The relationship between the hydrogen content of the experimental base plate material and the porosity level of the welds made at high dewpoints is plotted in Figures 30 through 33. In general, there can be seen a trend to a higher porosity level with increasing hydrogen content for the plates. The trend is particularly noticeable for the plates with high chemical content. The sole exception to the relationships observed above was for the 3/4-inch-thick X2014 base plate. All of the compositions plotted in Figure 33 had so much scatter between plates that no general conclusions were drawn.

Figures 34 through 37 show that no definite general relationship existed between porosity level and hydrogen content of the experimental filler wire for welds made on commercial base plate material. The points are scattered in all of the figures in a random manner.

Summary of the Porosity Level Determinations

The average porosity level and standard deviation for the welds on each alloy, composition type, and base plate thickness is listed in Table 25. Inspection of this table will show that some of the highest average porosity levels also have the higher standard deviations. Thus, any comparison between composition types for each alloy and thickness should consider both the size of the average porosity level and the size of the standard deviation for each porosity level.

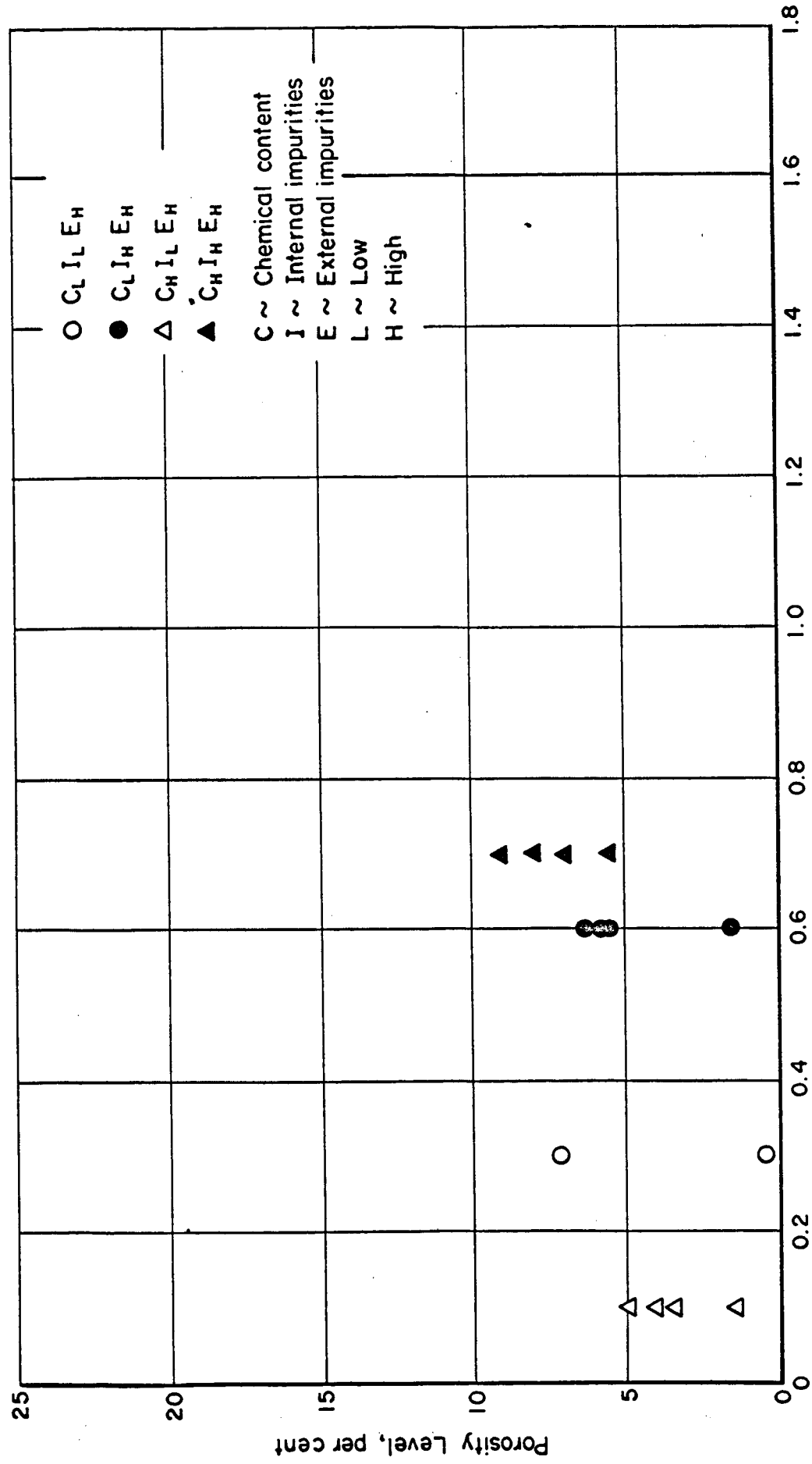

FIGURE 30. RELATIONSHIP OF POROSITY LEVEL TO HYDROGEN CONTENT FOR 1/4-INCH-THICK X2219 BASE PLATE

Each plotted point denotes an average plate porosity.

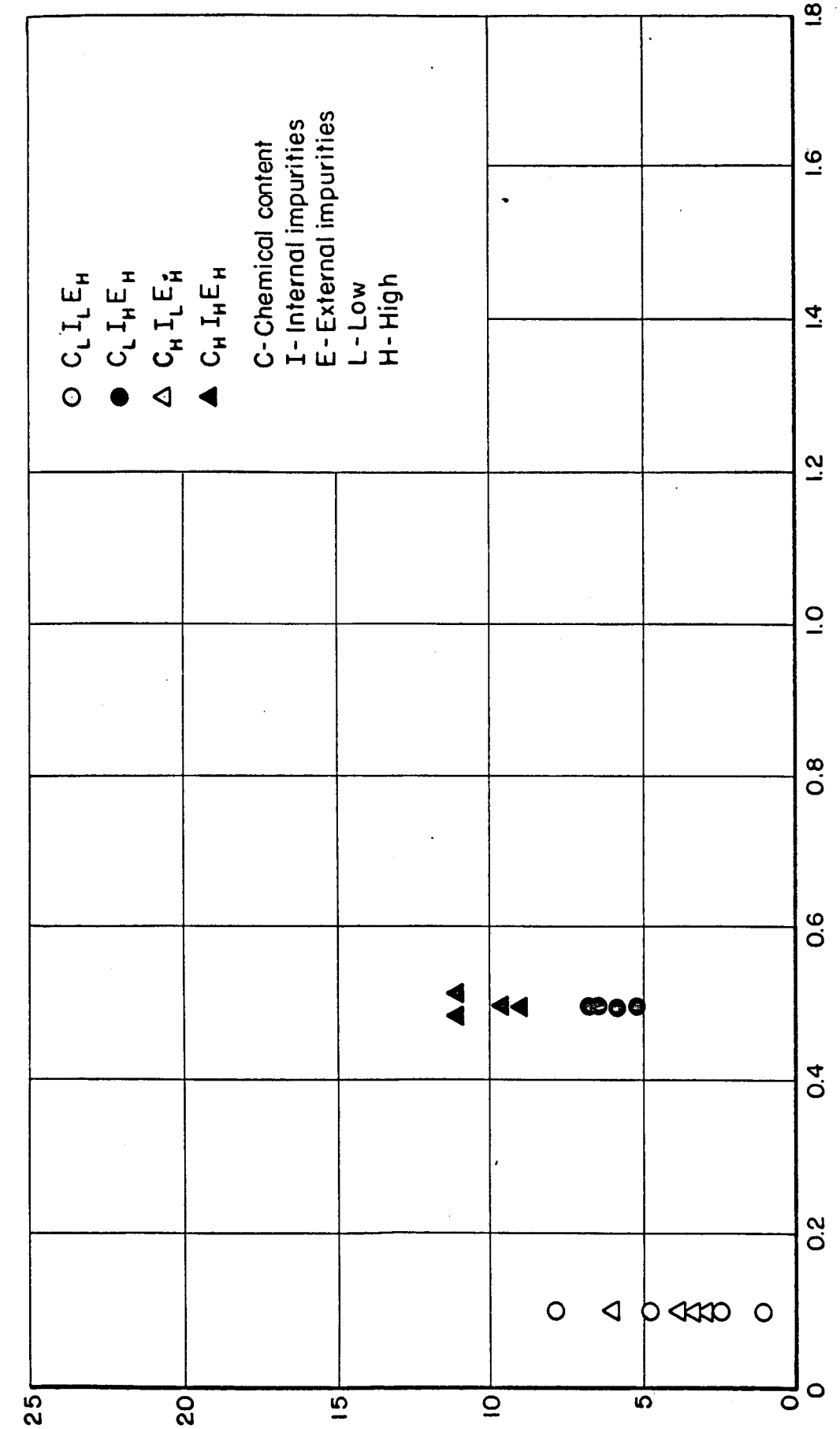

FIGURE 31. RELATIONSHIP OF POROSITY LEVEL TO HYDROGEN CONTENT FOR 3/4-INCH-THICK X2219 BASE PLATE

Each plotted point denotes an average plate porosity.

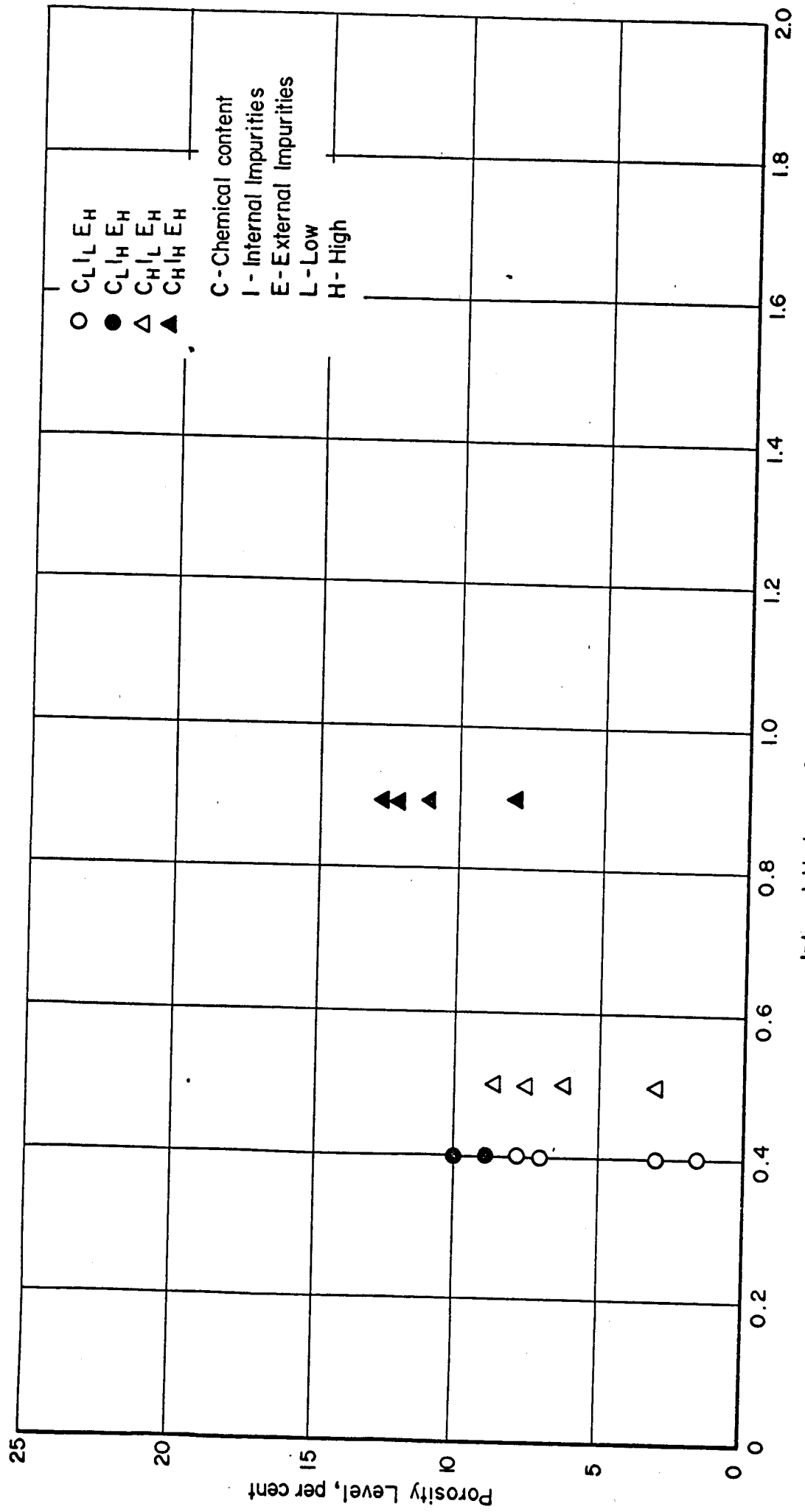

FIGURE 32. RELATIONSHIP OF POROSITY LEVEL TO HYDROGEN CONTENT FOR 1/4-INCH-THICK X2014 BASE PLATE

Each plotted point denotes an average plate porosity.

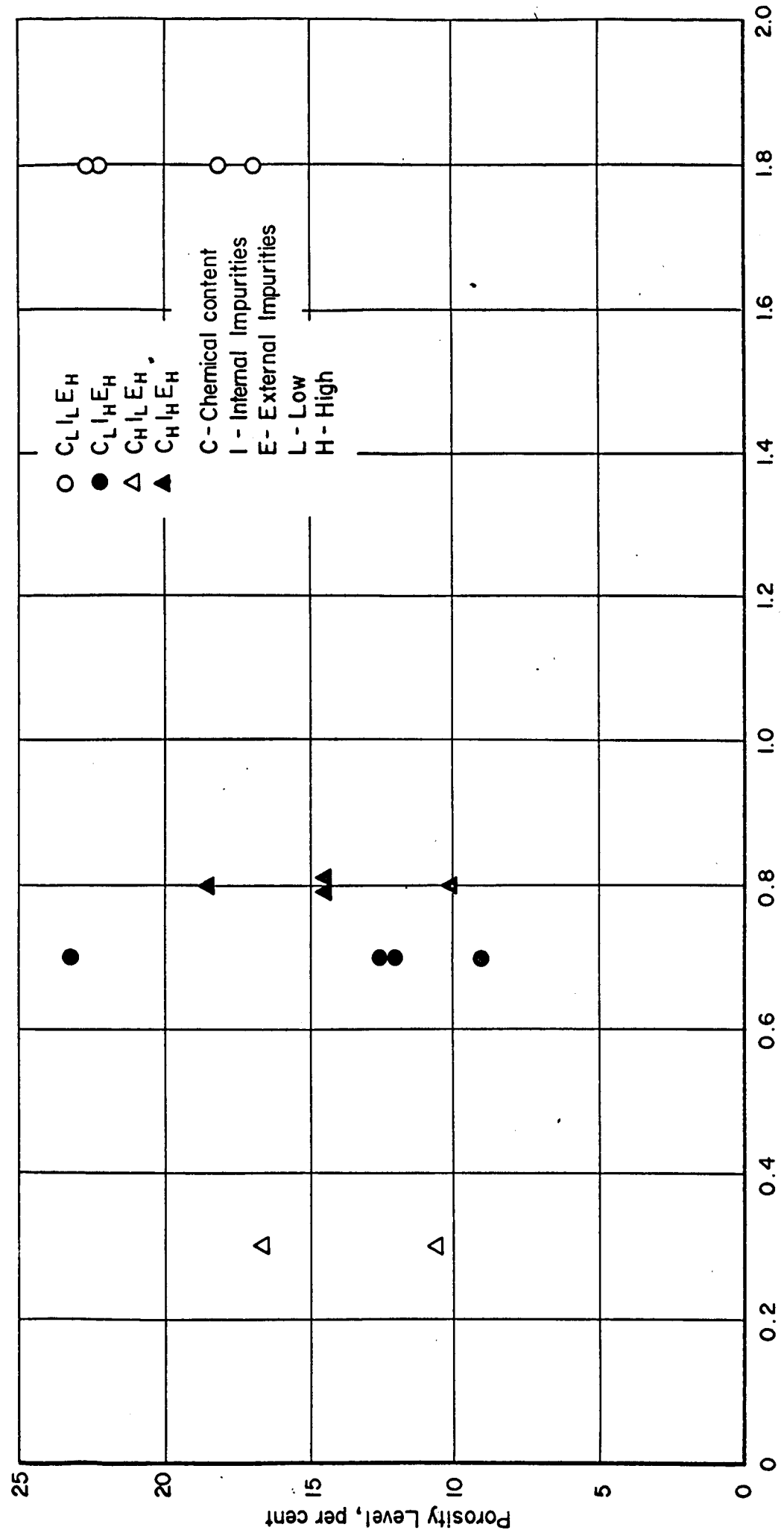

FIGURE 33. RELATIONSHIP OF POROSITY LEVEL TO HYDROGEN CONTENT FOR 3/4-INCH-THICK X2014 BASE PLATE

Each plotted point denotes an average plate porosity.

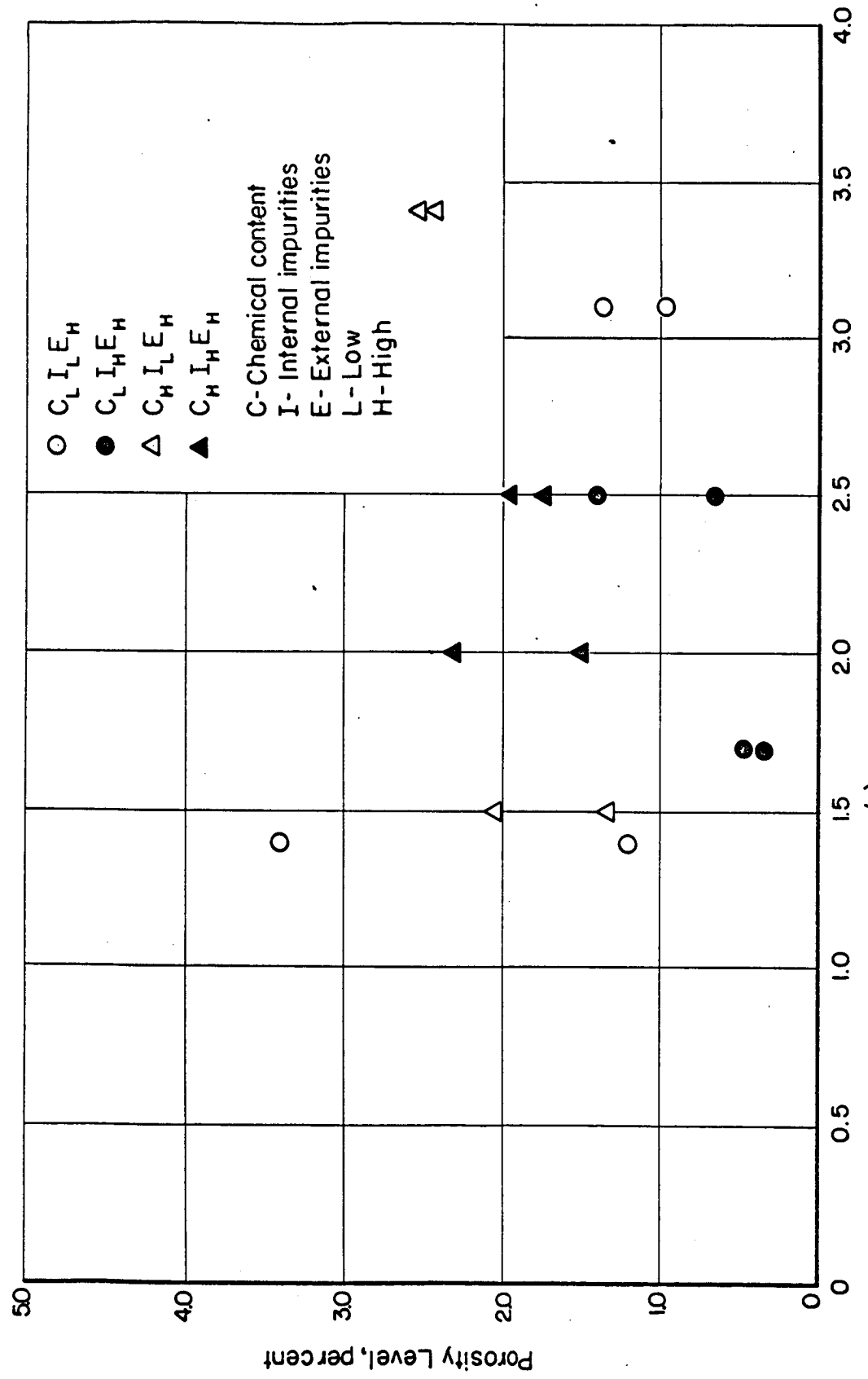

FIGURE 34. RELATIONSHIP OF POROSITY LEVEL TO HYDROGEN CONTENT FOR X2319 WIRE

1/4-inch-thick 2219 base plate.
Each plotted point denotes an average plate porosity level.
(a) See previous text.

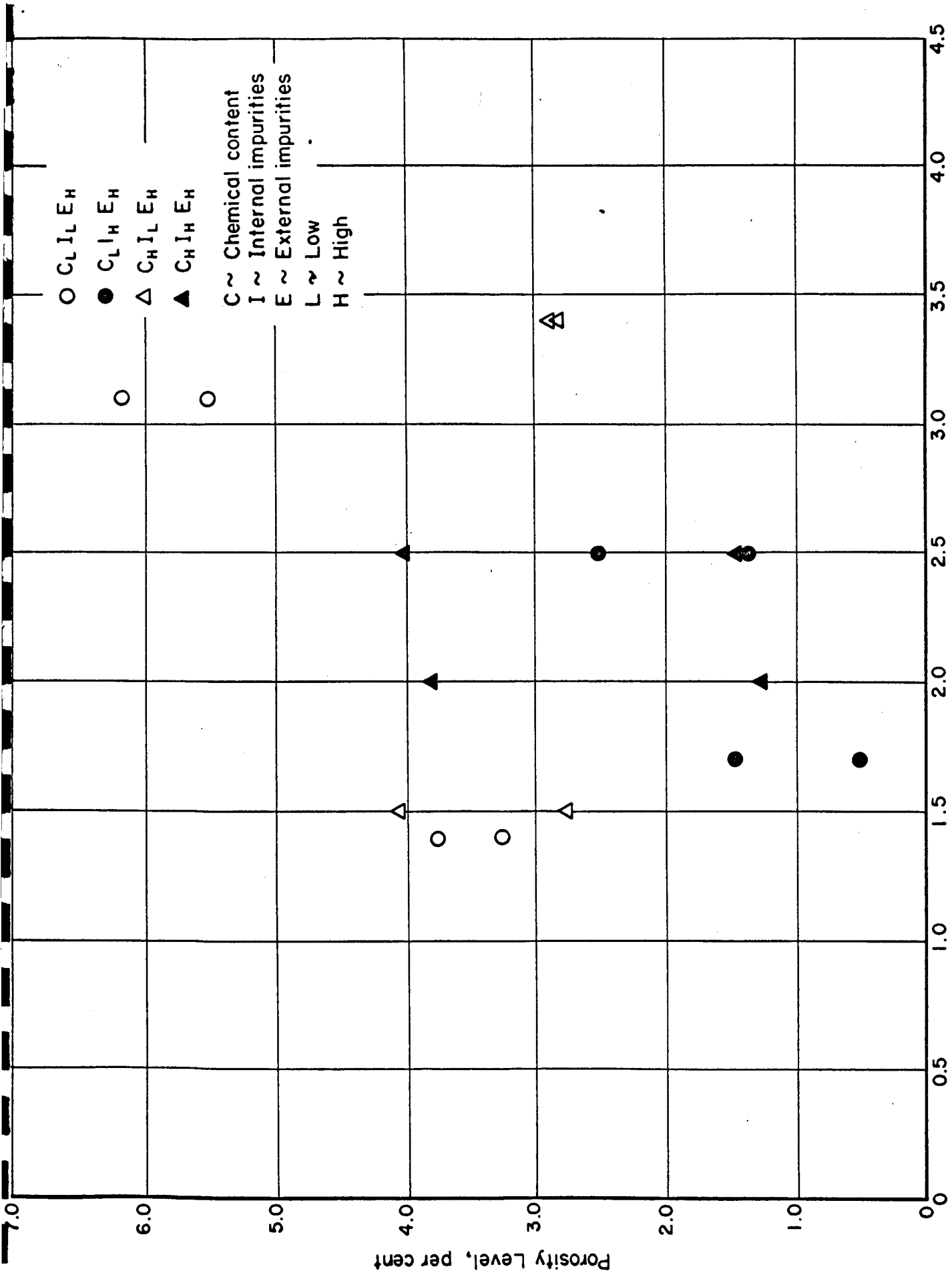

FIGURE 35. RELATIONSHIP OF POROSITY LEVEL TO HYDROGEN CONTENT FOR X2319 WIRE

3/4-inch-thick 2219 base plate
Each plotted point denotes an average plate porosity level.
(a) See previous text.

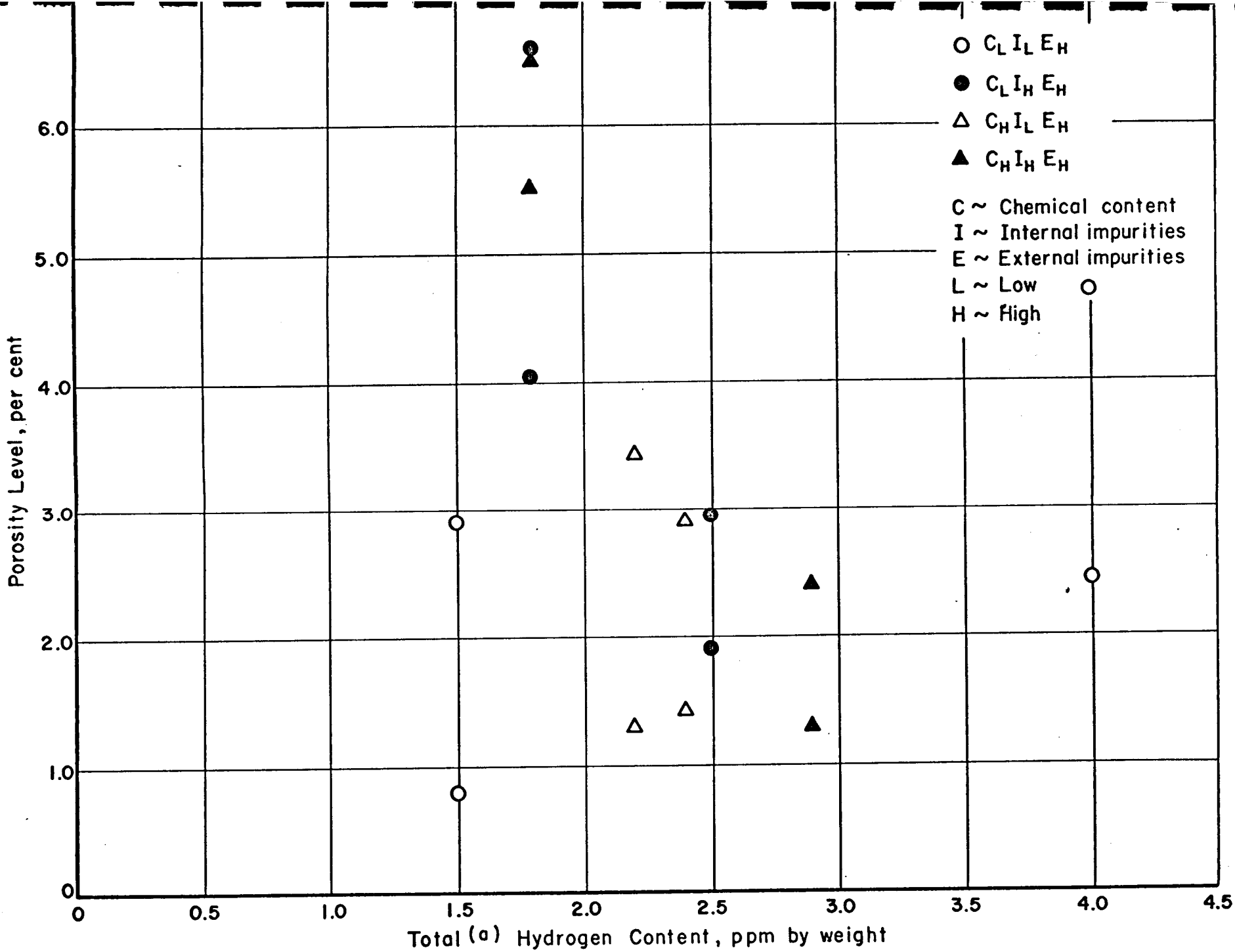

FIGURE 36. RELATIONSHIP OF POROSITY LEVEL TO HYDROGEN CONTENT OF X4043 WIRE

1/4-inch-thick 2014 plate.
Each plotted point denotes an average plate porosity level.
(a) See previous text.

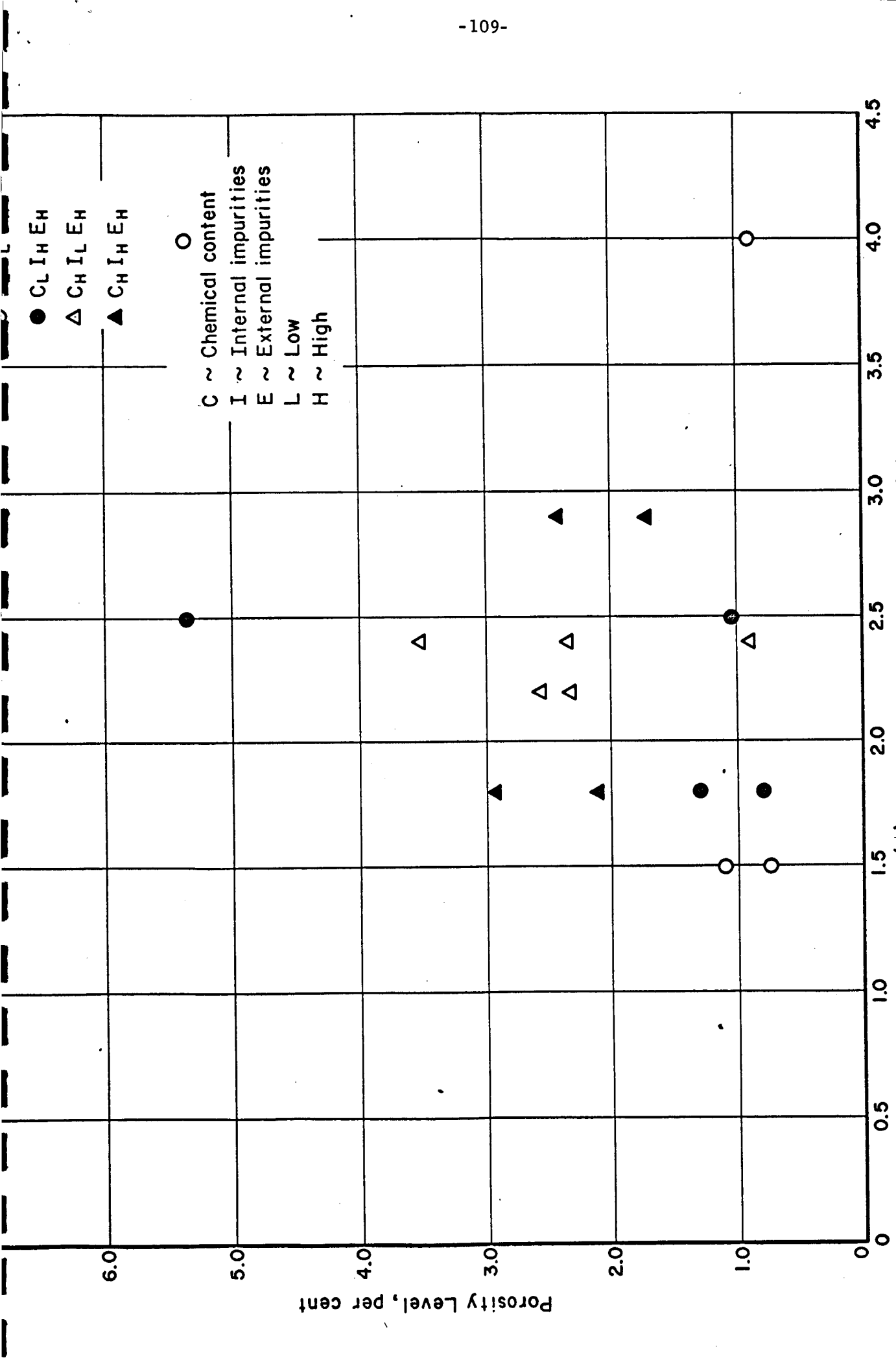

FIGURE 37. RELATIONSHIP OF POROSITY LEVEL TO HYDROGEN CONTENT OF X4043 WIRE
3/4-inch-thick 2014 base plate.
Each plotted point denotes an average plate porosity level.
(a) See previous text.

TABLE 25. AVERAGE POROSITY LEVEL AND STANDARD DEVIATION

Type	1/4-Inch Thick Base Plate		3/4-Inch Thick Base Plate	
	Average Porosity Level, percent	Standard Deviation, percent	Average Porosity Level, percent	Standard Deviation, percent
		X2219 Base Plate		
1(a)	0	----	0	----
2(a)	0	----	0	----
3	4.9	2.14	6.0	3.29
4	4.0	2.83	4.3	3.26
5(a)	0	----	0	----
6(a)	0	----	0	----
7	3.7	1.32	3.9	2.07
8	7.2	2.54	10.2	2.84
		X2014 Base Plate		
1(a)	0	----	0	----
2(a)	0	----	0	----
3	9.6	1.20	14.2	5.95
4	4.9	3.13	19.7	3.51
5(a)	3.1	2.58	0	----
6(a)	3.0	1.46	0	----
7	6.1	2.22	13.5	4.64
8	11.1	2.23	15.3	3.80
		X2319 Filler Wire		
1	2.3	1.51	3.0	1.34
2	0.4	0.03	1.0	0.61
3	1.0	0.66	2.2	0.53
4	1.2	0.57	5.8	1.76
5	2.5	0.39	2.8	0.42
6	1.9	1.20	2.7	1.49
7	1.7	0.47	3.4	0.77
8	1.9	0.66	2.5	2.03
		X4043 Filler Wire		
1	1.9	1.32	0.9	0.32
2	5.6	1.46	1.1	0.30
3	2.4	0.64	2.3	1.43
4	3.6	2.02	3.1	2.67
5	2.2	0.86	2.9	1.10
6	6.0	1.08	2.5	1.18
7	2.4	1.41	2.4	0.62
8	1.9	1.24	2.1	0.57

(a) Welded with low external impurities.

DISCUSSION OF PROGRAM RESULTS

The results obtained during the program allowed a large number of conclusions to be drawn regarding the effects of welding material composition upon weld defects. Additional conclusions which were related to the program were also made.

Effects of Welding Material Composition

The results of the program are based upon the study of welds made using eight experimental compositions of two base plate alloys and eight experimental compositions of two filler metal alloys each deposited upon two thicknesses of commercial base plate. Two of the experimental alloys, X2219 and X2319, studied, were variations of the same basic alloy. The X2014 alloy is similar to X2219 and X2319 since all three are primarily aluminum-copper alloys. The X4043 alloy differed from the other three since it is essentially an aluminum-silicon alloy. The variations of welding materials and welding conditions within the program made the drawing of conclusions of a general nature more difficult than if only one or two variations of alloy or base plate thickness had been studied.

The results of the study of the four factors of composition gave the following results.

External Impurities

The level of external impurities was the single factor to which the occurrence of weld defects was most significantly* related. In all but two of the sixteen combinations of alloy, composition, and base plate thickness welded in helium with a low (-60 F) dewpoint--low external impurities--the variations in the other three factors--chemical content, internal impurities, and hydrogen--were accompanied by very low porosity levels. The two exceptions were X2014 Type 5 and 6.

Stated another way--variations in chemical content, internal impurities, and gas content had no effect on porosity formation when welds were made under ideal conditions characteristic of low external impurity conditions. Welds in this series had so little porosity that it would normally be considered inconsequential.

The statistical degrees of certainty for the effect of external impurities in Phase I were the highest attained by any of the composition factors during the program (93%, 99.9%, >99.9%).

Because moisture is an external impurity which can be introduced into the welding arc because of poor shielding, leaks, or inadequate cleaning, the high significance of external impurities reaffirms the necessity of preventing moisture from entering the welding arc. Attempts to produce high quality welds with very few pores in the materials studied during this program should first concentrate on achieving low external impurity conditions in

*The word "significant" is used to denote that a high degree of certainty as calculated by statistical methods.

the welding arc. The use of special materials with the other three composition factors at specified levels can then be considered.

Chemical Content

The level of the chemical content of the materials studied was related less strongly to the weld porosity level than was external impurities. In comparison with the strength of the level of internal impurities, the significance of the level of chemical content was, apparently, slightly greater. However, the results of the statistical analysis of most of the paired comparisons indicated a strong interaction between chemical content and internal impurities. For example when internal impurities, gas content (0.1 ppm) and external impurities remained constant, the change in the porosity level was not significant when the level of chemical content for 1/4-inch-thick X2219 base plate was changed. However, when internal impurities and external impurities remained at the same level as previously, and hydrogen content was held constant at 0.5 ppm, an increased porosity level was related to the increased chemical content level with a 99.8% degree of certainty. This behavior was also noted for welds made on 1/4-inch-thick commercial base plate with X2319 filler wire with a 97.8% degree of certainty.

The comparisons for X4043 filler do not show the interaction between chemical content and internal impurities quite as clearly because the necessary paired comparisons could not be arranged from the results. For welds on both

1/4- and 3/4-inch-thick 2014 base plate using X4043 filler wire, the change in porosity level for a change from low chemical content and high internal impurities to high chemical content and low internal impurities was not significant (external impurities fixed, hydrogen content 2.4 and 2.5 ppm). For the same materials, the porosity level increased as chemical content and internal impurities both increased from low to high (external impurities fixed, hydrogen content at 1.5 and 1.8 ppm) with a degree of certainty of 91% (for the 1/4-inch-thick base plate and 93% for the 3/4-inch-thick base plate. The behavior of all of the materials studied indicates that a general interaction occurred between chemical content and internal impurities which strongly affected the relationship of the weld porosity level to the level of each separate factor. In general, as long as the chemical content remained low, changes in the internal impurity level did not change the porosity level signficantly.

Internal Impurities

The significance of the level of internal impurities upon the resulting weld porosity, as previously discussed, was minor compared to external impurities and was probably somewhat less than that of chemical content. Changes in the porosity level for welds on X2319 and X4043 in both base plate thickness were related to changes in the internal impurity level with anywhere from no degree of certainty to a low (87.5%) degree of certainty in all but

one case. For X4043 filler wire used with 1/4-inch-thick 2014 base plate, a decrease in porosity level was related to an increase in internal impurity level with a 91% degree of certainty when the external impurities and chemical content remained fixed at high levels. The relationship of the decreasing porosity level appears anomalous when compared to the previous observations.

Apparently, an increase in the level of the weld porosity was related significantly to an increase in the internal impurity level when the chemical content was high.

Hydrogen Content

The effect of the level of the hydrogen content upon weld defect occurrence had the lowest significance for all of the paired comparisons of the four composition factors. This was partly due to the inability to study the effect of the hydrogen content for the base plate where the experimental material made up 100% of the weld metal. The only direct comparisons of the effect of the hydrogen content were made for the experimental filler wire which composed an estimated 10 to 20% of the weld metal. The result of increasing the hydrogen content as much as 1.9 ppm was a small increase (with a degree of certainty of 81 to 85%) or an insignificant change in the porosity level of welds made with X2319 filler wire. Of 6 comparisons for welds using X4043 filler wire with increasing hydrogen content, only 2 showed that the changes in weld porosity level were significant. The change in hydrogen content from 1.8 to 2.9 ppm (high chemical content, internal impurities, and external impurities)accompanied a decrease in porosity level with a high (97.1%) degree of certainty for X4043 filler wire on 1/4-inch-thick base plate. This result is anomalous and contradictory when compared to the other program results.

The relationship observed between the hydrogen content and the experimental base plate composition as in Figure 27 might possibly explain why increasing porosity levels accompanied the increasing hydrogen contents in Figures 30 through 32. Since an increasing level of hydrogen content and porosity level have each been separately related with a high degree of certainty to increasing levels of the chemical content and the internal impurities in three specific examples, then a plot of these two variables (hydrogen content and porosity level) should show a linear relationship for welds on experimental base plate such as in Figures 30 through 32. However, none of the observed relationships indicate whether hydrogen content, hydrogen content and material composition, or both have a cause and effect relationship with the weld porosity level. The results of the program would indicate that changes in both the hydrogen content and material composition of the base plate cause changes in the porosity level.

Comparison of the Material Compositions

Inspection of Table 25 in which the average porosity levels and standard deviations are tabulated, allows selection of the material type that had the highest porosity level with a relatively small standard deviation for each thickness and alloy. After considering the standard deviation the material types in Table 26 were selected as the welds with the most consistent high porosity level for each thickness and type. These selections indicate that materials with a high level of chemical content, internal impurities,

TABLE 26. MATERIAL TYPES WHOSE WELDS HAD THE MOST CONSISTENT HIGH POROSITY LEVEL

Material	Type	Base Plate Thickness, inch	Composition		Hydrogen Content, ppm
			Chemical Content	Internal Impurities	
X2219	8	1/4	High	High	0.7
X2219	8	3/4	High	High	0.5
X2014	8	1/4	High	High	0.9
X2014	4	3/4	Low	Low	1.8
X2319	5	1/4	High	Low	3.4
X2319	7	3/4	High	Low	1.5
X4043	6	1/4	High	High	1.8
X4043	5	3/4	High	Low	2.4

and hydrogen content have a higher defect potential. However, the results of Table 26 do seem to indicate that the weld defect potential is high for a high chemical content level regardless of the internal impurity level. The single exception to the requirement of a high chemical content was 3/4-inch-thick X2014 Type 4 base plate which had both a low chemical content and internal impurities content. The hydrogen content of this composition (1.8 ppm) was achieved by placing a moistened graphite rod in the molten aluminum. This was more than 2 times higher than the hydrogen content of any other X2014 base plate which was welded with high external impurities (3/4-inch-thick Type 8 was 0.8 ppm). This single observation would indicate that the porosity level of the welds on experimental X2014 base plate was strongly related to the hydrogen content of 1.9 ppm. However, statistical statements on the effect of the hydrogen content upon the base plate weld porosity level could not be made. For this reason, the level is unknown at which the porosity level of welds on experimental base plate is more significantly related to the hydrogen content than to the chemical content or internal impurities.

Metallurgical Considerations

The causes for the dependence of weld porosity occurrence upon the welding material composition are metallurgical in nature. The individual relationships of the weld composition to (1) the kinds and amounts of intermetallic formed, (2) the freezing range of the alloy, and (3) the dendritic

growth all combine to form a complex metallurgical situation that must be analyzed to develop a hypothesis explaining pore formation. Salter and Milner (Reference 4 in Appendix G) have stated that the predominant form of porosity in aluminum welds is numerous, round pores which they would expect only if the pores were primarily bubbles formed mainly in the liquid and were then frozen by the advancing solidification front. If this observation were true in all cases, the inference from their statement would be that understanding the nucleation and growth of pores in aluminum would be of great value to determine how porosity might be minimized. However, the role of composition in supplying the intermetallics which form interfaces to allow nucleation of hydrogen bubbles would also be of equal importance in nucleation studies. The observation in this program of segregation layers within the weld and the preferential occurrence of pores within the impoverished regions again imply the dependence of pore formation upon weld composition. In this case, the freezing range and dendritic growth dependence upon weld composition would be more important factors. Brown and Adams present a discussion of the solidification rate of 2014 aluminum alloy in Reference 1 and point out that 0.9% silicon content is probably as influential as 4.4% copper in controlling the dendrite configuration in welds.

Thus, it can be readily seen that any study of porosity formation which does not consider variations in composition of the alloys studied could yield results of limited applicability. Also, it should be noted that any technique of welding which would change the segregation pattern of the weld or which would somehow affect hydrogen bubble nucleation could be expected to change the weld porosity level, pore distribution, or both.

Discussion of Other Results

Other results related to, but not pertaining directly to the objective of this program were obtained.

Pore Formation

The observation illustrated in Figure 22 of preferential occurrence of pores within the less hard (impoverished) segregation layers when combined with the observed appearance of cross sections such as Figure 23 implies that the form of the ordering of the pores within the welds was related to the composition of the weld metal. A comparison of microphotographs such as Figures E3 and E4 in Appendix E indicates that the size of pores in the experimental X2219 base plate of the same hydrogen content is possibly related to the chemical content and internal impurity level or the hydrogen content, or both of the base plate. The implication of these observations is that pore size and pore occurrence can be controlled by the welding material composition or by other factors which affect weld solidification so that a porosity distribution could be achieved that could have little effect upon the weld joint performance. Other factors which control or affect weld solidification are time-temperature relationships of the weld metal or outside effects such as stirring or agitating the solidifying weld metal.

The ordering of the pores into layers or zones along the weld (as shown by Figure 23) explains why the variations in porosity level along the same weld were so great. Because the pores were not uniformly distributed along the weld, the random sections taken along the welds could not be expected to have the same porosity level. Any investigation of porosity in welds which determines the amount of porosity present by methods similar to those used within the program should plan on examining several sections per weld.

Effect of Arc Variations

The statistical study of the effect of exceeding the maximum arc variations specified for the program (given in Table 14) indicated that the limits imposed were unnecessary for successful completion of the program. The lack of significant difference between microphotographs of weld sections where specified maximum arc variations were and were not exceeded may have been due partly to the wide variation in porosity levels that occurred along the welds studied. Possibly, if the standard deviation of the porosity level along a weld was small enough, the effect of exceeding the arc variations might have been apparent. However, this effect probably would still have been small.

The weld sections which were cut out for microphotographs during the program were carefully taken at points where the arc variations did not exceed the specified maximum variations by more than 1-1/2 times.

Electrode Shape

The variations of the arc voltage and arc current were successfully decreased by proper selection of the tungsten electrode shape. In addition, weld penetration could be increased by changing the electrode shape and keeping the arc voltage and current constant. The significant effects that the tungsten electrode configuration had on the welds requires that a standard shape should be used in gas, tungsten-arc welding where reproducible, and carefully-controlled welding conditions are desired.

Arc Contaminant Monitor

The observed variation in the arc voltage and current waveforms when the arc contained moisture could form the basis of a very simple and uncomplicated monitor of the shielding gas quality. An oscilloscope or a more sophisticated electronic counting circuit and electrical connnections to the welding electrodes would be required. The operator could monitor the arc waveforms on the oscilloscope and shut off the welding process if spikes or inflection points developed on the oscilloscope traces. These inflection points are characteristic of a welding arc in a contaminated atmosphere. The other type of monitor could simply count the spikes or measure the abruptness of changes in the arc waveforms over a fixed period of time. When the count or inflections exceed a preset level, the monitor would signal the welding operator or would shut down the welding process.

The potential simplicity of using this sort of system for monitoring shielding gas purity is a significant consideration. The monitors could be easily installed on welding fixtures with no increase in bulk within the immediate welding area. The monitor itself could be placed at any convenient point and could be composed of off-the-shelf electrical instruments or components.

CONCLUSIONS

On the basis of the observations, results, and statistical analyses of the program, five major conclusions were made.

Effect of the Four Factors

The relative strength of the relationship between weld porosity (the only weld defect observed) and each of the four factors was determined primarily by the statistical analyses. The factors are listed in a general order of decreasing significance of the relation of porosity level to the factor for the materials studied:

1. External impurities
2. Chemical content
3. Internal impurities
4. Hydrogen content.

The level of the external impurities had the strongest influence of any of the factors on the occurrence of weld porosity. The factor of the porosity level was not as significantly related to the factor of chemical content as to external impurities but was stronger than the relation to internal impurities. An interaction existed between the factors of chemical content and internal impurities such that the relationship of weld porosity to the level of one factor was dependent upon the level of the other factor. Increasing weld porosity levels were related to increasing base plate hydrogen content but an interaction between the material composition and hydrogen content prevented any conclusions regarding a definite cause and effect relationship. For X2014 base plate, however, a hydrogen content of 1.8 ppm, by weight, was sufficient to overshadow the strength of the chemical content and internal impurities to cause a high porosity level. For the filler wires studied, changes in the porosity level were not significant for changes in the hydrogen content of up to 1.9 ppm, by weight, except in one anomalous result where an increasing porosity level was related to a decreased hydrogen content. The weld defect potential for welds made with the materials studied would be lowest when all four factors (chemical content, internal impurities, hydrogen content, and external impurities) were low.

Pore Occurrence and Weld Composition

The composition of the weld metal was related to the pore size and the pore distribution within the welds. Segregation layers of alternately enriched and impoverished weld metal occurred regularly within the weld in groupings that depended upon the weld composition. Pores within the welds grouped themselves preferentially in the impoverished segregation layers.

Hydrogen Content and Base Plate Composition

The hydrogen content of the experimental X2219-T87 and X2014-T6 base plate was quite independent of the chlorination times and melting atmosphere. The hydrogen content of the experimental base plate significantly increased as the plate composition was increased from low chemical content and low internal impurities to high chemical content and high internal impurities. The filler wire internal hydrogen content was controlled well by the casting methods used.

Hydrogen Content and Porosity Level

As the hydrogen content of the experimental base plate increased, the weld porosity level of welds on the base plate also increased. This was probably partly due to the interaction of the material composition and hydrogen content. For 1/4-inch-thick X2014 plate, an internal hydrogen content of 1.9 ppm appeared to cause a high porosity level. Increasing hydrogen content of the filler metals for the levels studied was not related to increasing weld porosity levels.

Arc Waveform and Shielding Gas

The arc voltage and arc amperage waveforms changed from smooth waveforms when the weld shielding gas contained essentially no moisture to irregular waveforms with large numbers of inflections when the arc shielding gas contained water vapor. The arc voltage waveform also changed shape when contaminants were present in the shielding gas.

RECOMMENDATIONS

The following recommendations are made to assist in using the results of this program.

External Impurities

All possible sources of moisture contamination of the welding arc should be minimized when critical aluminum alloy assemblies composed of the materials studied in this program are welded. A means should be provided to determine the actual quality of the weld shielding gas in the arc during the welding of aluminum alloys.

Minimization of Weld Defect Potential

One or more of three basic approaches to the minimization of the weld defect potential for the materials studied should be followed. Each approach would determine and decrease the defect potential of the commercial materials to a degree depending upon the available time and applicable priority considerations.

Approach 1

In accordance with the conclusions of this investigation, the specifications for chemical content should be lowered to approach the low levels used in this study*. The ranges of hydrogen content of the commercial materials should be determined initially until the analyses show the variations of hydrogen content to be at a level low enough to have little weld defect potential.

Approach 2

An extensive testing program should be conducted to determine the magnitude of variations in hydrogen content, chemical content, and internal impurity content of commercial base plate and filler wire. These results would be used with the conclusions of this program to draw up material specifications.

Approach 3

A determination should be made of the relation of intermediate levels of chemical content and internal impurities or of specific metallic elements to the weld defect potential. This determination could take a new program approach or an approach extending this program.

---

* Before such changes are made, due consideration should be given to the consequences of such an action. Lowering the specified chemical content may impose undue restrictions on the aluminum producers and may also affect other alloy properties such as strength or stress corrosion resistance.

The new approach would require casting, fabricating, welding, and defect analysis of large numbers of plate compositions. The extension approach would study presently existing welds in existing variations of weld metal composition. This study would be similar to the extension proposed April 6, 1965, by Battelle to NASA-MSFC. The location of hydrogen would be determined within the weld and the base plate metal and any relationship between the occurrence of the hydrogen with any particular element would be identified. In addition, the relative significance of the base plate hydrogen content to the weld porosity level should be determined. The occurrence of pores should also be related, if possible, to specific metallic elements by this examination.

Pore Formation

Studies of the effect of specific elements upon the occurrence of porosity on a microscopic scale should be conducted as in the extension proposed by Battelle to NASA-MSFC on April 6, 1965. The composition of the segregation layers observed in welds and distribution of hydrogen within the segregation layers should be determined so that the effect of weld composition upon pore size and distribution can be understood rather than observed. These studies can result in the recommendation of welding material composition, which will distribute porosity in a weld at points and in sizes that will not impair the performance of the welded joint.

Hydrogen Content

After determination of the variations of hydrogen content of the materials studied, the hydrogen content of the materials studied during the program does not need to be specified or tested regularly if the hydrogen content of the base plate materials supplied is, generally, under 1.0 ppm, by weight. The hydrogen content of the filler wire should be of little concern if the internal hydrogen content of the filler wire is less than 3.0 ppm, as determined by the Battelle vacuum-fusion method. This limit could possibly be higher because the hydrogen contents of the filler wire studied were never much higher than 3 ppm.

Welding Arc Monitor

A feasibility study of the arc atmosphere monitor described in this report should be made. This study should determine the specific cause of the inflection points on the arc waveforms when the arc atmosphere is contaminated. The study should determine the sensitivity of the system, the applicability of the monitor to different power supplies, and the level at which the monitor should indicate contamination of the arc.

All data compiled during this project are in Battelle Laboratory Books Nos. 21573 and 21574.

APPENDIX A

CASTING AND FABRICATION DATA

TABLE A-1. COMMERCIAL MATERIALS USED DURING CASTING

Material	Source	Reported Analyses					
		Mn	Si	Fe	Ca	Zr	Ga
Super Purity Aluminum							
Lot 674-1 (1500 lb)	Apex Smelting Co.	0.001	0.003	0.001	0.002	0.001	--
50157-4 (170 lb)	Ditto	--	0.004	0.001	--	0.001	0.003
54297-4 (360 lb)	"	0.001	0.003	0.002	--	0.001	0.002
50639 (310 lb)	"	0.001	0.002	0.001	--	0.002	0.002
Al-50Cu Master	Foote Mineral Co.	49.2Cu-0.2Fe, 0.01Si, <0.05Mn, <0.05Mg 0.05Zn					
Al-25Si Master	Ditto	24.7Si					
Al-6Ti Master	"	5.93Ti, 0.29Fe, 0.24Si, 0.13V, 0.02Cu, <0.02Mg, <0.02Zn, <0.01Mn					
Al-25Mn Master	"	26.0Mn, 0.09Fe, 0.08Si, 0.03Cu, <0.02Zn <0.02Mg					
Al-2-1/2V Master	"	2.60V, 0.22Fe, 0.027Si					
Al-10Cr Master	"	10.6Cr, 0.12Fe, 0.019Si					
High Purity Silicon							
Grade No.3 (2.2 lb)	Dow Corning Corp.						
Sub Solar Grade 2 lb)	E.I.duPont deNemours and Co., Inc.						
Zone Refined (15 lb)	Foote Mineral Co.						
Copper	Battelle stock	OFHC					
Iron	Ditto	Standard purity					
Magnesium	"	>99.8Mg					
Zinc	"	>99.99Zn					
Zirconium	"	High-purity sponge zirconium					

TABLE A-2. HIGH-PURITY MASTER ALLOYS PREPARED AT BATTELLE

Nominal Composition	Amount, pounds	Analysis, weight percent
Al-25Cu		
No.1	60	24.8Cu
No.2	60	25.1Cu
No.3	60	25.3Cu
Al-20Si	11	18.6Si
Al-10Fe		
No.1a	2.5	8.58Fe
No.1b	6.0	6.42Fe
No.2	28	9.66Fe
No.3	9.5	7.49Fe
No.4	20	9.90Fe
Al-17.5Cu-7.5Zr	~1 each	Individual arc-melted master alloys made for each zirconium addition

TABLE A-3. MELTING AND CASTING CONDITIONS FOR X2219 INGOTS

Melt Number	X2219-1	X2219-2	X2219-3	X2219-4
Date Melted	10/6/64 pm	9/17/64 am	9/17/64 pm	10/9/64 pm
Average Temperature, F	70	76	80	70
Average Humidity, %	35	82	74	39
Order of Alloying and Temperature (F) at Start of Addition	Al-Cu:1230 Al-Mn:1350 Al-Cu-Zr:1450 Al-V:1460 Al-Ti:1450	Al-Cu Al-Si Zn:1240 Al-Mn:1350 Al-Cu-Zr:1445 Al-V:1465 Al-Ti:1460 Al-Fe:1460 Mg:1450	Al-Cu Al-Si Zn:1225 Al-Mn:1345 Al-Cu-Zr:1430 Al-V:1460 Al-Ti:1450 Al-Fe:1480 Mg:1450	Al-Cu:1230 Al-Mn:1340 Al-Cu-Zr:1460 Al-V:1460 Al-Ti:1460
Total Time First Heating,[a] min	77	56	68	73
Alloying Time, min	55	29	23	43
Cl_2 Time, min	15	11	20	7
Cl_2 Temperature Range, F	1440-1380	1485 → 1510	1440 → 1365	1475-1510
Hold Time, min	7	19	8	23[b]
Maximum Temperature, F	1495	1510	1498	1520
Casting Temperature, F	1290	1325	1300	1300
Total Time Second Heating,[b] min	57	39	60	37
Cl_2 Time, min	12	8	14	6
Cl_2 Temperature Range, F	1450-1385	1470 → 1533	1450 → 1398	1420-1470
Hold Time, min	9	11	6	14
Maximum Temperature, F	1505	1533	1510	1470
Casting Temperature, F	1280	1350	1300	1300

TABLE A-3. (CONTINUED)

Melt Number	X2219-5	X2219-6	X2219-7	X2219-8
Date Melted	10/9/64 am	9/16/64 am	10/6/64 am	9/16/64 pm
Average Temperature, F	70	68	68	82
Average Humidity, %	48	72	50	58
Order of Alloying and Temperature (F) at Start of Addition	Al-Cu:1220 Al-Mn:1335 Al-Cu-Zr:1435 Al-V:1445 Al-Ti:1450	Al-Cu Al-Si Zn:1345 Al-Mn:1380 Al-Cu-Zr:1430 Al-V:1460 Al-Ti:1460 Al-Fe:1460 Mg:1450	Al-Cu:1230 Al-Mn:1350 Al-Cu-Zr:1360 Al-V:1450 Al-Ti:1460	Al-Cu Al-Si Zn:1225 Al-Mn:1350 Al-Cu-Zr:1400 Al-V:1405 Al-Ti:1410 Al-Fe:1410 Mg:1495
Total Time First Heating,[a] min	82	80	79	71
Alloying Time, min	55	20	55	17
Cl_2 Time, min	8	14	16	15
Cl_2 Temperature Range, F	1430-1480	1410 → 1330	1465-1380	1425 → 1545 ← 1470
Hold Time, min	19[b]	8	8	19
Maximum Temperature, F	1480	1500	1510	1545
Casting Temperature, F	1320	1320	1300	1300
Total Time Second Heating,[c] min	30	50	44	46
Cl_2 Time, min	5	15	10	12
Cl_2 Temperature Range, F	1425-1485	1510 → 1395	1465-1375	1420 → 1545 ← 1410
Hold Time, min	13[c]	8	4	7
Maximum Temperature, F	1490	1510	1495	1545
Casting Temperature, F	1350	1300	1290	1350

(a) Ingot for 3/4-inch-thick plate

(b) Fuel gas burned over melt for 5 minutes at start of hold period with mild stirring of melt.

(c) Ingot for 1/4-inch-thick plate

TABLE A-4. MELTING AND CASTING CONDITIONS FOR X2014 INGOTS

Melt Number	X2014-1	X2014-2	X2014-2	X2014-3	X2014-4
Date Melted	10/19/64	8/27/64	10/21/64	8/27/64	10/23/64
Average Temperature, F	72	95	75	85	73
Average Humidity, %	35	65	31	68	28
Order of Alloying and Temperature (F) at Start of Addition	Al-Cu:1230 Al-Si:1335 Al-Mn:1330 Mg:1385	Al-Si:1240 Al-Cu:1240 Zn:1220 Al-Mn:1295 Al-Cr:1310 Al-Fe:1315 Al-Ti:1310 Mg:1380 (after Cl_2)	Al-Cu:1220 Al-Si:1235 Zn:1250 Al-Mn:1265 Al-Cr:1350 Al-Fe:1400 Al-Ti:1450 Mg:1450	Al-Si:1225 Al-Cu:1230 Zn:1235 Al-Mn:1300 Al-Cr:1310 Al-Fe:1320 Al-Ti:1340 Mg:1480 (after Cl_2)	Al-Cu:1220 Al-Si:1310 Al-Mn:1350 Mg:1410 H_2 added[a]
Total Time First Heating,[b] min	83	--	72	75	
Alloying Time, min	50	--	37	35	
Cl_2 Time, min	--	--	--	16	
Cl_2 Temperature Range, F	--	--	--	1365→1475	
Hold Time, min	33	--	35	24	
Maximum Temperature, F	1450	--	1465	1495	
Casting Temperature, F	1310	--	1285	1370	
Total Time Second Heating,[c] min	48	54	--	28	44
Cl_2 Time, min	--	13	--	3	--
Cl_2 Temperature Range, F	--	1440→1375	--	1360→1460	--
Hold Time, min	48	8	--	17	44[a,d]
Maximum Temperature, F	1450	1450	--	1495	1475
Casting Temperature, F	1275	1280	--	1375	1325

TABLE A-4. (CONTINUED)

Melt Number	X2014-4	X2014-5	X2014-5	X2014-6	X2014-7	X2014-7	X2014-8
Date melted	11/5/64	10/21/65	10/23/64	10/20/64	10/23/64	11/5/64	10/22/64
Average Temperature,F	72	72	69	68	69	72	71
Average Humidity,%	35	35	46	38	46	35	42
Order of Alloying and Temperature (F) at Start of Addition	Scrap from 3/4-inch-thick plate which cracked during rolling Mg:1360	Al-Cu:1220 Al-Si:1250 Al-Mn:1325 Mg:1400	Al-Cu:1220 Al-Si:1280 Al-Mn:1335 Mg:1400	Al-Si:1240 Al-Cu:1320 Zn:1390 Al-Mn:1280 Al-Cr:1340 Al-Fe:1350 Al-Ti:1365 Mg:1400	Al-Cu:1220 Al-Si:1280 Al-Mn:1335 Mg:1400	Scrap from 3/4-inch-thick plate which cracked during rolling. Mg:1355	Al-Cu:1220 Al-Si:1265 Zn:1300 Al-Mn:1350 Al-Cr:1380 Al-Fe:1400 Al-Ti:1400 Mg:1420
Total Time First Heating,(b) min	34	--	70	90	--	80	85
Alloying Time, min	15	--	50	60	--	45	67
Cl_2 Time, min	10	--	--	--	--	20	--
Cl_2 Temperature Range,F	1425→1450	--	--	--	--	1400→1310	--
Hold Time, min	9	--	20(d)	30	--	15	28(d)
Maximum Temperature,F	1460	--	1470	1470	--	1470	1500
Casting Temperature,F	1350	--	1340	1275	--	1300	1320
Total Time Second Heating,(c) min	--	39	--	47	47	--	32
Cl_2 Time, min	--	--	--	--	--	--	--
Cl_2 Temperature Range,F	--	--	--	--	--	--	--
Hold Time, min	--	39	--	87	47(d)	--	32(e)
Maximum Temperature,F	--	1485	--	1460	1505	--	1495
Casting Temperature,F	--	1275	--	1290	1300	--	1325

(a) Melt stirred with graphite rod which was wet in water at frequent intervals.
(b) Ingot for 3/4-inch-thick plate.
(c) Ingot for 1/4-inch-thick plate.
(d) Fuel gas burned over melt for 10 minutes at start of hold period with mild stirring of melt.
(e) Fuel gas burned over melt for 5 minutes at start of hold period with mild stirring of melt.

TABLE A-5. MELTING AND CASTING CONDITIONS FOR X2319 INGOTS

Melt Number	X2319-1 and -4	X2319-2 and -3	X2319-6 and -8	X-2319-5 and -7
Date Melted	9/30/64 am	9/23/64 am	9/23/64 am	9/30/64 pm
Average Temperature, F	72	78	82	74
Average Humidity, %	55	68	42	46
Order of Alloying and Temperature (F) at Start of Addition	Al-Cu:<1200 Al-Mn: 1355 Al-Cu-Zn:1435 Al-V:1445 Al-Ti:1450	Al-Cu, Al-Si in melt down Zn:1230 Al-Mn:1350 Al-Cu-Zr:1450 Al-Fe:1450 Al-V:1450 Al-Ti:1454 Mg:1440 (after Cl_2)	Al-Cu, Al-Si in melt down Zn:1225 Al-Mn:1350 Al-Cu-Zr:1450 Al-Fe:1450 Al-V:1450 Al-Ti:1450 Mg:1500 (after Cl_2)	Al-Cu:1200 Al-Mn:1350 Al-Cu-Zr:1450 Al-V: 1450 Al-Ti:1450
Total Time First Heating, min	64	65	65	60
Alloying Time, min	39	41	39	40
Cl_2 Time, min	10	10	11	10
Cl_2 Temperature Range, F	1450 → 1505	1460 → 1505	1460 → 1515	1460 → 1510
Hold Time, min	15	17	15	10
Maximum Temperature, F	1505	1505	1515	1520
Casting Temperature, F	1325 (X2319-4)	1350 (X2319-2)	1325 (X2319-8)	1350 (X2319-5)
Total Time Second Heating, min	17	19	22	25
Cl_2 Time, min	1445 → 1380	15	17	17
Cl_2 Temperature Range, F	2	1410 → 1335	1390 → 1340	1440 → 1380
Hold Time, min	1455	2	3	6
Maximum Temperature, F	1300 (X2319-1)	1420	1400	1460
Casting Temperature, F		1300 (X2319-3)	1300 (X2319-6)	1300 (X2319-7)

TABLE A-6. MELTING AND CASTING CONDITIONS FOR X4043 INGOTS

Melt Number	X4043-1 and -4	X4043-2 and -3	X4043-5 and -7	X4043-6 and -8
Date Melted	1/11/65	1/12/65	1/11/65	1/12/65
Average Temperature, F	--	--	--	--
Average Humidity, %	35	40	--	--
Order of Alloying and Temperature (F) at Start of Addition	Si:1335 (a)	Si:1300 (a) Al-Cu:1310 Zn:1320 Al-Mn: 1340 Al-Ti:1345 Al-Fe:1335 Mg:1350 (b)	Si:1360 (a)	Si:1290 (a) Al-Cu:1280 Zn:1290 Al-Mn:1300 Al-Ti:1310 Al-Fe:1375 Mg:1390 (b)
Total Time First Heating, min	88	93	80	81
Alloying Time, min	49	50	40	32
Cl_2 Time, min	15	15	15	15
Cl_2 Temperature Range, F	1435→1310	1410→1350	1450→1400	1435→1390
Hold Time, min	24	28	25	24
Maximum Temperature, F	1525	1440	1505	1460
Casting Temperature, F	1280 (X4043-1)	1280 (X4043-3)	1280 (X4043-7)	1280 (X4043-6)
Total Time Second Heating, min	48	50	57	41
Cl_2 Time, min	--	--	--	--
Cl_2 Temperature, F	--	--	--	--
Hold Time, min	33 (c)	21 (d)	20 (d)	21 (d)
Maximum Temperature, F	1450	1480	1510	1455
Casting Temperature, F	1350 (X4043-4)	1350 (X4043-2)	1350 (X4043-5)	1350 (X4043-8)

(a) Silicon was added as lump silicon rather than as master alloy to minimize the chance for composition errors.
(b) Added after chlorination.
(c) Gas flame burning over melt with surface agitation for about 20 minutes.
(d) Gas flame burning over melt with surface agitation for about 15 minutes.
(e) Estimated, thermocouple defective.

TABLE A-7. SUMMARY OF HOT ROLLING OF X2219 AND X2014 BASE PLATE

Composition	Thickness, inch		Preheat Conditions		Intermediate Scalping		Rolling Temperature, F	Final Condition
	Initial	Final	Temperature, C	Time, hours	Amount per Side, inch	Thickness After Scalping, inch		
1/4-Inch-Plate Fabrication								
X2219-1	1.87	0.27	950	16	0.03	0.87	930-900	Good
-2	1.83	0.27	850	24	0.03	0.80	930-900	Good
-3	1.82	0.27	850	24	0.02	0.82	930-900	Good
-4	1.90	0.27	950	16	0.06	1.13	930-900	Good
-5	1.92	0.27	950	16	0.04	1.16	930-900	Good
-6	1.84	0.27	850	24	0.02	0.82	930-900	Good
-7	1.89	0.27	950	16	0.03	0.87	930-900	Good
-8	1.85	0.27	850	24	0.03	0.81	930-900	Good
X2014-1	1.83	0.25	880	6	0.09	1.08	870-850	Good
-2	1.92	0.25	850	24	0.03	0.80	900-880	Good
-3	1.93	0.25	850	24	0.04	1.18	900-880	Good
-4	1.90	0.25[a]	880	6	0.08	1.16	880-860	Good
-5	1.80	0.25	880	6	0.07	1.11	870-850	Good
-6	1.76	0.25[a]	880	6	0.08	1.11	850	Fair
-7	1.91	0.25	880	6	0.08	1.15	880-860	Good
-8	1.85	0.25	880	6	0.10	1.12	880-860	Good
3/4-Inch-Plate Fabrication								
X2219-1	2.36	0.82	950	16	0.05	1.03	930-900	Good
-2	2.35	0.81	850	24	0.05	1.16	930-900	Good
-3	2.35	0.81	850	24	0.04	1.18	930	Good
-4	2.35	0.81	950	16	0.06	1.01	930-900	Good
-5	2.36	0.82	950	16	0.08	1.38	930-900	Good
-6	2.38	0.82	850	24	0.03	1.14	930-900	Good
-7	2.37	0.81	950	16	0.06	1.01	930-900	Good
-8	2.32	0.81	850	24	0.03	1.14	930-900	Good
X2014-1	2.29	0.75	880	6	0.11	1.83	870-850	Fair
-2	2.35	0.75	880	6	0.08	1.27	870-850	Good
-3	2.39	0.75	850	24	0.05	2.04 and 1.22	900-880	Good
-4	2.35	0.75	880	6	0.15	1.11	860	Fair
-5	2.38	0.75	880	6	0.10	1.42	880-860	Good
-6	2.38	0.74	880	6	0.09	1.27	870-850	End split
-7	2.36	0.74	880	6	0.14	1.12	860	Good
-8	2.40	0.75	880	6	0.08	1.46	880-860	Good

(a) Cross rolled after intermediate surface scalping.

TABLE A-8. HOT ROLLING OF X2219 BASE PLATE

Description of Material Composition	Section[a]	Thickness, inches Initial	Final	Rolling Temperature, F	Number of Passes	Remarks
X2219-1	1	2.370	1.130	930	7	Light surface cracks
	2	2.365	1.130	930	7	Light surface cracks
	3	1.870	0.925	930	6	Very light surface cracks
X2219-1 (after surface milling)	1	1.026	0.816	900	2	Good quality
	2	1.026	0.815	900	2	Good quality
	3	0.871	0.274	900	5	Good quality
X2219-2	1	2.350	1.258	850 → 900	8	Light surface cracks
	2	2.350	1.261	850 → 900	8	Light surface cracks
	3	1.830	0.861	850 → 900	9	Very light surface cracks
X2219-2 (after surface milling)	1	1.160	0.813	930	4	Good quality
	2	1.170	0.812	930	4	Good quality
	3	0.800	0.268	930	6	Good quality
X2219-3	1	2.352	1.261	850 → 900	8	Light surface cracks
	2	2.356	1.262	850 → 900	8	Light surface cracks
	3	1.815	0.861	850 → 900	9	Very light surface cracks
X2219-3 (after surface milling)	1	1.175	0.808	930	4	Good quality
	2	1.205	0.807	930	4	Good quality
	3	0.821	0.271	930	6	Good quality
X2219-4	1	2.350	1.126	930	7	Moderate surface cracks
	2	2.310	1.127	930	7	Moderate surface cracks
	3	1.905	1.235	930	4	Light surface cracks
X2219-4 (after surface milling)	1	1.010	0.810	900	3	Good quality
	2	1.045	0.809	900	3	Good quality
	3	1.128	0.271	900	7	Good quality
X2219-5	1	2.365	1.445	930	5	Moderate surface cracks
	2	2.360	1.605	930	4	Moderate surface cracks
	3	1.920	1.237	930	4	Light surface cracks
X2219-5 (after surface milling)	1	1.293	0.816	900	5	Good quality
	2	1.479	0.817	900	6	Good quality
	3	1.164	0.272	900	7	Good quality
X2219-6	1	2.380	1.195	900	8	Light surface cracks
	2	2.400	1.193	900	8	Moderate furface cracks
	3	1.840	0.861	900	9	Very light surface cracks
X2219-6 (after surface milling)	1	1.135	0.817	930	4	Good quality
	2	1.150	0.817	930	4	Good quality
	3	0.818	0.271	930	6	Good quality
X2219-7	1	2.380	1.131	930	7	Light surface cracks
	2	2.355	1.132	930	7	Light surface cracks
	3	1.893	0.925	930	6	Very light surface cracks
X2219-7 (after surface milling)	1	1.004	0.811	900	3	Good quality
	2	1.012	0.812	900	3	Good quality
	3	0.873	0.275	900	5	Good quality

TABLE A-8. (CONTINUED)

Description of Material		Thickness, inches		Rolling Temperature, F	Number of Passes	Remarks
Composition	Section(a)	Initial	Final			
X2219-8	1	2.320	1.195	900	8	Moderate surface cracks
	2	2.330	1.195	900	8	Moderate surface cracks
	3	1.850	0.861	900	9	Very light surface cracks
X2219-8 (after surface milling)	1	1.155	0.806	930	4	Good quality
	2	1.125	0.810	930	4	Good quality
	3	0.806	0.271	930	6	Good quality

(a) Sections 1 and 2 were rolled to 3/4-inch-thick plate; Section 3 was rolled to 1/4-inch-thick plate.

TABLE A-9. HOT ROLLING OF X2014 BASE PLATE

Description of Material		Thickness, inches		Rolling Temperature, F	Number of Passes	Remarks
Composition	Section(a)	Initial	Final			
X2014-1	1	2.286	2.087	870	2	Heavy surface cracking
	2	2.292	2.015	870	2	Heavy surface cracking
	3	1.834	1.270	870	4	Heavy surface cracking
X2014-1 (after surface milling)	1	1.829	0.752	870-850	9	Fair quality, edge cracks
	2	1.830	0.747	870-850	9	Fair quality, edge cracks
	3	1.084	0.248	850	11	Good quality
X2014-2	1	2.349	1.445	870	5	Slight surface cracking
	2	2.353	1.445	870	5	Slight surface cracking
	3	1.915	0.866		9	Very light surface cracks
X2014-2 (after surface milling)	1	1.300	0.751	850	6	Good quality
	2	1.270	0.748	850	6	Good quality
	3	0.803	0.250	880	5	Good quality
X2014-3	1	2.394	2.130	850→900	3	Deep edge crack
	2	2.394	1.260	850→900	8	Light surface cracks
	3	1.928	1.260	900	6	Moderate edge crack
X2014-3 (after surface milling)	1	2.036	0.749	880	9	Good quality
	2	1.217	0.749	880	4	Good quality
	3	1.178	0.252	880	7	Good quality
X2014-4	1	2.358	1.405	880	7	Light surface cracking
	2	2.355	1.405	880	7	Light surface cracking
	3	1.904	1.319	880	7	Light surface cracking
X2014-4 (after surface milling)	1	1.115	0.750	860	4	Good quality
	2	1.105	0.751	860	4	Good quality
	3	1.160(a)	0.246	860	17	Good quality
X2014-5	1	2.384	1.620	880	6	Slight surface cracking
	2	2.383	1.620	880	6	Slight surface cracking
	3	1.795	1.280	870	4	Light surface cracks
X2014-5 (after surface milling)	1	1.460	0.751	880-860	10	Good quality
	2	1.420	0.752	880-860	10	Good quality
	3	1.108	0.250	850	11	Good quality
X2014-6	1	2.370	1.450	870	5	Slight surface cracking
	2	2.380	1.448	870	5	Slight surface cracking
	3	1.766	1.280	870	4	Slight surface cracking
X2014-6 (after surface milling)	1	1.300	0.745	850	6	End split, short plate
	2	1.245	0.744	850	6	End split, short plate
	3	1.108(a)	0.250	850	11	Good quality
X2014-7	1	2.363	1.403	880	7	Light surface cracking
	2	2.364	1.400	880	7	Light surface cracking
	3	1.907	1.321	880	7	Slight surface cracking
X2014-7 (after surface milling)	1	1.150	0.740	860	4	Good quality
	2	1.108	0.743	860	4	Good quality
	3	1.150	0.251	860	17	Good quality

TABLE A-9. (CONTINUED)

Description of Material		Thickness, inches		Rolling Temperature, F	Number of Passes	Remarks
Composition	Section(a)	Initial	Final			
X2014-8	1	2.399	1.627	880	6	Slight surface cracking
	2	2.398	1.620	880	6	Slight surface cracking
	3	1.855	1.327	880	7	Slight surface cracking
X2014-8 (after surface milling)	1	1.440	0.753	880-860	10	Good quality
	2	1.475	0.752	880-860	10	Good quality
	3	1.125	0.251	860	17	Good quality

(a) Sections 1 and 2 were rolled to 3/4-inch-thick plate; Section 3 was rolled to 1/4-inch-thick plate.

TABLE A-10. DRAWING RECORD OF EXPERIMENTAL WIRE

Material Composition	Initial Area Reduction,[a] percent	Diameter at First Anneal,[b] inch	Diameter at Second Anneal, inch	Diameter at Third Anneal, inch	Finish Diameter, inch
X2319-1	87	0.125	----	----	0.0625
X2319-2	25	0.298	0.198	0.114	0.0625
X2319-3	25	0.298	0.198	0.114	0.0625
X2319-4	87	0.125	----	----	0.0625
X2319-5	48	0.250	0.125	----	0.0625
X2319-6	48	0.250	0.170	0.114	0.0625
X2319-7	25	0.298	0.150	0.091	0.0625
X2319-8	48	0.250	0.150	0.102	0.0625
X4043-1	87	0.125	----	----	0.0625
X4043-2	76	0.170	0.125	----	0.0625
X4043-3	60	0.218	0.125	----	0.0625
X4043-4	87	0.125	----	----	0.0625
X4043-5	87	0.125	----	----	0.0625
X4043-6	67	0.198	0.125	----	0.0625
X4043-7	87	0.125	----	----	0.0625
X4043-8	76	0.125	0.125	----	0.0625

(a) Original diameters of wire were 0.340 and 0.350 inch.

(b) Standard anneal for 2000 series aluminum used for X2319: Heat to 750 F, hold 2 hours, cool to 500 F at no more than 50 F per hour, air cool to room temperature.

PROGRAM NUMBERING SYSTEM

During the program, two different numbering systems were used to identify the composition and the thickness of the welding materials. The type number designated the material composition. Table A-11 tabulates the values of the four composition factors for each material studied.

The sample numbers were assigned as follows:

1 through 4	1/4-inch-thick base plate
6 through 9	3/4-inch-thick base plate

During Phase I, 6 and 7 were located on opposite sides of the same plate as were 8 and 9. All of the remaining welds were made on individual plates.

TABLE A-11. VALUE OF THE FOUR FACTORS FOR EACH TYPE NUMBER

Type Number	Chemical Content	Internal Impurities	Actual Hydrogen Content, ppm by weight						Phase I External Impurities	Phase II External Impurities
			X2219[a]		X2014[a]		X2319[b]	X4043[b]		
			1/4-inch plate	3/4-inch plate	1/4-inch plate	3/4-inch plate				
1	Low	Low	0.1	0.3	0.3	0.3	1.4	1.5	Low	High
2	Low	High	0.8	0.5	0.7	1.9	1.7	1.8	Low	High
3	Low	High	0.6	0.5	0.4	0.7	2.5	2.5	High	High
4	Low	Low	0.3	0.1	0.4	1.8	3.1	4.0	High	High
5	High	Low	1.1	0.7	0.6	0.5	3.4	2.4	Low	High
6	High	High	0.5	0.4	0.8	0.7	2.5	1.8	Low	High
7	High	Low	0.1	0.1	0.5	0.3	1.5	2.2	High	High
8	High	High	0.7	0.5	0.9	0.8	2.0	2.9	High	High

(a) Internal hydrogen content.
(b) Internal hydrogen content plus surface hydrogen correction factor.

APPENDIX B

THE BATTELLE VACUUM-FUSION ANALYSIS OF HYDROGEN

BATTELLE VACUUM-FUSION ANALYSIS OF HYDROGEN

All analyses of hydrogen content made during the program were conducted at Battelle with the use of vacuum-fusion apparatus.

Selection of Samples

The hydrogen content of the ingots prior to fabrication was determined from a sample taken at an ingot corner after the outer surface of the ingot had been milled off. The hydrogen content of the fabricated plate was determined from a 10- to 15-gram sample taken at the midpoint of the plate along one edge. The edge was selected so that the sample was taken at the center of the ingot for the 3/4-inch-thick plate and at or near the center of the ingot for the 1/4-inch-thick plate. A single sample was taken for each thickness of each experimental composition type. The use of a single section from the center of each ingot gave results representative of the entire ingot as was illustrated by the analysis of 3/4-inch-thick X2219 Type 2 plate. The 3/4-inch-thick plate was analyzed at three points which were located approximately at the ingot center, a corner at the top on one side, and a corner at the bottom on the opposite side. The hydrogen content of all three specimens was 0.5 ppm by weight. Despite this indication of homogeneous hydrogen content throughout plates fabricated from the same ingot, the hydrogen content of each thickness of each type of each experimental alloy base plate was considered to be the reported hydrogen content $\pm$ 0.1 ppm, by weight. Therefore, when two types were compared, the types were considered to have a significant difference in hydrogen content when the difference between the two analyses was 0.2 ppm or greater.

Selection of Filler-Wire Samples

The hydrogen content of the 1/16-inch-diameter experimental filler wire was obtained from a 5-gram sample which was removed from the wire reel directly after making the necessary welds with the wire. Care was taken during handling to prevent scoring or otherwise contaminating the wire. Four samples each of Type 1 X2319 and X4043 filler were analyzed and the results gave an indication of the variation of hydrogen content along the wire and the variation in the analysis methods. For the X2319 wire the total-hydrogen analyses were 0.9, 1.4, 1.3, and 1.6 ppm, by weight. The first value in each case was one of the first total-hydrogen content analyses made in the series of tests. The closeness of the values reported for the succeeding three analyses tends to refute the first values. However, there were no definite reasons determined that could justify ignoring the first results.

Sample Cleaning

The samples of experimental base plate submitted for analysis were cut using a band saw and then draw filed to remove surface markings and contamination. The base-plate samples as supplied were smooth and bright. Prior to analysis, the base-plate samples were filed again on all external surfaces with a clean, flat bastard file to remove about 0.001 inch from each surface.

The freshly filed samples were exposed to air for 25 minutes before being placed in the evacuated vacuum-fusion apparatus. The correction factor for the hydrated surface oxide formed during this period has been found to be quite constant and reproducible.

The filer wire samples were abraded with 320-grit silicon carbide paper and then degreased with C.P. acetone. The clean wire was then carefully wound into a coil to allow fitting the sample into the vacuum-fusion apparatus. The freshly abraded wire samples were exposed to air for 25 minutes before being placed in the vacuum-fusion apparatus.

Calculation of Surface Hydrogen Correction Factor

A correction factor for the hydrogen on the surface of the sample was calculated for each alloy. The factor corrects for the introduction of hydrogen into the analysis by the rapid formation of a hydrated aluminum oxide on the sample surface directly after cleaning and before the sample was placed in the evacuated vacuum-fusion apparatus. The time of exposure to air was standardized at 25 minutes. Experience has indicated that, after this period of time, the formation of the hydrated oxide is much less rapid.

The surface hydrogen correction factor was determined by a separate set of analyses of at least three identical samples. The following procedure was used for each sample:

Sample Number 1. After the standard surface preparation and exposure to air, one sample was placed in the vacuum-fusion apparatus. The total hydrogen evolved from the sample during the analysis was determined.

Sample Number 2. After the standard surface preparation and exposure to air, a second sample was placed in the evacuated vacuum-fusion apparatus and preheated for 5 hours at 977 F to remove all surface hydrogen and some of the internal hydrogen. After the preheat, the sample

was analyzed for the residual hydrogen content. (The sample was not reabraded or re-exposed to the air.)

Sample Number 3. After the standard surface preparation and exposure to air, a third sample was placed along with Sample No. 2 in the evacuated vacuum-fusion apparatus and preheated for 5 hours at 977 F. After removal of the surface hydrogen and some of the internal hydrogen, the sample was removed from the apparatus and reabraded by the standard procedure. After the standard exposure to air, the sample was placed in the vacuum-fusion apparatus and the external plus the residual hydrogen content was determined.

These three analyses determined the total "as-received" hydrogen content, the residual hydrogen content, and the external plus residual hydrogen content. The calculations can then be made to determine the internal hydrogen content and the external hydrogen content (surface hydrogen correction factor) as follows:

A. Total Hydrogen Content: Sample Number 1

B. Residual Hydrogen Content: Sample Number 2

C. External plus Residual Hydrogen Content: Sample Number 3

D. External Hydrogen Content: C-B

E. Internal Hydrogen Content: A-(C-B)=A-D

Analysis for Total Hydrogen Content

The sample, after the standard cleaning and exposure treatment, was sealed in the glass vacuum-fusion apparatus. The tin bath in the

apparatus was heated by an induction coil while the apparatus was outgassed. The tin bath was maintained at 1200 F throughout the analyses. After a suitable outgassing period, the blank rate of the hydrogen evolved from the apparatus, seals, tin bath, and samples was determined. Analyses were not made until the blank rate was 0.006-milliliter STP or less over a 20-minute period (equivalent to 10-microns pressure rise).

The number of samples that could be analyzed with one pumpdown of the apparatus was limited by the size of the apparatus and the necessity of maintaining a volume ratio of aluminum to tin not exceeding 1:19 in the bath.

After the blank rate of the apparatus was determined to be low and constant, the first sample was placed in the molten tin bath. Readings of the evolved gas pressure were taken every five minutes on a McLeod gage. If the pressure change between the readings at 15 and 20 minutes after placement of the sample in the tin bath was less than 3 microns of mercury at STP, the collection was stopped. If the pressure rise was still high, the collection of the gas evolved from the bath was not stopped until the pressure rise over five minutes was less than 3 microns.

When the pressure rise was sufficiently low, the collected gas was circulated by a diffusion pump through a closed system containing heated copper oxide and a dry ice-acetone-cooled trap. The hydrogen present within the gas was oxidized by the copper oxide to form water vapor which then was frozen at the cold trap. The drop in the pressure of the system (related to water vapor freezing out) was measured every minute until two consecutive readings were obtained. The total hydrogen collected from the bath was determined from the pressure drop due to the freezing out of

the hydrogen as water vapor. After correcting for the copper oxide outgassing and the blank rate of the bath, the total hydrogen evolved for the sample weight was known. Correction for the external hydrogen content and division by the sample weight yielded the internal hydrogen content in parts per million, by weight. The sensitivity of the apparatus for a 10-gram sample was approximately 0.04 ppm, by weight.

After the blank rate of the apparatus was again suitably low, the next sample was immersed in the tin bath.

Other Analysis Methods

The measurement of the small amounts of hydrogen within aluminum alloys has been considered more difficult than the measurement of hydrogen within most metals and alloys. Two specific articles describing methods and results of hydrogen analyses for aluminum are References 6 and 7 in Appendix G. Brandt and Cochran (7) describe the methods and results of vacuum-fusion analyses and solid extraction analyses of hydrogen in aluminum. Brandt and Cochran concluded that reproducible hydrogen contents of aluminum alloy samples could be secured by either solid extraction or vacuum-fusion analysis. They also concluded that the rapidity of vacuum-fusion analysis is a decided advantage for this method of analysis over solid-extraction analysis.

Vacuum-fusion analysis of the hydrogen within the materials used for this study was utilized because the method has been shown to yield reproducible results both by Battelle and by other investigators. In addition, considerable experience with vacuum-fusion analysis of aluminum and other alloys has been amassed by Battelle. Finally, the

cost and time required per sample for vacuum-fusion analyses were much less compared to other comparable analysis methods. Although the absolute levels of hydrogen contents were determined, the approach to the program was such that any method yielding an accurate measure of the differences in hydrogen contents among the materials would have sufficed.

APPENDIX C

WELDING EQUIPMENT

WELDING EQUIPMENT

1. ATMOSPHERE CHAMBER: 30 inch diameter, 8 feet long; equipped with a jacket for steam or cooling water; vacuum-purged to <10 micron mercury; helium-filled from 0.2 to 1.0 psig.

2. ARC CONTROL: Airco Heliarc HMH-E automatic welding unit with HMC-B control box.

3. ARC MOVEMENT: Threaded screw and nut driven by Lee Type R-35H, 1/25 horsepower motor.
   Speed Reduction: 50 to 1 (by worm gears)
   Motor Response: 0 to 5000 rpm in 0.5 seconds
   Motor Speed Variation: ± 0.5 per cent at 4700 rpm
   Motor Driving Speed: Approximately 4700 rpm for travel speed of 11 inches per minute

4. POWER SUPPLY: P and H DC arc welder, DC 201, 3 phase rectifier, 300 amperes (Phase I only)

   Vickers Controlarc d-c arc welder, 3 phase rectifier, 400 amperes, Type 51E30-2 (Phase II only)

   Amperage Variation: ± 0.5 per cent at 150 amperes

5. WELDING TORCH: Linde Heliarc HW-13, water cooled with 3/32 inch diameter, 1 per cent thoriated tungsten electrode.

6. WIRE FEEDER: Airco HMF-A (Phase II only).

Welding Torch Positioner

The welding torch positioner at the right of the recording potentiometer in Figure 6 (see text), was placed in the horizontal position. The positioner was connected by a double universal joint to a precision ground shaft, which entered the chamber through a vacuum seal. The seal employed a ball bushing to prevent binding of the positioner in the positioner drive rolls. The shaft passed through a single O-ring seal which prevented atmosphere leakage in either direction. During the program the necessity of providing a smoothly-operating feedthrough seal was demonstrated. For Phase II, careful counterbalancing of the shaft outside the chamber was necessary to offset the weight of the torch, filler wire feeder, and filler wire speed monitor inside the chamber. Lubrication of the shaft was also critical. Vacuum grease was the most satisfactory lubricant used on the shaft since the difference between the static and kinetic friction coefficients was less than with other suitable lubricants, such as vacuum-pump oil. Satisfactory operation of the feedthrough was necessary to assure close control of the arc voltage by the automatic head positioner.

The dewpoint meter is shown in the center of Figure 6. At the extreme right, part of the travel movement drive is visible at the top. At the lower right, the compound mechanical vacuum pump used with the chamber is shown.

The travel movement inside the chamber consisted of a machine-screw driven platform using ball bushings riding on precision ground shafts. The trunnion-mounted work holder was positioned so that the base plate to be welded was in the horizontal position perpendicular

to the welding torch axis. The plates were clamped in the workholder at three points on one-foot centers at the top and bottom of the plate. The total contact area of the clamp at each point was one-half square inch at the front and one-half square inch at the back. During Phase II, the clamping surface was insulated by a 3-mil thickness of mica sheet. A modification made to the torch was a copper collar brazed to the end of the torch collet. The collar firmly engaged the tungsten electrode when a setscrew was tightened. The voltage lead from the torch was directly connected to the torch and thus avoided recording variations of the voltage across the arc which were due only to variations in collet tightening.

The variable-speed travel drive motor and a 5 to 1 worm gear speed reducer were located outside the chamber. The speed reducer output shaft was connected by a double universal joint through a vacuum seal into the chamber where a second double universal joint connected the feedthrough-seal shaft to the machine screw. The use of double universal joints reduced the binding and subsequent irregular travel motion that might have occurred in the drive. Backlash through the entire system was less than 5° at the machine screw.

Filler Wire Equipment for Phase II

During Phase II a pull-type wire feeder was used to feed 1/16-inch-diameter filler wire into the arc in the forehand position. The wire was fed into the arc pool at 3 to 4 o'clcok at an angle of about 15° to the base plate. The tip of the wire feeder was less than 1/2

inch from the tungsten electrode. The filler wire feeder employed smooth, grooved drive rolls and contained a clean plastic liner at all points. The filler wire feeder was attached directly to the welding torch.

APPENDIX D

WELDING INSTRUMENTATION AND DISCUSSION

WELDING INSTRUMENTATION AND DISCUSSION

1. ARC VOLTAGE: Measured between a collar attached to the tungsten electrode and the plate being welded

   Voltage Divider: 1500 to 1

   Recorder: Honeywell Brown recording electronic millivolt potentiometer
   Model SY 153X (28)-(VV)-II-III-(6)-N4
   2 pen recorder
   Response: full scale in 0.5 seconds
   Accuracy: ± 0.25 per cent
   Full Scale Reading: 10 millivolts
   Chart Speed: 6 inches per minute

2. ARC AMPERAGE: Measured at the welding power supply

   Precision Shunts: Calibrated for 50 millivolts at 200 or 300 amperes

   Recorder: Same as for arc voltage except
   Full Scale Reading: 50 millivolts

3. ARC SPEED: Measured at motor output shaft

   Measuring Device: Servo-Tek industrial tachometer-generator SA-757B-1
   Output: 20.7 volts per 1000 rpm
   RMS Ripple: less than 3 per cent of d-c value

   Voltage Divider: 2000 to 1

   Recorder: Honeywell Brown recording electronic millivolt potentiometer
   Model Y 153X (12) V-X-(IV)6V
   Response: full scale in 1 second
   Accuracy: ± 0.25 per cent
   Full Scale Reading: 50 millivolts
   Chart Speed: 6 inches per minute
   Timer Relay: alternated arc speed and welding wire speed signals (Phase II only)

4. FILLER WIRE SPEED: Measured directly on the filler wire (Phase II only)

   Measuring Device: A filler-wire-driven roll connected by a 1:5 precision gear increase drove a Servo-Tek industrial tachometer-generator SA-757B-1
   Output: 20.7 volts/1000 rpm
   RMS Ripple: less than 3 per cent of d-c value

   Voltage Divider: 200 to 1

   Recorder: Same as for arc speed
   (a timer relay alternated the two signals; Phase II only)

5. VACUUM GAGE: National Research Model 0701 meter with Type 501 thermocouple vacuum gage

6. DEWPOINTER: Alnor 7000 U
   Nominal range for helium: room temperature to -130 F

CALIBRATION: All voltage dividers and shunts are traceable to standards of the National Bureau of Standards. Recorders are checked against at least secondary standards of the U.S. Bureau of Standards.

Discussion of Recording Specifications

Contract NAS8-11445 specified a high equipment and recorder accuracy. Future programs might be conducted with even greater precision if additional important recording factors were specified which also affect the recorded signal accuracy. These factors are dynamic response, damping, and sensitivity. They can be defined as follows:

(1) Dynamic Response. The time with which the recorder can move from one input value to another. This value is commonly specified as full-scale response (number of seconds to go from zero to the full-scale reading). For a changing, dynamic signal, the recorded maximum and minimum variations from the recorded value depend upon how rapidly the recorder can follow the variations. An oscilloscope is one of the most rapid recorders of dynamic variations. Figure D-1 illustrates the recording made of the same signal by two similar recorders with two different response times. The variations are seen to be much greater in the recorder with the faster response.

(2) Damping. This factor is specified by the damping factor. Damping is necessary to prevent the mechanical inertia of the recorder from carrying the recorder pen far above the actual input value when a sudden variation occurs. The damping factor can be measured directly from the recording instrument.

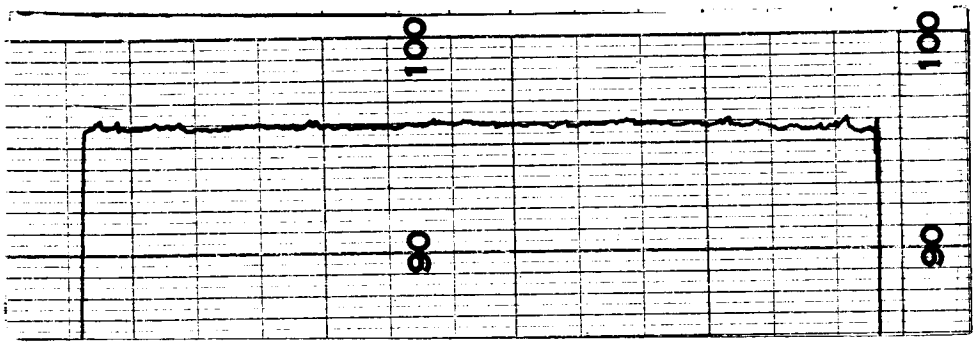

a. Recording at 1.0 Second Full Scale Response ± 0.4 units recorded variation.

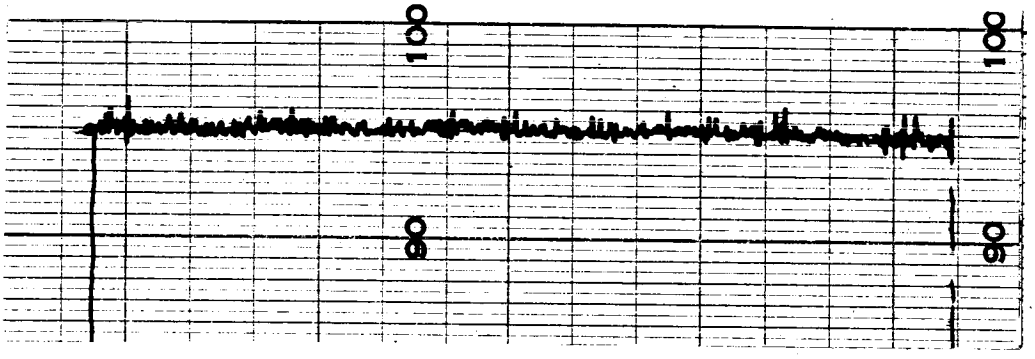

b. Recording at 0.5 Second Full Scale Response ± 1.3 units recorded variation.

FIGURE D-1. EFFECT OF RECORDER RESPONSE TIME

These two recordings were made simultaneously from the same input signal. Chart speed difference has affected x-axis lengths.

(3) Sensitivity. This factor specifies the ability of the recorder to detect and record small, short signals. An oscilloscope is one of the most sensitive instruments available. An example is that when the recording electronic millivolt potentiometer was scribing a perfectly linear arc voltage recording an oscilloscope trace showed voltage varying from 2.5 to 14 volts several hundred times each second.

In addition to the inclusion of these three recording factors, the point at which each of the recorded quantities is measured should be specified. The best example to show the desirability of such a specification would be a filler-wire feeder. If the motor speed instead of the wire speed is measured directly, the recording will never show variations in filler-wire speed due to slippage on the drive rolls. The accuracy of the recording instruments can be easily negated by unreliable mechanical connections beyond the recording transducer.

APPENDIX E

TYPICAL WELD CROSS SECTIONS

a. 1/4-Inch-Thick Base Plate

b. 3/4-Inch-Thick Base Plate

FIGURE E-1. TYPICAL CROSS SECTIONS OF WELDS ON X2219, TYPE 1 BASE PLATE

a. 1/4-Inch-Thick Base Plate

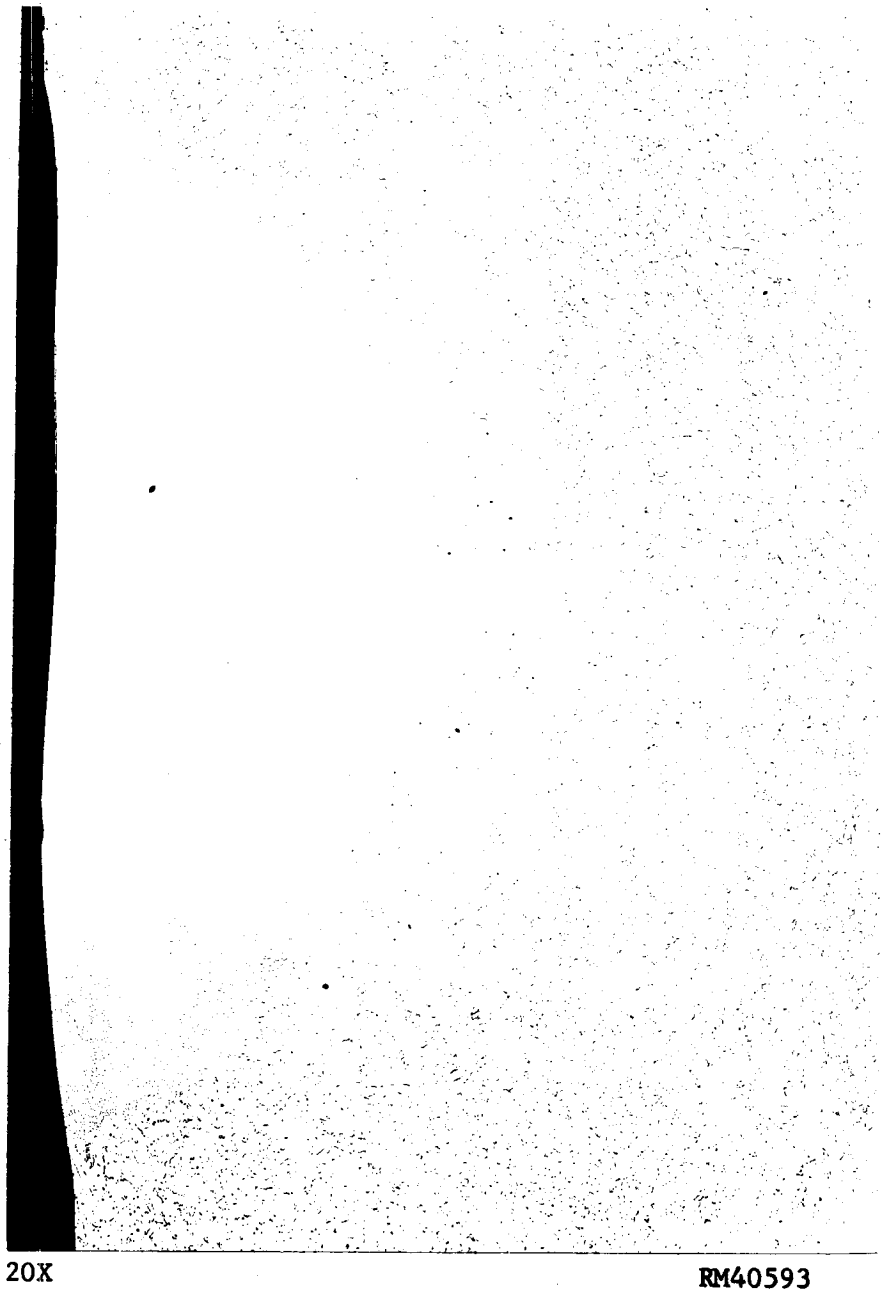

b. 3/4-Inch-Thick Base Plate

FIGURE E-2. TYPICAL CROSS SECTIONS OF WELDS ON X2219, TYPE 2 BASE PLATE

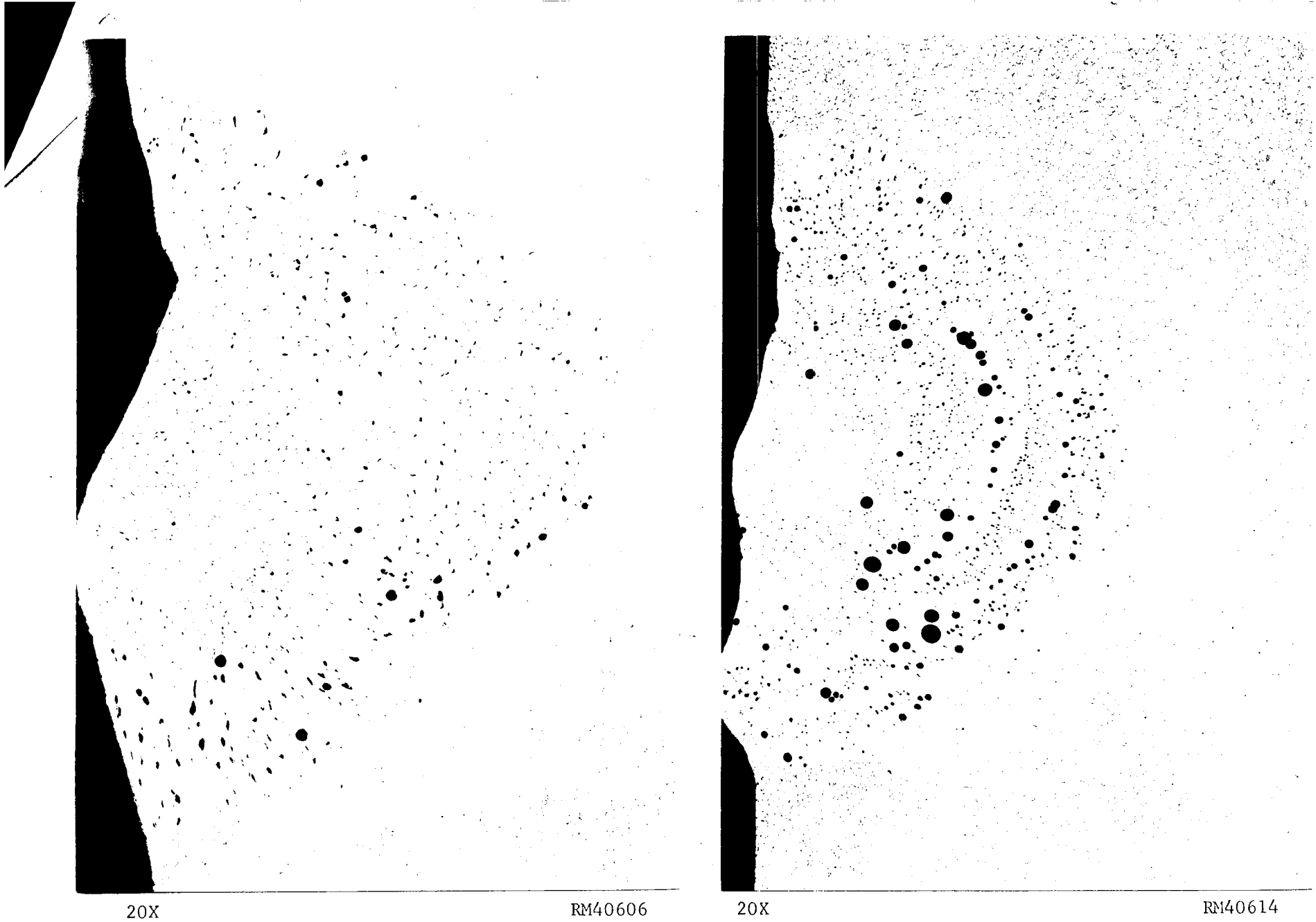

a. 1/4-Inch-Thick Base Plate

b. 3/4-Inch-Thick Base Plate

FIGURE E-3. TYPICAL CROSS SECTIONS OF WELDS ON X2219, TYPE 3 BASE PLATE

a. 1/4-Inch-Thick Base Plate

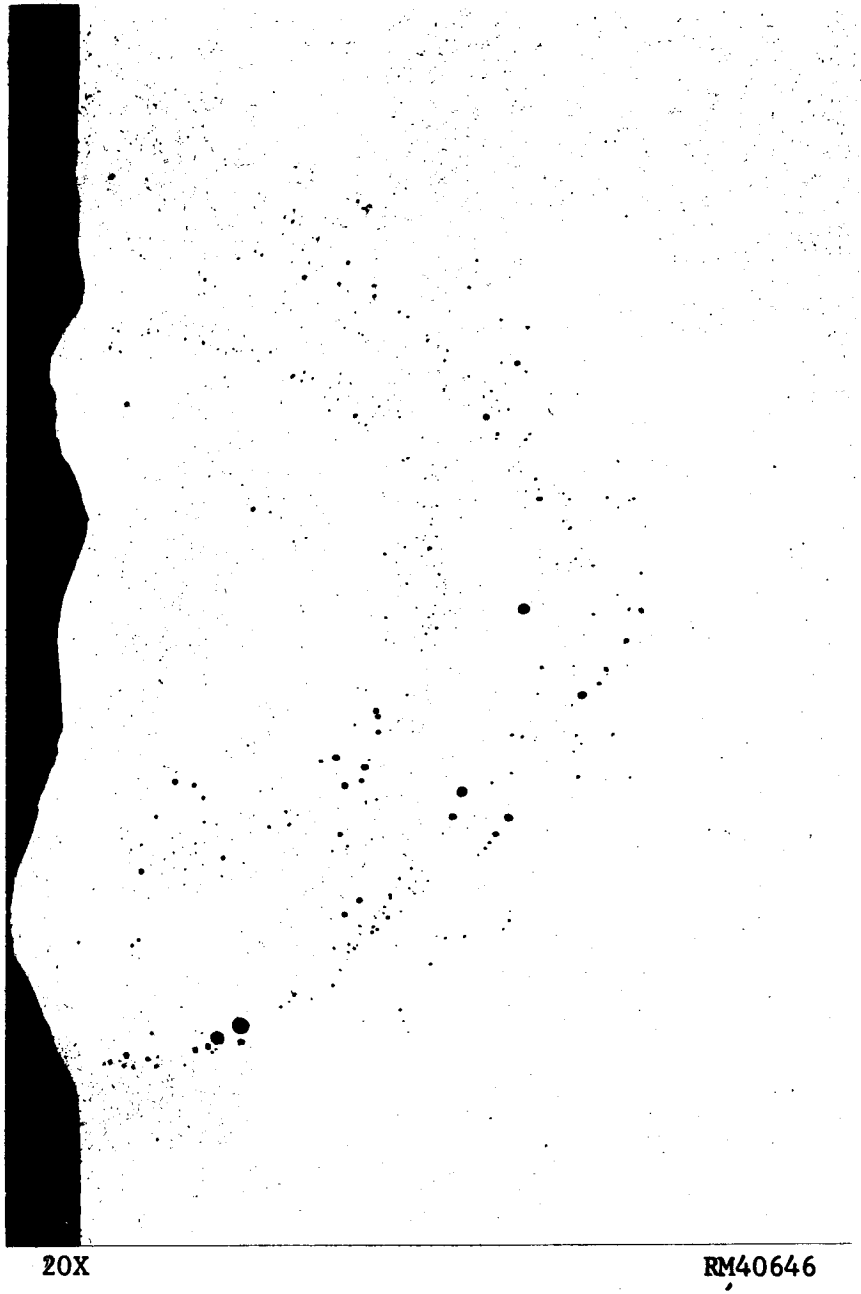

b. 3/4-Inch-Thick Base Plate

FIGURE E-4. TYPICAL CROSS SECTIONS OF WELDS ON X2219, TYPE 4 BASE PLATE

a. 1/4-Inch-Thick Base Plate

b. 3/4-Inch-Thick Base Plate

FIGURE E-5. TYPICAL CROSS SECTIONS OF WELDS ON X2219, TYPE 5 BASE PLATE

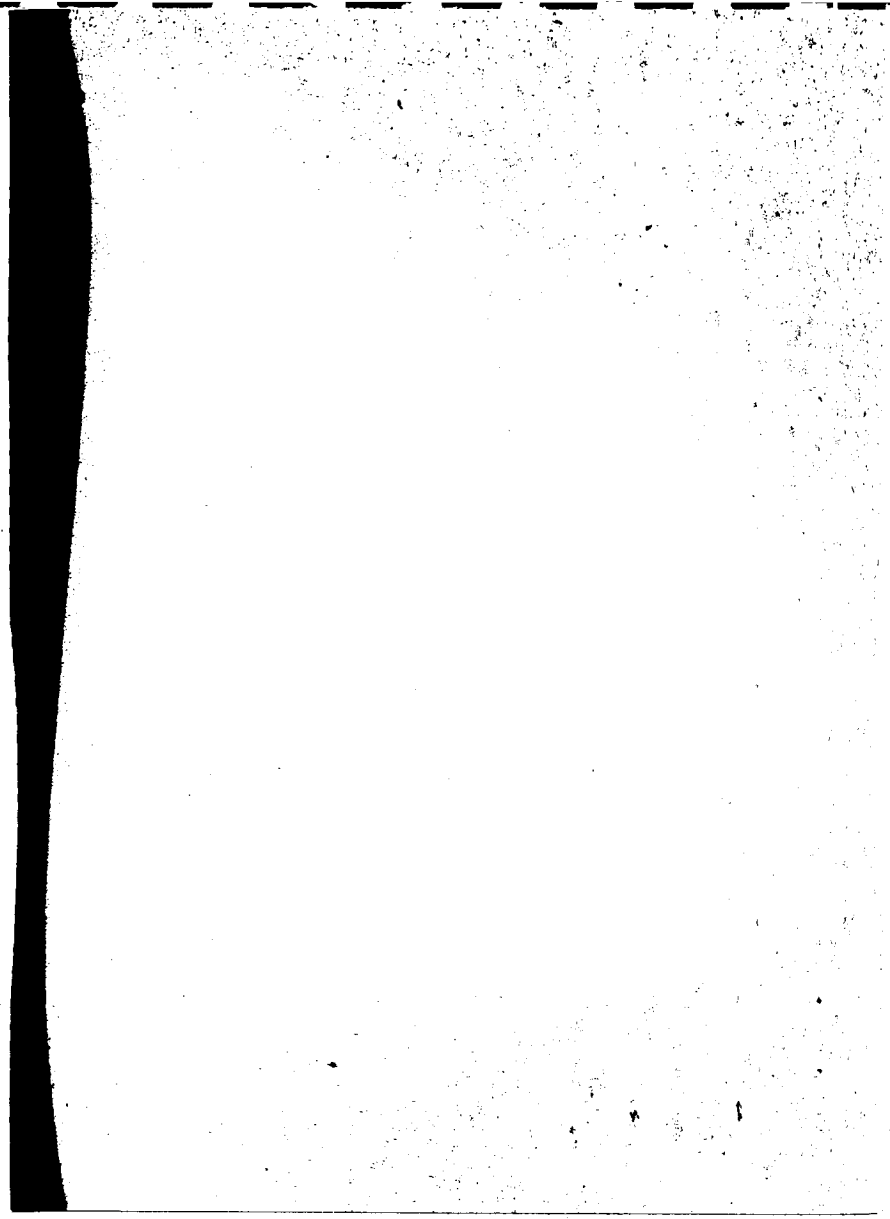

20X RM40413

a. 1/4-Inch-Thick Base Plate

20X RM40085

b. 3/4-Inch-Thick Base Plate

FIGURE E-6. TYPICAL CROSS SECTIONS OF WELDS ON X2219, TYPE 6 BASE PLATE

a. 1/4-Inch-Thick Base Plate

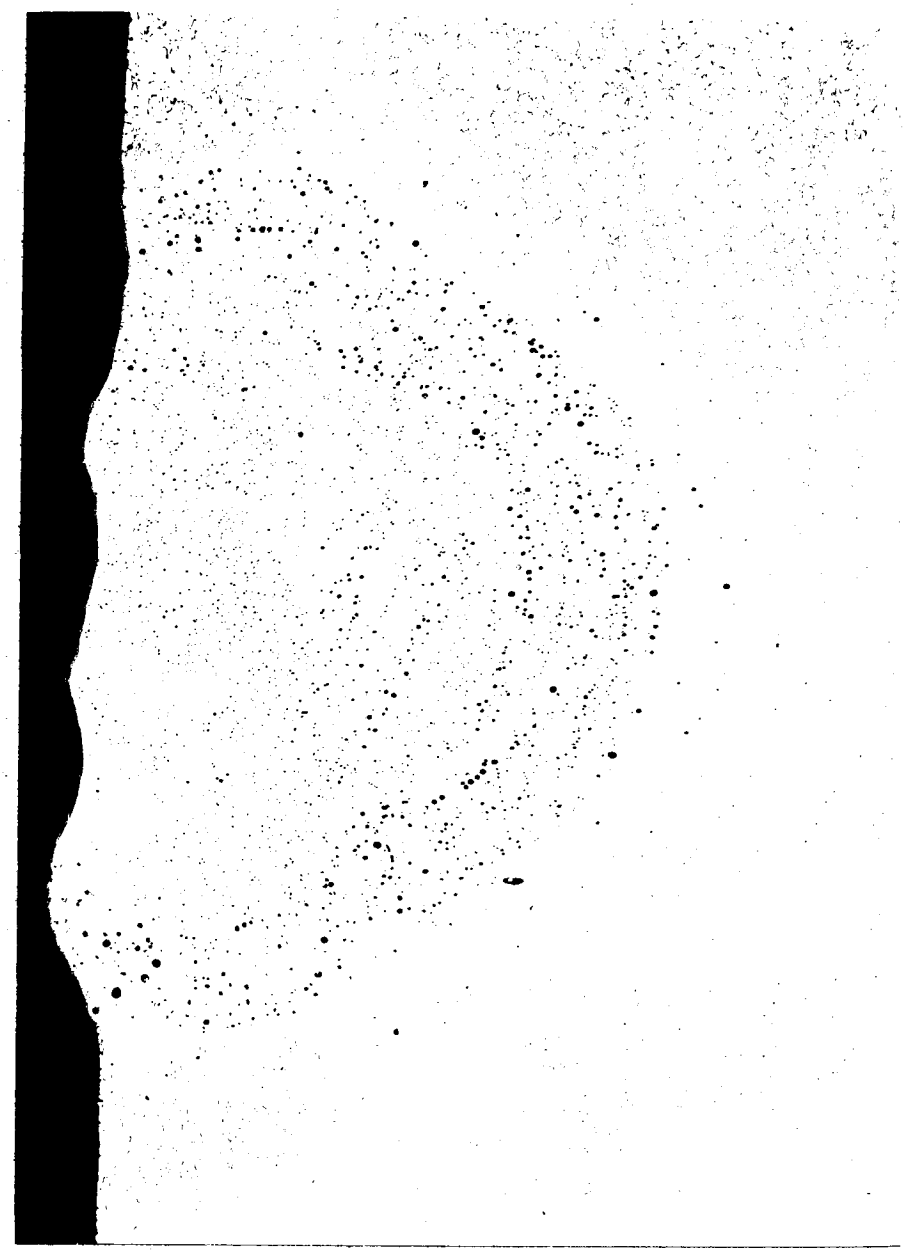

b. 3/4-Inch-Thick Base Plate

FIGURE E-7. TYPICAL CROSS SECTIONS OF WELDS ON X2219, TYPE 7 BASE PLATE

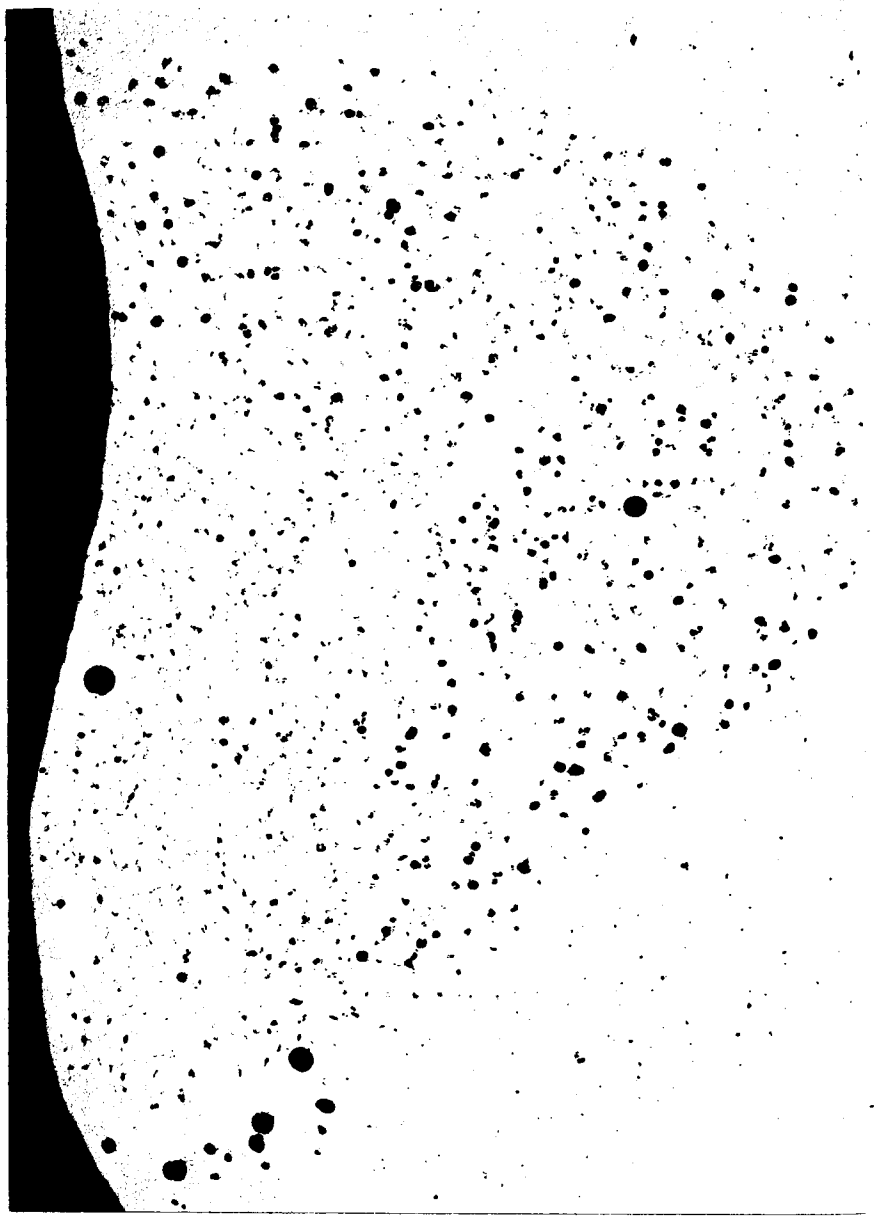

a. 1/4-Inch-Thick Base Plate

b. 3/4-Inch-Thick Base Plate

FIGURE E-8. TYPICAL CROSS SECTIONS OF WELDS ON X2219, TYPE 8 BASE PLATE

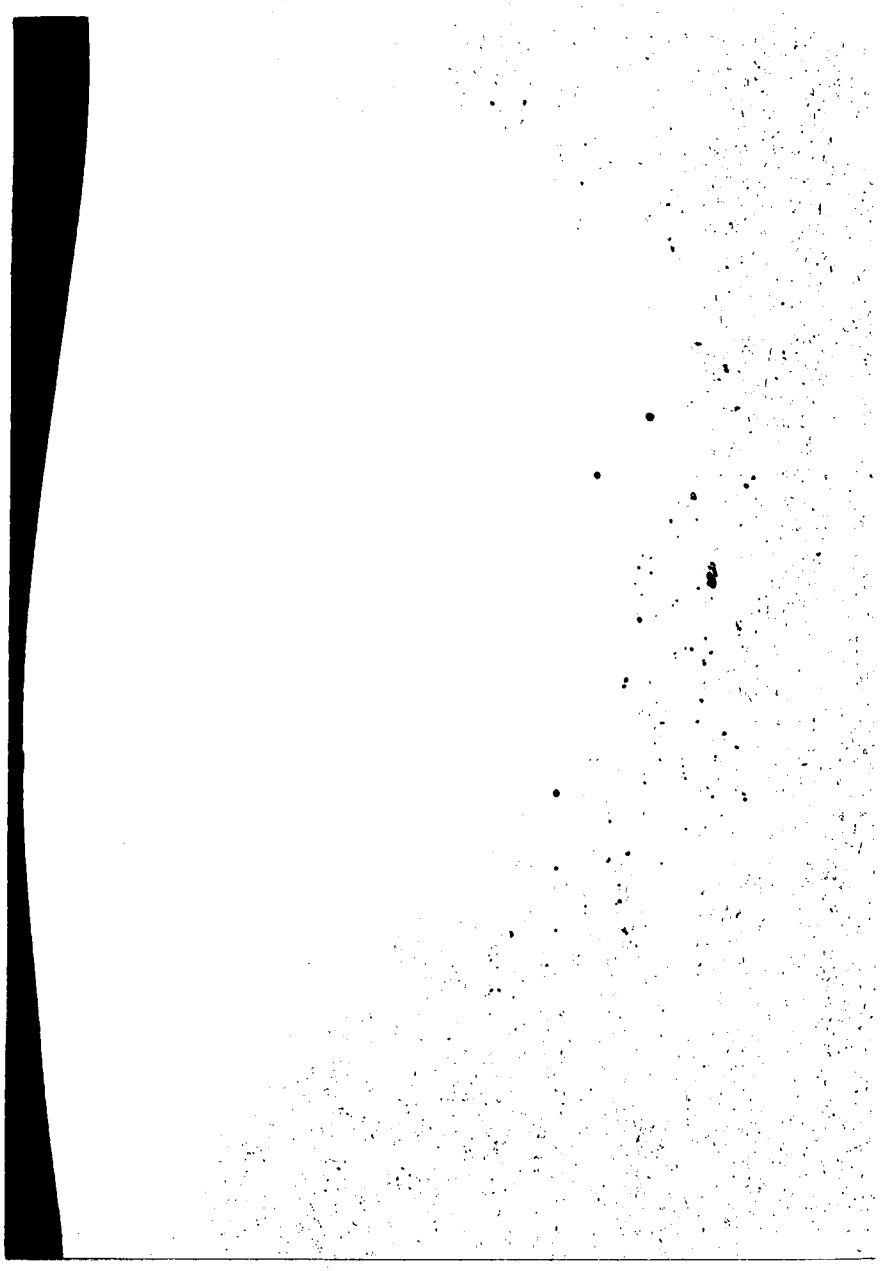

a. 1/4-Inch-Thick Base Plate

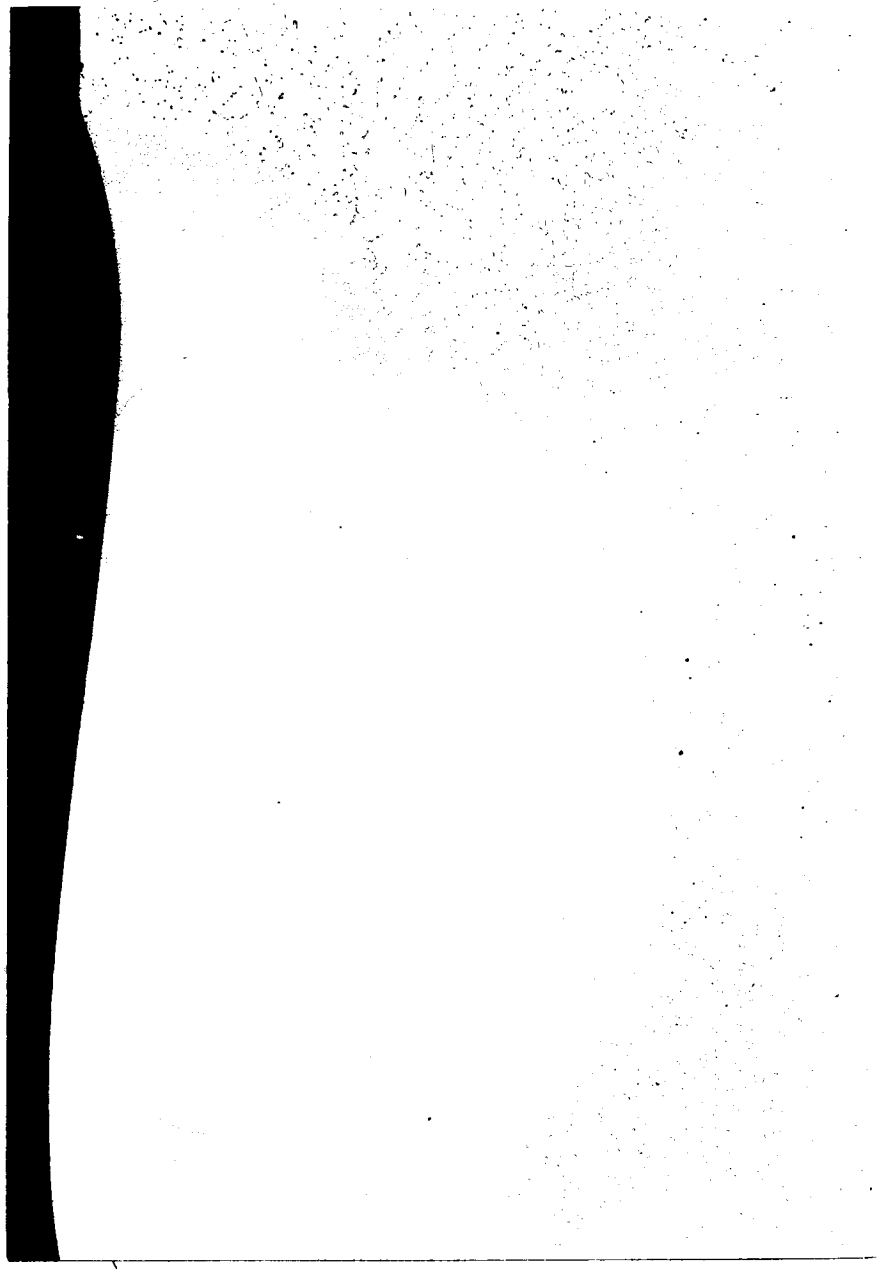

b. 3/4-Inch-Thick Base Plate

FIGURE E-9. TYPICAL CROSS SECTIONS OF WELDS ON X2014, TYPE 1 BASE PLATE

a. 1/4-Inch-Thick Base Plate

b. 3/4-Inch-Thick Base Plate

FIGURE E-10. TYPICAL CROSS SECTIONS OF WELDS ON X2014, TYPE 2 BASE PLATE

20X RM41684

a. 1/4-Inch-Thick Base Plate

20X RM41757

b. 3/4-Inch-Thick Base Plate

FIGURE E-11. TYPICAL CROSS SECTIONS OF WELDS ON X2014, TYPE 3 BASE PLATE

a. 1/4-Inch-Thick Base Plate

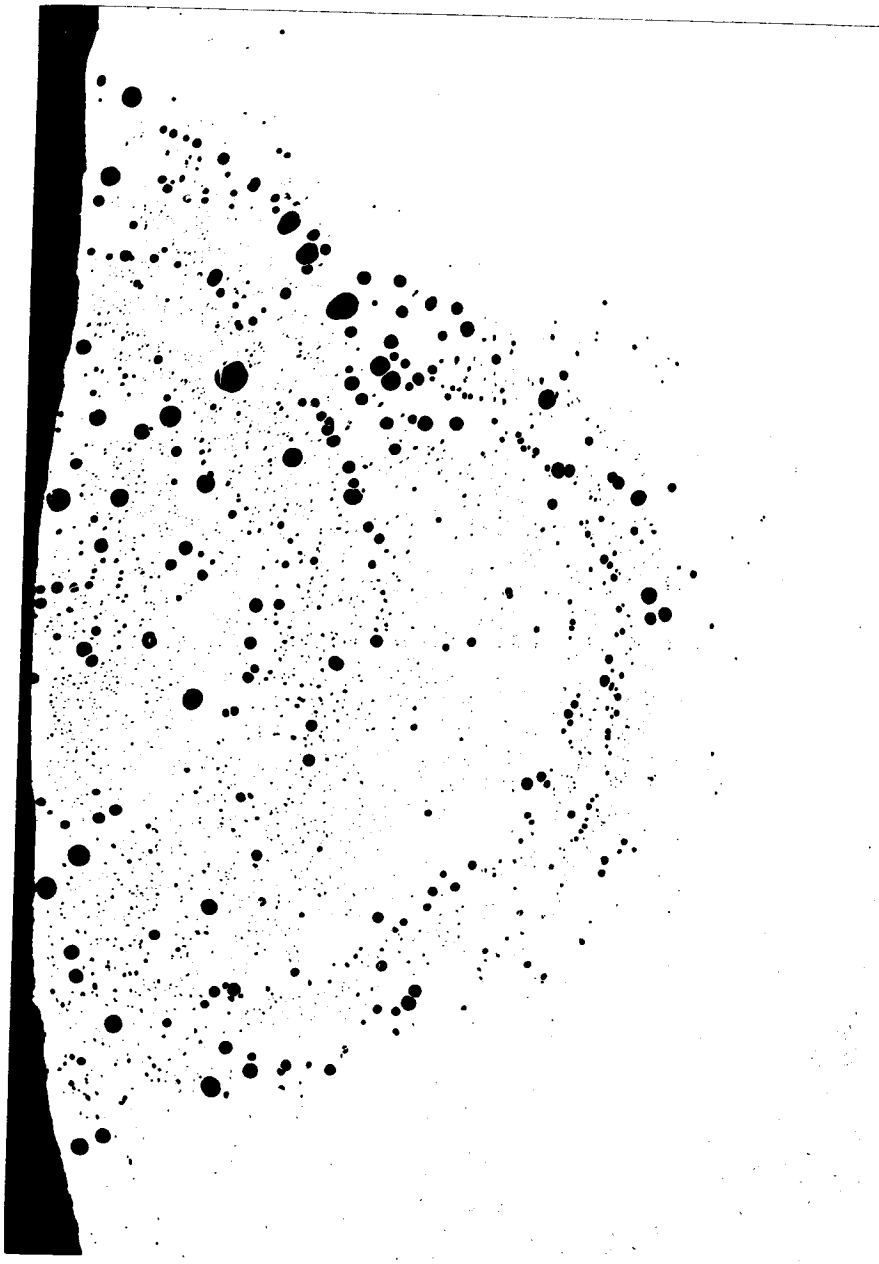

b. 3/4-Inch-Thick Base Plate

FIGURE E-12. TYPICAL CROSS SECTIONS OF WELDS ON X2014, TYPE 4 BASE PLATE

20X RM41024

a. 1/4-Inch-Thick Base Plate

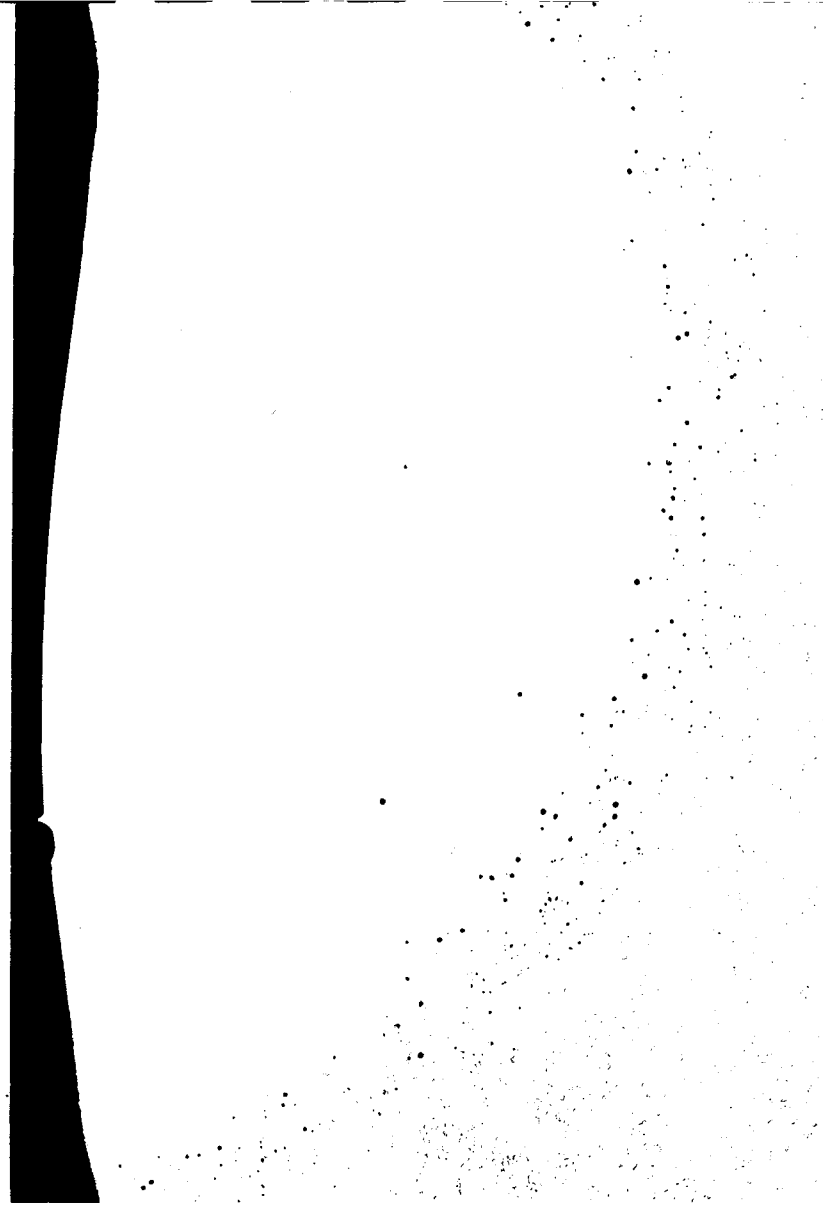

20X RM41614

b. 3/4-Inch-Thick Base Plate

FIGURE E-13. TYPICAL CROSS SECTIONS OF WELDS ON X2014, TYPE 5 BASE PLATE

20X RM41619

a. 1/4-Inch-Thick Base Plate

20X RM41629

b. 3/4-Inch-Thick Base Plate

FIGURE E-14. TYPICAL CROSS SECTIONS OF WELDS ON X2014 , TYPE 6 BASE PLATE

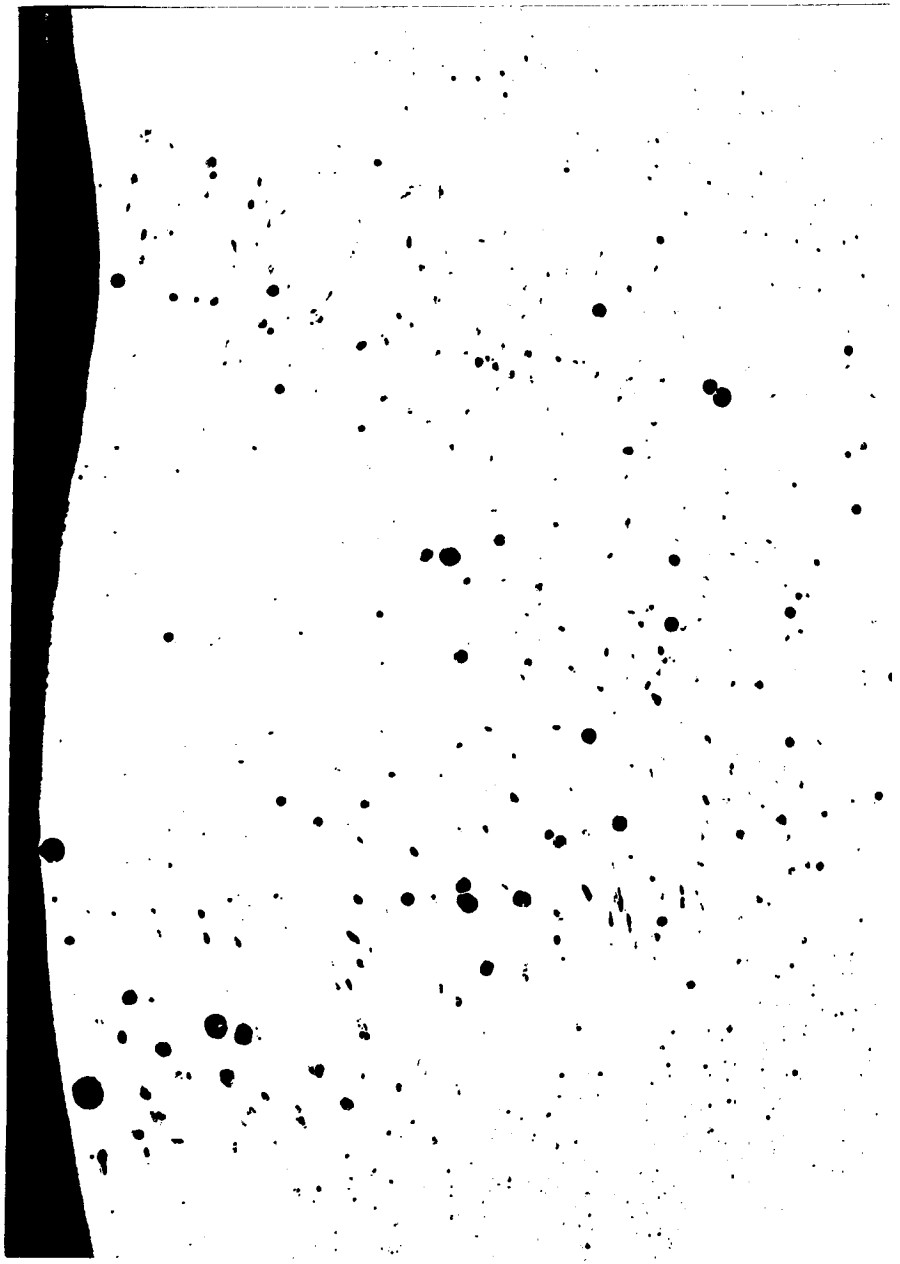

20X RM41695

a. 1/4-Inch-Thick Base Plate

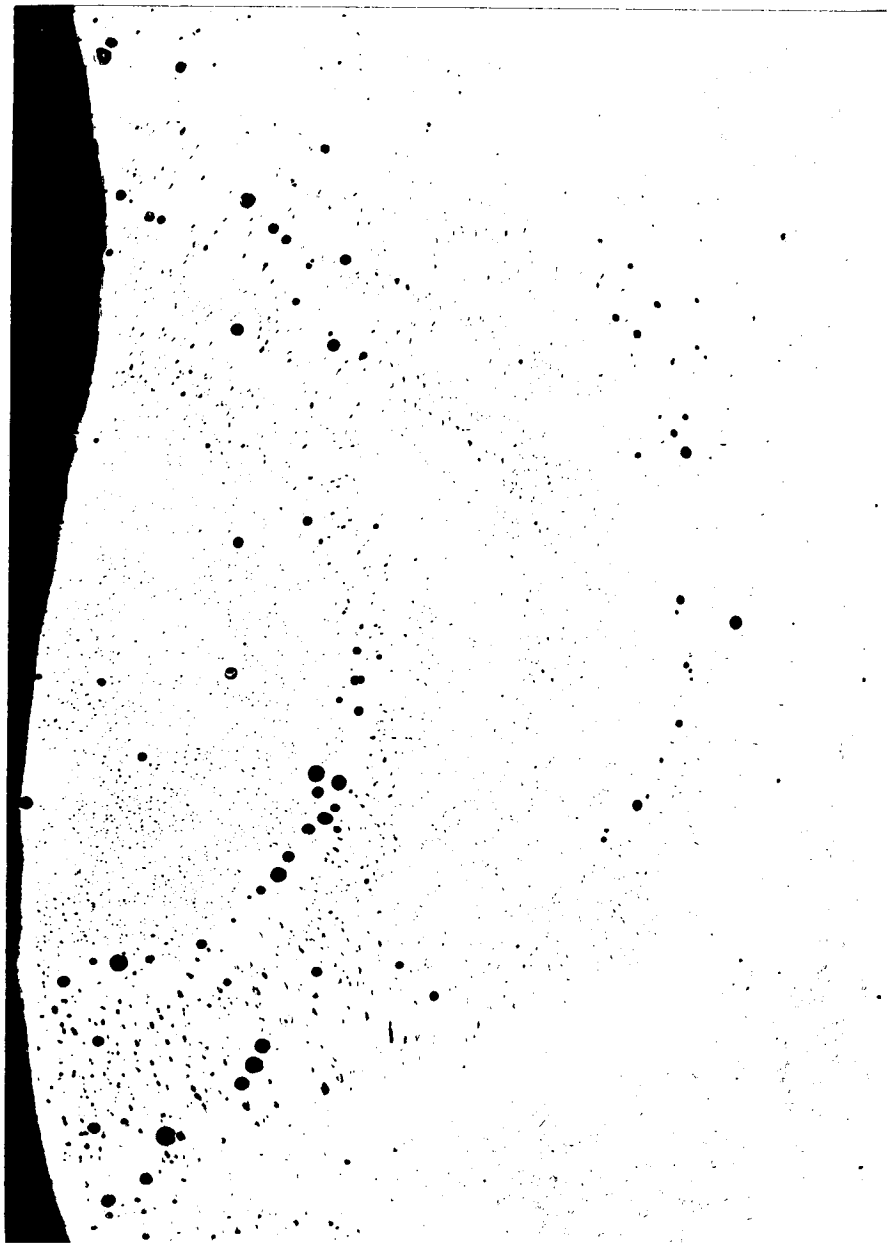

20X RM41748

b. 3/4-Inch-Thick Base Plate

FIGURE E-15. TYPICAL CROSS SECTIONS OF WELDS ON X2014, TYPE 7 BASE PLATE

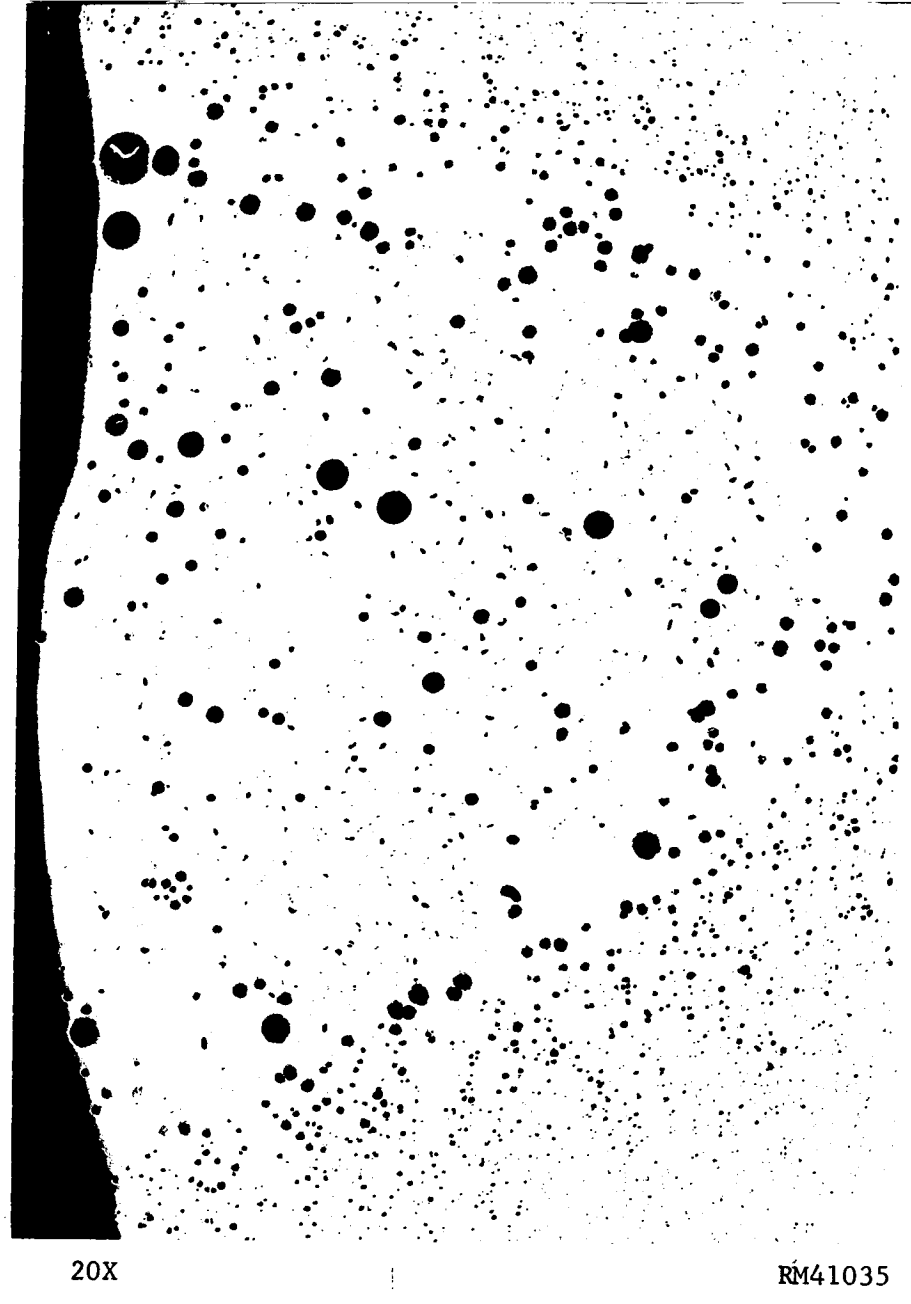

a. 1/4-Inch-Thick Base Plate

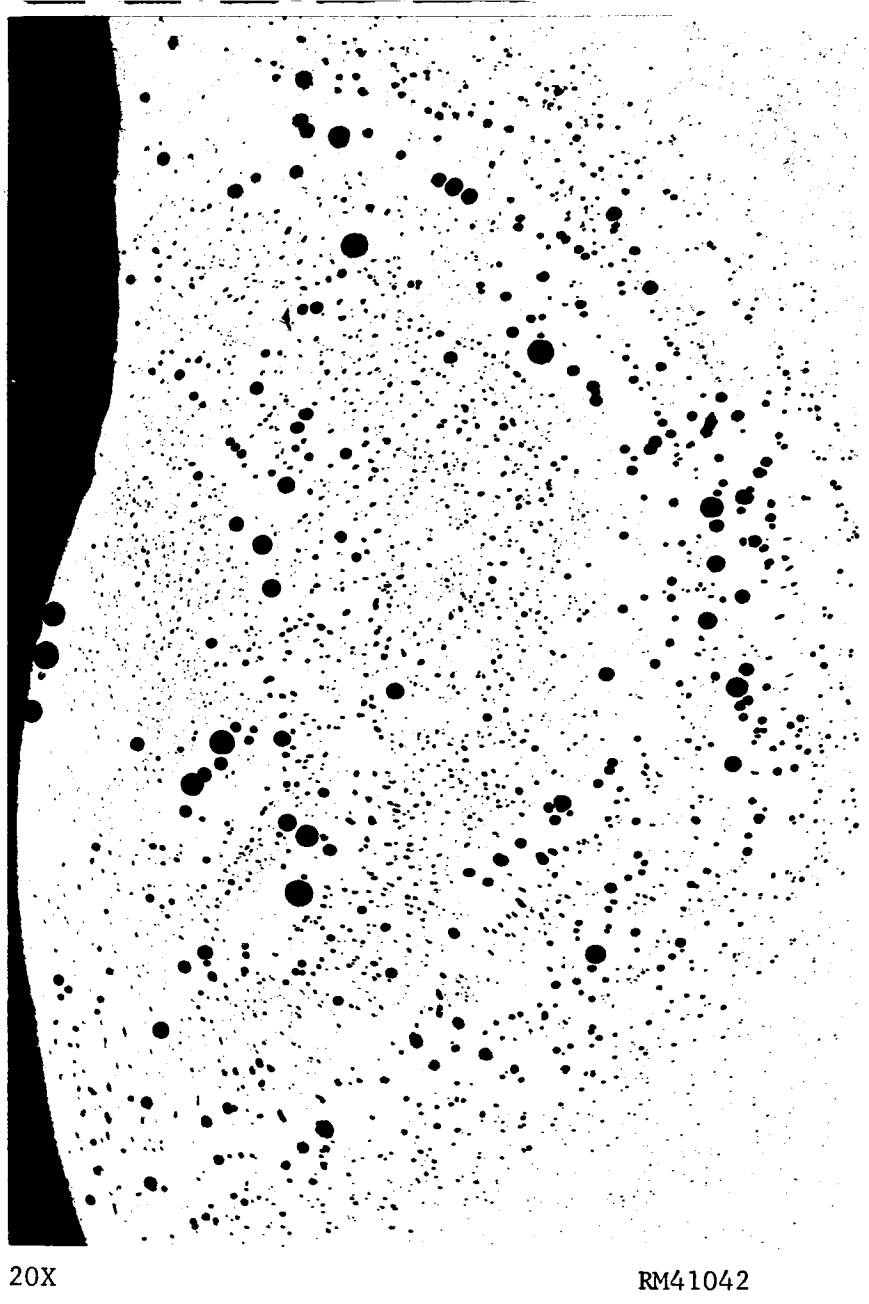

b. 3/4-Inch-Thick Base Plate

FIGURE E-16. TYPICAL CROSS SECTIONS OF WELDS MADE ON X2014, TYPE 8 BASE PLATE

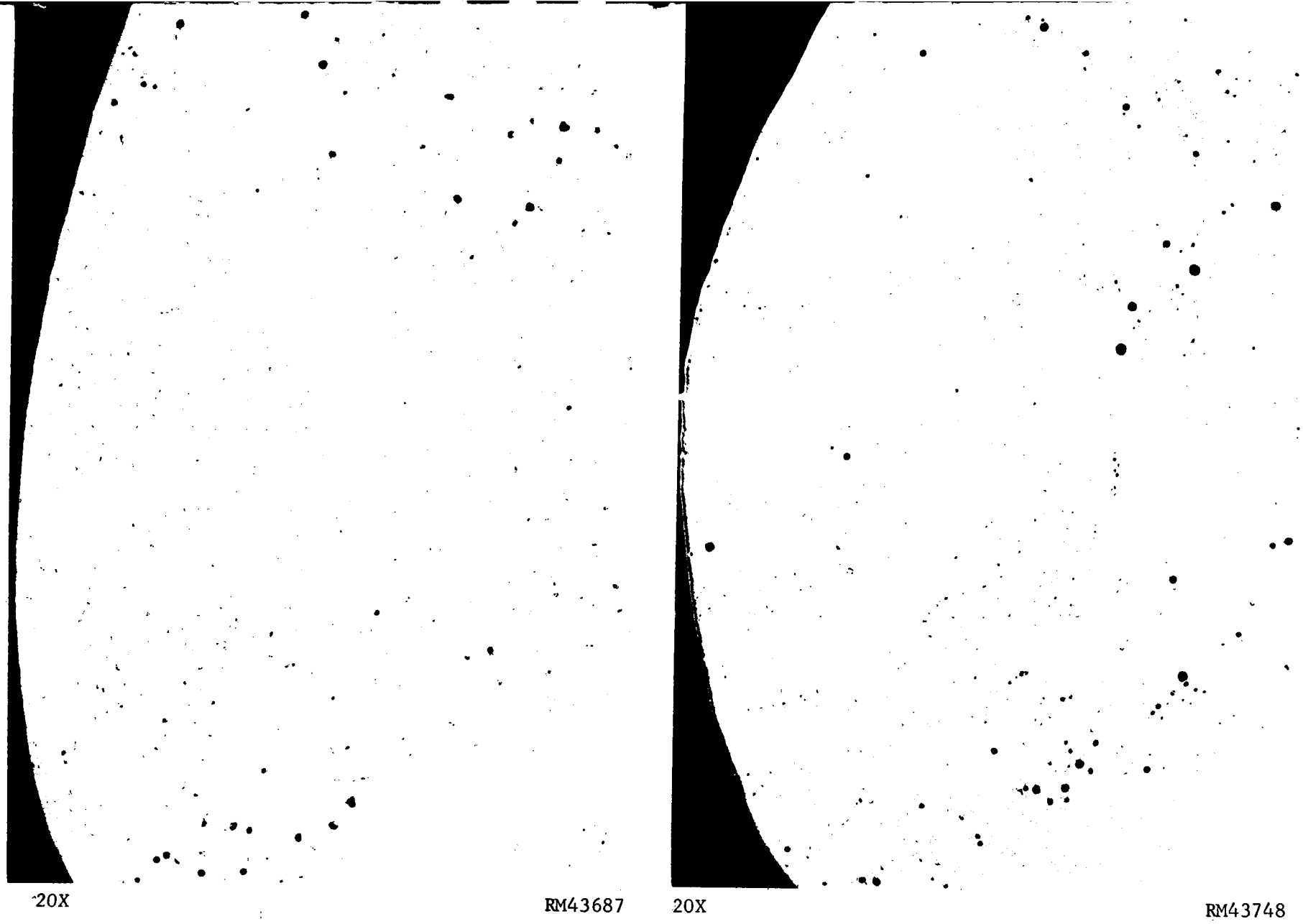

a. 1/4-Inch-Thick 2219 Plate

b. 3/4-Inch-Thick 2219 Plate

FIGURE E-17. TYPICAL CROSS SECTIONS OF WELDS WITH X2319, TYPE 1 FILLER WIRE

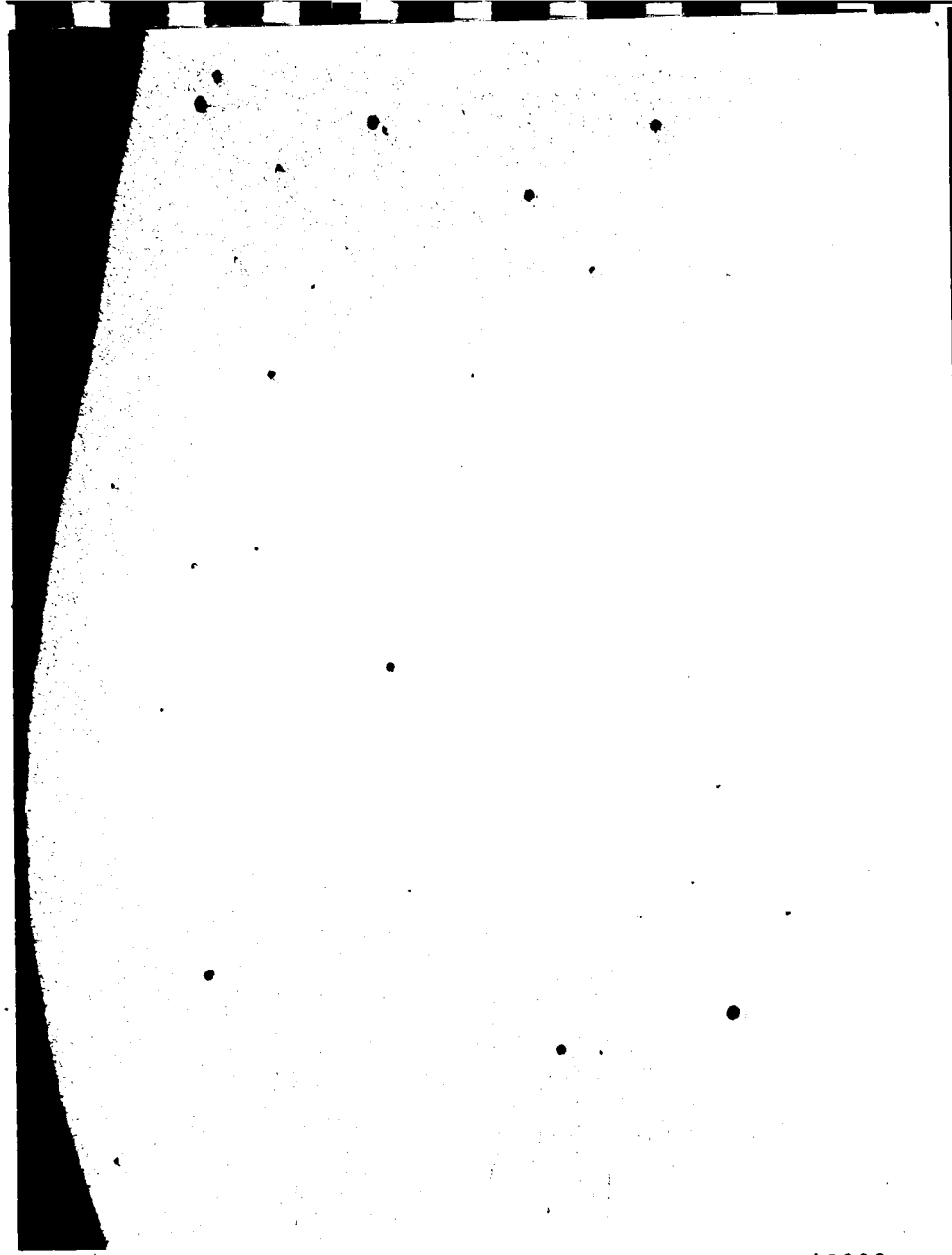

20X RM43999

a. 1/4-Inch-Thick 2219 Plate

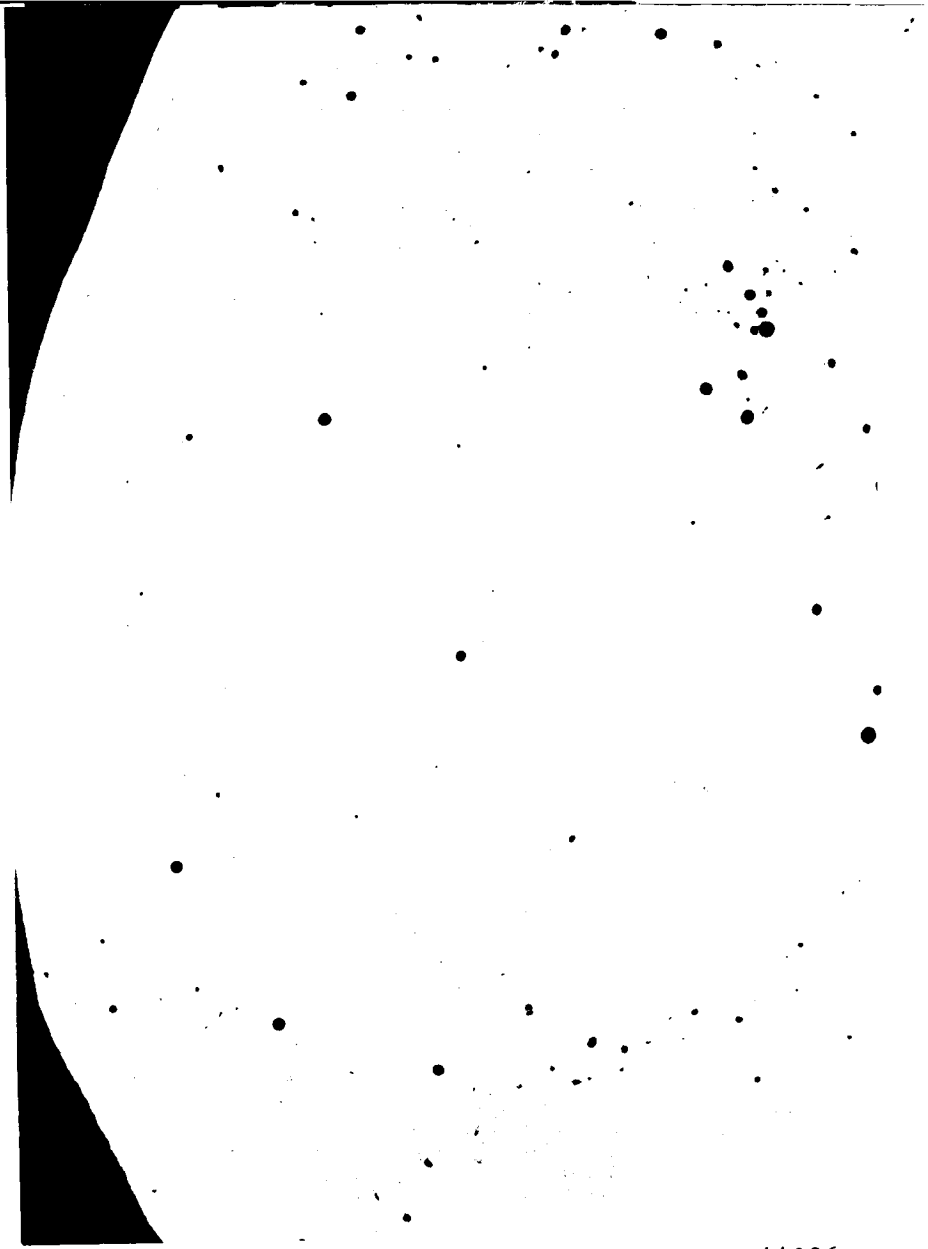

20X RM44006

b. 3/4-Inch-Thick 2219 Plate

FIGURE E-18. TYPICAL CROSS SECTIONS OF WELDS WITH X2319, TYPE 2 FILLER WIRE

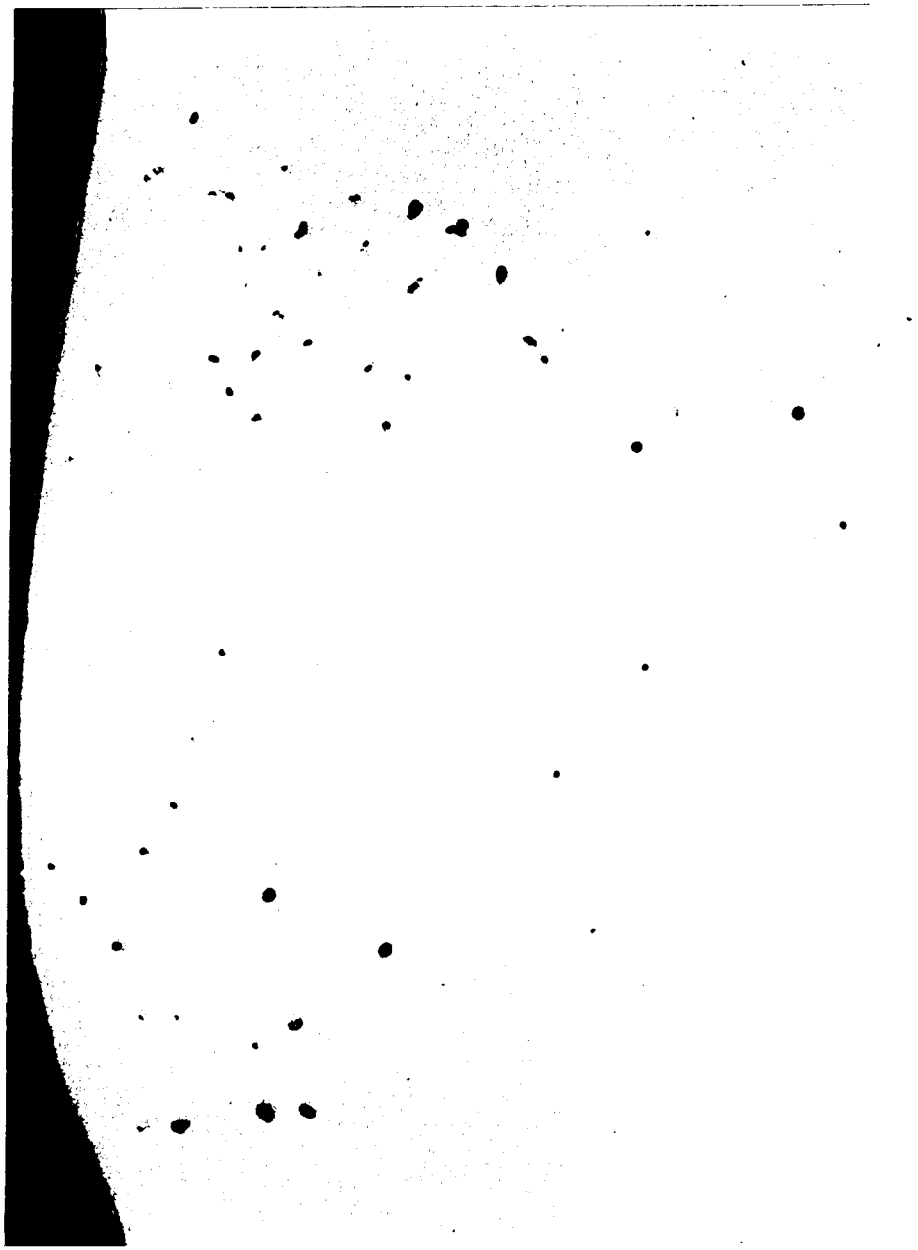

a. 1/4-Inch-Thick 2219 Plate

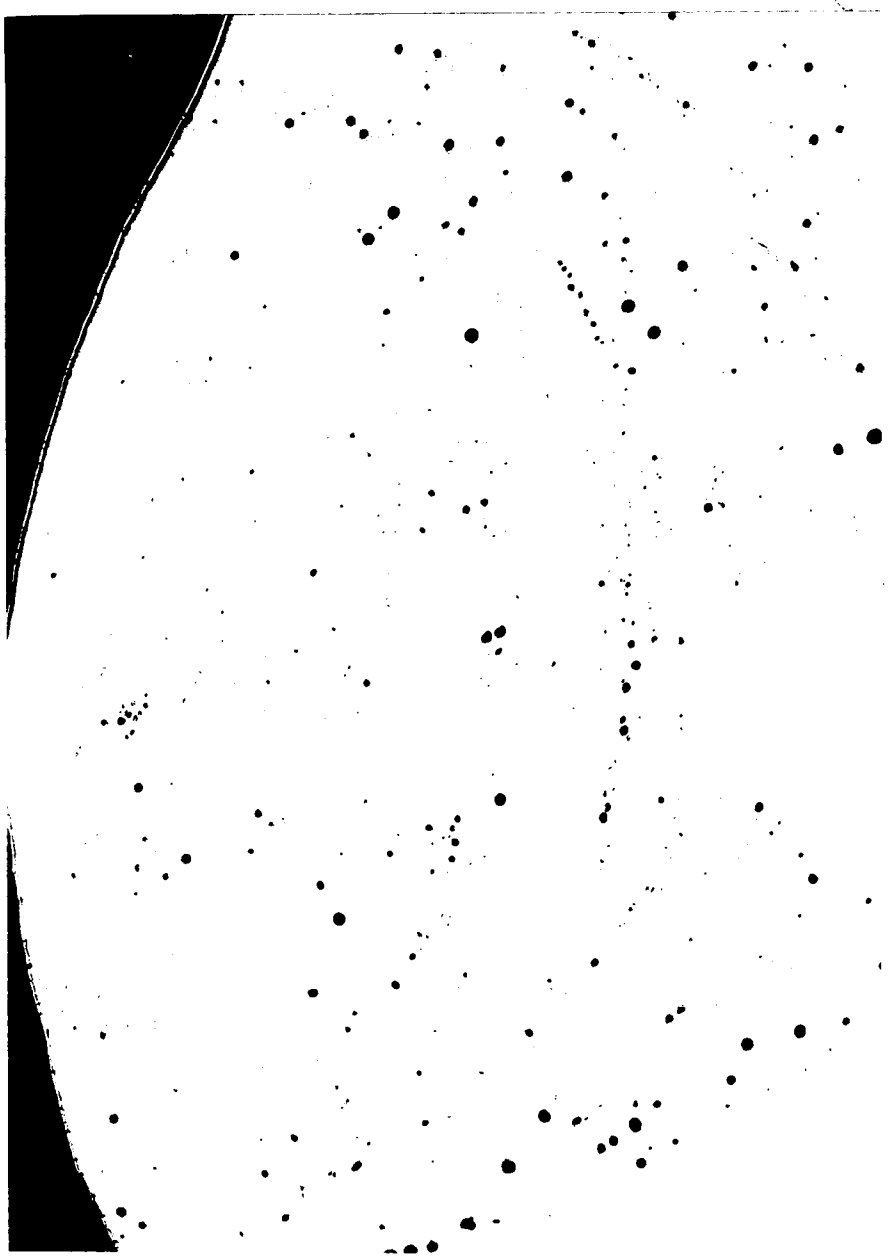

b. 3/4-Inch-Thick 2219 Plate

FIGURE E-19. TYPICAL CROSS SECTIONS OF WELDS WITH X2319, TYPE 3 FILLER WIRE

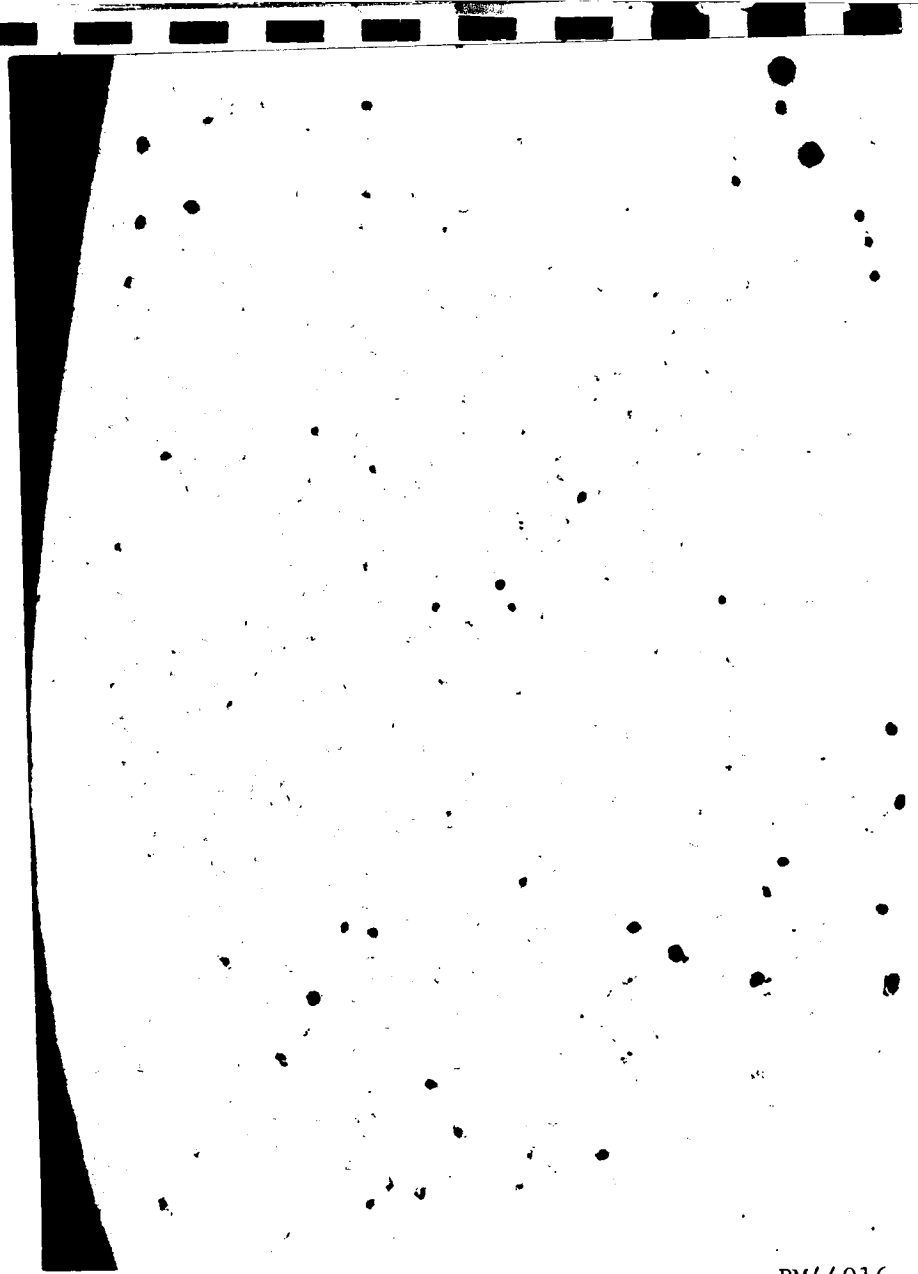

a. 1/4-Inch-Thick 2219 Plate

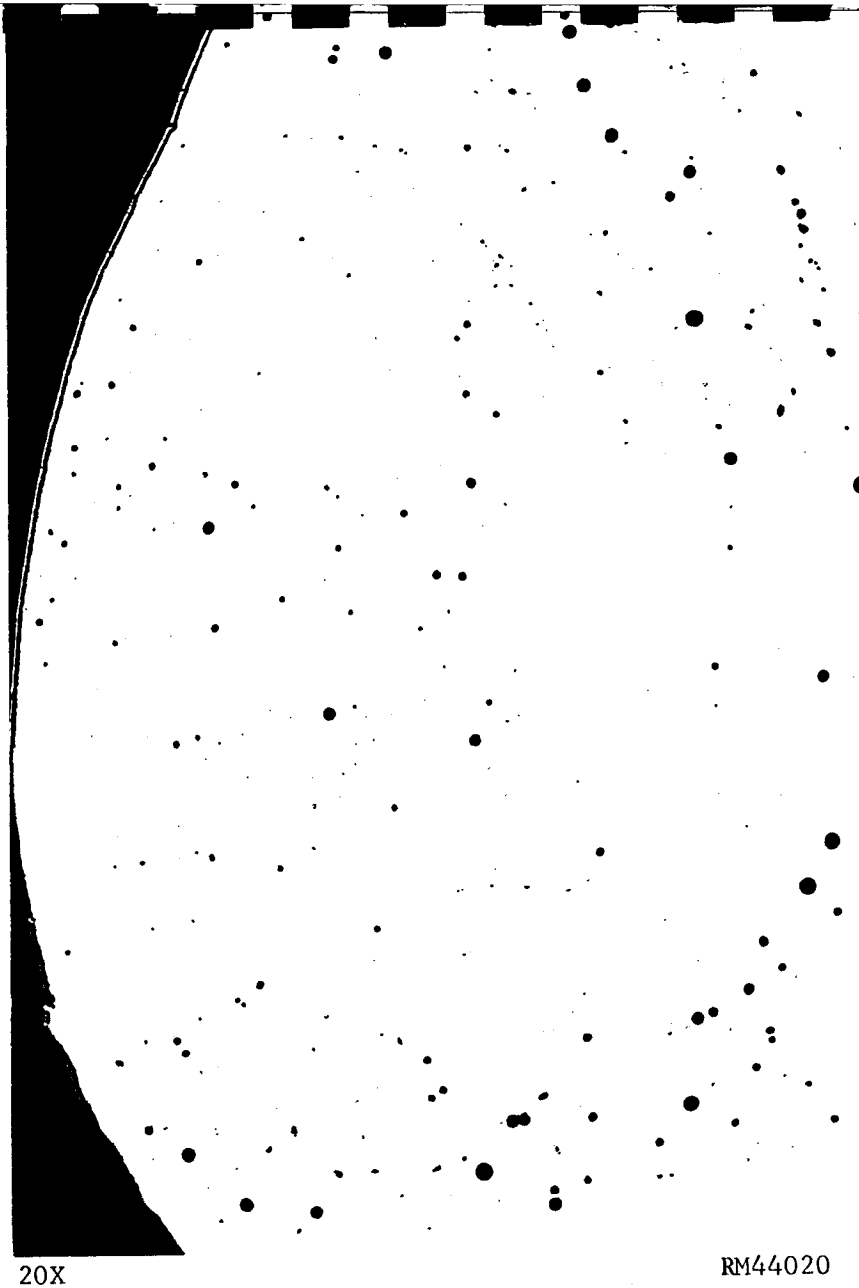

b. 3/4-Inch-Thick 2219 Plate

FIGURE E-20. TYPICAL CROSS SECTIONS OF WELDS WITH X2319, TYPE 4 FILLER WIRE

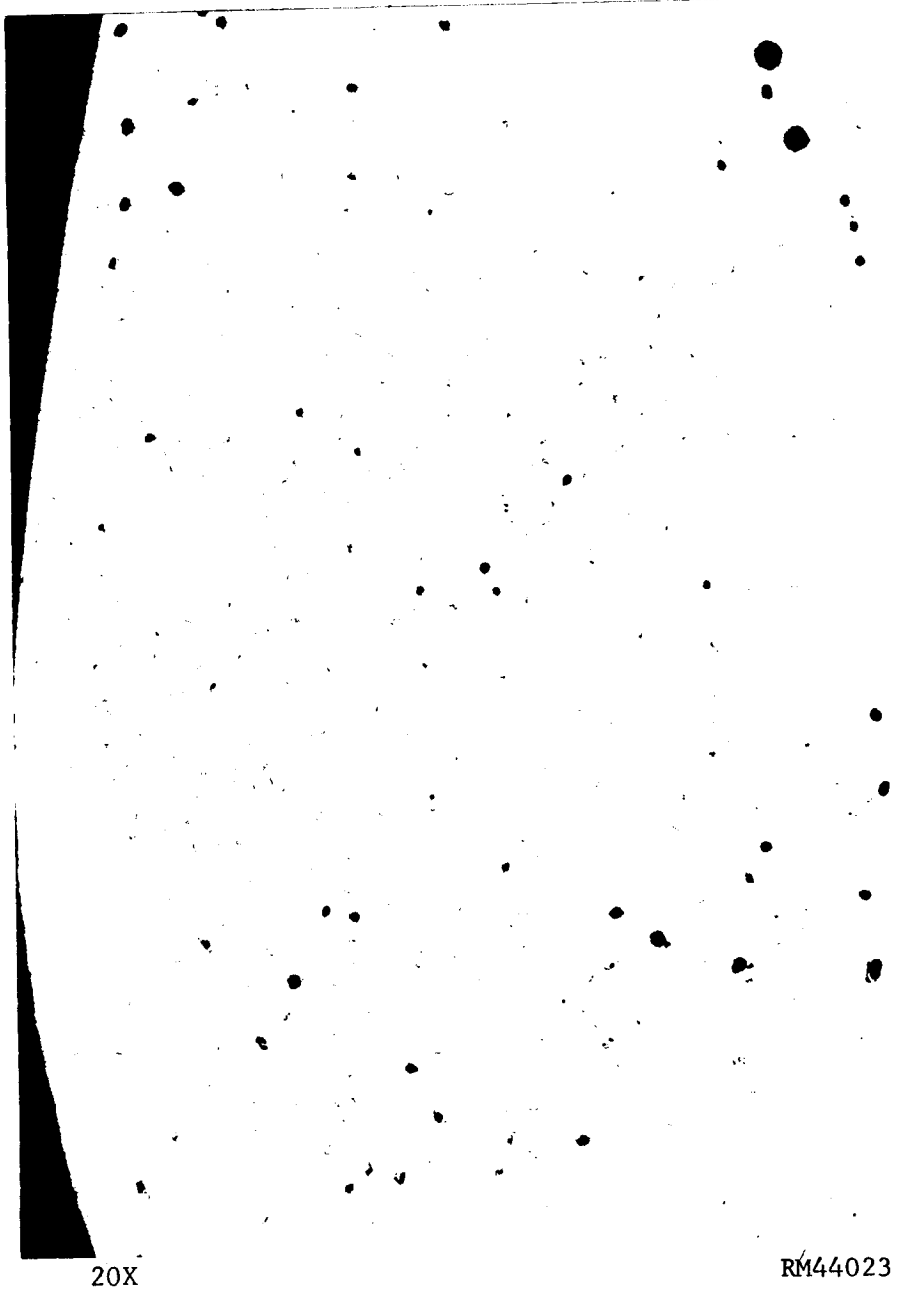

a. 1/4-Inch-Thick 2219 Plate

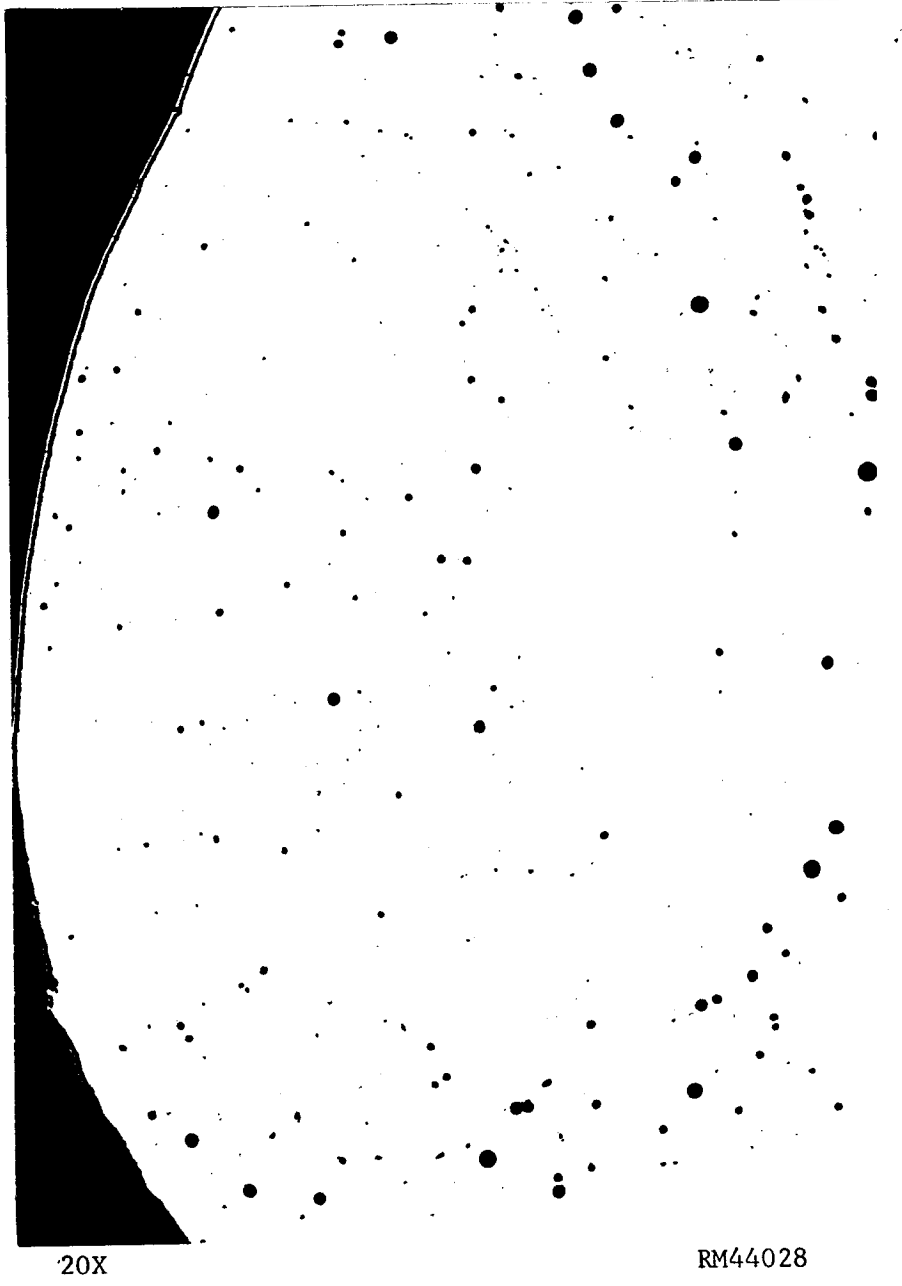

b. 3/4-Inch-Thick 2219 Plate

FIGURE E-21. TYPICAL CROSS SECTIONS OF WELDS WITH X2319, TYPE 5 FILLER WIRE

a. 1/4-Inch-Thick 2219 Plate

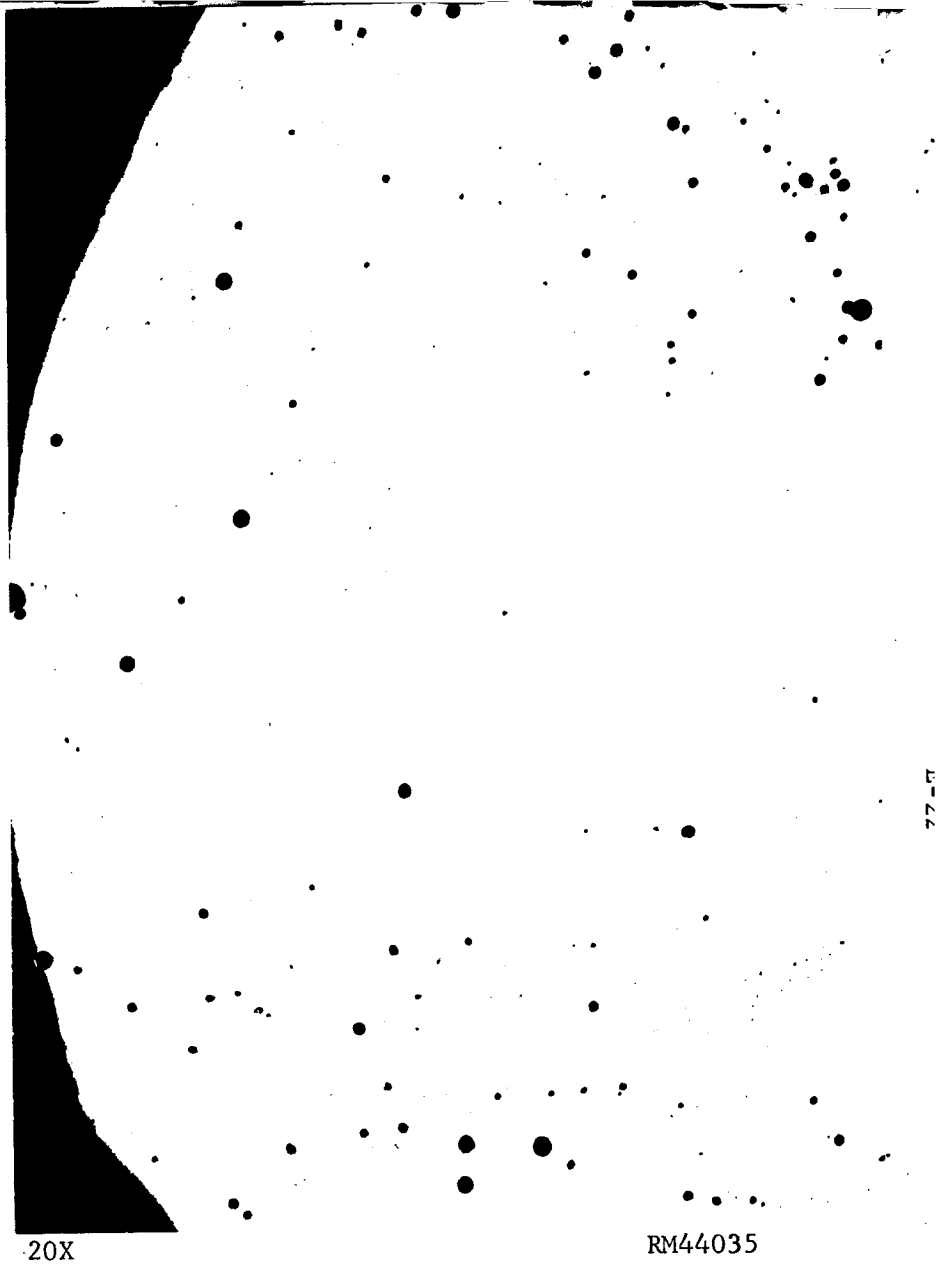

b. 3/4-Inch-Thick 2219 Plate

FIGURE E-22. TYPICAL CROSS SECTIONS OF WELDS WITH X2319, TYPE 6 FILLER WIRE

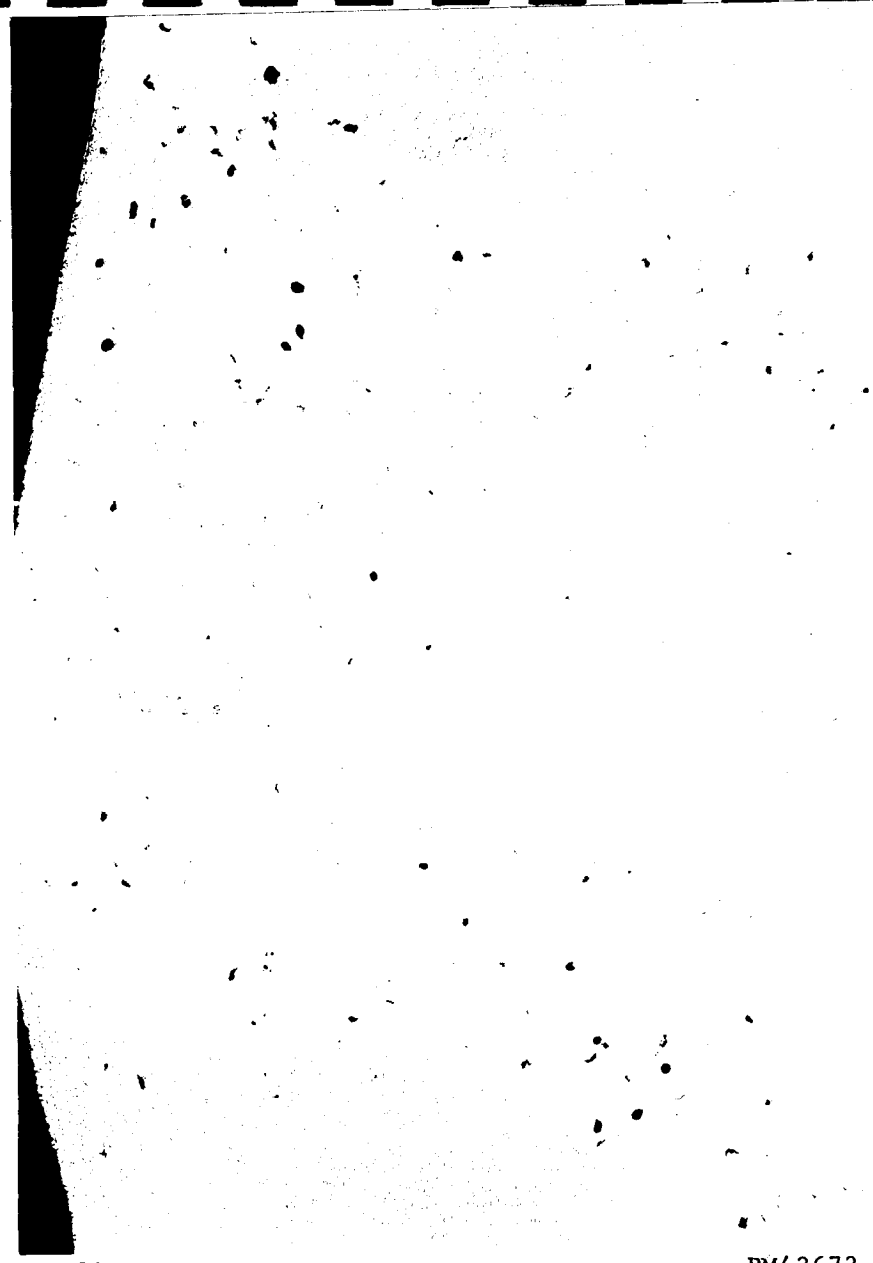

a. 1/4-Inch-Thick 2219 Plate

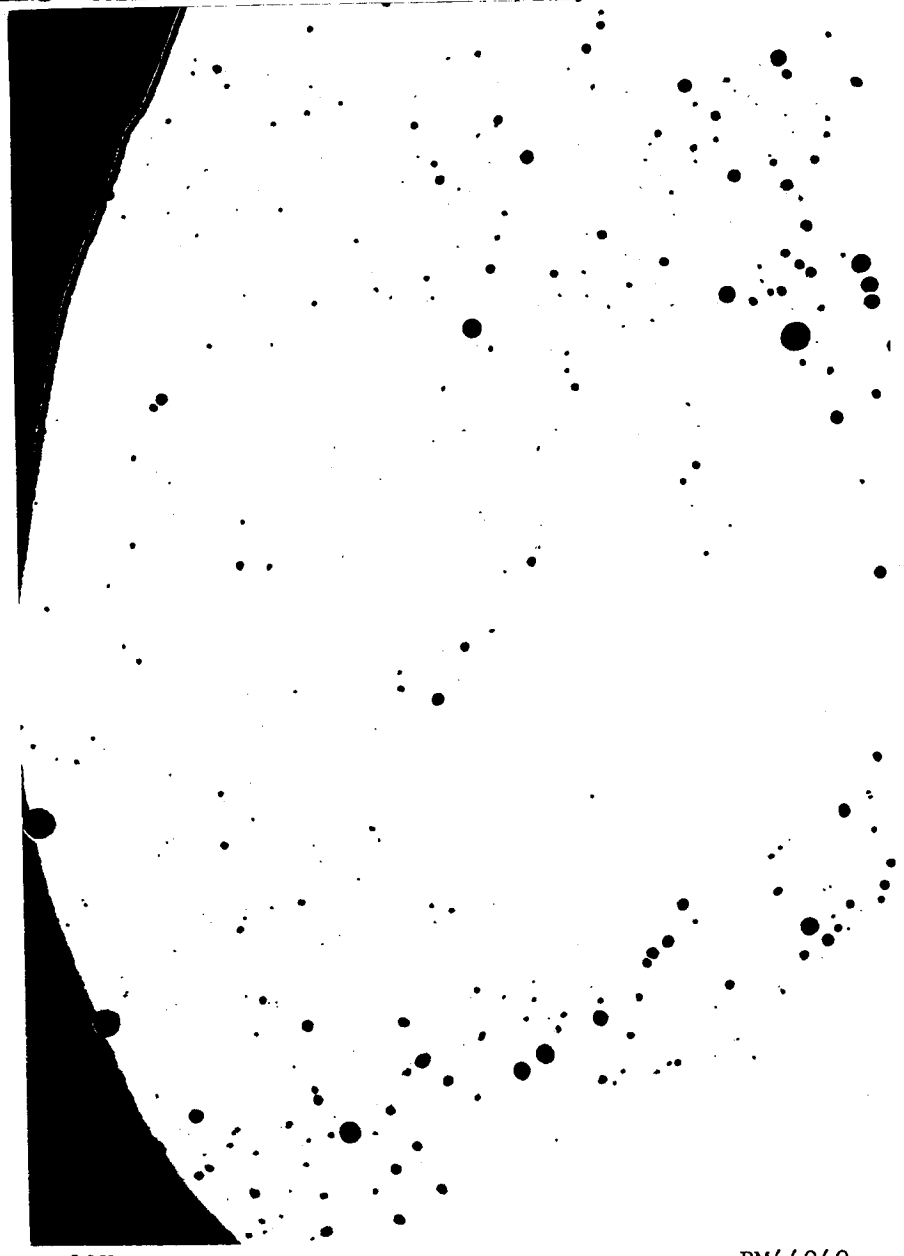

b. 3/4-Inch-Thick 2219 Plate

FIGURE E-23. TYPICAL CROSS SECTIONS OF WELDS WITH X2319, TYPE 7 FILLER WIRE

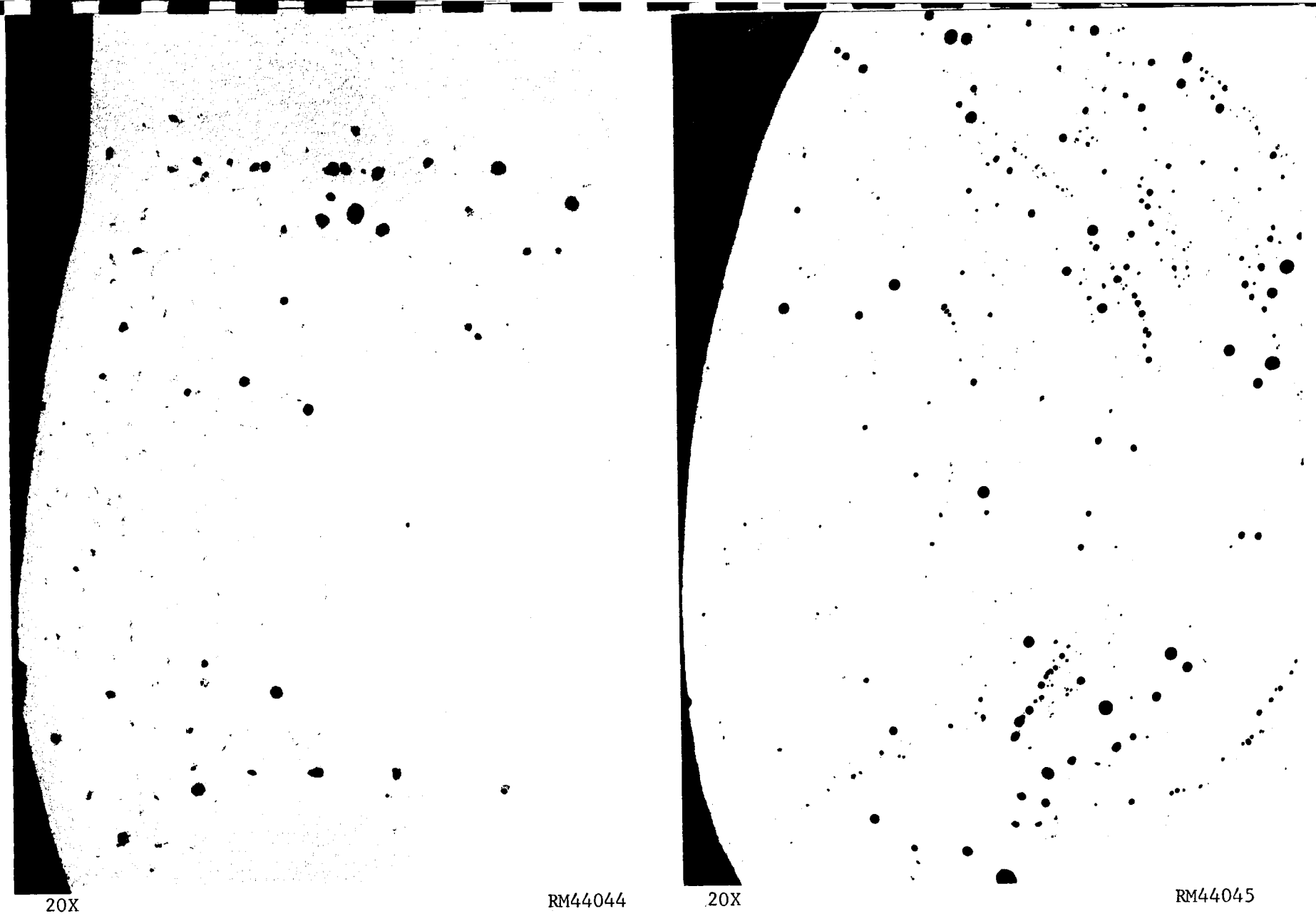

a. 1/4-Inch-Thick 2219 Plate

b. 3/4-Inch-Thick 2219 Plate

FIGURE E-24. TYPICAL CROSS SECTIONS OF WELDS WITH X2319, TYPE 8 FILLER WIRE

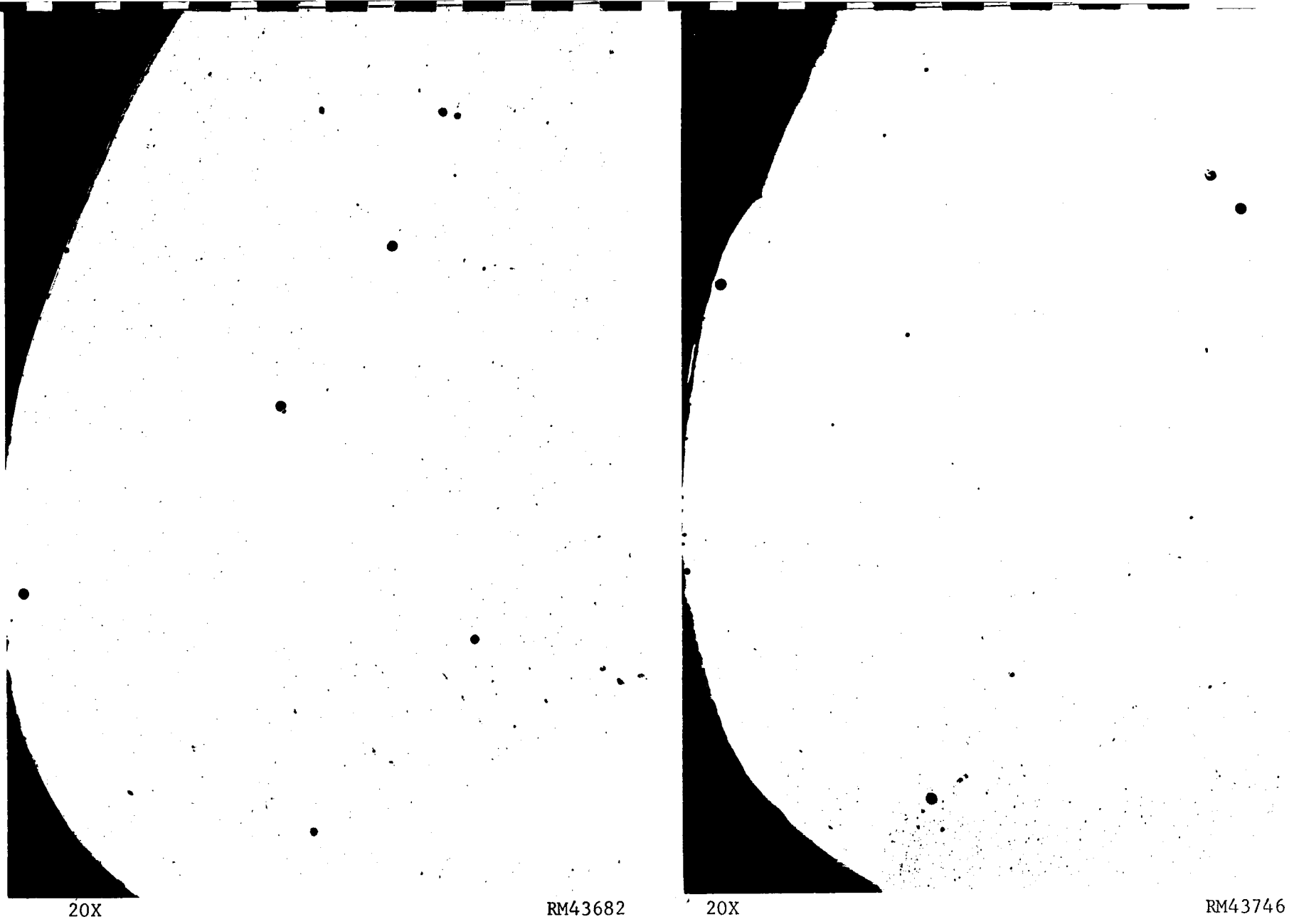

a. 1/4-Inch-Thick 2014 Plate

b. 3/4-Inch-Thick 2014 Plate

FIGURE E-25. TYPICAL CROSS SECTIONS OF WELDS WITH X4043, TYPE 1 FILLER WIRE

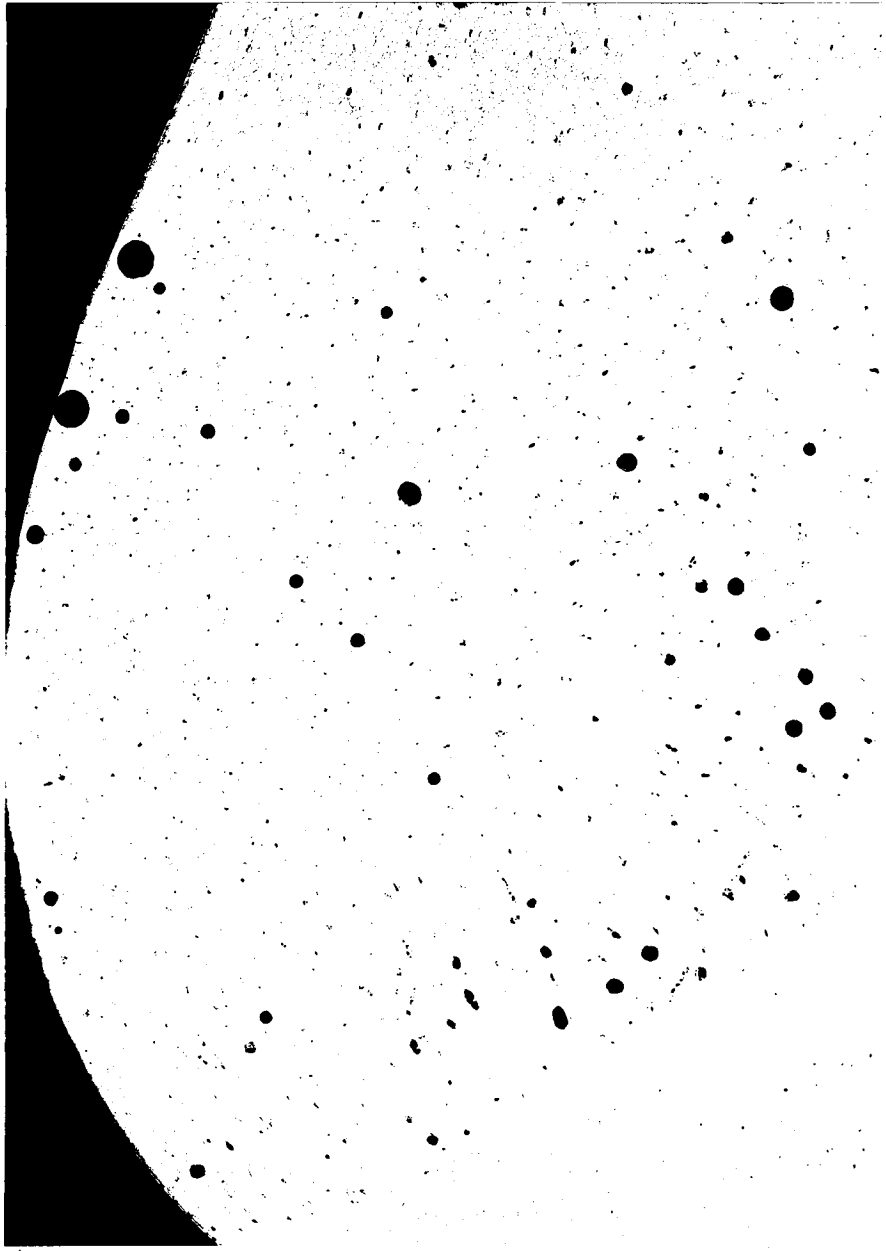

a. 1/4-Inch-Thick 2014 Plate

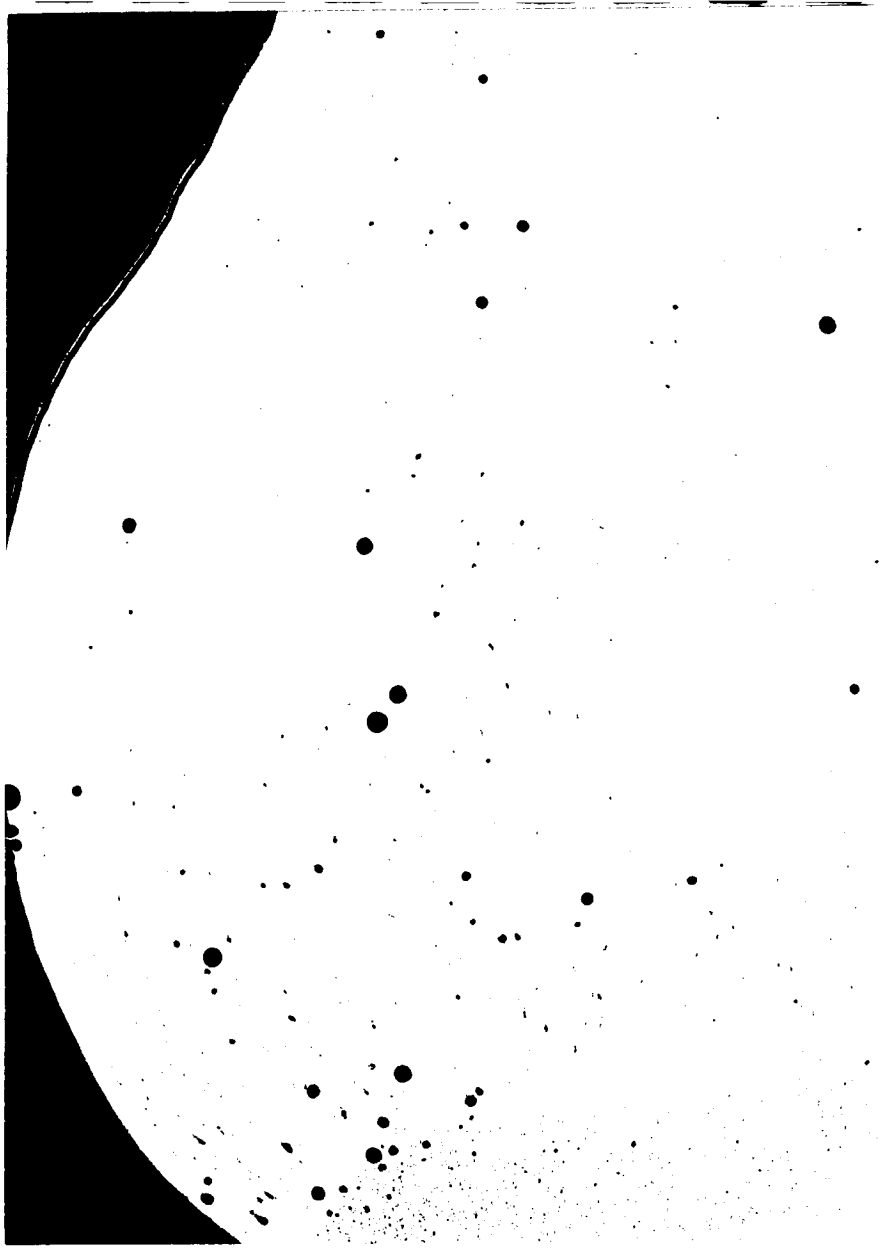

b. 3/4-Inch-Thick 2014 Plate

FIGURE E-26. TYPICAL CROSS SECTIONS OF WELDS WITH X4043, TYPE 2 FILLER WIRE

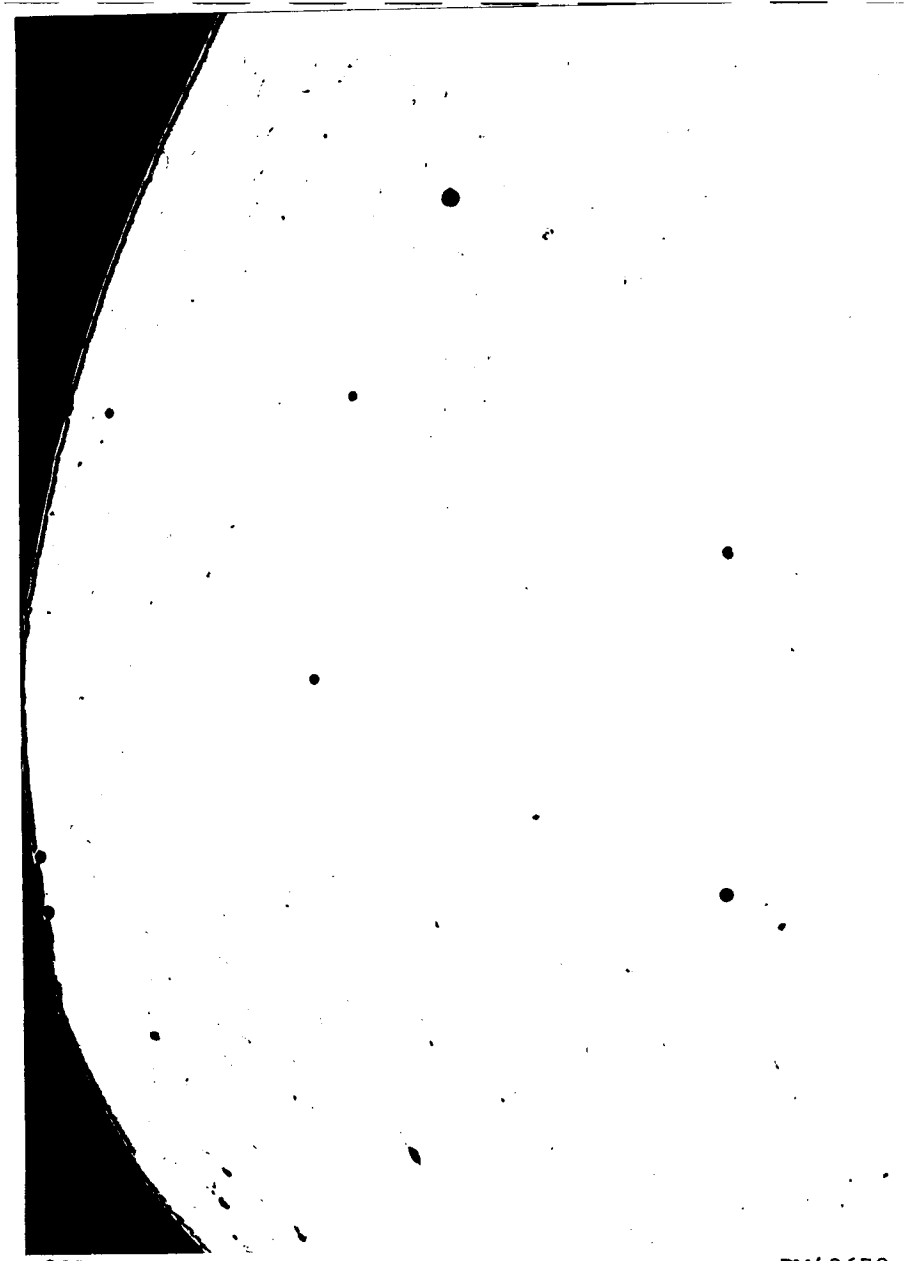

a. 1/4-Inch-Thick 2014 Plate

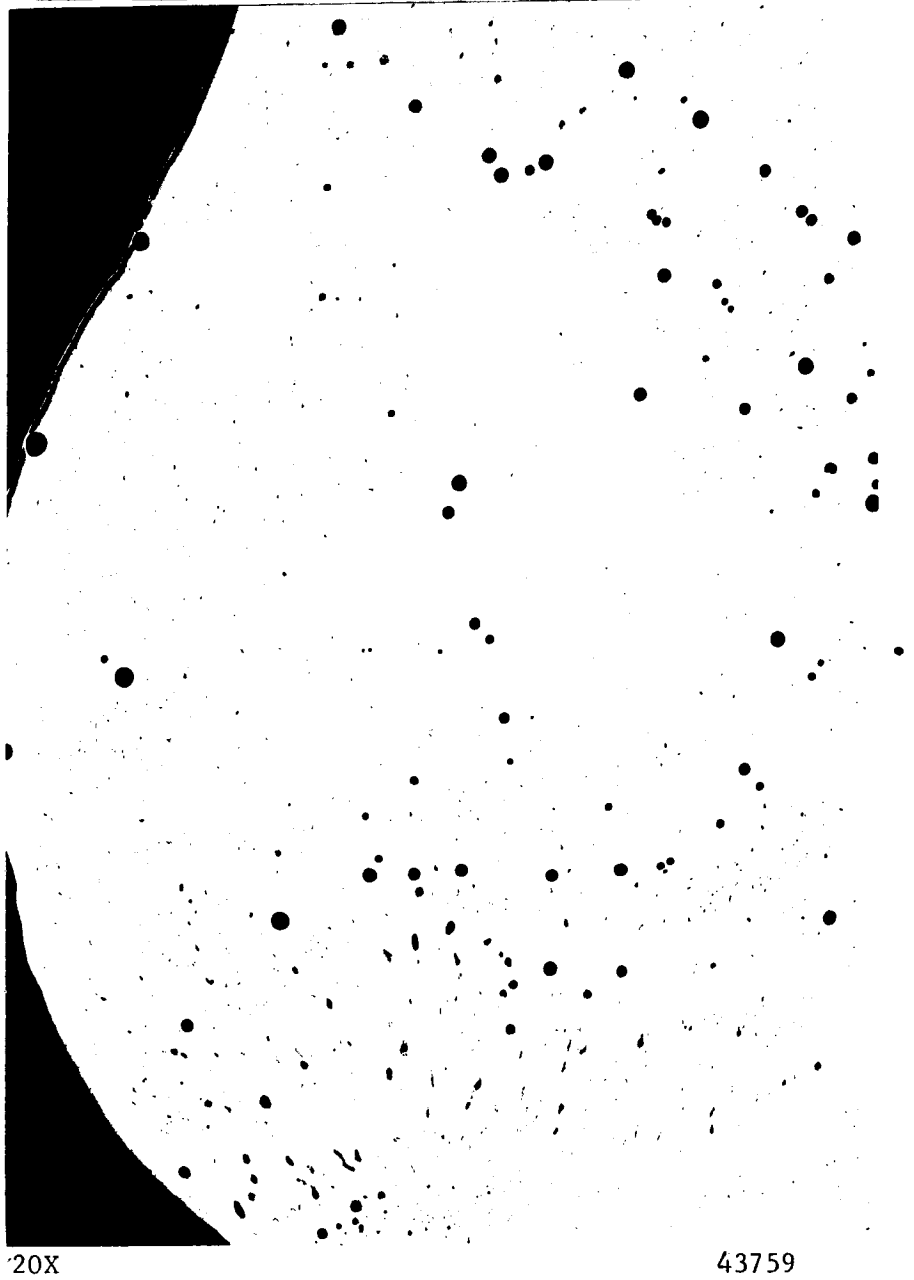

b. 3/4-Inch-Thick 2014 Plate

FIGURE E-27. TYPICAL CROSS SECTIONS OF WELDS WITH X4043, TYPE 3 FILLER WIRE

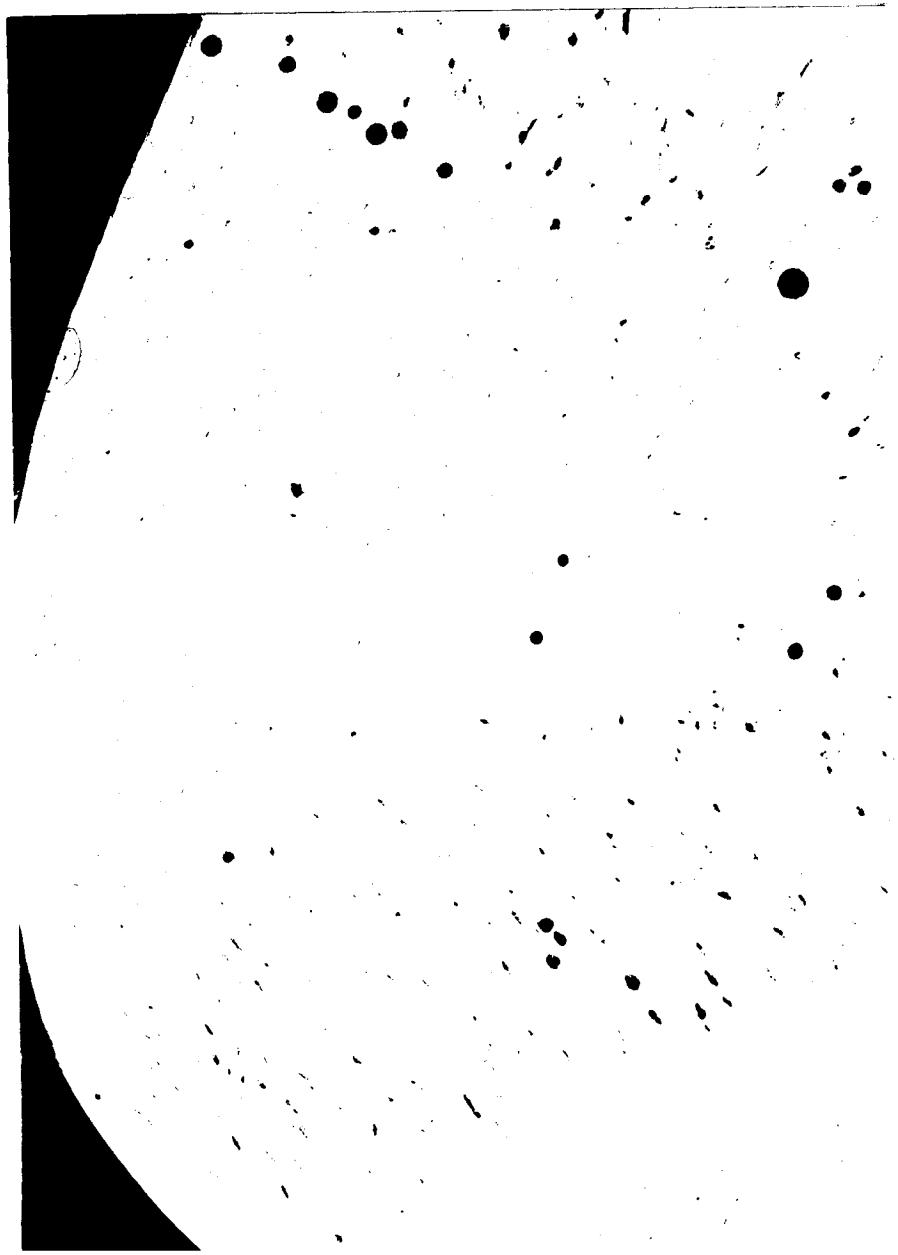

a. 1/4-Inch-Thick 2014 Plate

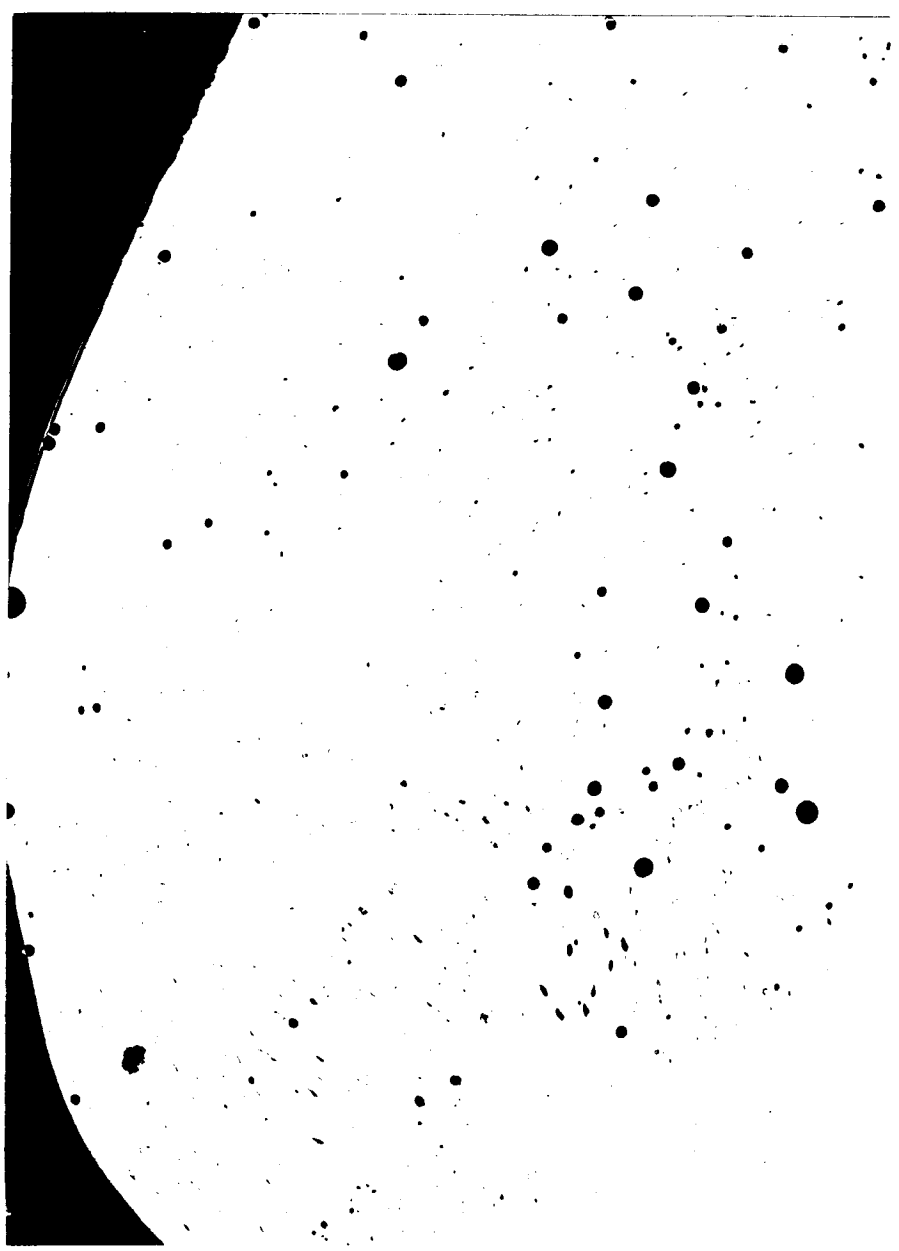

b. 3/4-Inch-Thick 2014 Plate

FIGURE E-28. TYPICAL CROSS SECTIONS OF WELDS WITH X4043, TYPE 4 FILLER WIRE

a. 1/4-Inch-Thick 2014 Plate

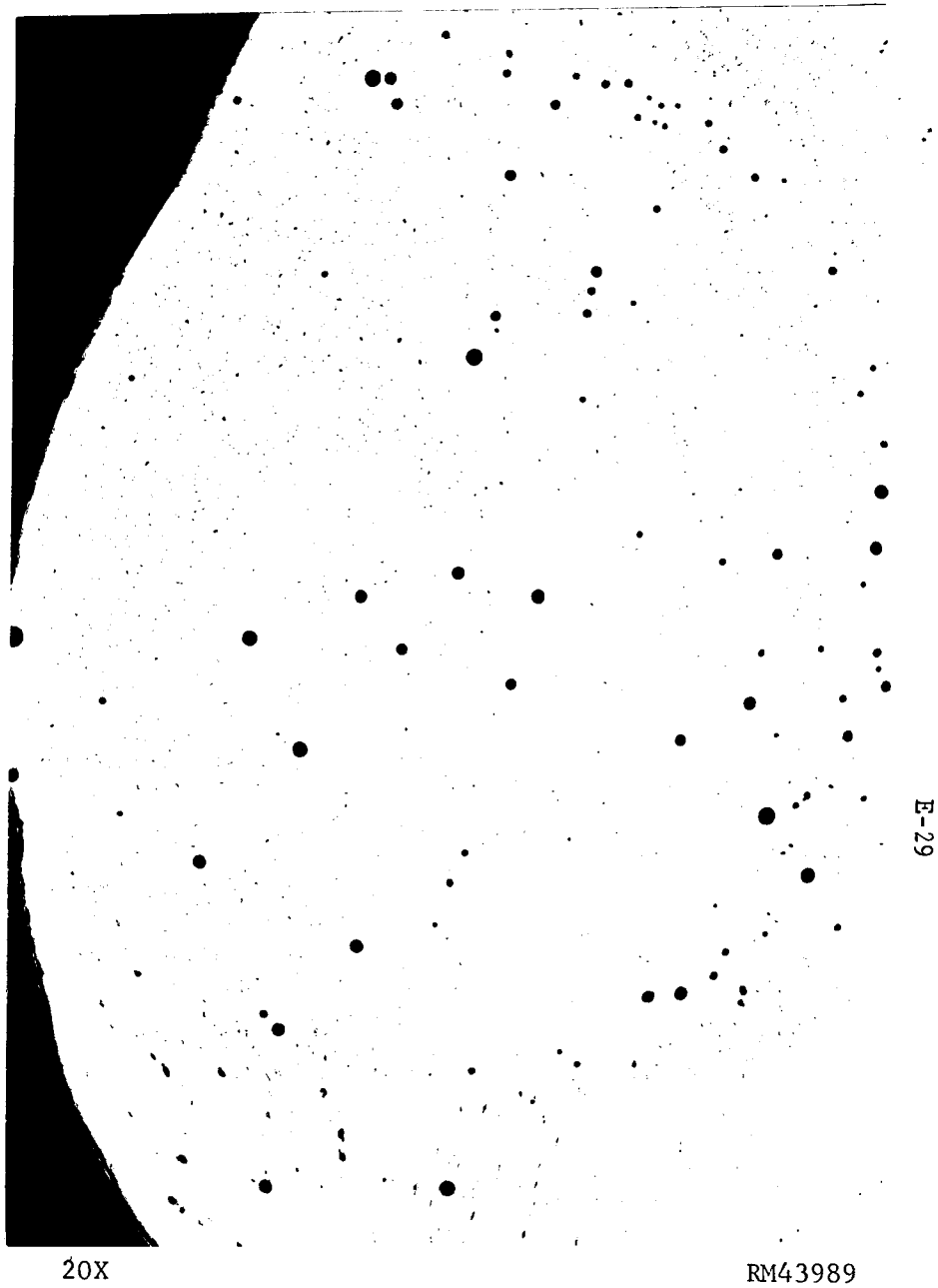

b. 3/4-Inch-Thick 2014 Plate

FIGURE E-29. TYPICAL CROSS SECTIONS OF WELDS WITH X4043, TYPE 5 FILLER WIRE

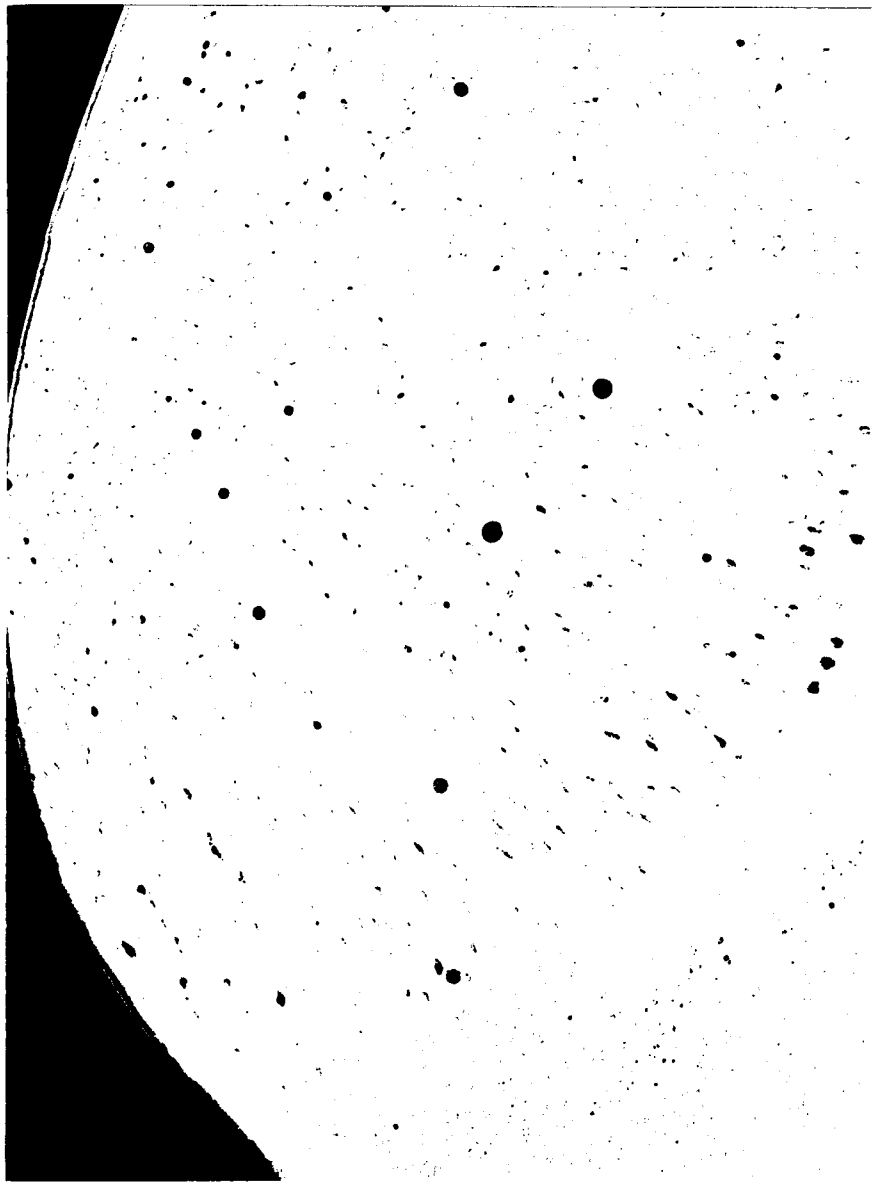

a. 1/4-Inch-Thick 2014 Plate

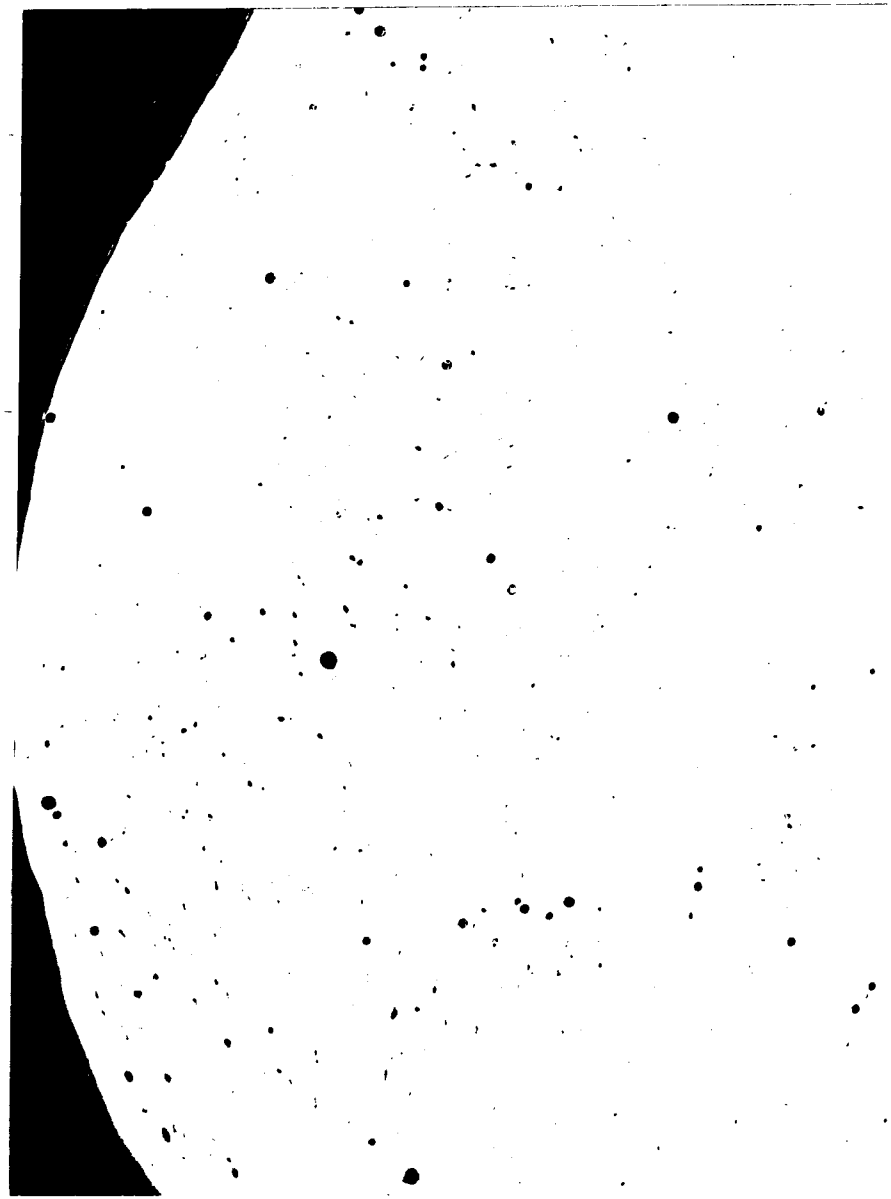

b. 3/4-Inch-Thick 2014 Plate

FIGURE E-30. TYPICAL CROSS SECTIONS OF WELDS WITH X4043, TYPE 6 FILLER WIRE

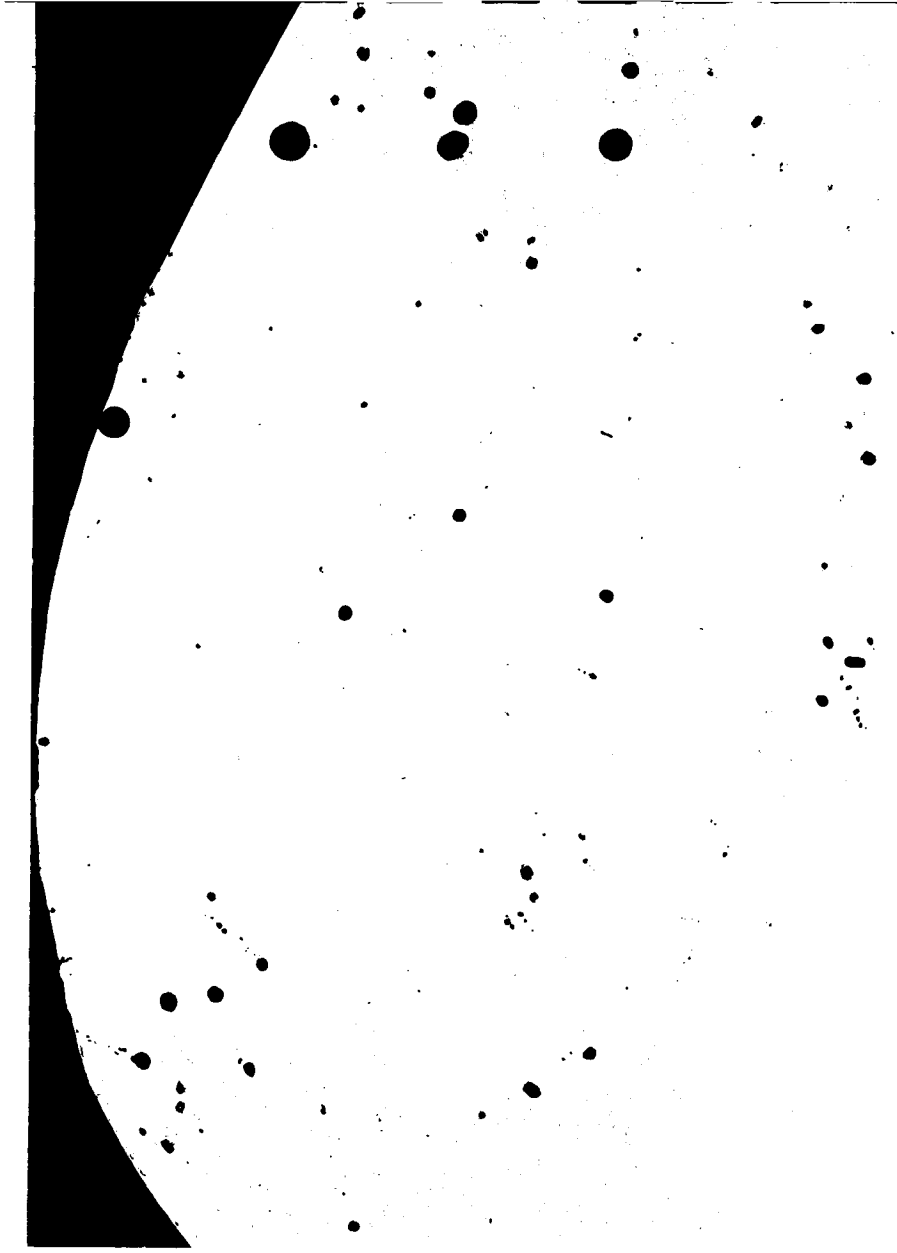

a. 1/4-Inch-Thick 2014 Plate

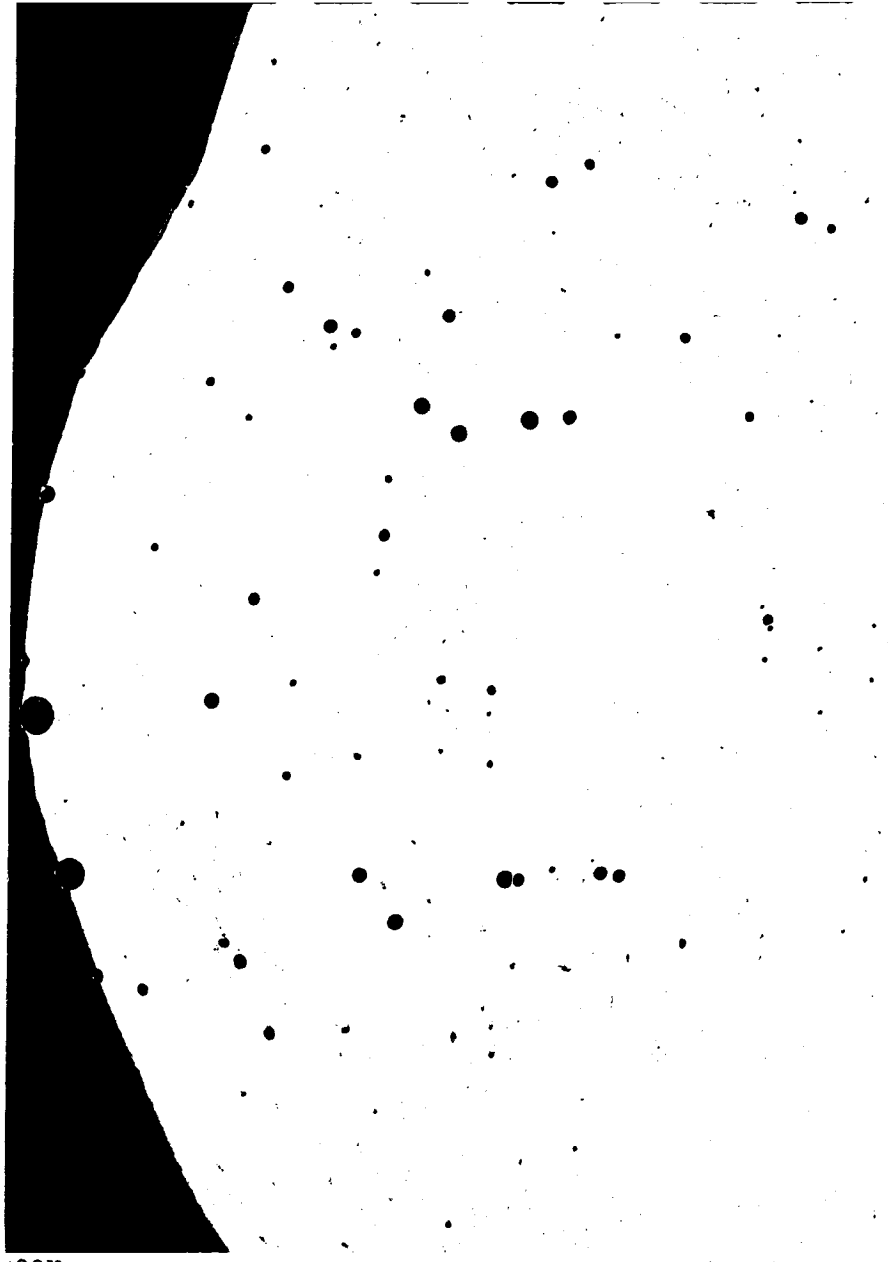

b. 3/4-Inch-Thick 2014 Plate

FIGURE E-31. TYPICAL CROSS SECTIONS OF WELDS WITH X4043, TYPE 7 FILLER WIRE

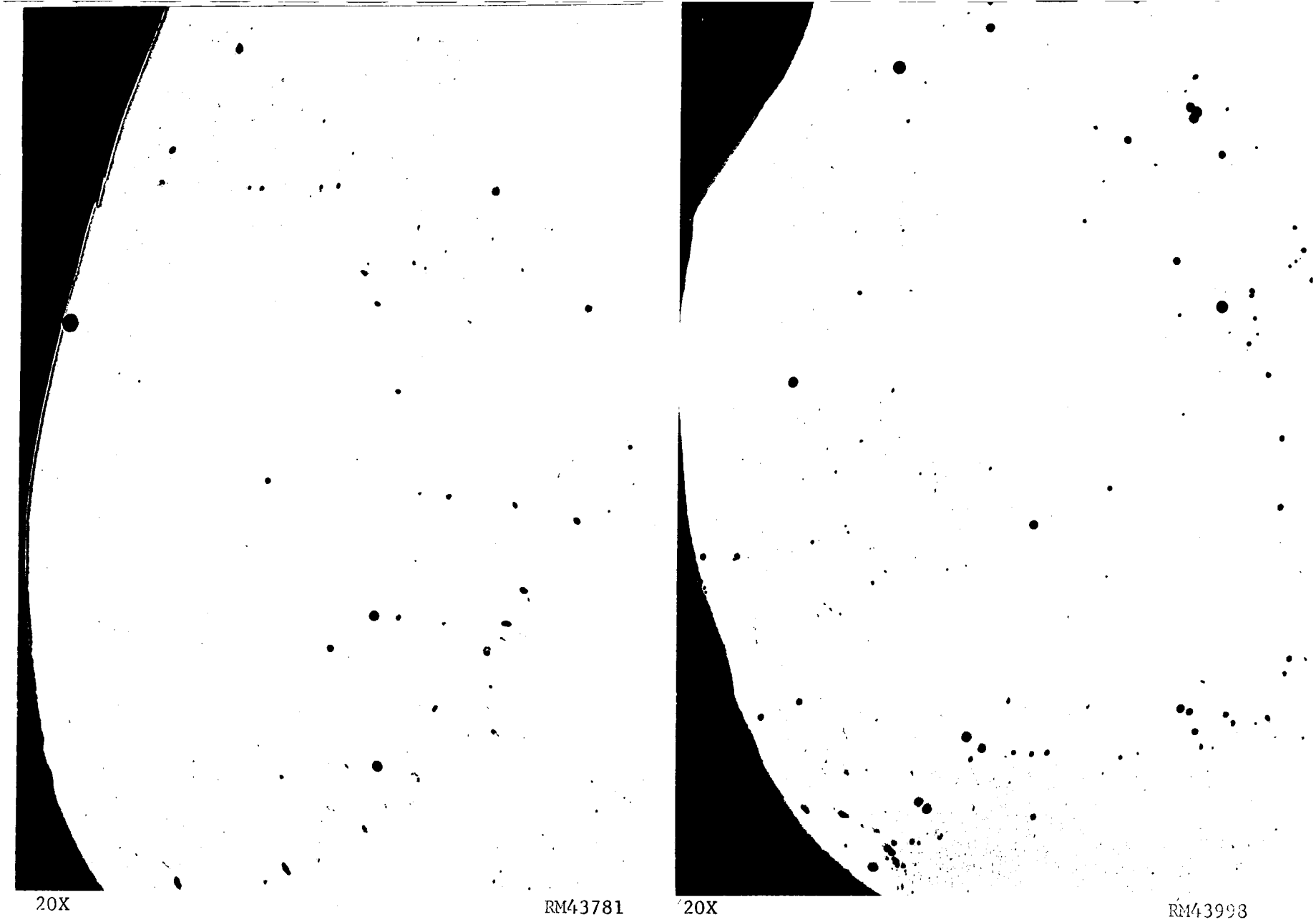

a. 1/4-Inch-Thick 2014 Plate

b. 3/4-Inch-Thick 2014 Plate

FIGURE E-32. TYPICAL CROSS SECTIONS OF WELDS WITH X4043, TYPE 8 FILLER WIRE

APPENDIX F

STATISTICAL ANALYSIS

Statistical Design

The experimental program was planned according to accepted statistical practice. The statistical design that was utilized was a half replicate of a factorial arrangement of the 16 possible combinations of 2 levels of each of the following 4 variables: external impurities, internal impurities, chemical content, and gas content. High and low levels of these variables were combined as follows:

Run	C	E	G	I
1	L	L	L	L
2	L	L	H	H
3	L	H	H	L
4	L	H	L	H
5	H	L	H	L
6	H	L	L	H
7	H	H	L	L
8	H	H	H	H

In the above table, an entry L indicates the low level of a factor and an entry H the high level. Column C specifies the levels of chemical content, Column E the levels of external impurities, Column G the levels of gas content, and Column I the levels of internal impurities.

It was recognized that, in selecting this design, the type of information provided by numerical analysis of the resulting data was thereby predetermined. Tests of statistical significance of the separate effects (on porosity) of the 4 factors are provided by the analysis. However, only linear effects of these factors can be detected. In order to measure curvilinear effects, at least 3 levels of each variable would be required. Furthermore, interaction effects are not measurable. So if porosity changed with joint changes in two or more of the experimental variables, this fact could not be established. In Table F-1 are listed the measurable effects for the selected design.

TABLE F-1. MEASURABLE EFFECTS

Effect*	Alias	Degrees of Freedom
E	ICG	1
I	ECG	1
C	EIG	1
G	EIC	1
EI	CG	1
EC	IG	1
EG	IC	1
Plate		24
Total		31

E = external impurities
I = internal impurities
C = chemical content
G = gas content

Analysis of Variance

"Analysis of variance" is a widely used statistical tool. It is used primarily in the numerical analysis of data obtained from experiments which have been planned in accordance with sound statistical principles. The fractional factorial design, which was employed in the present task, fits this requirement.

A variance analysis is essentially a method of breaking the total variation in a set of observations into components which can be associated with identifiable factors. These factors are usually the experimental variables, whose real effects are unknown. The key component of variation is "experimental error". This also goes by other names such as repeatability, random variation, and so on. This is the standard of comparison for all the other factors.

The variation in the data caused by a test factor, when compared with experimental error, provides a statistical test of significance of that factor. The outcome of such a test is expressed as a percentage* which may be thought of as the "degree of certainty" that the factor in question exerts a real effect on the measured characteristic. The terms "high degree of certainty" and "high significance" are often used interchangeably. If this percentage is low, the factor probably has little, if any, effect; if this percentage is high, the factor probably has an appreciable effect. The dividing point between a "low" and a "high" percentage is called the "level of significance". It is customary to set the significance level at 95 per cent, but this is largely arbitrary and is affected by individual circumstances.

The ability of a significance test to detect an effective factor is greatly dependent on the number of "degrees of freedom" associated with experimental error. A degree of freedom is a concept linked to the size of a sample. It may be regarded as that portion of a sample which is reserved for the measurement of a given effect. A sample of n observations has a total of n degrees of freedom which can be assigned various tasks. The success of an experiment depends very often on the ability of the researcher to control the size of experimental error and to measure it with sufficient degrees of freedom for the purpose at hand.

Revised Analysis

When the level of the gas content of the compositions cast for Phase I were incompletely controlled to form two distinct levels by the casting method, the resulting compositions did not fit into the

* Statisticians recognize this percentage as a fractile of an F-distribution associated with m and n degrees of freedom.

original statistical plan. An analysis of variance was used to analyze the results in Phase I. For Phase II, the factor of external impurities was fixed instead of varied as in Phase I. Also, the gas content of the materials was not controlled at the two levels needed for statistical analysis. An analysis of variance was conducted on the Phase II results also. A sample calculation for the analysis of variance is included in Table F-2.

TABLE F-2. SAMPLE CALCULATION OF ANALYSIS OF VARIANCE 3/4-INCH-THICK X2219 BASE PLATE, POROSITY LEVEL IN PER CENT

	Type 4					Type 7					
Sample	1	2	3	4		1	2	3	4		
	1.6	8.4	7.1	2.5		6.4	5.3	5.6	1.5		
	0.7	1.3	8.6	1.1		5.9	4.3	5.7	0.8		
				4.0				1.9	6.1		
								2.3	5.9		
Sum	2.3	9.7	15.7	7.6	35.3	12.3	9.6	15.5	14.3	51.7	87.0
Number	2	2	2	3	9	2	2	4	4	12	21
Average	1.1	4.9	7.8	2.53	3.92	6.1	4.8	3.9	3.6	4.31	

Correlation = $(87.0)^2 \div 21 = 360.428571$

Total = $(1.6)^2 + \ldots + (5.9)^2$ - correlation = 493.14 - cor. = 132.711429

P = $\frac{(2.3)^2}{2} + \ldots + \frac{(14.3)^2}{4}$ - correlation = 425.098333 - cor. = 64.669762

Type = $\frac{(35.3)^2}{9} + \frac{(51.7)^2}{12}$ - correlation = 0.766706

		Sum of Square		Degree of Freedom	Variance	F Ration	Degree of Certainty
		0.766706		1	0.766706	0.072 (1,6)	Not Significant
P-(Type)		63.903056		6	10.650509		
	P		64.669762	7	9.238537	1.77 (7,13)	81%
	R		68.041667	13	5.233974		
	T		132.711429	20			

APPENDIX G

REFERENCES

References

The following references were found to be relevant to the work, observations, and conclusions of the program. The references were grouped under five categories.

Weld Solidification

(1) Paul E. Brown and C. M. Adams, Jr., "Fusion Zone Structures and Properties in Aluminum Alloys", Welding Journal Research Supplement, Vol. 42 No. 12, pp 520-s to 524-s (December, 1963)

(2) H. S. Guren and R. D. Stout, "Solidification Phenomena in Inert Gas Metal-Arc Welds", Welding Journal Research Supplement, Vol. 42 No. 7, pp 298-s to 310-s (July, 1963)

Aluminum, Hydrogen, and Porosity

(3) M. D. Randall, P. A. Kammer, R. E. Monroe, and D. C. Martin, "Minimization of Influences of Wire Surface Conditions on the Automatic Welding of Aluminum". Final Report, October 31, 1962, Battelle Memorial Institute, Contract NAS8-2593. (Also reported in Welding Journal Research Supplement, Vol. 42 No. 10, pp 433-s to 440-s (October, 1963)).

(4) G. R. Salter and D. R. Milner, "Gas Metal Arc Reactions in Arc Welding", British Welding Journal, Vol. 12 No. 3, pp 222 to 228

(5) D. E. J. Talbot and D. A. Granger, "Secondary Hydrogen Porosity in Aluminum", Journal of the Institute of Metals, Vol. 92, pp 290 to 297 (1963-1964)

Hydrogen Analysis

(6) James L. Brandt and C. Norman Cochran, "Gas Content of Solid Aluminum by Solid Extraction and Vacuum Fusion", Transactions AIME, Journal of Metals, Vol. 8 No. 12, pp 1672 to 1674 (December, 1956)

(7) C. B. Griffith and M. W. Mallet, "Determination of Hydrogen in Wrought Aluminum Alloys", Analytical Chemistry, Vol. 25 No. 7, pp 1085 to 1087 (July, 1953)

Microscopic Studies

(8) J. H. Brophy and M. J. Sinnott, "Quantitative Metallographic Analysis of Graphite Size in Cast Iron", American Society for Metals Transactions Quarterly, Vol. 54 No. 1, pp 65 to 71, (March, 1961)

(9) T. Gladman and J. H. Woodhead, "The Accuracy of Point Counting in Metallographic Investigations", Journal of the Iron and Steel Institute, Vol. 194, pp 189 to 193 (February, 1960)

(10) Ervin E. Underwood, "Quantitative Metallography", Metals Engineering Quarterly, Vol. 1, No. 3, pp 70 to 81 (August, 1961), and Vol. 1, No. 4, pp 62 to 71 (November, 1961)

Welding Arc Behavior

(11) D. M. Kenyon, "Arc Behavior and Its Effect on the Tungsten-Arc Welding of Magnesium Alloys", Journal of the Institute of Metals, Vol. 93, No. 3, pp 85 to 89 (November, 1964)